

Design of Linear and Non-linear MIMO
Transceivers: Single and Multiple User Systems
with Different Channel Knowledge Assumptions.

DESIGN OF LINEAR AND NON-LINEAR MIMO
TRANSCEIVERS: SINGLE AND MULTIPLE USER SYSTEMS
WITH DIFFERENT CHANNEL KNOWLEDGE ASSUMPTIONS.

By

Michael Botros Shenouda, B.Sc., M.Sc.

AUGUST 2008

A Thesis

Submitted to the Department of Electrical & Computer Engineering

and the School of Graduate Studies

in Partial Fulfilment of the Requirements

for the Degree of

Doctor of Philosophy

McMaster University

© Copyright by Michael Botros Shenouda, August 2008

DOCTOR OF PHILOSOPHY (2008)
(Electrical & Computer Engineering)

McMaster University
Hamilton, Ontario

TITLE: Design of Linear and Non-linear MIMO Transceivers:
Single and Multiple User Systems with Different Channel
Knowledge Assumptions.

AUTHOR: Michael Botros Shenouda
B.Sc. (Communications and Electronics Engineering),
M.Sc. (Communications and Electronics Engineering)
Cairo University, Egypt

SUPERVISOR: Timothy N. Davidson, Associate Professor

NUMBER OF PAGES: xvii, 227

Dedications

To the lasting memory of my father.

To a very loving mother, and a wonderful sister.

Abstract

This thesis considers wireless multi-input multi-output (MIMO) communication systems in block flat-fading environments. It develops novel designs of transmission and reception schemes for single-user and multi-user systems. The designs are developed under different models for the information about the communication channel that is available at the transmitter.

For single-user systems, the thesis studies the class of non-linear MIMO transceivers that implement sequential interference (pre-) subtraction, namely transceivers with Tomlinson-Harashima precoding (THP) and transceivers with decision feedback equalization (DFE). For these transceivers, a novel design framework is developed to unify the design of these two dual systems when channel state information (CSI) is available at both the transmitter and the receiver. The framework encompasses a broad range of performance criteria, and generates closed-form expressions for the optimal designs under these criteria. The framework reveals that a single transceiver design is optimal for a large subclass of these performance criteria, and shows that this unique optimal design is (strictly) superior to the corresponding optimal linear transceiver for the same performance criterion. The framework also characterizes another class of design criteria for which the optimal non-linear transceiver reduces to the optimal linear transceiver for the same criterion. This novel design framework brings the design of non-linear MIMO transceivers to a level

of maturity similar to the linear counterparts, and will impact the design of practical wireless communication systems that implement these interference subtraction schemes. The framework is then generalized to the case of DFE transceivers that satisfy an additional zero-forcing (ZF) constraint and operate in a “limited feedback” regime in which CSI is available only to the receiver and there is a limited rate feedback channel between the receiver and the transmitter. The proposed limited feedback system is the first that involves a “precoded” DFE transceiver.

The multi-user part of the thesis develops multi-user transceivers that are robust to uncertainties in the available information about the users’ channels. These uncertainties are inevitable in most practical multi-user communication systems, and can result in significant performance degradation.

The first component of the multi-user part develops robust broadcast channel transceivers with quality of service (QoS) requirements for communication scenarios with bounded channel uncertainty at the transmitter. It formulates design problems for QoS requirements that can be expressed as constraints on the signal-to-interference-plus-noise-ratio (SINR) of each user, or as constraints on the mean square error (MSE) each user’s received signal. For both formulations, convex and efficiently-solvable design approaches are proposed. These design approaches are used to derive solutions to other related design problems, such as robust counterparts of the fair broadcasting problem.

The second component of the multi-user part develops robust designs for multi-user transceivers that minimize different MSE criteria subject to a power constraint. The designs are obtained for different models of channel uncertainty: stochastic uncertainty models and bounded uncertainty models. For each channel uncertainty model, the robust multi-user designs are developed for both linear and non-linear MIMO transceivers, for both broadcast channels (BC) and multiple access channels

(MAC).

Simulation studies demonstrate the impact of the proposed robust designs on the performance of multi-user systems, and show that by incorporating robustness in the design one can significantly reduce the sensitivity of these systems to channel uncertainty and mitigate its deleterious effects.

Acknowledgment

“I thank God through Jesus Christ our Lord.” (*Romans 7: 25*).

I would like to express my thanks to my advisor Dr. Timothy N. Davidson. I owe him a debt of gratitude for his abundant guidance, invaluable support, and continuous encouragement throughout my PhD, and for his open office and approachability, even during his busiest time. I would like also to thank my supervisory committee members, Prof. K. M. Wong and Prof. T. Kirubarajan, for their insightful remarks and encouraging comments during the committee meetings.

I would like to sincerely thank my friends and colleagues at McMaster University: E. Anis, N. Fahmy, S. Saad, B. Balasingam and S. Abdelkader for their support that I have always valued. My thanks extend to our friendly administrative staff members, Mrs. C. Gies and Mrs. H. Jachna, and our expert technical staff members Mr. T. Greenlay and Mr. C. Coroiu.

I am very indebted to many friends for their continuing moral support and encouragement. In particular, I am grateful to St. Mina Coptic Orthodox Church in Hamilton, Ontario, and I owe special thanks to Father Metias Ibrahim and Mr. M. Wadie. I would like also to express my deep gratitude to S. Kirolos, S. Mina, S. Philopater Mercurius, and S. George for their support throughout the past years.

Finally, I wish to express my thanks to my beloved family for their understanding and endless love.

List of Acronyms

BC	Broadcast Channel
BER	Bit Error Rate
CSI	Channel State Information
DFE	Decision Feedback Equalization
LMI	Linear Matrix Inequality
MAC	Multiple Access Channel
MIMO	Multiple Input Multiple Output
MMSE	Minimum Mean Square Error
ML	Maximum Likelihood
MSE	Mean Square Error
QoS	Quality of Service
SDP	Semidefinite Program
SINR	Signal-to-Interference-plus-Noise-Ratio
SNR	Signal-to-Noise-Ratio
SOCP	Second Order Cone Program
THP	Tomlinson-Harashima Precoding
ZF	Zero-Forcing

Contents

Abstract	iv
Acknowledgment	vii
List of Acronyms	viii
1 Introduction	1
1.1 Wireless Communications and MIMO Systems	1
1.1.1 Single-user Systems	5
1.1.2 Multi-user Systems	6
1.2 Thesis Contributions	7
1.2.1 Contributions to Single-user MIMO Systems	8
1.2.2 Contributions to Multi-user MIMO Systems	10
I Single-user Systems	16
2 A Unified Design Framework for Non-Linear MIMO Transceivers	17
2.1 Introduction	18
2.2 Two Dual Non-Linear MIMO Transceivers	21
2.2.1 Transceivers with Decision Feedback Equalization	21

2.2.2	Transceivers with Tomlinson-Harashima Precoding	22
2.2.3	General Model	24
2.3	Optimal feedforward and feedback matrices	25
2.3.1	Optimal feedforward matrix \mathbf{G}	25
2.3.2	Optimal feedback matrix \mathbf{B}	26
2.3.3	Optimality in the sense of maximizing individual SINRs	27
2.4	Design of the Precoding matrix: Preliminaries	28
2.4.1	A Multiplicative Majorization Inequality	29
2.4.2	An Additive Majorization Inequality	29
2.4.3	Schur-convex and Schur-concave functions	30
2.5	Optimal Precoding Matrix: Schur-convex objectives	31
2.5.1	Optimal Precoding Matrix	31
2.5.2	Properties of the optimal design	33
2.5.3	Examples of Schur-convex objectives	35
2.6	Optimal Precoding Matrix: Schur-concave objectives	39
2.6.1	Optimal Precoding Matrix	39
2.6.2	Examples of Schur-concave objectives	40
2.7	Simulation Studies	41
2.7.1	Validation of the design assumptions	41
2.7.2	Comparisons with linear transceivers	42
2.7.3	Comparisons with other interference (pre)subtraction designs	44
2.8	Conclusion	46
3	Design Framework for Limited Feedback MIMO Systems with Zero-Forcing DFE	49
3.1	Introduction	50

3.2	Zero-forcing DFE with Limited Feedback	52
3.3	Unified Framework for Zero-Forcing DFE	53
3.3.1	ZF-DFE Receiver Design	54
3.3.2	Transmitter Design	55
3.4	Statistical Distribution of Optimal Precoder for Schur-Convex Objectives	58
3.5	Precoder Selection and Codebook design	60
3.5.1	Precoding Matrix Selection	60
3.5.2	Grassmann Packing and Codebook Design	60
3.5.3	Codebook Design Criteria for Strictly Schur-convex Objectives	62
3.5.4	Codebook Design Criteria for Objectives that are Both Schur-convex and Schur-concave	64
3.5.5	Comparison with ZF-Linear Schemes	65
3.6	Simulation Studies	66
3.6.1	Comparisons with Limited Feedback Zero-forcing DFE Schemes	67
3.6.2	Comparisons with Limited Feedback Linear Zero-forcing Schemes	72
3.7	Conclusion	75

II Multi-user Systems 76

4 Robust Linear Broadcasting with QoS Constraints: SINR Formulations 77

4.1	Introduction	78
4.2	System Model	81
4.2.1	Precoding with QoS Constraints: Perfect CSI Case	82
4.2.2	Bounded Channel Uncertainty Model	84
4.3	Precoding with QoS Constraints: Uncertain CSI Case	85

4.4	Conservative Approaches	87
4.4.1	Robust SOCP with Independent Uncertainty	87
4.4.2	Robust SDP with Unstructured Uncertainty	89
4.4.3	Robust SDP with Structured Uncertainty	90
4.4.4	Some Comparisons	92
4.4.5	Maximum Allowable Uncertainty Size	95
4.5	Fair SINR Maximization	96
4.6	Numerical Results	98
4.7	Conclusion	108
5	Robust Non-Linear and Linear Broadcasting with QoS Constraints:	
	MSE Formulations	109
5.1	Introduction	110
5.2	System Model	112
5.3	Transceiver Design with MSE Constraints: Perfect CSI case	115
5.4	General Class of Bounded Channel Uncertainty Models	119
5.5	Transceiver Design with MSE Constraints: Uncertain CSI Case	120
5.5.1	Case of Intersecting Uncertainty Sets for each \mathbf{h}_k	122
5.5.2	Largest Feasible Uncertainty Size	123
5.5.3	Robust Broadcasting with QoS requirements: MSE versus SINR constraints	124
5.6	Robust Counterpart of Fair Minimax Transceiver Design	127
5.7	Numerical Studies	129
5.7.1	Performance Comparisons against SINR Requirements	131
5.7.2	Performance Comparisons against Uncertainty Size	133
5.8	Conclusion	136

6	Robust Linear Transceivers for Multi-user Systems	138
6.1	Introduction	139
6.2	Broadcast Channel with Linear Transceivers	142
6.3	Channel Uncertainty Models	144
6.3.1	Stochastic uncertainty model	144
6.3.2	Bounded uncertainty model	144
6.4	Statistically Robust design Via BC-MAC duality	146
6.4.1	Dual Multiple Access Channel with Linear Transceivers	147
6.4.2	BC-MAC Duality with Stochastic Uncertainty and Linear Transceivers	148
6.4.3	Statistically Robust Transceiver Design for the Dual MAC	149
6.5	Downlink Minimax Robust Design with Individual Channel Uncertainties	151
6.5.1	Multiple Intersecting Uncertainties for Each User	153
6.6	Downlink Minimax Robust Design with Overall Channel Uncertainty	154
6.7	Uplink Minimax Robust Designs	158
6.8	Simulation Studies	159
6.8.1	Statistically robust transceiver design	160
6.8.2	Robust minimax transceiver designs	164
6.9	Conclusion	167
7	Robust Non-Linear Transceivers for Multi-user Systems	168
7.1	Introduction	169
7.2	System Model	171
7.3	Statistically Robust design Via BC-MAC duality	173
7.3.1	Dual Multiple Access Channel with Non-Linear Transceivers	174

7.3.2	BC-MAC Duality with Stochastic Uncertainty and Non-Linear Transceivers	176
7.3.3	Statistically Robust Transceiver Design for the Dual MAC	177
7.4	Robust Design with Bounded Channel Uncertainties	178
7.5	Uplink Minimax Robust Designs	181
7.6	Simulation Studies	182
7.6.1	Statistically Robust Designs	183
7.6.2	Minimax Robust Designs	186
7.7	Conclusion	188
8	Summary and Future Directions	191
8.1	Summary	191
8.2	Future Directions	194
A	Proofs of Schur-convex objectives	196
B	Proofs of Schur-concave objectives	199
C	Proof of Theorem 3.1	201
C.1	Optimal Precoder for Schur-convex Functions	201
C.2	Optimal Precoder for Schur-concave Functions	203
D	Incorporating different power constrains	204
E	Proof of Lemma 5.1	206
F	Derivation of Design Formulations 1 and 2	208
G	Proof of Theorem 6.1	210

List of Figures

1.1	A single-user MIMO system	4
2.1	Single-user MIMO transceiver using DFE	21
2.2	Single-user MIMO transceiver using THP	23
2.3	Validation of the design assumptions for DFE and THP transceivers .	43
2.4	BER comparison of the proposed Schur-convex designs with linear transceiver designs	44
2.5	BER comparison of the proposed Schur-convex designs with other in- terference (pre-)subtraction designs	46
2.6	Another BER comparison of the proposed Schur-convex designs with other interference (pre-)subtraction designs	47
3.1	MIMO transceiver with DFE using limited feedback.	53
3.2	BER comparison of the proposed codebooks and ZF-DFE with other ZF-DFE schemes and limited feedback	68
3.3	Another BER comparison of the proposed codebooks and ZF-DFE with other ZF-DFE schemes and limited feedback	69
3.4	Comparison of the Gaussian mutual information of the proposed code- book and ZF-DFE with other ZF-DFE schemes and limited feedback	70
3.5	BER comparison of the proposed ZF-DFE limited feedback scheme with ZF-linear schemes and limited feedback	73

3.6	Another BER comparison of the proposed ZF-DFE limited feedback scheme with ZF-linear schemes and limited feedback	74
4.1	Percentage of channel realizations for which the robust QoS guarantee can be made against the uncertainty size δ	101
4.2	Average of the transmitted power versus uncertainty size δ	102
4.3	Empirical CDF of lower bounds on δ_{\max}	103
4.4	Percentage of channel realizations, for which the robust QoS guarantee can be made against the required SINRs	104
4.5	Maximum achievable (equal) SINRs against the average transmitted power	105
4.6	Empirical CDF of SINR_{\max}	106
4.7	Empirical CDF of the actual received SINRs of all users	107
5.1	Broadcast channel with Tomlinson-Harashima precoding at the transmitter.	114
5.2	Equivalent linear model for the transmitter.	114
5.3	Percentage of channel realizations for which robust QoS guarantee can be made against the required SINRs: comparison between different linear and non-linear designs	132
5.4	Average transmitted power versus SINR requirements: comparison between different linear and non-linear approaches	134
5.5	Percentage of channel realizations for which the robust QoS guarantee can be made against the uncertainty size δ : comparison between different linear and non-linear designs	135
5.6	Average transmitted power versus uncertainty size δ for different different linear and non-linear designs	136

6.1	Comparison of the statistically robust linear design with non-robust designs	161
6.2	Another comparison of the statistically robust linear design with non-robust designs for different system configuration	162
6.3	Comparison of the statistically robust linear design with other robust designs	163
6.4	Comparison between minimax linear design for “per-user” and “system-wide” uncertainty models and other non-robust designs . . .	165
6.5	Another comparison between minimax linear design for “per-user” and “system-wide” uncertainty models and other non-robust designs . . .	166
7.1	BC with Tomlinson-Harashima precoding.	172
7.2	Equivalent linear model for the transmitter.	172
7.3	The Dual MAC with decision feedback equalization.	175
7.4	Comparison of the statistically robust THP design with non-robust designs	184
7.5	Comparison of the statistically robust THP design with other robust designs	185
7.6	Comparison of the minimax robust THP design with non-robust designs	187
7.7	Comparison of the minimax robust THP design with non-robust designs: Scenario with near and far users	189

Chapter 1

Introduction

This thesis considers the (joint) design of the transmitter and receiver for multiple-input multiple-output (MIMO) communications systems. The designs include both linear and non-linear transmission and reception techniques, for both single-user and multi-user systems, and they are based on different assumptions of the nature and the extent of the available channel knowledge. In this chapter, we will highlight some of the desirable features of MIMO communication systems that make them suitable for wireless communications.¹ We will also present the contributions of the thesis to the development of this area.

1.1 Wireless Communications and MIMO Systems

Wireless communication systems constitute a substantial and rapidly growing sector of the communication industry. In addition to the almost-ubiquitous cellular

¹The vector model of MIMO systems can also be applied to wired multi-channel systems such as Digital Subscriber Line (DSL) systems.

telephone networks, wireless local area networks are covering an increasing number of business and educational environments, and wireless wide area networks are extending to many areas in which installing wired communication networks is a less economical option. The mobility offered by the wireless communication systems and the relatively low cost of deployment has spawned a variety of services, from conventional voice, email, internet access, and audio and video conferencing, to remote sensing and distributed control, such as monitoring the elderly and automation of the transportation networks.

However, the wireless medium possesses some characteristics that can make reliable communication rather challenging. One of these characteristics is the multipath fading phenomenon, which results from the propagation of the transmitted signal along different paths to the receiver. Each path has its own attenuation and delay, and these different multipath components do not necessarily add in a constructive manner at the receiver. Furthermore, small changes in the position of the transmitter, the receiver, or the scatterers can result in substantial changes in the phase relationships between these paths, and hence the received signal power may fluctuate quite rapidly. When the relative delays between the multiple propagation paths are significantly smaller than the signaling interval, the accumulated gains of these paths can be approximated by a complex scalar, and the channel is said to be a flat fading channel. When this condition does not hold, the channel is said to be a frequency-selective fading channel. In the frequency selective scenario, multi-carrier transmission techniques can be used to partition the transmitted signal over a (large) number of parallel subchannels, each of which can be treated as a flat-fading channel; e.g., [1].² Hence, flat fading channels will be considered throughout this thesis. This thesis will also adopt an independent block fading channel model in which the fading

²Typically, the design of multi-carrier techniques is more involved than those for a single flat fading channel.

gains are considered constant for few channel uses, and then they take on independent values. This model well approximates a wide range of communication scenarios with slow fading; e.g., [2]. For this model, channel state information can be obtained at the receiver using training techniques. When transmission and reception are multiplexed in time with a short “ping-pong” time, the reciprocity of the channel allows the transmitter to obtain an estimate of the communication channel. Otherwise, obtaining channel state information at the transmitter would require feedback from the receiver; e.g., [2].

One of the potential applications of multiple antennas systems is to meet the challenge of fading. MIMO systems can exploit the availability of the different communication links between each transmit and receive antennas to enhance the quality of the received signal. One way of doing so is by through sending linearly scaled versions of the same data stream from the different transmit antennas in a way that enables the signals from the received antennas to be linearly combined in a constructive way to extract the transmitted data. In this way, multiple fading links are combined in a controlled way to construct a more reliable channel. This approach is often called beamforming, and is an example of linear transmitter and receiver processing. In these beamforming MIMO systems, the optimal design of the scaling weights of each transmit antenna and the combining weights of the receive antennas typically requires the availability of the channel state information (CSI) at both the transmitter and the receiver [3,4].

Other challenging characteristics of wireless communication are the limitations on the bandwidth and power of the transmitted signal that are imposed by the transmission device (e.g., a cell phone), or the standards of the particular wireless application. These constrained resources limit the growth of the achievable data rates. MIMO

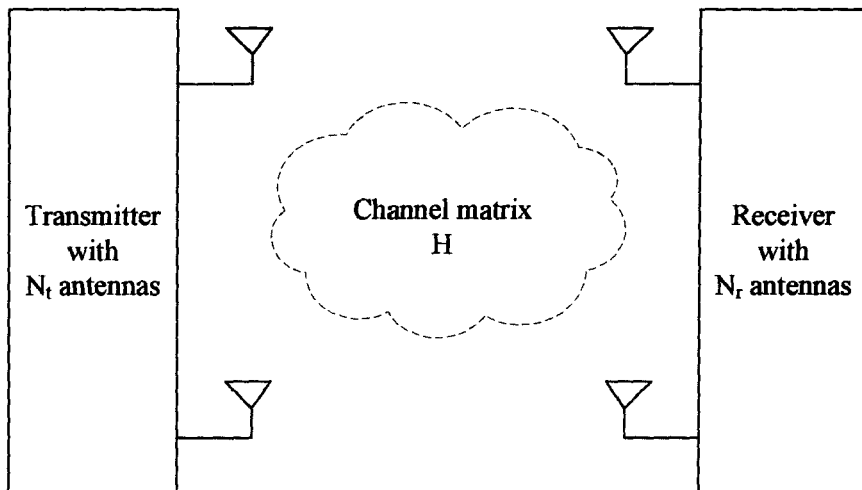


Figure 1.1: A single-user MIMO system with N_t transmit antennas and N_r receive antennas. The element H_{ij} of the channel matrix \mathbf{H} represents the gain from the j^{th} transmit antenna to the i^{th} receive antenna.

communication systems provide the potential for a significant increase in the achievable data rate by facilitating the transmission of multiple simultaneous data streams. This characteristic of MIMO systems is termed spatial multiplexing, and it offers a new dimension to the conventional time and frequency multiplexing dimensions in single-input single-output (SISO) systems. For example, consider a single-user MIMO communication system with N_t transmit antennas and N_r receive antennas as depicted in Fig 1.1. In a richly scattered environment, at moderate to high signal-to-noise-ratios (SNRs), the growth of the achievable data rate with the (logarithm of the) transmitted power in this MIMO system is $\min(N_t, N_r)$ times that of the corresponding SISO system.

1.1.1 Single-user Systems

One approach to employing spatial multiplexing to achieve these potential gains is through sending a different linear combination of the multiple data messages from each transmit antenna, and processing the received signals linearly to separate these data messages. This linear approach to transmitter processing (precoding) and receiver processing (equalization) generalizes beamforming to the case of simultaneous transmission of multiple data streams. Because of the rather low computational complexity of the joint linear transmitter and receiver (transceiver) approach, its optimal designs were studied for a large number of design objectives; e.g., [5], and a unifying design approach for many of these objectives was developed in [6]. These designs considered scenarios in CSI is available at both the receiver and the transmitter.

An attractive alternative to linear transceiver design is the class of non-linear MIMO transceivers. These transceivers have the potential for significant gains over linear transceivers, and yet can be implemented with comparable complexity. The performance gains are achieved by implementing sequential interference (pre-) subtraction at either the transmitter, as in Tomlinson-Harashima Precoding (THP) systems, or at the receiver, as in systems with Decision Feedback Equalization (DFE). Interference subtraction in these systems is implemented in a way that mitigates the interference that is created by the channel. However, because of the non-linearity of these systems, the joint design of the transmitter and the receiver has been more challenging than in the case of linear transceivers. While the optimal transceiver design is known for a few communication design objectives [7], the optimal designs for many other objectives have remained an open problem.

In the single-user part of this thesis, we study the optimal design of this class of non-linear transceivers for a wide range of communication objectives, and we develop a unifying design framework that complements the existing framework for linear

transceivers [6]. In Chapter 2, we focus on communication scenarios that assume the availability of perfect (CSI) at both the transmitter and the receiver, and in Chapter 3 we generalize the optimal designs and the unifying framework to scenarios with limited feedback that assume perfect CSI at the receiver only and a low-rate feedback channel between the receiver and the transmitter.

1.1.2 Multi-user Systems

In multi-user scenarios, the design of the processing schemes at the transmitter and receiver becomes more dependant on the availability of the users' channel state information, due to the physically disjoint nature of the users. For example, consider a broadcast channel (BC) that uses N_t antennas at the base station to simultaneously send independent data streams to K users, each with one receive antenna. The users of this BC are unable to cooperate, and hence they can not jointly detect their data messages. In this scenario, precoding at the transmitter plays a critical role in mitigating interference at the receivers, but its effectiveness is rather sensitive to the available channel knowledge. In particular, let $\mathbf{s} \in \mathbb{C}^K$ denote the vector of symbols intended to each user, $\mathbf{h}_k \in \mathbb{C}^{1 \times N_t}$ denote the k^{th} user's channel, \mathbf{P} denote the linear precoding matrix used at the transmitter, and \mathbf{p}_j denote the j^{th} column of \mathbf{P} . Then, the received signal, y_k at the k^{th} user can be written as

$$y_k = \mathbf{h}_k \mathbf{p}_k s_k + \sum_{j \neq k} \mathbf{h}_k \mathbf{p}_j s_j + n_k, \quad (1.1)$$

where the first term represents the useful signal carrying the intended messages, the second term represents the multi-user interference, and the third term is the additive noise of the k^{th} receiver. From (1.1), it is apparent that the design of the precoder \mathbf{P} in order to mitigate the interference terms at the receivers will depend on the availability (and quality) of the information that the transmitter has regarding each

user's channel.

In practical communication systems, the CSI available at the transmitter is usually imperfect. For example, in broadcast systems with uplink-downlink reciprocity (e.g., time division duplex systems), the base station can estimate the users' channels by exploiting the fact that it acts as receiver during some of the time slots. In a slow fading environment, the dominant impairment in this estimate is that due to estimation errors. In systems in which users can estimate their channel, quantize it, and feed it back to the transmitter, e.g., [8,9], the uncertainty in the channel is usually dominated by quantization errors. The performance of broadcasting systems is quite sensitive to these uncertainties, which can result in serious degradation of the quality of the signal received by each user [8]. These facts, motivate the multi-user part of this thesis, in which we study the design of multiuser transceivers, both linear and non-linear, under different models of channel uncertainty. In that part, the thesis considers two broad classes of transceiver design problem. In the first class, the objective is to minimize the transmission power necessary to guarantee specified quality of service (QoS) requirement for each user. In the other class, the objective is to optimize the fidelity of the users' signals subject to a power constraint at the transmitter.

1.2 Thesis Contributions

The focus of the thesis is on the design of MIMO transceivers for both single-user and multi-user systems for different channel state information assumptions.

1.2.1 Contributions to Single-user MIMO Systems

Chapter 2, develops a novel and broadly applicable framework for the the design of non-linear transceivers with Tomlinson-Harashima precoding or decision feedback equalization. The framework unifies the design of these dual systems. It uses concepts from majorization theory and convex optimization theory to develop optimal closed-form designs for a broad range of objectives. In addition, scenarios under which the optimally designed non-linear transceivers are (strictly) superior to their linear counterparts are characterized. One of the interesting results of this unified framework is that one of the derived optimal designs can simultaneously optimize a large class of performance objectives, including maximizing the Gaussian mutual information, minimizing the total bit error rate and minimizing the total mean square error — a property that can not be achieved by a linear transceiver. This class is characterized through the use of majorization theory. Another interesting result is that for a second class of design objectives, the optimal non-linear transceiver reduces to the optimal linear transceiver for the same design objective.

The transceiver design framework in Chapter 2 assumes the availability of accurate channel information at both the transmitter and the receiver. In many practical schemes the receiver can estimate the channel using a training sequence, but the channel information available at the transmitter can be rather limited. The design of non-linear MIMO transceivers with limited channel information at the transmitter results in an even more challenging design problem. Chapter 3 generalizes the design framework developed in Chapter 2 to scenarios with limited CSI at the transmitter. In particular, we consider a communication system with a linear precoder at the transmitter, zero-forcing decision feedback equalization at the receiver, and a low-rate feedback channel that enables communication from the receiver to the transmitter. In this limited feedback scheme, receiver selects a suitable precoder from a codebook and

feeds back the index of this precoder to the transmitter. In this chapter, the statistical distribution of the optimal precoder in a standard Rayleigh fading environment is characterized for a broad range of design objectives. This distribution is then used to show that codebooks constructed from Grassmann packings minimize an upper bound on average distortion measures for this range of objectives. The proposed limited feedback system is, to the best knowledge of the author, the first that involves a “precoded” DFE transceiver.

The contribution of the single-user part of this thesis were summarized in the following two journal articles

- M. Botros Shenouda and T. N. Davidson, “A framework for designing MIMO systems with decision feedback equalization or Tomlinson Harashima precoding,” *IEEE J. Select. Areas Commun.*, vol. 26, no. 2, pp. 401–411, Feb. 2008,
- M. Botros Shenouda and T. N. Davidson, “A design framework for limited feedback MIMO systems with zero-forcing DFE,” Submitted to *IEEE J. Select. Areas Commun.*, Accepted March 2008.

and were presented in the following conferences

- M. Botros Shenouda and T. N. Davidson, “A framework for designing MIMO systems with decision feedback equalization or Tomlinson-Harashima precoding,” in *Proc. IEEE Int. Conf. Acoustics, Speech, Signal Processing*, Honolulu, April 2007, pp. III-209 – III-212. (Finalist Best Student Author Award.)
- M. Botros Shenouda and T. N. Davidson, “Minimum SER zero-forcing transmitter design for MIMO channels with interference pre-subtraction,” in *Proc. IEEE Veh. Technol. Conf.*, Dublin, 2007, pp. 2109–2113.

- M. Botros Shenouda and T. N. Davidson, “Limited feedback design of MIMO systems with zero-forcing DFE using Grassmann codebooks,” in *Proc. IEEE Canadian Wrkshp Info. Theory*, Edmonton, June 2007, pp. 118–123.

1.2.2 Contributions to Multi-user MIMO Systems

This section will describe the contributions of this thesis to the robust design of multi-user transceivers that explicitly include the nature of channel uncertainty in the design formulations. Chapters 4 and 5 study the design of robust transceivers for communication schemes with quality of service (QoS) requirements for each user, while Chapters 6 and 7 study the design of robust transceivers based on mean-square error (MSE) performance criteria subject to a transmission power constraint.

1.2.2.1 Robust Broadcasting Transceivers with QoS Constraints

Chapters 4 and 5 consider the design of broadcasting schemes with quality of service constraints and uncertain channel information. Transceiver designs that guarantee QoS are essential for practical communication systems with interactive data, such as video and audio conference applications, and in cellular systems in which users are offered different grades of service. A central design problem in this area is that of designing the transmitter of the downlink so as minimize the transmission power required to to guarantee that all users’ QoS requirements are satisfied. When accurate channel information of all users is available, the transmitter employs transmit precoding techniques to spatially precode the messages intended to different users in a way that mitigates the multiuser interference at the (non-cooperating) receivers. The transmitter’s ability to mitigate interference at the receivers is dependent on the availability of (accurate) channel state information for all the users’ channels. When the channel state information is imperfect, the QoS of all users may incur significant

degradation.

Chapter 5 considers a deterministically-bounded model for the channel uncertainty of each user, and the goal is to design a robust linear precoder that minimizes the total transmission power required to satisfy the users' signal-to-interference-plus-noise (SINR) constraints for all channels within a specified uncertainty region around the transmitter's estimate of each user's channel. The constraints on the received SINR of each user can be translated into equivalent constraints on the symbol error rate or the achievable data rate of the user, and hence they constitute a general constraint on the quality of service. Chapter 5 demonstrates that this QoS problem is equivalent to a semi-infinite convex optimization problem whose tractability is still an open problem. The theories of robust and convex optimization are then used to derive three conservative design approaches that yield efficiently-solvable convex design formulations that guarantee that the SINR constraints are met. These three approaches yield semidefinite program (SDP) formulations that offer different trade-offs between the degree of conservatism and the size of the SDP. It will be also shown that these three approaches can be used to solve other related problems, such as the robust counterpart of the fair transceiver design problem that seeks to maximize the QoS of the "weakest" user subject to a given power constraint. For these problems, conservative, but efficiently-solvable, quasi-convex design formulations are derived.

Chapter 6 formulates each user's QoS requirement as a constraint on the mean square error (MSE) in each user's received signal, and shows that these MSE constraints imply constraints on the received SINR of each user. Using the MSE constraints, this chapter presents a unified design approach for robust linear and non-linear transceivers with QoS requirements. The proposed designs provide an exact solution to the robust transceiver problem with MSE constraints, thus overcoming the need for the conservative designs that are presented in Chapter 5. Furthermore, this

approach provides computationally-efficient design formulations for a general model of channel uncertainty that subsumes many natural choices for the uncertainty region. As in Chapter 5, the designs can also be utilized to solve the robust fair transceiver design problem.

The contributions of the first component of the multi-user part of the thesis were summarized in the following journal articles

- M. Botros Shenouda and T. N. Davidson, “Convex conic formulations of robust downlink precoder designs with quality of service constraints,” *IEEE J. Select. Topics Signal Processing*, vol. 1, no. 4, pp. 714–724, Dec. 2007.
- M. Botros Shenouda and T. N. Davidson, “Non-linear and linear broadcasting with QoS requirements: Tractable approaches for bounded channel uncertainties,” Submitted to *IEEE Trans. Signal Processing* Dec. 2007. Revised May 2008. See also <http://arxiv.org/abs/0712.1659v1>.

and also presented in the following conferences:

- M. Botros Shenouda and T. N. Davidson, “Linear matrix inequality formulations of robust QoS precoding for broadcast channels,” in *Proc. IEEE Canadian Conf. Elec. & Comp. Engineering*, Vancouver, April 2007, pp. 324–328.
- M. Botros Shenouda and T. N. Davidson, “Quality constrained broadcasting with channel uncertainty: Semidefinite and quasi-convex formulations,” in *Proc. Int. Conf. Continuous Optimization*, Hamilton, Aug. 2007.
- M. Botros Shenouda and T. N. Davidson, “Tractable approaches to fair QoS broadcast precoding under channel uncertainty,” in *Int. Conf. Acoustics, Speech, Signal Processing*, Las Vegas, April 2008, pp. 3125–3128.

- M. Botros Shenouda and T. N. Davidson, “Design of fair multi-user transceivers with QoS and imperfect CSI,” in *Commun. Networks Services Research Conf.*, Halifax, May 2008, pp. 191–197.

1.2.2.2 Robust MSE Designs of Multi-user Transceivers

Chapters 6 and 7 consider robust minimum MSE designs for multi-user transceivers for linear and non-linear transceivers, respectively, subject to a transmission power constraint. They consider robust transceiver designs for both multiple access channels and broadcast channels, with emphasis on the BC case, under two different models for the uncertainty in the information regarding each users’ channel: a stochastic model, and a deterministically-bounded model.

The stochastic model of channel uncertainty suits communication systems in which channel uncertainties are dominated by estimation errors; e.g., time division duplex systems. For this uncertainty model, the designs are based on a derived generalization of the mean square error (MSE) duality between the broadcast channels (BC) and multiple access channels (MAC) to scenarios with uncertain channels. The existence of such duality complements the proven lack of duality of the users’ signal-to-interference-plus-noise-ratio (SINR) region for the same stochastic channel model. Using this duality, it can be shown that the achievable regions for the average, over channel uncertainty, of users’ MSEs are equivalent for the BC and MAC. The equivalence of the MSE regions holds under a linear transformation between the BC and MAC transceivers. As a result, the design of robust transceivers for the BC so as to optimize objectives that are arbitrary functions of the average MSEs can be solved by obtaining the optimal MAC transceivers for the same objective and then applying this linear transformation. For example, the joint design of the linear transceiver for

the BC so as to minimize the total average MSEs is a non-convex problem. However, using the derived duality result the non-convex BC transceiver design can be obtained as an affine transformations of the corresponding optimal transceiver for the dual MAC, which is itself a convex optimization problem that can be efficiently solved.

The deterministically-bounded channel uncertainty models suit communication systems in which quantized channel feedback is employed. For these systems, the broadcast channel and multiple access channel transceivers are designed to minimize the worst-case value of the total MSE, over all admissible channels. While it is shown that the design problem is non-convex, an efficient iterative optimization algorithm that is based on efficiently-solvable convex conic formulations is proposed. The designs are also generalized to the case when the channel uncertainty is described using the intersection of multiple uncertainty sets. The framework is quite flexible, and can incorporate different bounded uncertainty models as well as a variety of power constraints, such as per-antenna power constraints and spatial shaping power constraints.

The contributions of the second component of the multi-user part of the thesis were summarized in the following journal articles

- M. Botros Shenouda and T. N. Davidson, “On the design of linear transceivers for multi-user systems with channel uncertainty,” To appear in *IEEE J. Select. Areas Commun.*, Accepted Jan. 2008.
- M. Botros Shenouda and T. N. Davidson, “Tomlinson-Harashima precoding for broadcast channels with uncertainty,” *IEEE J. Select. Areas Commun.*, vol. 25, no. 7, pp. 1380–1389, Sept. 2007.

and were presented in the following conferences

- M. Botros Shenouda and T. N. Davidson, “Robust linear precoding for uncertain MISO broadcast channels,” in *Proc. IEEE Int. Conf. Acoustics, Speech, Signal Processing*, Toulouse, May 2006, pp. IV-37–IV-40. (Best Student Author Award.)
- M. Botros Shenouda and T. N. Davidson, “Transmitter design with interference pre-subtraction for uncertain broadcast channels,” in *Proc. Allerton Conf. Comm., Control, Computing*, Monticello Illinois, Sept. 2006.
- M. Botros Shenouda and T. N. Davidson, “Minimax linear precoding for MISO broadcast channels with bounded uncertainty,” in *Proc. IEEE Global Telecommun. Conf.*, San Francisco, Nov. 2006, pp. 1–6.
- M. Botros Shenouda and T. N. Davidson, “Non-linear transceiver design for broadcast channels with statistical channel state information,” in *Proc. IEEE Int. Symp. Signal Processing Inform. Tech.*, Cairo, Dec. 2007, pp. 311–316.
- M. Botros Shenouda and T. N. Davidson, “Statistically robust transceiver design for broadcast channels with uncertainty,” in *IEEE Canadian Conf. Elec. & Comp. Engineering*, Vancouver, April 2007, pp. 320–323.
- M. Botros Shenouda and T. N. Davidson, “Linear multiuser transceivers: Robustness via worst scenario MSE approach,” in *Wireless Commun. Networking Conf.*, Las Vegas, March 2008, pp. 1008–1013.
- M. Botros Shenouda and T. N. Davidson, “Sequential interference subtraction multi-user transceivers: Designs for general bounded channel uncertainty models,” To appear *Proc. IEEE European Signal Process. Conf.*, August 2008.

Finally, the thesis is concluded by Chapter 8, which also provides suggestions for further research directions.

Part I

Single-user Systems

Chapter 2

A Unified Design Framework for Non-Linear MIMO Transceivers

In this chapter, we consider joint transceiver design for general single-user (point-to-point) multiple-input multiple-output communication systems that implement interference (pre-) subtraction; i.e., Decision Feedback Equalization (DFE) or Tomlinson-Harashima precoding (THP). For systems in which perfect channel state information (CSI) is available, a unified framework is developed for joint transceiver design of these two dual systems by considering design criteria that are expressed as functions of the (logarithm of the) Mean Square Error (MSE) of the individual data streams. By deriving two inequalities that involve the logarithms of the individual MSEs, optimal designs are obtained for two broad classes of communication objectives, namely those that are Schur-convex and Schur-concave functions of these logarithms. These two classes embrace several design criteria for which the optimal transceiver design has remained an open problem. For Schur-convex objectives, the optimal design results in data streams with equal MSEs. In addition to other desirable properties, this design

simultaneously minimizes the total MSE and the average bit error rate, and maximizes the Gaussian mutual information; a property that is not achieved by a linear transceiver. Moreover, we show that the optimal design yields objective values that are superior to the corresponding optimal objective value for a linear transceiver. For Schur-concave objectives, the optimal DFE design results in linear equalization and the optimal THP design results in linear precoding. The proposed design framework embraces a wide range of design objectives and can be regarded as a counterpart of the existing framework of linear transceiver design.

2.1 Introduction

In the previous chapter, we have mentioned that one of the key advantages of Multiple-Input Multiple-Output (MIMO) communications schemes is that they facilitate the simultaneous transmission of multiple data streams. In single-user (point-to-point) applications, such schemes typically involve processing of the data streams at the transmitter (precoding) to “match” the transmission to the channel and processing of the received signals (equalization) to mitigate the interference between the received streams at reasonable computational cost. One approach to the design of such a scheme is to focus on linear precoding and linear equalization; e.g., [5, 6]. An alternative approach that offers the potential for performance improvements over the linear approach is to allow interference (pre-)subtraction at either the transmitter or the receiver. This approach includes schemes with linear precoding and Decision Feedback Equalization (DFE), and schemes with Tomlinson-Harashima precoding (THP) and linear equalization, and will be the focus of this chapter. The DFE and THP schemes were initially introduced as receiver and transmitter (pre)equalization schemes, respectively, for single input single output (SISO) channels with inter-symbol

interference, e.g., [10].

A large number of joint design strategies have been proposed for the class of linear MIMO transceivers (e.g., [5]), and a unified framework that encompasses many of these designs was proposed in [6]. That framework is based on the classes of communication objectives that are Schur-convex or Schur-concave functions of the mean square error (MSE) of each data stream, and encompasses a broad range of design objectives. For DFE-based systems, joint transceiver designs based on a minimum MSE criterion were considered in [7, 11–13], and designs subject to a zero-forcing constraint were considered in [14, 15]. However, for many of the design criteria for which (jointly) optimal linear transceivers are known, the jointly optimal DFE-based transceiver has remained an open problem. Furthermore, the development of a unifying design framework for DFE-based transceivers that encompasses these designs has appeared to be a challenging problem. For THP schemes, designs based on minimum MSE criteria were considered in [10, 13], and designs subject to a zero-forcing constraint were considered in [10, 16]. However, the approach in [13] considers a lower bound on the MSE, and the approaches in [10, 16] do not use all the degrees of design freedom available in a single-user system. Hence, the approaches in [10, 13, 16] yield suboptimal designs. In addition to the absence of a minimum MSE transceiver, the design of (jointly) optimal TH-based transceivers for other design criteria, and the development of a unifying framework have remained open problems.

In this chapter, we develop a broadly applicable framework for joint transmitter and receiver design for MIMO systems with DFE or THP. (A related DFE-centric framework was developed, independently, in [17, 18].) We consider the broad range of design criteria that can be expressed as either Schur-convex or Schur-concave functions of the logarithm of the MSE of each data stream, and we provide optimal transceiver designs for these two classes. In addition to providing a generalization of

existing DFE designs based on the overall MSE, these classes of functions embrace other design criteria, such as minimizing the maximum of the individual MSEs, minimizing a general p -norm of the MSEs, and minimizing the product of the individual MSEs, which is equivalent to maximizing the Gaussian mutual information. Moreover, design criteria expressed in terms of the signal-to-interference-plus-noise ratio (SINR) and bit error rate (BER) of each stream are included in the set of objectives covered by these classes; e.g., maximizing the harmonic mean of the SINRs, maximizing a general p -norm of the SINRs, and minimizing the the total BER of all streams. Interestingly, the optimal design for both Schur-convex and Schur-concave objectives yields a diagonal MSE matrix. Hence, communication over the MIMO channel is decomposed into a number of uncorrelated subchannels. For Schur-convex objectives the optimal design results in data streams with equal MSEs. This property is not achieved by the previously proposed (suboptimal) designs for THP systems (e.g., [10, 13]), and hence ordering the symbols prior to interference subtraction is necessary for those designs, as it is in multi-user schemes [19]. This ordering is unnecessary for the optimal transceiver designs derived herein. Another property of our optimal design for Schur-convex objectives is that it simultaneously minimizes the total MSE, minimizes the average bit error rate, and maximizes the Gaussian mutual information. This property is not achieved by the optimal linear transceiver. For any Schur-convex objective, our optimal design yields an objective value that is superior to the corresponding optimal objective value for a linear transceiver. For Schur-concave objectives, the optimal DFE design results in linear equalization and optimal THP design results in linear precoding. From a broader perspective, the proposed framework can be viewed as a counterpart for the design of DFE-based and TH-precoding-based transceivers of the unified framework for the design of linear transceivers in [6].

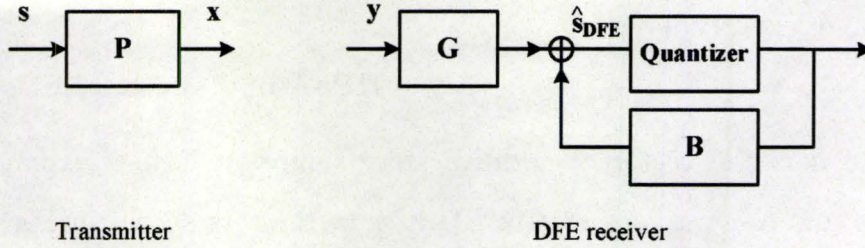


Figure 2.1: Single-user MIMO transceiver using Decision Feedback Equalization.

2.2 Two Dual Non-Linear MIMO Transceivers

We consider a generic MIMO communication system described by the channel matrix $\mathbf{H} \in \mathbb{C}^{n_r \times N_t}$, e.g., [20], and we denote by K the number of data streams transmitted simultaneously over the channel. We will consider the design of two communication architectures: systems with linear precoding (pre-equalization) at the transmitter and DFE at the receiver; and systems with Tomlinson-Harashima precoding at the transmitter and linear equalization at the receiver. We will assume that full channel state information (CSI) is available at both the transmitter and the receiver. However, the framework developed herein will be extended to scenarios with limited CSI at the transmitter in Chapter 3.

2.2.1 Transceivers with Decision Feedback Equalization

As shown in the DFE model in Fig. 2.1, the vector $\mathbf{s} \in \mathbb{C}^K$ that contains the current data symbol of each stream is linearly precoded by the matrix $\mathbf{P} \in \mathbb{C}^{N_t \times K}$ to generate the transmitted vector

$$\mathbf{x} = \mathbf{P}\mathbf{s}, \quad (2.1)$$

where we assume, without loss of generality, that $\mathbb{E}\{\mathbf{s}\mathbf{s}^H\} = \mathbf{I}$. Hence, the average transmitted power constraint can be written as $\mathbb{E}_{\mathbf{s}}\{\mathbf{x}^H\mathbf{x}\} = \text{tr}(\mathbf{P}^H\mathbf{P}) \leq P_{\text{total}}$. The

received vector \mathbf{y} is

$$\mathbf{y} = \mathbf{H}\mathbf{P}\mathbf{s} + \mathbf{n}, \quad (2.2)$$

where \mathbf{n} is the vector of additive noise samples which is assumed to have zero-mean and a covariance matrix $\mathbb{E}\{\mathbf{n}\mathbf{n}^H\} = \mathbf{R}_n$. As shown in Fig. 2.1, the DFE is implemented using a feedforward matrix $\mathbf{G} \in \mathbb{C}^{K \times n_r}$ and a feedback matrix filter $\mathbf{B} \in \mathbb{C}^{K \times K}$. In this scenario, the detection of the k^{th} symbol is preceded by subtracting the effect of previously decoded symbols. Assuming correct previous decisions, the input to the quantizer, $\hat{\mathbf{s}}$, can be written as (e.g., [7])

$$\hat{\mathbf{s}}_{\text{DFE}} = (\mathbf{G}\mathbf{H}\mathbf{P} - \mathbf{B})\mathbf{s} + \mathbf{G}\mathbf{n}, \quad (2.3)$$

where \mathbf{B} is a strictly lower triangular matrix.¹ Using the error signal $\mathbf{e} = \hat{\mathbf{s}}_{\text{DFE}} - \mathbf{s}$, we can define the Mean Square Error matrix,

$$\mathbf{E} = \mathbb{E}_s\{\mathbf{e}\mathbf{e}^H\} = \mathbf{C}\mathbf{C}^H - \mathbf{C}\mathbf{P}^H\mathbf{H}^H\mathbf{G}^H - \mathbf{G}\mathbf{H}\mathbf{P}\mathbf{C}^H + \mathbf{G}\mathbf{H}\mathbf{P}\mathbf{P}^H\mathbf{H}^H\mathbf{G}^H + \mathbf{G}\mathbf{R}_n\mathbf{G}^H, \quad (2.4)$$

where $\mathbf{C} = \mathbf{I} + \mathbf{B}$ is a unit diagonal lower triangular matrix.

2.2.2 Transceivers with Tomlinson-Harashima Precoding

As shown in Fig. 2.2(a), in a THP system the transmitter performs successive interference pre-subtraction and precoding using the strictly lower triangular matrix \mathbf{B} and the precoding matrix \mathbf{P} , respectively. We assume that the elements of \mathbf{s} are chosen from a square QAM constellation \mathcal{S} with cardinality M and that $\mathbb{E}_s\{\mathbf{s}\mathbf{s}^H\} = \mathbf{I}$. The Voronoi region, \mathcal{V} , of this constellation is a square whose side length is D . Following pre-subtraction of the effect of previously precoded symbols, the transmitter uses the modulo operation so that the symbols of \mathbf{v} lie within the boundaries of \mathcal{V} . The effect

¹In general, the estimator in (2.3) is biased, but the effect of this bias can be mitigated by scaling the decision regions of the quantizer [21]. At operating points at which one can reasonably assume correct previous decisions, the effect of the bias is typically small [21].

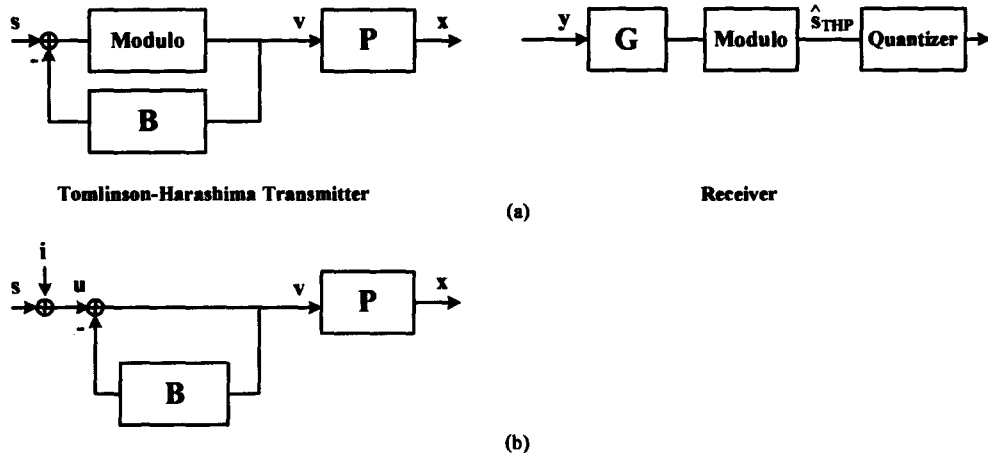


Figure 2.2: (a) MIMO transceiver with Tomlinson-Harashima precoding (b) Equivalent linear transmitter model for Tomlinson-Harashima precoding system

of the modulo operation is equivalent to the addition of $\mathbf{i}_k = \mathbf{i}_k^{re} D + j \mathbf{i}_k^{imag} D$ to \mathbf{s}_k , where $\mathbf{i}_k^{re}, \mathbf{i}_k^{imag} \in \mathbb{Z}$. Using this observation, we obtain the linearized model of the transmitter shown in Fig. 2.2(b), e.g., [10], in which

$$\mathbf{v} = (\mathbf{I} + \mathbf{B})^{-1} \mathbf{u} = \mathbf{C}^{-1} \mathbf{u}, \quad (2.5)$$

where $\mathbf{u} = \mathbf{i} + \mathbf{s}$ is the modified data symbol and $\mathbf{C} = \mathbf{I} + \mathbf{B}$. As a result of the modulo operation, the elements of \mathbf{v} are almost uncorrelated and uniformly distributed over the Voronoi region \mathcal{V} [10, Th. 3.1], [16, Fig. 3]. Therefore, the symbols of \mathbf{v} will have slightly higher average energy than the input symbols \mathbf{s} . This slight increase in the average energy is termed precoding loss [10]. For example, for square M -ary QAM we have $\sigma_v^2 = E\{|\mathbf{v}_k|^2\} = \frac{M}{M-1} E\{|\mathbf{s}_k|^2\}$ for all k except the first one [10, Sec. 3.2.6]. For moderate to large values of M this power increase can be neglected and the approximation $E\{\mathbf{v}\mathbf{v}^H\} = \mathbf{I}$ is often used; e.g., [16], [13]. We will assume negligible precoding loss, and hence the average transmitted power constraint can be written as $E_{\mathbf{v}}\{\mathbf{x}^H \mathbf{x}\} = \text{tr}(\mathbf{P}^H \mathbf{P}) \leq P_{\text{total}}$.

The vector of received signals in a THP system can be written as

$$\mathbf{y} = \mathbf{HPC}^{-1}\mathbf{u} + \mathbf{n}, \quad (2.6)$$

where \mathbf{n} is the vector of additive noise which is assumed to have zero-mean and a covariance matrix $E\{\mathbf{nn}^H\} = \mathbf{R}_n$. At the receiver, the feedforward processing matrix \mathbf{G} is used to obtain an estimate $\hat{\mathbf{u}} = \mathbf{GHPC}^{-1}\mathbf{u} + \mathbf{Gn}$ of the modified data symbols \mathbf{u} . Following this linear receive processing step, the modulo operation is used to obtain $\hat{\mathbf{s}}_{\text{THP}}$ by eliminating the effect of the periodic extension of the constellation caused by the integer vector \mathbf{i} . In terms of the modified data symbols, the error signal

$$\mathbf{e} = \hat{\mathbf{u}} - \mathbf{u} = \mathbf{GHPv} + \mathbf{Gn} - \mathbf{Cv} \quad (2.7)$$

can be used to define a Mean Square Error matrix

$$\mathbf{E} = E_{\mathbf{v}}\{\mathbf{ee}^H\} = \mathbf{CC}^H - \mathbf{CP}^H\mathbf{H}^H\mathbf{G}^H - \mathbf{GHPC}^H + \mathbf{GHPP}^H\mathbf{H}^H\mathbf{G}^H + \mathbf{GR}_n\mathbf{G}^H. \quad (2.8)$$

Assuming negligible precoding loss and that the vector \mathbf{i} is eliminated by the receiver modulo operation (which occurs with high probability, even at reasonably low SNRs), the error signal in (2.7) is equivalent to $\hat{\mathbf{s}}_{\text{THP}} - \mathbf{s}$. Hence, the mean square error matrix, \mathbf{E} , of the estimate $\hat{\mathbf{s}}_{\text{THP}}$ of the THP model is the same as that of the estimate $\hat{\mathbf{s}}_{\text{DFE}}$ of the DFE model under the assumption of correct previous decisions in the DFE.

2.2.3 General Model

From (2.4) and (2.8), we observe that the MSE matrix of both systems can be rewritten as:

$$\mathbf{E} = \mathbf{CC}^H - \mathbf{CP}^H\mathbf{H}^H\mathbf{G}^H - \mathbf{GHPC}^H + \mathbf{GR}_y\mathbf{G}^H, \quad (2.9)$$

where $\mathbf{R}_y = \mathbf{HPP}^H\mathbf{H}^H + \mathbf{R}_n$. It can also be observed that linear transceivers are a special subclass of both system models with the feedback matrix $\mathbf{B} = \mathbf{0}$ (or, equivalently, $\mathbf{C} = \mathbf{I}$); see Figs 2.1 and 2.2. Our objective is to jointly design the matrices

\mathbf{G} , \mathbf{C} and \mathbf{P} according to criteria that are functions of \mathbf{E} , subject to a constraint on the average transmitted power.

2.3 Optimal feedforward and feedback matrices

We will consider the joint design of the transceiver matrices \mathbf{G} , \mathbf{C} and \mathbf{P} so as to optimize system design criteria that are expressed as (increasing) functions of the (logarithm of the) MSE of each individual data stream, \mathbf{E}_{ii} , subject to the transmitted power constraint $\text{tr}(\mathbf{P}^H\mathbf{P}) \leq P_{\text{total}}$. We will adopt a three-step design approach. First, an expression for the optimal feedforward matrix \mathbf{G} will be found as a function of \mathbf{C} and \mathbf{P} . Second, using the expression for the optimal \mathbf{G} , an expression for the optimal \mathbf{C} will be found as a function of \mathbf{P} . Finally, using the obtained expressions for the optimal \mathbf{G} and \mathbf{C} , we will design the optimal precoder \mathbf{P} .

2.3.1 Optimal feedforward matrix \mathbf{G}

For given \mathbf{C} and \mathbf{P} , the MSE of the i^{th} data stream, \mathbf{E}_{ii} , is a convex quadratic function of the i^{th} row of \mathbf{G} , and is independent of other rows. Therefore, the rows of \mathbf{G} can be independently optimized to minimize the individual MSEs, and the resulting \mathbf{G} is optimal for any transceiver objective that is an increasing function of the individual MSEs. (A similar property was observed in [6] for linear transceivers.) Since \mathbf{G} is unconstrained and the MSE of the i^{th} data stream is a smooth convex function of the i^{th} row of \mathbf{G} , we can obtain an expression for optimal \mathbf{G} by setting the gradient of \mathbf{E}_{ii} with respect to the i^{th} row of \mathbf{G} to zero. Hence, the optimal \mathbf{G} can be written as (e.g., [7]):

$$\mathbf{G} = \mathbf{C}\mathbf{P}^H\mathbf{H}^H\mathbf{R}_y^{-1}. \quad (2.10)$$

Using this expression, the MSE matrix for a system with the optimal \mathbf{G}

$$\mathbf{E} = \mathbf{C}(\mathbf{I} + \mathbf{P}^H \mathbf{H}^H \mathbf{R}_n^{-1} \mathbf{H} \mathbf{P})^{-1} \mathbf{C}^H = \mathbf{C} \mathbf{M} \mathbf{C}^H, \quad (2.11)$$

where the matrix inversion lemma has been used, and $\mathbf{M} = (\mathbf{I} + \mathbf{P}^H \mathbf{H}^H \mathbf{R}_n^{-1} \mathbf{H} \mathbf{P})^{-1}$.

2.3.2 Optimal feedback matrix \mathbf{B}

From (2.11) we observe that the MSE of each data stream, \mathbf{E}_{ii} , is a convex quadratic function of the i^{th} row of $\mathbf{C} = \mathbf{I} + \mathbf{B}$ and is independent of the other rows. Using a similar argument to that for \mathbf{G} above, the matrix \mathbf{C} whose rows independently minimize the individual MSEs is optimal for the transceiver objectives that we will consider. However, \mathbf{C} is constrained to be a unit diagonal lower triangular matrix and these constraints must be incorporated in the design. To do so, we observe that the matrix \mathbf{C} that minimizes the individual MSEs can be obtained by minimizing any convex combination of \mathbf{E}_{ii} . By choosing that convex combination to be the sum, our goal reduces to minimizing $\text{tr}(\mathbf{C} \mathbf{M} \mathbf{C}^H)$ subject to \mathbf{C} being unit diagonal lower triangular matrix. Using the Cholesky decomposition

$$\mathbf{M} = \mathbf{L} \mathbf{L}^H, \quad (2.12)$$

where \mathbf{L} is a lower triangular matrix with positive real diagonal elements, we can rewrite the objective as $\text{tr}(\mathbf{C} \mathbf{M} \mathbf{C}^H) = \|\mathbf{C} \mathbf{L}\|_F^2$, where the product $\mathbf{C} \mathbf{L}$ is a positive definite lower triangular matrix [22]. Let $\lambda_1(\mathbf{C} \mathbf{L}) \geq \dots \geq \lambda_K(\mathbf{C} \mathbf{L})$ and $\sigma_1(\mathbf{C} \mathbf{L}) \geq \dots \geq \sigma_K(\mathbf{C} \mathbf{L})$ denote the ordered eigenvalues and singular values, respectively, of the matrix $\mathbf{C} \mathbf{L}$. Then the unit diagonal lower triangular \mathbf{C} that minimizes $\text{tr}(\mathbf{C} \mathbf{M} \mathbf{C}^H)$

can be obtained using the following lower bound,

$$\|\mathbf{CL}\|_F^2 = \sum_{i=1}^K \sigma_i^2(\mathbf{CL}) \geq \sum_{i=1}^K \lambda_i^2(\mathbf{CL}) \quad (2.13)$$

$$= \sum_{i=1}^K [\mathbf{CL}]_{ii}^2 = \sum_{i=1}^K \mathbf{L}_{ii}^2, \quad (2.14)$$

where the bound in (2.13) is obtained by applying Weyl's inequality [23], and (2.14) follows from the fact that \mathbf{CL} is lower triangular and \mathbf{C} is unit diagonal. The expression on the right hand side of (2.14) is a lower bound on $\|\mathbf{CL}\|_F^2$ that is independent of \mathbf{C} . Furthermore, the inequality in (2.13) is satisfied with equality when the matrix is normal [23]. Since our matrix \mathbf{CL} is a triangular matrix, it can only be normal if it is diagonal [22, pp 103]. Therefore, the matrix \mathbf{C} that attains the lower bound in (2.14), and hence is optimal, is

$$\mathbf{C} = \text{Diag}(\mathbf{L}_{11}, \dots, \mathbf{L}_{KK}) \mathbf{L}^{-1}. \quad (2.15)$$

Using this optimal \mathbf{C} , the MSE matrix can be rewritten as

$$\mathbf{E} = \text{Diag}(\mathbf{L}_{11}^2, \dots, \mathbf{L}_{KK}^2). \quad (2.16)$$

We observe that for any given precoding matrix \mathbf{P} , the optimal feedforward and feedback matrices will yield a diagonal MSE matrix, with the individual MSEs being $\mathbf{E}_{ii} = \mathbf{L}_{ii}^2$.

2.3.3 Optimality in the sense of maximizing individual SINRs

For any given channel and precoder, the minimum MSE design of the matrices \mathbf{G} and \mathbf{B} for a DFE system, is also optimal in sense of maximizing the signal-to-interference-plus-noise (SINR) of each stream [24–26]. Using this optimal minimum MSE design of

the feedforward and feedback matrices, the SINR of the i^{th} stream is given by [24, 27]

$$\text{SINR}_i = (1/\mathbf{E}_{ii}) - 1. \quad (2.17)$$

Under the assumptions stated in Section 2.2, the estimate vector $\hat{\mathbf{s}}_{\text{THP}}$ has the same covariance matrix as the vector $\hat{\mathbf{s}}_{\text{DFE}}$ at the input to the quantizer in the DFE system. Hence, the individual SINRs for both systems are the same for any given input covariance matrix, $\mathbf{E}\{\mathbf{ss}^H\}$, and noise covariance matrix, \mathbf{R}_n . An analogous relation between SINR_i and \mathbf{E}_{ii} holds under a zero-forcing constraint for both the DFE model (e.g., [27]), and the THP model under similar assumptions to those stated in Section 2.2; e.g., [16]. (Similar relations also hold in the multiuser case; e.g., [28].) Since linear precoding is a special subclass of both models when $\mathbf{B} = \mathbf{0}$, the same relation between SINR_i and \mathbf{E}_i holds for minimum MSE design of the receiver matrix \mathbf{G} ; e.g., [6]. Using the expression for the individually minimized MSEs in (2.16), the individually maximized SINR of each data stream is given by

$$\text{SINR}_i = (1/\mathbf{L}_{ii}^2) - 1. \quad (2.18)$$

2.4 Design of the Precoding matrix: Preliminaries

Given the expressions for the optimal \mathbf{G} and \mathbf{C} , the remaining step is to design a precoding matrix \mathbf{P} to optimize design criteria that are expressed as functions of the individual MSE of each stream, \mathbf{L}_{ii}^2 . We will first derive two inequalities involving \mathbf{L}_{ii} that will enable us to characterize the optimal precoder. These inequalities will depend on the concepts of multiplicative and additive majorization [29].

2.4.1 A Multiplicative Majorization Inequality

The first inequality is derived using the concept of multiplicative majorization [23, 26, 29].

Definition 2.1 (Multiplicative Majorization). *For a vector $\mathbf{a} \in \mathbb{R}^K$, let $a_{[1]}, \dots, a_{[K]}$ denote the re-ordering of the elements of \mathbf{a} in a non-increasing order; i.e., $a_{[1]} \geq \dots \geq a_{[K]}$. Let \mathbb{R}_+ denote the set of positive real numbers, and let $\mathbf{a}, \mathbf{b} \in \mathbb{R}_+^K$. The vector \mathbf{b} is said to multiplicatively majorize \mathbf{a} , $\mathbf{a} \prec_{\times} \mathbf{b}$, if*

$$\prod_{i=1}^j \mathbf{a}_{[i]} \leq \prod_{i=1}^j \mathbf{b}_{[i]} \quad \text{for } j = 1, \dots, K-1, \quad (2.19)$$

$$\prod_{i=1}^K \mathbf{a}_{[i]} = \prod_{i=1}^K \mathbf{b}_{[i]}. \quad (2.20)$$

An important example of the multiplicative majorization is the relation between the eigenvalues and singular values of a square matrix, and is given by the following lemma.

Lemma 2.1 (Weyl [23]). *Let $\mathbf{A} \in \mathbb{C}^{K \times K}$ and let $\lambda_i(\mathbf{A})$ and $\sigma_i(\mathbf{A})$ denote the eigenvalues and singular values of \mathbf{A} , respectively. Then we have $[|\lambda_1(\mathbf{A})|^2, \dots, |\lambda_K(\mathbf{A})|^2] \prec_{\times} [\sigma_1^2(\mathbf{A}), \dots, \sigma_K^2(\mathbf{A})]$. If \mathbf{A} is normal, then $|\lambda_i(\mathbf{A})| = \sigma_i(\mathbf{A})$. \square*

Applying the above lemma to the positive definite lower triangular matrix \mathbf{L} , we obtain

$$[\mathbf{L}_{11}^2, \dots, \mathbf{L}_{KK}^2] \prec_{\times} [\sigma_1^2(\mathbf{L}), \dots, \sigma_K^2(\mathbf{L})]. \quad (2.21)$$

2.4.2 An Additive Majorization Inequality

The second inequality involves the more common notation of additive majorization [29].

Definition 2.2 (Additive Majorization). *Let $\mathbf{a}, \mathbf{b} \in \mathbb{R}^K$. The vector \mathbf{b} is said to majorize \mathbf{a} , $\mathbf{a} \prec \mathbf{b}$, if*

$$\sum_{i=1}^j \mathbf{a}_{[i]} \leq \sum_{i=1}^j \mathbf{b}_{[i]} \quad \text{for } j = 1, \dots, K-1, \quad (2.22)$$

$$\sum_{i=1}^K \mathbf{a}_{[i]} = \sum_{i=1}^K \mathbf{b}_{[i]}. \quad (2.23)$$

□

We observe that if elements of \mathbf{a} and \mathbf{b} are positive, then $\mathbf{a} \prec_{\times} \mathbf{b} \Leftrightarrow \log(\mathbf{a}) \prec \log(\mathbf{b})$. Consequently, (2.21) can be written as:

$$\mathbf{l} \prec \mathbf{m}, \quad (2.24)$$

where $\mathbf{l} = [\log \mathbf{L}_{11}^2, \dots, \log \mathbf{L}_{KK}^2]$ and $\mathbf{m} = [\log \sigma_1^2(\mathbf{L}), \dots, \log \sigma_K^2(\mathbf{L})]$.

To derive the second inequality, we will use the following consequence of additive majorization: Any vector $\mathbf{a} \in \mathbb{R}^K$ majorizes its mean vector $\bar{\mathbf{a}}$, whose elements are all equal to the mean; i.e., $\bar{\mathbf{a}}_i = \frac{1}{K} \sum_{i=1}^K \mathbf{a}_i$. That is, $\bar{\mathbf{a}} \prec \mathbf{a}$. Now, since $\mathbf{M} = \mathbf{L}\mathbf{L}^H$, we know that $\prod_{i=1}^K \mathbf{L}_{ii}^2 = \det(\mathbf{L}\mathbf{L}^H) = \det(\mathbf{M})$. As a result, we have $\sum_{i=1}^K l_i = \log \det(\mathbf{M})$ and hence

$$\bar{\mathbf{l}} \prec \mathbf{l}, \quad (2.25)$$

where $\bar{l}_i = \frac{1}{K} \log \det(\mathbf{M})$.

2.4.3 Schur-convex and Schur-concave functions

The proposed designs will be based on the following classes of functions [29].

Definition 2.3 (Schur-convex and Schur-concave functions). *A real-valued function $f(\mathbf{x})$ defined on a subset \mathcal{A} of \mathbb{R}^K is said to be Schur-convex if $\mathbf{a} \prec \mathbf{b}$ on $\mathcal{A} \Rightarrow f(\mathbf{a}) \leq f(\mathbf{b})$, and is said to be Schur-concave if $\mathbf{a} \prec \mathbf{b}$ on $\mathcal{A} \Rightarrow f(\mathbf{a}) \geq f(\mathbf{b})$. □*

In particular, we will consider communication objectives that can be expressed as the minimization of increasing functions of the MSEs of each data stream, $g(\mathbf{L}_{11}^2, \dots, \mathbf{L}_{KK}^2) = g(e^{l_1}, \dots, e^{l_K}) = g(e^{\mathbf{l}})$, that are either Schur-convex or Schur-concave functions of \mathbf{l} .

2.5 Optimal Precoding Matrix: Schur-convex objectives

In this section, we will present a closed-form expression for the optimal precoding matrix \mathbf{P} for the class of Schur-convex objectives. We will also study the properties of the optimal solution and compare it to optimal linear transceiver designs. Finally, we will present examples of design objectives $g(e^{\mathbf{l}})$ that are Schur-convex functions of \mathbf{l} .

2.5.1 Optimal Precoding Matrix

If $g(e^{\mathbf{l}})$ is a Schur-convex function of \mathbf{l} , then from (2.25) we have that $g(e^{\bar{\mathbf{l}}}) \leq g(e^{\mathbf{l}})$, and that equality is obtained if the elements of \mathbf{l} are equal. Our approach to finding the optimal precoder is to characterize the family of precoders that minimize the lower bound $g(e^{\bar{\mathbf{l}}})$ subject to the power constraint, and then to show that within this family there is a precoder that results in all of the elements of \mathbf{l} being equal, and hence attains the minimized lower bound.

Since the objective is an increasing function of the individual MSEs, and since $\bar{l}_i = \frac{1}{K} \log \det(\mathbf{M})$, where \mathbf{M} was defined following (2.11), the problem of minimizing

the lower bound subject to the power constraint can be formulated as:

$$\max_{\mathbf{P}} \log \det(\mathbf{I} + \mathbf{P}^H \mathbf{H}^H \mathbf{R}_n^{-1} \mathbf{H} \mathbf{P}) \quad (2.26a)$$

$$\text{subject to } \text{tr}(\mathbf{P}^H \mathbf{P}) \leq P_{\text{total}}. \quad (2.26b)$$

This formulation is equivalent to maximizing the Gaussian mutual information, and hence the family of optimal precoders is obtained using a standard water-filling algorithm [30]. To state this family, we use the eigenvalue decomposition

$$\mathbf{R}_{\mathbf{H}} = \mathbf{H}^H \mathbf{R}_n^{-1} \mathbf{H} = \mathbf{U}_{\mathbf{H}} \mathbf{\Lambda}_{\mathbf{H}} \mathbf{U}_{\mathbf{H}}^H, \quad (2.27)$$

where $\mathbf{\Lambda}_{\mathbf{H}} = \text{Diag}(\lambda_{\mathbf{H},1}, \dots)$, and $\lambda_{\mathbf{H},i}$ are eigenvalues of $\mathbf{R}_{\mathbf{H}}$ in descending order. In the water-filling algorithm, power is allocated to K_{wf} eigenvalues of $\mathbf{R}_{\mathbf{H}}$, where K_{wf} is the maximum integer j satisfying $(P_{\text{total}} + \sum_{i=1}^j \lambda_{\mathbf{H},i}^{-1}) \geq j/\lambda_{\mathbf{H},j}$, [30]. If we define $\hat{K} = \min(K_{\text{wf}}, K)$, the family of optimal precoders can be written as

$$\mathbf{P} = \mathbf{U}_{\mathbf{H},1} \hat{\Phi} \mathbf{V} = \mathbf{U}_{\mathbf{H},1} [\hat{\Phi} \quad \mathbf{0}] \mathbf{V}, \quad (2.28)$$

where $\mathbf{U}_{\mathbf{H},1} \in \mathbb{C}^{N_t \times \hat{K}}$ contains the eigenvectors of $\mathbf{R}_{\mathbf{H}}$ corresponding to the largest \hat{K} eigenvalues, $\mathbf{V} \in \mathbb{C}^{K \times K}$ is a unitary matrix degree of freedom, and the diagonal matrix $\hat{\Phi}$ is

$$\hat{\Phi}_{ii} = \mu - 1/\lambda_{\mathbf{H},i}, \quad (2.29)$$

where the “water” level μ is given by $\frac{1}{\hat{K}}(P + \sum_{i=1}^{\hat{K}} \lambda_{\mathbf{H},i}^{-1})$.

To complete the design of \mathbf{P} , we need to select the unitary matrix \mathbf{V} in (2.28) so that the minimized lower bound is attained; i.e., so that the Cholesky decomposition of $\mathbf{M} = \mathbf{L}\mathbf{L}^H$ yields an \mathbf{L} factor with equal diagonal elements. Using (2.28),

$$\begin{aligned} \mathbf{M} &= \left(\mathbf{V}^H (\mathbf{I} + \hat{\Phi}^T \mathbf{\Lambda}_{\mathbf{H},1} \hat{\Phi})^{-1/2} \right) \left((\mathbf{I} + \hat{\Phi}^T \mathbf{\Lambda}_{\mathbf{H},1} \hat{\Phi})^{-1/2} \mathbf{V} \right) \\ &= \mathbf{L}\mathbf{L}^H = \mathbf{R}^H \mathbf{R} = (\mathbf{Q}\mathbf{R})^H (\mathbf{Q}\mathbf{R}), \end{aligned} \quad (2.30)$$

where $\mathbf{\Lambda}_{\mathbf{H},1}$ is the diagonal matrix containing the largest \hat{K} eigenvalues of $\mathbf{R}_{\mathbf{H}}$, and \mathbf{Q} is a matrix with orthonormal columns. Hence, finding \mathbf{V} is equivalent to finding a \mathbf{V} such that QR decomposition of $(\mathbf{I} + \hat{\mathbf{\Phi}}^T \mathbf{\Lambda}_{\mathbf{H},1} \hat{\mathbf{\Phi}})^{-1/2} \mathbf{V}$ has an R-factor with equal diagonal. This problem was solved in [14] and \mathbf{V} can be obtained by applying the algorithm in [14] to the matrix $(\mathbf{I} + \hat{\mathbf{\Phi}}^T \mathbf{\Lambda}_{\mathbf{H},1} \hat{\mathbf{\Phi}})^{-1/2}$; see also [7, 31, 32].

2.5.2 Properties of the optimal design

In this section we describe some interesting properties of the optimal transceiver design for Schur-convex objectives.

2.5.2.1 Independence of the optimal transceiver design on the design objective $g(e^l)$

We observe that the above derivation of the optimal precoder design is independent of the actual design objective, $g(e^l)$. (A similar property holds for linear transceiver design, but with objectives that are Schur-convex functions of the individual MSEs themselves.) Therefore, the desirable properties of the DFE transceiver that minimizes the total MSE generalize to other Schur-convex objectives for both DFE and THP models. For example, the DFE transceiver that minimizes the total MSE has asymptotically the same symbol error rate as the transceiver that employs the optimal precoder with maximum likelihood detection [32]. This property is now applicable to all DFE and THP transceivers with Schur-convex objectives.

2.5.2.2 For any Schur-convex objective $g(e^l)$, the optimal transceiver is information lossless

Since maximizing the Gaussian mutual information is a Schur-convex objective, it follows that the optimal design for any Schur-convex objective is information lossless, in the sense that optimizing the chosen objective does not incur any reduction of the Gaussian mutual information. In addition to being information lossless, the properties of the matrix \mathbf{V} in Section 2.5.1 mean that the optimal Schur convex design results in a uniform decomposition of the mutual information [32]. As a result, the SINR on each subchannel is the same. This result generalizes the information lossless property of MMSE-DFE receivers (e.g., [11, 25]), and that of minimum MSE DFE-based transceivers [7], to designs for DFE and THP transceivers with an arbitrary Schur-convex objective, $g(e^l)$. This property does not hold in general for the linear transceiver designs because the precoder that maximizes the Gaussian mutual information does not necessarily optimize other criteria.

2.5.2.3 Relation to linear transceiver designs

Using the majorization results in (2.24) and (2.25), we can show the following interesting result for any Schur-convex objective $g(e^l)$.

Proposition 2.1. *For design criteria with a Schur-convex objective $g(e^l)$, the optimal THP or DFE design yields a lower bound on the objective value obtained by any linear transceiver.* □

Proof. For any linear transceiver, $\mathbf{C} = \mathbf{I}$. It follows from (2.15) that \mathbf{L} is diagonal and hence $\mathbf{L}_{ii}^2 = \sigma_i^2(\mathbf{L})$, or equivalently $\mathbf{l} = \mathbf{m}$. Since the optimal THP or DFE transceiver corresponds to $\mathbf{l} = \bar{\mathbf{l}}$ and we have $\bar{\mathbf{l}} \prec \mathbf{m}$, it follows that $g(\bar{\mathbf{l}}) \leq g(\mathbf{m})$, for any Schur-convex objective $g(\cdot)$. □

This result shows that the optimal DFE or THP transceiver for any Schur-convex objective $g(e^{\mathbf{l}})$ will yield an objective value that is less than or equal to the objective value achieved by the optimal linear transceiver for the same objective. Furthermore, a stronger results can be obtained by considering the subclass of strictly Schur-convex objectives. For this class of objectives, $f(\mathbf{a}) < f(\mathbf{b})$, whenever $\mathbf{a} \prec \mathbf{b}$ and \mathbf{a} is not a permutation of \mathbf{b} . Since the optimal transceiver corresponds to $\mathbf{l} = \bar{\mathbf{l}}$, and any linear transceiver corresponds to $\mathbf{l} = \mathbf{m}$, it follows from $\bar{\mathbf{l}} \prec \mathbf{m}$ that $g(e^{\bar{\mathbf{l}}}) < g(e^{\mathbf{m}})$, for every strictly Schur-convex function $g(\cdot)$ whenever \mathbf{m} is not equal to a permutation of $\bar{\mathbf{l}}$. Since all elements of $\bar{\mathbf{l}}$ are equal, it follows that $g(e^{\bar{\mathbf{l}}}) < g(e^{\mathbf{m}})$ whenever $\bar{\mathbf{l}} \neq \mathbf{m}$. The case $\bar{\mathbf{l}} = \mathbf{m}$ corresponds to the optimal design of \mathbf{L} being a diagonal matrix with equal diagonal elements; i.e., a scaled identity matrix. This case can arise from water-filling over $K \leq K_{\text{wf}}$ equal eigenvalues of the matrix $\mathbf{R}_{\mathbf{H}}$.

2.5.3 Examples of Schur-convex objectives

In this section we present examples of design objectives that are Schur-convex functions of \mathbf{l} , the vector of logarithms of the individual MSEs. (Sketches of the proofs are provided in Appendix A.) Before we do so, we point out that by using the composition properties of Schur-convex functions [29] one can prove the following result.

Lemma 2.2. *Let $\mathbf{y} = e^{\mathbf{l}}$. If $g(\mathbf{y})$ is Schur-convex in \mathbf{y} , then $g(e^{\mathbf{l}})$ is Schur-convex in \mathbf{l} .*

Using this lemma and the results in [6], functions such as the total MSE and the average BER can be shown to be to Schur-convex functions of \mathbf{l} . However, by analyzing $g(e^{\mathbf{l}})$ directly, we will obtain stronger results. For example, we will show that the total MSE is *strictly* Schur-convex in \mathbf{l} . (It is not strictly Schur-convex in the MSEs themselves.) We will also show that the average BER of certain constellations,

including 16-QAM, is a Schur-convex function of \mathbf{l} for the entire range of the MSE, whereas it is a Schur-convex function of the MSEs only for limited ranges of the MSE [6]. In addition, by taking the direct approach we will be able to show that several objectives that are not Schur-convex functions of the MSEs are Schur-convex functions of the logarithm of the MSEs; e.g., the Gaussian mutual information and the geometric mean of the SINRs.

2.5.3.1 Minimization of the total MSE

Minimization of total MSE (or the arithmetic mean of the MSEs) corresponds to minimization of

$$g(\mathbf{e}^l) = \sum_{i=1}^K e^{l_i}, \quad (2.31)$$

which is a strictly Schur-convex function of \mathbf{l} . Hence, the optimal precoder is given by the closed-form expression derived in Section 2.5.1. For the DFE model, transceiver design based on minimization of the total MSE was considered in [7], and the solution therein is, as expected, the same as that in Section 2.5.1. For the THP model, a design approach based on a bound on the total MSE was presented in [13], but that approach does not necessarily minimize the total MSE. Furthermore, the THP designs in [10, 16] do not exploit all the available degrees of design freedom. Using the approach presented in this section, we obtain a jointly optimal design for THP model for the total MSE objective.

2.5.3.2 Minimization of product of MSEs and maximization of Gaussian mutual information

Given the diagonal structure of the matrix \mathbf{E} in (2.16), minimization of the product of the MSEs (or the geometric mean of the MSEs) is equivalent to minimization of the determinant of \mathbf{E} . Furthermore, maximization of the Gaussian mutual information is

equivalent to minimization of $\log \det(\mathbf{E})$, [11]. Therefore, these three objectives are equivalent and correspond to minimization of

$$g(e^{\mathbf{l}}) = \log \prod_{i=1}^K e^{l_i} = \sum_{i=1}^K l_i. \quad (2.32)$$

In Appendix A, we show that $g(e^{\mathbf{l}})$ is both a Schur-convex and a Schur-concave function of \mathbf{l} . Hence, the optimal design in (2.28) is information lossless for both the DFE and THP models. (This is consistent with the MMSE-DFE being a ‘canonical receiver’ [11], and examples of existing designs that apply these criteria to DFE-based transceivers appear in [7, 11, 12].) Since the expression in (2.32) is also Schur-concave, a design that maximizes the Gaussian mutual information can also be obtained using the Schur-concave approach in Section 2.6, below. That approach results in a linear transceiver with a standard water-filling power allocation [30]. (Of course, both approaches yield the same maximized Gaussian mutual information.)

2.5.3.3 Minimization of maximum MSE (Maximization of minimum SINR)

Minimization of the maximum MSE corresponds to minimization of the following Schur-convex function of \mathbf{l}

$$g(e^{\mathbf{l}}) = \max_{1 \leq i \leq K} (e^{l_i}). \quad (2.33)$$

According to (2.17), the stream with the maximum MSE is the one with the minimum SINR. Hence, this objective is equivalent to maximization of the minimum SINR.

2.5.3.4 Minimization of p -norm of MSEs

In this case, the objective is to minimize

$$g(e^{\mathbf{l}}) = \left(\sum_{i=1}^K (e^{l_i})^p \right)^{1/p}, \quad p \geq 1. \quad (2.34)$$

This design criteria includes the minimization of total MSE, $p = 1$, and the minimization of the maximum MSE, $p = \infty$, among several other norms of the vector of MSEs of each data stream.

2.5.3.5 Maximization of the harmonic mean of SINRs

In this case, the objective is to minimize

$$g(e^l) = \sum_{i=1}^K \frac{1}{\text{SINR}_k} = \sum_{i=1}^K \frac{1}{e^{-l_i} - 1}, \quad l_i < 0. \quad (2.35)$$

2.5.3.6 Maximization of product of SINRs

Maximization of the product of the SINRs (or the geometric mean of the SINRs) can be expressed as the minimization of

$$g(e^l) = -\log \prod_{i=1}^K (e^{-l_i} - 1) = -\sum_{i=1}^K \log(e^{-l_i} - 1). \quad (2.36)$$

2.5.3.7 Minimization of average BER

Assuming that each each data stream employs the same constellation, the average BER is given by

$$g(e^l) = \frac{1}{K} \sum_{i=1}^K \text{BER}(\text{SINR}_i) = \frac{1}{K} \sum_{i=1}^K \text{BER}(e^{-l_i} - 1), \quad (2.37)$$

where $\text{BER}(\cdot)$ is the bit error rate of the chosen constellation as function of the SINR. For many constellations, such as M -ary QAM, the bit error rate function $\text{BER}(\text{SINR})$ can be closely approximated by [33, eq. 18], [34, eq. 13]:

$$\text{BER}(\text{SINR}) = c_2 Q(\sqrt{c_1 \text{SINR}}), \quad (2.38)$$

where c_1 and c_2 are constants that depend on the size of constellation M , and $Q(x) = \frac{1}{\sqrt{2\pi}} \int_x^\infty e^{-z^2/2} dz$. For BPSK and QPSK, we have $c_1 = c_2 = 1$ and the approximation

becomes exact. In Appendix A we show that the objective in (2.38) is a Schur-convex function of \mathbf{l} for BPSK and M -ary QAM up to $M = 16$, and that for higher-order QAM it is Schur-convex under the mild constraint that the SINR is above a small threshold. (The design of DFE-based systems with an average BER objective was considered in [7].)

2.6 Optimal Precoding Matrix: Schur-concave objectives

2.6.1 Optimal Precoding Matrix

If $g(e^{\mathbf{l}})$ is a Schur-concave function of \mathbf{l} , then from (2.24) we have $g(e^{\mathbf{m}}) \leq g(e^{\mathbf{l}})$, and the optimal value is obtained when

$$\mathbf{L}_{ii} = \sigma_i(\mathbf{L}). \quad (2.39)$$

According to Lemma 2.1, this equality holds when \mathbf{L} is normal matrix. Since \mathbf{L} is a lower triangular matrix, in order to be normal it must be a diagonal matrix [22]. The optimal \mathbf{C} in that case is \mathbf{I} , and hence the optimal feedback matrix is $\mathbf{B} = \mathbf{0}$. That is, in the case of Schur-concave functions of \mathbf{l} , the optimal DFE design results in linear equalization and optimal THP design results in linear precoding.

This result shows that for Schur-concave objectives the design problem reduces to that for the special subclass of linear transceivers; e.g., [5,6]. What remains is to compare the direct linear designs with those that we have derived from the optimization of DFE and THP transceivers with Schur-concave objectives of the logarithm of the individual MSEs, $g(e^{\mathbf{l}})$. Using the composition properties of Schur-concave functions [29] the following counterpart to Lemma 2.2 can be established.

Lemma 2.3. *Let $\mathbf{y} = e^{\mathbf{l}}$. If $g(e^{\mathbf{l}})$ is Schur-concave in \mathbf{l} , then $g(\mathbf{y})$ is Schur-concave in \mathbf{y} .*

A consequence of this result is that the optimal DFE or THP transceiver design for an objective that is Schur-concave in the logarithm of the individual MSEs is the optimal linear transceiver for the corresponding Schur-concave function of the individual MSEs themselves. As shown in [6], that optimal precoder will depend on the objective. This is in contrast to the Schur-convex designs, which are independent of the objective; see Section 2.5.

2.6.2 Examples of Schur-concave objectives

We now briefly present some examples of design objectives that are Schur-concave functions of \mathbf{l} . (Sketches of the proofs are provided in Appendix B.)

2.6.2.1 Minimization of harmonic mean of MSEs

This objective corresponds to the minimization of

$$g(e^{\mathbf{l}}) = \frac{1}{\sum_{i=1}^K e^{-l_i}}. \quad (2.40)$$

2.6.2.2 Maximization of p -norm of SINRs

In this case, the objective is to minimize

$$g(e^{\mathbf{l}}) = -\left(\sum_{i=1}^K (e^{-l_i} - 1)^p\right)^{1/p}, \quad p \geq 1. \quad (2.41)$$

2.6.2.3 Minimization of a subclass of weighted products of MSEs (weighted geometric mean of MSEs)

The minimization of the weighted product of MSEs is equivalent to minimization of

$$g(e^{\mathbf{l}}) = \log \prod_{i=1}^K (e^{l_i})^{a_i} = \sum_{i=1}^K a_i l_i, \quad (2.42)$$

where, without loss of generality, we may assume that the MSEs are arranged in a decreasing order; i.e. $l_1 \geq \dots \geq l_K$. For this ordering, $g(e^l)$ is Schur-concave whenever the weights are in ascending order.

2.7 Simulation Studies

In this section, we provide some simulation results for systems designed using the proposed framework. We consider systems that transmit vectors of 16-QAM symbols over an independent Rayleigh fading channel (with perfect channel state information at both the receiver and transmitter). The same constellation is used for each data stream because the optimal transceiver design for the class of Schur-convex objectives results in equal SINR on each data stream; cf. Section 2.5.2.2. The coefficients of the $N_r \times N_t$ channel matrix \mathbf{H} are modelled as being independent rotationally-symmetric complex Gaussian random variables with zero mean and unit variance, and the elements of the additive noise vector \mathbf{n} are modelled as being independent rotationally-symmetric complex Gaussian random variables with zero mean and equal variance. For each design we will plot the average bit error rate (BER) of the K data streams against the signal-to-noise ratio (SNR), which is defined as the ratio of the total average transmitted power, $E\{\mathbf{x}^H \mathbf{x}\}$, to the total receiver noise power, $E\{\mathbf{n}^H \mathbf{n}\}$.

2.7.1 Validation of the design assumptions

In this section, we validate the assumptions that we made in the development of the proposed designs. For DFE systems we made the standard assumption that the previously detected symbols were correctly detected, and for THP systems we made the assumption of no precoding loss; see Section 2.2. To validate these assumptions, we consider the case of systems optimized for Schur-convex objectives. These designs

minimize the total MSE, as well as minimizing the average BER and maximizing the Gaussian mutual information. In Fig. 2.3 we compare the actual performance of the proposed designs to the performance that would have been achieved if the assumptions held precisely, in the case of a system with $N_t = N_r = K = 4$. In Fig. 2.3 the practical performance of the proposed jointly optimal THP transceiver is very close to that of a system that assumes no precoding loss, and the impact of the standard assumption of correct decisions in a DFE system is quite mild, especially at high SNRs. Indeed, the four curves coalesce at high SNRs. The slight advantage of the THP transceiver in Fig. 2.3 over the DFE transceiver can be attributed to the fact that interference subtraction at the transmitter is, inherently, free from error propagation.

2.7.2 Comparisons with linear transceivers

In this section, we compare the performance of the proposed (jointly optimal) DFE and THP transceiver designs to that of (jointly-optimized) linear transceivers. We compare the performance of the optimal Schur-convex design for the DFE and THP transceivers, which simultaneously minimizes the total MSE, minimizes the average BER and maximizes the Gaussian mutual information, with that of the (different) optimal linear transceivers that: minimize the total MSE, e.g., [5]; minimize the average BER [6, 35]; and maximize the Gaussian mutual information, e.g., [6, 30]. For reference, we also provide performance comparisons with a transceiver that implements maximum likelihood (ML) detection at the receiver and employs the precoder in (2.28) at the transmitter. (That precoder is the optimal Schur-convex design for the DFE receiver.) We compare the performance of these five methods in an $N_t = N_r = K = 4$ scenario in Fig. 2.4. By comparing the curves for the DFE and THP transceivers with that of the minimum BER linear transceiver, one can quantify

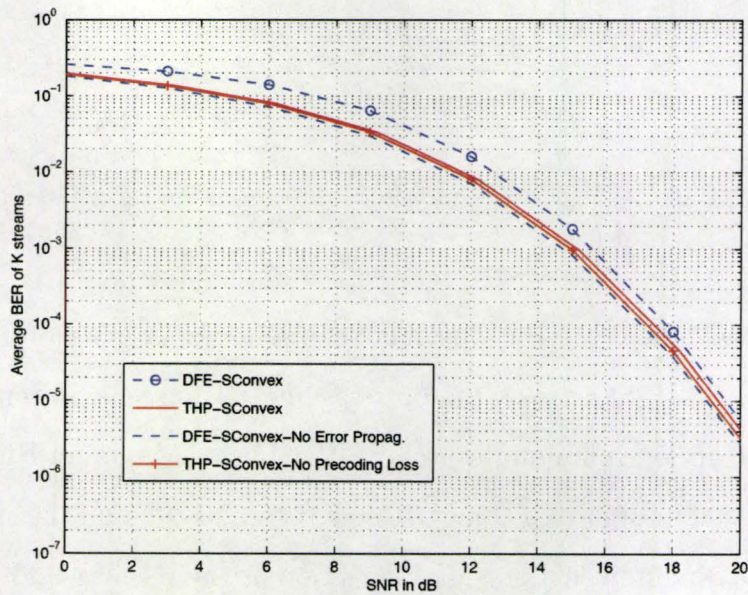


Figure 2.3: BERs of the optimal Schur-convex design of a DFE transceiver (DFE-SConvex), and a THP transceiver (THP-SConvex) for a system with $N_t = N_r = K = 4$. Also plotted is the BER of the optimal Schur-Convex DFE design in the absence of error propagation (DFE-SConvex-No Error Propag.), and the BER of the optimal Schur-Convex THP design with no precoding loss (THP-SConvex-No Precoding Loss).

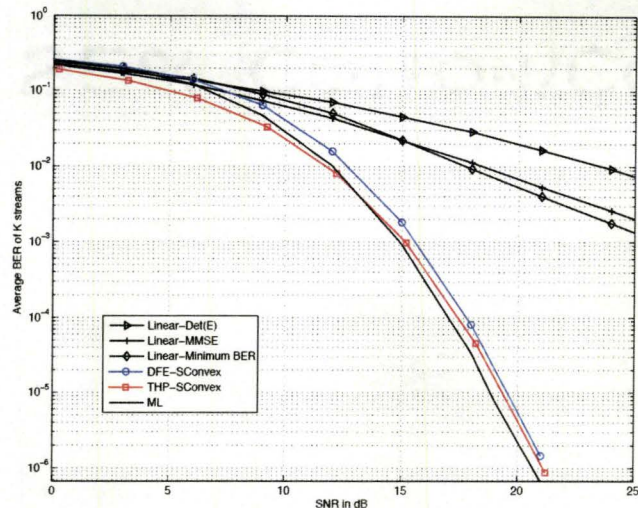


Figure 2.4: BERs of the optimal Schur-convex designs of DFE (DFE-SConvex) and THP (THP-SConvex), the optimal linear transceivers: minimum MSE (Linear-MMSE) e.g., [5], minimum average BER (Linear-Minimum BER) [6, 35], and maximum mutual information (Linear-Det(E)) e.g., [6, 30], and the transceiver that implements maximum likelihood (ML) detection at the receiver and employs the precoder in (2.28) at the transmitter, for a system with $N_t = N_r = K = 4$.

the statement in Proposition 1 that for Schur-convex design objectives, the DFE and THP transceivers provide provably better performance than the corresponding linear transceiver.

2.7.3 Comparisons with other designs for interference (pre)subtraction transceivers

In this section, we compare the performance of the proposed jointly optimal DFE and THP transceiver designs to that of some existing suboptimal designs for systems that

employ MMSE interference (pre-)subtraction. In particular, we will provide comparisons to systems with an identity precoder at the transmitter and an MMSE-DFE receiver with the ‘BLAST’ [36] detection ordering [10,37], or an unordered MMSE-DFE receiver. We will also provide comparisons with the performance of the MMSE-THP transceiver design in [10], with both BLAST ordering and the natural ordering, and for reference we will also provide performance comparisons with a transceiver that implements maximum likelihood (ML) detection at the receiver and employs the precoder in (2.28) at the transmitter. We compare the performance of these seven methods in an $N_t = N_r = K = 4$ scenario in Fig. 2.5, and in an $N_t = K = 4, N_r = 5$ scenario in Fig. 2.6. These comparisons are appropriate because the MMSE-DFE approach in [10,37] and the MMSE-THP design in [10] can be represented by special cases of our system model in which the precoder \mathbf{P} is restricted to be a permutation matrix. The significantly lower BERs of the proposed designs demonstrate that the exploitation of all the available degrees of design freedom in the proposed approach can have a substantial impact on performance. (In fact, the performance of the optimized DFE transceiver is close to that of the transceiver with ML detection and the optimized precoding matrix.) Moreover, the permutation-based approaches in [10,37] result in data streams with different MSEs (and SINRs), and hence different ordering algorithms are required for different performance objectives. For example, for error performance criteria the BLAST ordering [36] is appropriate, as it attempts to maximize the SINR of the weakest data stream, but maximizing the Gaussian mutual information requires a different ordering [38]. In contrast to these permutation-based approaches, the proposed approach exploits all the degrees of design freedom in the system and results in data streams with equal SINRs, and hence no ordering algorithm is necessary. It is worth pointing out that while precoding generalizes ordering for point-to-point DFE or THP models, in the corresponding multi-user models ordering

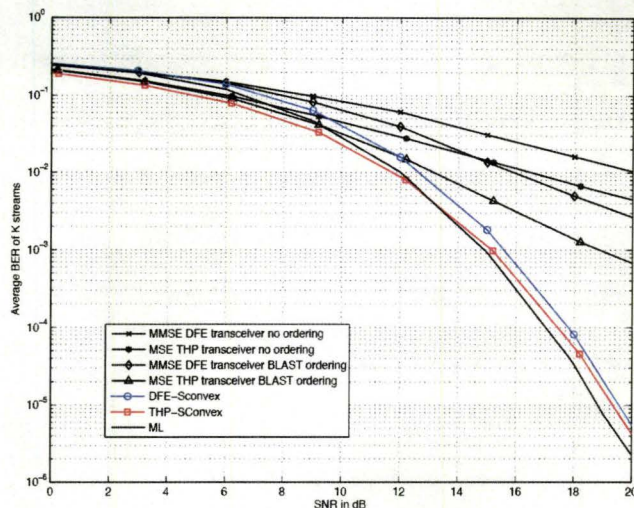


Figure 2.5: BERs of the optimal Schur-convex designs for DFE (DFE-SConvex) and THP (THP-SConvex) transceivers, other interference (pre-)subtraction approaches: MMSE DFE with BLAST ordering [10, 37], and MMSE DFE with no ordering, THP transceiver MMSE design in [10] with BLAST ordering and with no ordering, and the transceiver that implements maximum likelihood (ML) detection at the receiver and employs the precoder in (2.28) at the transmitter, for a system with $N_t = N_r = K = 4$.

must be considered in conjunction with precoder design because on the uplink the transmitters cannot cooperate, and on the downlink the receivers cannot cooperate; cf. [19].

2.8 Conclusion

In this chapter, a unified framework was developed for joint transceiver design for interference (pre-)subtraction schemes for communication over generic point-to-point MIMO channels, and we have obtained optimal designs for two broad classes of

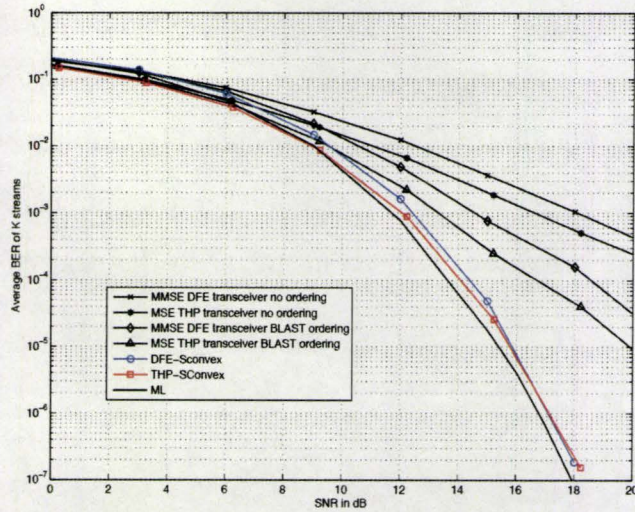


Figure 2.6: BERs of the optimal Schur-convex designs for DFE (DFE-SConvex) and THP (THP-SConvex) transceivers, other interference (pre-)subtraction approaches: MMSE DFE with BLAST ordering [10,37], and MMSE DFE with no ordering, THP transceiver MMSE design in [10] with BLAST ordering and with no ordering, and the transceiver that implements maximum likelihood (ML) detection at the receiver and employs the precoder in (2.28) at the transmitter, for a system with $N_t = K = 4$, $N_r = 5$.

communication objectives, namely those that are Schur-convex and Schur-concave functions of the logarithms of the (individual) MSEs of each data stream. For Schur-convex objectives, the optimal transceiver results in equal individual MSEs, and simultaneously minimizes the total MSE, minimizes the average bit error rate, and maximizes the Gaussian mutual information. Furthermore, that design yields objective values that are superior to the corresponding optimal objective value for a linear transceiver. For the class Schur-concave objectives, the optimal DFE design results in linear equalization and the optimal THP design results in linear precoding. The developed framework will be extended to communication scenarios with limited channel state information at the transmitter in the next chapter.

Chapter 3

Design Framework for Limited Feedback MIMO Systems with Zero-Forcing DFE

The previous chapter presented a unifying design framework for non-linear MIMO transceivers that implement interference (pre-)subtraction. The framework provided optimal transceiver designs for a wide range of design objectives. These designs were obtained for communication scenarios that assume perfect channel state information (CSI) at both the transmitter and the receiver. In this chapter, we will generalize that framework to scenarios with limited CSI at the transmitter. We will consider the design of multiple-input multiple-output communication systems with a linear precoder at the transmitter, zero-forcing decision feedback equalization (ZF-DFE) at the receiver, and a low-rate feedback channel that enables communication from the receiver to the transmitter. The channel state information available at the receiver is assumed to be perfect, and based on this information the receiver selects a suitable

precoder from a codebook and feeds back the index of this precoder to the transmitter. Our approach to the design of the components of this limited feedback scheme is based on the development, herein, of a unified framework for the joint design of the precoder and the ZF-DFE under the assumption that perfect CSI is available at both the transmitter and the receiver. The framework is the zero-forcing counterpart of the one developed in Chapter 2, and it enables us to characterize the statistical distribution of the optimal precoder in a standard Rayleigh fading environment. Using this distribution, it will be shown that codebooks constructed from Grassmann packings minimize an upper bound on an average distortion measure, and hence are natural candidates for the codebook in limited feedback systems. Our simulation studies show that the proposed limited feedback scheme can provide significantly better performance at a lower feedback rate than existing schemes in which the detection order is fed back to the transmitter.

3.1 Introduction

In many communication schemes, such as frequency division duplex systems, obtaining accurate CSI at the transmitter may require a considerable amount of feedback to the transmitter. An approach that allows the designer to limit the required amount of the feedback is to quantize the transmitter design. In these limited feedback schemes [39], the receiver uses its CSI to choose the best transmitter design from a codebook of available designs, and then feeds back the index of this precoder to the transmitter. This strategy has been considered for beamforming schemes (e.g., [40–46]), diagonal precoding [47], unitary precoding with linear equalization (e.g., [48]), and unitary precoding for orthogonal space time block codes [49, 50]. For zero-forcing DFE schemes, a limited feedback scheme in which the receiver feeds back

the order of interference cancellation was proposed in [51, 52].

In this chapter, we consider the design of a limited feedback scheme for systems with a (general) linear precoder at the transmitter and zero-forcing DFE at the receiver. Our designs are based on a unified framework, developed herein, for the joint design of the precoder and the ZF-DFE in the presence of perfect CSI. Similar to the framework that is obtained in absence of the zero-forcing criteria, it embraces a wide range of design criteria that can be expressed as Schur-convex or Schur-concave functions of the logarithm of the mean square error (MSE) of each data stream. In particular, it will be shown that the optimal precoder for the rich class of Schur-convex objectives is a scaled unitary matrix that is isotropically distributed (over the Stiefel manifold of unitary matrices). Using this distribution, it will be shown that codebooks constructed from Grassmann subspace packings minimize an upper bound on an average distortion measure, and hence are excellent candidates for the codebook in limited feedback schemes for systems with zero-forcing DFE. In contrast, the application of Grassmann codebooks in limited feedback schemes with linear receivers (e.g., [48]) involves an inherent compromise, because the optimal precoder in the presence of perfect CSI and a total power constraint is not unitary. Since the scheme that we propose involves the construction of codebooks for isotropically distributed unitary matrices, our scheme subsumes that in [51, 52], in which the precoder is, by construction, a permutation matrix. Our simulation studies suggest that the additional degrees of freedom available in our approach enable our scheme to provide significantly better performance than that in [51, 52] while using a lower feedback rate.

3.2 Zero-forcing DFE with Limited Feedback

We consider a point-to-point communication system with N_t transmit antennas and N_r receive antennas that transmits K data streams simultaneously, where K is no greater than the rank of the channel matrix \mathbf{H} . We adopt a narrow band block fading channel model, and we consider MIMO communications systems that use (generalized) zero-forcing decision feedback equalization, e.g., [7, 11], for spatial equalization. Similar to the DFE system model in Section 2.2.1, the input data vector at the transmitter, \mathbf{s} , is linearly precoded using \mathbf{P} to generate the transmitted data vector \mathbf{x} ,

$$\mathbf{x} = \mathbf{P}\mathbf{s}. \quad (3.1)$$

Without loss of generality, we will assume that $E\{\mathbf{s}\mathbf{s}^H\} = \mathbf{I}$, and hence the total transmitter power constraint can be written as $E\{\mathbf{x}^H\mathbf{x}\} = \text{tr}(\mathbf{P}^H\mathbf{P}) \leq P_{\text{total}}$.

The vector of received signals is given by

$$\mathbf{y} = \mathbf{H}\mathbf{P}\mathbf{s} + \mathbf{n}, \quad (3.2)$$

where \mathbf{H} is the channel matrix and \mathbf{n} is the vector of additive noise which is assumed to have zero-mean and a covariance matrix $E\{\mathbf{n}\mathbf{n}^H\} = \sigma_n^2\mathbf{I}$. As illustrated in Fig. 3.1, following linear processing using the feedforward matrix \mathbf{G} , the receiver makes successive decisions on each symbol by subtracting the effect of previously decided symbols. Hence, the feedback matrix \mathbf{B} is strictly lower triangular. This system model embraces linear precoding and equalization as a special case when $\mathbf{B} = \mathbf{0}$. Assuming correct previous decisions, the vector of inputs to the quantizer is given by

$$\hat{\mathbf{s}} = (\mathbf{G}\mathbf{H}\mathbf{P} - \mathbf{B})\mathbf{s} + \mathbf{G}\mathbf{n}. \quad (3.3)$$

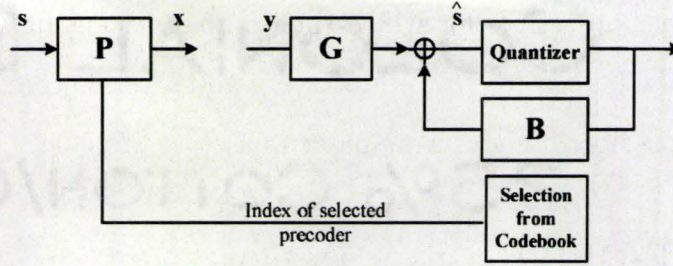


Figure 3.1: MIMO transceiver with DFE using limited feedback.

Using the error signal $\mathbf{e} = \mathbf{s} - \hat{\mathbf{s}}$, the mean square error matrix can be written as

$$\mathbf{E} = E\{\mathbf{e}\mathbf{e}^H\} = \mathbf{C}\mathbf{C}^H - \mathbf{C}\mathbf{P}^H\mathbf{H}^H\mathbf{G}^H - \mathbf{G}\mathbf{H}\mathbf{P}\mathbf{C}^H + \mathbf{G}\mathbf{H}\mathbf{P}\mathbf{P}^H\mathbf{H}^H\mathbf{G}^H + \sigma_n^2\mathbf{G}\mathbf{G}^H, \quad (3.4)$$

where $\mathbf{C} = \mathbf{I} + \mathbf{B}$ is a unit diagonal lower triangular matrix.

We will consider communication schemes in which perfect CSI is available only at the receiver. Based on its channel knowledge, the receiver selects a suitable precoding matrix from a codebook of precoders \mathcal{P} of size $|\mathcal{P}|$, and feeds that index back to the transmitter using $\log_2 |\mathcal{P}|$ information bits; see Fig 3.1. In order to develop effective methods for quantizing the precoding matrix, we first need to characterize the optimal precoding matrix for different design criteria in the presence of perfect CSI. We will then use the statistical distribution of this optimal precoder to define the distortion measures that are required to design the codebook for the limited feedback scheme.

3.3 Unified Framework for Zero-Forcing DFE

In this section, we develop a general framework for the joint design of the transceiver matrices \mathbf{G} , $\mathbf{C} = \mathbf{I} + \mathbf{B}$, and \mathbf{P} in the presence of perfect CSI and a zero-forcing criterion. The proposed framework embraces a wide range of design objectives that can be expressed as functions of the (logarithm of the) MSE of the individual data streams

\mathbf{E}_{ii} It includes objectives for which the optimal designs of ZF-DFE transceivers are already available (e.g., the total MSE, [7]), and several other objectives for which the optimal transceiver design has remained an open problem.

3.3.1 ZF-DFE Receiver Design

The zero-forcing design criterion implies

$$\mathbf{GHP} - \mathbf{B} = \mathbf{I}. \quad (3.5)$$

Given the assumption that $K \leq \text{rank}(\mathbf{H})$, the condition in (3.5) can be achieved so long as \mathbf{P} is chosen such that $\text{rank}(\mathbf{HP}) = K$. In that case, the feedforward matrix \mathbf{G} is given by

$$\mathbf{G} = \mathbf{C}(\mathbf{HP})^\dagger. \quad (3.6)$$

Since \mathbf{HP} has full column rank, the pseudo-inverse in (3.6) can be written as

$$(\mathbf{HP})^\dagger = (\mathbf{P}^H \mathbf{H}^H \mathbf{HP})^{-1} \mathbf{P}^H \mathbf{H}^H. \quad (3.7)$$

Using the expression for \mathbf{G} in (3.6), the MSE matrix in (3.4) reduces to

$$\mathbf{E} = \mathbf{CNC}^H, \quad (3.8)$$

where $\mathbf{N} = \sigma_n^2 (\mathbf{P}^H \mathbf{H}^H \mathbf{HP})^{-1}$ is a positive definite Hermitian matrix. Using the derivation in Section 2.3.2, the optimal matrix \mathbf{C} , that minimizes the MSE of each individual data stream, subject to being unit diagonal and lower triangular, is given by

$$\mathbf{C} = \text{Diag}(\mathbf{L}_{11}, \dots, \mathbf{L}_{KK}) \mathbf{L}^{-1}, \quad (3.9)$$

where $\mathbf{N} = \mathbf{LL}^H$ is the Cholesky factorization of \mathbf{N} , and \mathbf{L} is a lower triangular matrix with strictly positive diagonal entries. Using this optimal \mathbf{C} , the MSE matrix can be rewritten as

$$\mathbf{E} = \text{Diag}(\mathbf{L}_{11}^2, \dots, \mathbf{L}_{KK}^2), \quad (3.10)$$

where \mathbf{L}_{ii} is the i^{th} diagonal element of \mathbf{L} . Hence, the SNR of each data stream is

$$\text{SINR}_k = \frac{1}{\mathbf{E}_{kk}} = \frac{1}{\mathbf{L}_{kk}^2}. \quad (3.11)$$

3.3.2 Transmitter Design

Given the optimal \mathbf{G} and \mathbf{C} , our next step is to design a precoding matrix \mathbf{P} so as to optimize design criteria that are expressed as functions of the (logarithm of the) MSE of each individual stream,

$$\mathbf{l} = (\ln \mathbf{L}_{11}^2, \dots, \ln \mathbf{L}_{KK}^2). \quad (3.12)$$

The following lemma provides two main inequalities that include the logarithm of the MSEs, \mathbf{l} , and can be proved using similar arguments to those used in deriving the inequalities in (2.24) and (2.25).

Lemma 3.1. *For the Cholesky factorization $\mathbf{N} = \mathbf{L}\mathbf{L}^H$, the following inequalities hold:*

$$\frac{\ln \det(\mathbf{N})}{K} (1, \dots, 1) \prec \mathbf{l} \prec (\ln \lambda_1(\mathbf{N}), \dots, \ln \lambda_K(\mathbf{N})),$$

where $\lambda_k(\mathbf{N})$ is the k^{th} largest eigen value of \mathbf{N} . □

Let $\mathbf{H}^H\mathbf{H} = \mathbf{U}_H\mathbf{\Lambda}_H\mathbf{U}_H^H$ be the eigen value decomposition of $\mathbf{H}^H\mathbf{H}$ such that the entries of the diagonal matrix $\mathbf{\Lambda}_H$ are squared singular values of \mathbf{H} , $\sigma_k^2(\mathbf{H})$, in descending order. Let $\mathbf{U}_{H,1}$ and $\mathbf{\Lambda}_{H,1}$ be the first K columns of \mathbf{U}_H and $\mathbf{\Lambda}_H$, respectively. The optimal precoders for the two classes of Schur-convex and Schur-concave design criteria are given by the following theorem.

Theorem 3.1. *The optimal precoder for the class of objectives for which $g(e^{\mathbf{l}})$ is a Schur-convex function of the logarithm of the MSEs is independent of the actual form of $g(\cdot)$ and is given by:*

$$\mathbf{P} = \sqrt{\frac{P_{\text{total}}}{K}} \mathbf{U}_{H,1} \mathbf{V}(\mathbf{\Lambda}_{H,1}), \quad (3.13)$$

where $\mathbf{V}(\Lambda_{\mathbf{H},1})$ is a unitary matrix that results in the QR decomposition of $\Lambda_{\mathbf{H},1}^{-1/2}\mathbf{V}(\Lambda_{\mathbf{H},1}) = \mathbf{QR}$ having an \mathbf{R} factor with equal diagonal elements.

For the class of objectives for which $g(e^{\mathbf{l}})$ is a Schur-concave function of the logarithm of the MSEs, the optimal solution results in $\mathbf{B} = \mathbf{0}$, and hence the optimal zero-forcing linear transceiver is an optimal transceiver for a system with a zero-forcing DFE.

Proof. See Appendix C. □

As we mentioned in Chapter 2, algorithms for obtaining a matrix Ψ such that the R-factor of the QR decomposition of $\mathbf{A}\Psi$ has equal diagonal elements were introduced in [14, 53], and \mathbf{V} in (3.13) can be obtained by applying the algorithms therein to the matrix $\Lambda_{\mathbf{H},1}^{-1/2}$.

For design objectives that are expressed as functions of the vector of MSE of each data stream, $e^{\mathbf{l}}$, the Schur-convexity and Schur-concavity classification of these objectives with respect to \mathbf{l} are the same as their classification in Sections 2.5.3 and 2.6.2 in absence of the zero-forcing design criteria. However, for the design objectives that are expressed as functions of the vector of the SINR of each data stream, $e^{-\mathbf{l}}$, and hence the bit error rate of each stream, the classification may be different from their classification in Sections 2.5.3 and 2.6.2, in which the absence of the zero-forcing criteria means that $\text{SINR} = e^{-\mathbf{l}} - 1$. For example, maximization of the product of the SINRs is now a Schur-convex and Schur-concave objective of \mathbf{l} , while in absence of the zero-forcing constraint it is only a Schur-convex objective. Also, maximization of the Gaussian mutual information is now strictly Schur-convex, while in absence of the zero-forcing constraint it is both Schur-convex and Schur-concave. The following examples provides the Schur-convexity/Schur-concavity classification of some design objectives that are embraced by the design framework.

- *Minimization of the sum of the individual MSEs:* In this case the objective is

to minimize

$$g(e^{\mathbf{l}}) = \sum_{k=1}^K e^{\mathbf{l}_k}, \quad (3.14)$$

which is Schur-convex function of \mathbf{l} .

- *Minimization of the maximum MSE / Maximization of minimum SNR:* In this case the objective is to minimize

$$g(e^{\mathbf{l}}) = \max_k(e^{\mathbf{l}_k}), \quad (3.15)$$

which is Schur-convex function of \mathbf{l} .

- *Minimization of the average Bit Error Rate:* This corresponds to the minimization of the objective

$$g(e^{\mathbf{l}}) = \frac{1}{K} \sum_{k=1}^K BER(\text{SNR}_k) = \sum_{k=1}^K BER(e^{-\mathbf{l}_k}), \quad (3.16)$$

where the *BER* expression will depend on the constellation used, and we have assumed that the same constellation is used for each element of \mathbf{s} in (3.1). Similar to the proof in Appendix A, It can be verified that under a mild constraint on the SNR, the BER expressions for BPSK and M-QAM constellations are convex functions of \mathbf{l}_k . Hence, $g(e^{\mathbf{l}})$ is a Schur-convex function of \mathbf{l} .

- *Maximization of Gaussian mutual information* This corresponds to the minimization of

$$g(e^{\mathbf{l}}) = \sum_{k=1}^K -\log(1 + e^{-\mathbf{l}_k}), \quad (3.17)$$

which takes the form $\sum_{k=1}^K h(\mathbf{l}_k)$ for the convex function $h(\mathbf{l}_k) = -\log(1 + e^{-\mathbf{l}_k})$, and hence it is a Schur-convex function of \mathbf{l} .

- *Minimization of the product of MSEs:* Minimization of the product of the individual MSEs (or equivalently, the geometric mean of the MSEs) corresponds

to the minimization of

$$g(\mathbf{e}^l) = \log \prod_{k=1}^K e^{l_k} = \sum_{k=1}^K l_k, \quad (3.18)$$

which is both Schur-convex and Schur-concave. Furthermore, since $\sum_{k=1}^K l_k = -\sum_{k=1}^K \log(\text{SNR})$, at high SNR the minimization of the product of the MSEs corresponds to the maximization of the Gaussian mutual information.

As demonstrated by Theorem 3.1 and the above examples, the optimal precoder for a system with zero-forcing DFE and a design objective from the Schur-convex class simultaneously optimizes the total MSE, the average bit error rate, and the Gaussian mutual information. MIMO systems with linear precoding and equalization do not achieve this simultaneous optimality, and in the general case each of these objectives results in a different optimal precoder [6]. For design criteria that can be expressed as the minimization of objectives that are both Schur-convex and Schur-concave, both the optimal Schur-convex design in (3.13) and the optimal linear transceiver will yield the same objective value. In the following sections, we will consider the efficient design of codebooks for limited feedback systems with Schur-convex objectives. Our first step will be to obtain the statistical distribution of the optimal precoder.

3.4 Statistical Distribution of Optimal Precoder for Schur-Convex Objectives

The optimal precoder for the Schur-convex class of objectives can be written as

$$\mathbf{P} = \sqrt{\frac{P_{\text{total}}}{K}} \bar{\mathbf{P}}, \quad (3.19)$$

where the matrix $\bar{\mathbf{P}} = \mathbf{U}_{\mathbf{H},1} \mathbf{V}(\mathbf{\Lambda}_{\mathbf{H},1})$ belongs to the Stiefel manifold $\mathcal{S}(N_t, K)$ of complex $N_t \times K$ matrices with orthonormal columns. The statistical distribution of

$\bar{\mathbf{P}}$ in (3.19) plays a key role in the design of the codebooks, and is established in Theorem 2 below. First, we establish an intermediate result.

Lemma 3.2. *For an i.i.d. Rayleigh fading channel matrix \mathbf{H} , the matrices $\mathbf{U}_{\mathbf{H},1}$ and $\mathbf{V}(\Lambda_{\mathbf{H},1})$ are statistically independent. Furthermore, $\mathbf{U}_{\mathbf{H},1}$ is isotropically distributed over the manifold $\mathcal{S}(N_t, K)$.*

Proof. The proof follows directly from the isotropic distribution of the eigen vectors of the Wishart distributed matrix $\mathbf{H}^H \mathbf{H}$ and its independence of the eigen values. \square

Theorem 3.2. *For an i.i.d. Rayleigh fading channel matrix \mathbf{H} , the normalized optimal precoder matrix $\bar{\mathbf{P}}$ is isotropically distributed over the Stiefel manifold $\mathcal{S}(N_t, K)$.*

Proof. We first observe from Lemma 3.2 that $\mathbf{U}_{\mathbf{H},1}$ is isotropically distributed over the manifold $\mathcal{S}(N_t, K)$. Hence, its probability distribution $p(\mathbf{U}_{\mathbf{H},1})$ is unaffected by post-multiplication by any *deterministic* unitary matrix \mathbf{Z} ; i.e., $p(\mathbf{U}_{\mathbf{H},1}) = p(\mathbf{U}_{\mathbf{H},1} \mathbf{Z})$. Hence,

$$p(\bar{\mathbf{P}}) = \int p(\bar{\mathbf{P}}|\mathbf{V}) p(\mathbf{V}) d\mathbf{V} \quad (3.20)$$

$$= \int p(\mathbf{U}_{\mathbf{H},1}) p(\mathbf{V}) d\mathbf{V} = p(\mathbf{U}_{\mathbf{H},1}), \quad (3.21)$$

Since $\mathbf{U}_{\mathbf{H},1}$ is isotropically distributed, then so is $\bar{\mathbf{P}}$. \square

It is worth noting that for MIMO systems with linear precoding and equalization, the optimal precoder will not be isotropically distributed. That is true for a wide range of objectives under a total power constraint (e.g., [6] and the references therein), and holds for both zero-forcing and MMSE linear receivers. That said, some quantization methods for linear transceivers have been based on a suboptimal underlying scheme that selects the best unitary precoding matrix; e.g., [48]. In that case the distribution of the unquantized precoder is isotropic. In the case of systems with a zero-forcing DFE, we have shown that selection of the best unitary precoding matrix is optimal.

3.5 Precoder Selection and Codebook design

In order to study the codebook design problem, we will first consider the selection method for choosing the best precoding matrix from a given codebook \mathcal{P} .

3.5.1 Precoding Matrix Selection

Given a codebook for quantizing the normalized optimal precoding matrix $\bar{\mathbf{P}}$, $\mathcal{P} = \{\bar{\mathbf{P}}^j, j = 1, \dots, |\mathcal{P}|\}$, and a cost function $g(\cdot)$ associated with the design criterion, the receiver will select a normalized precoding matrix from the codebook that yields the minimum value for the cost function; i.e., the receiver will select the index

$$\arg \min_{j=1, \dots, |\mathcal{P}|} g(e^{\mathbf{l}^j}), \quad (3.22)$$

where \mathbf{l}^j is the vector containing the logarithm of the diagonal elements of \mathbf{L}^j , the Cholesky factor of $\mathbf{N}^j = \sigma_n^2 \left(\frac{K}{P_{\text{total}}} \bar{\mathbf{P}}^j H^H \mathbf{H} \bar{\mathbf{P}}^j \right)^{-1}$. The quality of a given codebook can be measured in terms of the average degradation in the value of the objective that is incurred by using a precoder from the codebook rather than the optimal precoder in Theorem 1. Borrowing terminology from the source coding literature, we will refer to this degradation, and various bounds thereon, as distortion measures for the quantization scheme.

3.5.2 Grassmann Packing and Codebook Design

In the following section we will consider the design of codebooks to minimize distortion measures for the broad class of objectives $g(e^{\mathbf{l}})$ that are Schur-convex in \mathbf{l} . As shown in the previous section, for these objectives the optimal normalized precoder is uniformly distributed over the Stiefel manifold $\mathcal{S}(N_t, K)$. We observe that the range

of the columns of any normalized precoding matrix $\bar{\mathbf{P}}$ represents a K dimensional subspace, $R_{\bar{\mathbf{P}}}$, of \mathbb{C}^{N_t} . Hence, the desired codebook $\mathcal{P} = \{\bar{\mathbf{P}}^j, j = 1, \dots, |\mathcal{P}|\}$ represents a set of subspaces $\mathcal{R} = \{R_{\bar{\mathbf{P}}^j}, j = 1, \dots, |\mathcal{P}|\}$, and each of these subspaces can be represented as a point in the associated quotient space, namely the Grassmann Manifold; e.g., [54,55]. In the next section, we will relate the problem of designing codebooks that minimize suitable distortion measures to the Grassmann packing problem that selects a set of subspaces such that the minimum pairwise distance between any two subspaces in the packing is maximized. The distances between two subspaces $R_{\bar{\mathbf{P}}^1}$ and $R_{\bar{\mathbf{P}}^2}$ can be defined in different ways [56]. For example, the projection 2-norm is defined as

$$\text{dist}_{\text{proj}2}(\bar{\mathbf{P}}^1, \bar{\mathbf{P}}^2) = \left\| \bar{\mathbf{P}}^1 \bar{\mathbf{P}}^1{}^H - \bar{\mathbf{P}}^2 \bar{\mathbf{P}}^2{}^H \right\|_2, \quad (3.23)$$

while the Fubini-Study distance is defined as

$$\text{dist}_{\text{FS}}(\bar{\mathbf{P}}^1, \bar{\mathbf{P}}^2) = \arccos \left| \det(\bar{\mathbf{P}}^1{}^H \bar{\mathbf{P}}^2) \right|. \quad (3.24)$$

For a given set or a packing of subspaces and a given distance measure, we will denote the minimum pairwise distance between any two subspaces in the packing by

$$d = \min_{1 \leq i < j \leq |\mathcal{P}|} \text{dist}(\bar{\mathbf{P}}^i, \bar{\mathbf{P}}^j). \quad (3.25)$$

In addition to the minimum distance of the packing d , we will also be interested in its density D ; e.g., [56]. In our context, the density is the probability that the range space of an isotropically distributed unitary matrix falls within a distance $d/2$ of any of the subspaces of the packing, and is function of d , $|\mathcal{P}|$ and the volume of the manifold; see [56]. In the following two sections, we will show that codebooks from certain optimized Grassmann packings minimize distortion measures that are appropriate for two subclasses of the Schur-convex objectives: the strict Schur-convex objectives, and the objectives that are both Schur-convex and Schur-concave functions of \mathbf{l} .

3.5.3 Codebook Design Criteria for Strictly Schur-convex Objectives

In this section we will present suitable distortion measures for objectives $g(e^{\mathbf{l}})$ that are Schur-convex functions of \mathbf{l} and are not Schur-concave; e.g., the sum of the MSEs, the maximum MSE and the BER. From the first principles, we can obtain the following bounds on the these objectives:

- *Minimization of the sum of MSE:*

$$g(e^{\mathbf{l}}) = \sum_{k=1}^K e^{l_k} \leq K \max_k e^{l_k} = \frac{K}{\min_k e^{-l_k}}. \quad (3.26)$$

- *Minimization of the maximum MSE / Maximization of minimum SNR:*

$$g(e^{\mathbf{l}}) = \max_k (e^{l_k}) = \frac{1}{\min_k e^{-l_k}}. \quad (3.27)$$

- *Minimization of the average Bit Error Rate:*

$$g(e^{\mathbf{l}}) = \sum_{k=1}^K \text{BER}(e^{-l_k}) \leq K \text{BER}(\min_k e^{-l_k}). \quad (3.28)$$

We observe that each of these bounds is expressed in terms of the minimum SNR over the K data streams, $\text{SNR}_{\min} = \min_k e^{-l_k}$.

Since each of these terms is bounded by the minimum SNR, a natural choice for the distortion measure for a given codebook is the average loss in the minimum SNR that one incurs by using a normalized precoder $\bar{\mathbf{P}}^{\text{quant}}$ chosen from the codebook \mathcal{P} instead of using the optimal normalized precoder $\bar{\mathbf{P}}^{\text{opt}}$. That is,

$$\begin{aligned} \mathcal{E} &= \mathbb{E}_{\mathbf{H}} \left\{ \text{SNR}_{\min}(\bar{\mathbf{P}}^{\text{opt}}) - \text{SNR}_{\min}(\bar{\mathbf{P}}^{\text{quant}}) \right\} \\ &= \frac{\mathbb{E}_{\mathbf{H}} \left\{ \sqrt[k]{\det \boldsymbol{\Lambda}_{\mathbf{H},1}} \right\}}{\sigma_n^2} - \mathbb{E}_{\mathbf{H}} \left\{ \max_{1 \leq j \leq |\mathcal{P}|} \min_{1 \leq k \leq K} e^{-l_k^j} \right\}, \end{aligned} \quad (3.29)$$

where (3.29) follows by observing that the optimal $\bar{\mathbf{P}}$ results in $l_k = \frac{\ln \det(\mathbf{N})}{K}$ for every k . Consider the second term in the distortion measure in equation (3.29). From the definition of the majorization relation $\mathbf{a} \prec \mathbf{b}$, we have $\mathbf{a}_{[1]} \leq \mathbf{b}_{[1]}$. Hence, from Lemma 1 we have

$$\max_{1 \leq k \leq K} l_k \leq \ln \lambda_1(\mathbf{N}) = \ln \left(\frac{\sigma_n^2}{\sigma_{\min}^2(\mathbf{HP})} \right), \quad (3.30)$$

from which it follows that

$$\mathbb{E}_{\mathbf{H}} \left\{ \max_{1 \leq j \leq |\mathcal{P}|} \min_{1 \leq k \leq K} e^{-l_k^j} \right\} \geq \mathbb{E}_{\mathbf{H}} \left\{ \max_{1 \leq j \leq |\mathcal{P}|} \frac{\sigma_{\min}^2(\mathbf{HP}^j)}{\sigma_n^2} \right\}. \quad (3.31)$$

Hence, the distortion measure in (3.29) is upper bounded by

$$\mathcal{E} \leq \frac{\mathbb{E}_{\mathbf{H}} \left\{ \sqrt[K]{\det \Lambda_{\mathbf{H},1}} \right\}}{\sigma_n^2} - \mathbb{E}_{\mathbf{H}} \left\{ \max_{1 \leq j \leq |\mathcal{P}|} \frac{\sigma_{\min}^2(\mathbf{HP}^j)}{\sigma_n^2} \right\}. \quad (3.32)$$

When codebooks are designed from a Grassmann packing using the projection 2-norm distance in (3.23), the expectation on the right hand side of (3.31) satisfies [48],

$$\mathbb{E}_{\mathbf{H}} \left\{ \max_{1 \leq j \leq |\mathcal{P}|} \sigma_{\min}^2(\mathbf{HP}^j) \right\} \geq \mathbb{E}_{\mathbf{H}} \left\{ \sigma_K^2(\mathbf{H}) \right\} D_{\text{proj}2} \left(1 - \frac{d_{\text{proj}2}^2}{4} \right), \quad (3.33)$$

where $d_{\text{proj}2}$ is the minimum pairwise distance of the packing (cf. (3.25)) for the projection 2-norm distance, and $D_{\text{proj}2}$ is the corresponding packing density; cf. [56].

In addition, for a given $|\mathcal{P}|$ the right hand side of (3.33) is an increasing function of the packing distance $d_{\text{proj}2}$. Using the inequality in (3.32), we obtain the following upper bound on the distortion:

$$\mathcal{E} \leq \frac{\mathbb{E}_{\mathbf{H}} \left\{ \sqrt[K]{\det \Lambda_{\mathbf{H},1}} \right\}}{\sigma_n^2} - \frac{\mathbb{E}_{\mathbf{H}} \left\{ \sigma_K^2(\mathbf{H}) \right\}}{\sigma_n^2} D_{\text{proj}2} \left(1 - \frac{d_{\text{proj}2}^2}{4} \right), \quad (3.34)$$

which, for a given $|\mathcal{P}|$, is a decreasing function of the packing distance $d_{\text{proj}2}$. The bound on the right hand side of (3.34) can be minimized by choosing the codebook from a Grassmann packing that is designed to maximize the packing distance d in (3.25) with projection 2-norm as the distance metric. Such designs correspond to minimizing the bound on the distortion.

Since permutation matrices are special cases of unitary matrices, the limited feedback approach in [51, 52], in which the precoder is chosen from a codebook of permutation matrices, is a special case of the codebooks that we consider. However, the resulting codebooks do not necessarily have the maximum packing distance. Furthermore, the size of the codebook in the approaches in [51, 52] is fixed for a given N_t and K , while the Grassmann packings can be constructed for an arbitrary number of codewords.

3.5.4 Codebook Design Criteria for Objectives that are Both Schur-convex and Schur-concave

For communication objectives $g(e^{\mathbf{l}})$ that are both Schur-convex and Schur-concave functions of \mathbf{l} , such as the minimization of product of the MSEs, we observe that the design problem corresponds to maximization of $\det(\mathbf{P}^H \mathbf{H}^H \mathbf{H} \mathbf{P})/\sigma_n^2$. Hence, a suitable distortion measure for the codebook is

$$\begin{aligned} \mathcal{E} &= \mathbb{E}_{\mathbf{H}} \left\{ \det(\bar{\mathbf{P}}^{\text{opt}H} \mathbf{H}^H \mathbf{H} \bar{\mathbf{P}}^{\text{opt}}) - \det(\bar{\mathbf{P}}^{\text{quant}H} \mathbf{H}^H \mathbf{H} \bar{\mathbf{P}}^{\text{quant}}) \right\} / \sigma_n^2 & (3.35) \\ &= \mathbb{E}_{\mathbf{H}} \{ \det \boldsymbol{\Lambda}_{\mathbf{H},1} \} / \sigma_n^2 - \mathbb{E}_{\mathbf{H}} \left\{ \max_{1 \leq j \leq |\mathcal{P}|} \det(\bar{\mathbf{P}}^jH \mathbf{H}^H \mathbf{H} \bar{\mathbf{P}}^j) \right\} / \sigma_n^2 \\ &\leq \mathbb{E}_{\mathbf{H}} \{ \det \boldsymbol{\Lambda}_{\mathbf{H},1} \} / \sigma_n^2 - \mathbb{E}_{\mathbf{H}} \{ \det \boldsymbol{\Lambda}_{\mathbf{H},1} \} \mathbb{E}_{\mathbf{H}} \left\{ \max_{1 \leq j \leq |\mathcal{P}|} \det(\bar{\mathbf{P}}^jH \mathbf{U}_{\mathbf{H},1} \mathbf{U}_{\mathbf{H},1}^H \bar{\mathbf{P}}^j) \right\} / \sigma_n^2. & (3.36) \end{aligned}$$

Here, (3.36) follows from the independence of $\mathbf{U}_{\mathbf{H}}$ and $\boldsymbol{\Lambda}_{\mathbf{H}}$. When codebooks are designed from a Grassmann packing using the Fubini-Study distance in (3.24), the last expectation on the right hand side of (3.36) satisfies the following inequality [48]:

$$\mathbb{E}_{\mathbf{H}} \left\{ \max_{1 \leq j \leq |\mathcal{P}|} \det(\bar{\mathbf{P}}^jH \mathbf{U}_{\mathbf{H},1} \mathbf{U}_{\mathbf{H},1}^H \bar{\mathbf{P}}^j) \right\} \geq D_{\text{FS}} \cos^2(d_{\text{FS}}/2). \quad (3.37)$$

Hence, we obtain the following upper bound on the distortion:

$$\mathcal{E} \leq \mathbb{E}_{\mathbf{H}} \{ \det \boldsymbol{\Lambda}_{\mathbf{H},1} \} (1 - D_{\text{FS}} \cos^2(d_{\text{FS}}/2)) / \sigma_n^2, \quad (3.38)$$

which, for a given $|\mathcal{P}|$, is a decreasing function of the packing distance d_{FS} . A similar upper bound was proposed for designing codebooks for MIMO systems with linear receivers [48].

3.5.5 Comparison with ZF-Linear Schemes

In this section, we will show that for a given codebook, the performance of the zero-forcing DFE with limited feedback provides an upper bound on the performance of its linear zero-forcing counterpart for any Schur-convex performance objective $g(e^{\mathbf{l}})$. As stated in the following lemma, this is true for any codebook, including those codebooks constructed from non-unitary matrices.

Lemma 3.3. *Consider a codebook of precoding matrices, \mathcal{P} , and a Schur-convex performance $g(e^{\mathbf{l}})$. For any given channel \mathbf{H} , let $\mathbf{l}_{\text{DFE}}^j$ denote the vector \mathbf{l} in (3.12) when the precoder \mathbf{P}^j is used, and let the $\mathbf{l}_{\text{Lin}}^j$ denote the corresponding vector for the case of linear equalization. Then*

$$\min_{j=1, \dots, |\mathcal{P}|} g(e^{\mathbf{l}_{\text{DFE}}^j}) \leq \min_{j=1, \dots, |\mathcal{P}|} g(e^{\mathbf{l}_{\text{Lin}}^j}).$$

Proof. Consider a given channel \mathbf{H} and any precoding matrix $\mathbf{P}^j \in \mathcal{P}$. For the linear zero-forcing receiver we have $\mathbf{C} = \mathbf{I}$. It follows from (3.9) that the corresponding matrix \mathbf{N}^j and its Cholesky factor \mathbf{L}^j are diagonal. Hence, $(\mathbf{L}_{ii}^j)^2 = \lambda_i(\mathbf{N}^j)$, or, equivalently,

$$\mathbf{l}_{\text{Lin}}^j = (\ln \lambda_1(\mathbf{N}^j), \dots, \ln \lambda_K(\mathbf{N}^j)).$$

On the other hand, for the DFE receiver we have

$$\mathbf{l}_{\text{DFE}}^j = (\ln(\mathbf{L}_{11}^j)^2, \dots, \ln(\mathbf{L}_{KK}^j)^2).$$

From Lemma 3.1, we have $\mathbf{l}_{\text{DFE}}^j \prec \mathbf{l}_{\text{Lin}}^j$, hence $g(e^{\mathbf{l}_{\text{DFE}}^j}) \leq g(e^{\mathbf{l}_{\text{Lin}}^j})$ and

$$\min_{j=1,\dots,|\mathcal{P}|} g(e^{\mathbf{l}_{\text{DFE}}^j}) \leq \min_{j=1,\dots,|\mathcal{P}|} g(e^{\mathbf{l}_{\text{Lin}}^j}).$$

□

3.6 Simulation Studies

In this section, we simulate the performance of the proposed limited feedback MIMO schemes over a standard i.i.d. Rayleigh block fading channel model.¹ For the error rate performance comparisons, we use 16-QAM signaling and we plot the average bit error rate (BER) of the K data streams against the signal-to-noise-ratio, which is defined as the ratio of the total average transmitted power P_{total} to the total receiver noise power $E\{\mathbf{n}^H \mathbf{n}\}$. We compare the performance of the proposed codebook designs for systems with zero-forcing DFE with that of the optimal zero-forcing DFE transceiver for the case of perfect CSI that was presented in Section 3.3. For the proposed limited-feedback schemes, the Grassmann codebooks are constructed using the design approach in [57]; see also [48]. (Grassmann codebooks could also be constructed using the optimization algorithms in [54,55]). We also provide simulation-based comparisons with the two limited feedback schemes for zero-forcing DFE systems in [52]. In addition, we provide performance comparisons with limited feedback schemes for linear zero-forcing transceivers that use Grassmann codebooks [48], and with the optimal zero-forcing linear transceiver designs for the case of perfect CSI for minimum MSE and minimum bit error rate design criteria [58].

¹The coefficients of the channel matrix \mathbf{H} are modelled as independent circularly symmetric complex Gaussian random variables with zero mean and unit variance.

3.6.1 Comparisons with Limited Feedback Zero-forcing DFE Schemes

In Fig 3.2, we consider a MIMO system with $N_t = 6$ transmit antennas and $N_r = 3$ receive antennas that transmits $K = 3$ independent data streams. We compare the performance of the proposed schemes with Grassmann codebook designs and precoder selection based on the minimization of the sum of the MSEs (Grassmann-6 bits- Sum MSE), minimization of the average BER (Grassmann-6 bits- Min BER), and the minimization of the maximum MSE (Grassmann-6 bits- Max MSE) which is equivalent to the maximization of minimum SINR. The codebooks consist of 64 unitary matrices, and hence 6 bits of feedback are used per block. We also make comparisons with the limited feedback schemes in [52] (Ordering Feedback ZF-DFE and Ordering Feedback2 ZF-DFE) in which the receiver feeds back the index of the selected permutation of the columns of \mathbf{H} from the set of possible $P_K^{N_t} = N_t!/(N_t - K)!$ permutation matrices. For the system under consideration, the number of possible permutations matrices is 120, almost twice the size of the Grassmann codebook. In the scheme denoted Ordering Feedback ZF-DFE the permutation matrix is selected based on the norms of the columns of \mathbf{H} , while the scheme denoted Ordering Feedback2 ZF-DFE the permutation is selected based on a greedy ordering of the QR decomposition of the channel matrix \mathbf{H} . In Fig. 3.2, we observe the close performance of the proposed codebooks with different Schur-convex selection criteria. This is to be expected, because in the limit of infinite feedback (i.e., perfect CSI), all these objectives result in the same optimal precoder design. We also observe that the Grassmann codebooks provide significantly better performance than the schemes that are based on precoding with permutation matrices, even though they employ fewer feedback bits. This is because codebooks constructed from permutation matrices are special cases

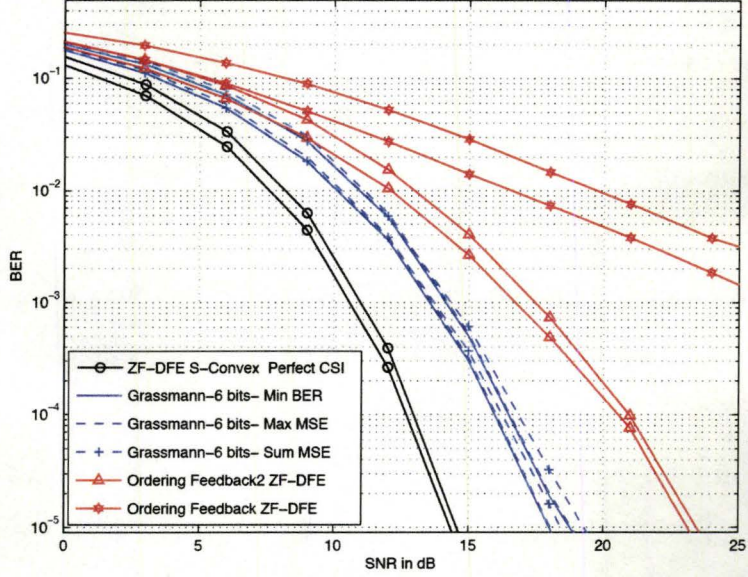


Figure 3.2: BER performance of various MIMO transmission schemes with zero-forcing DFE for a system with $N_t = 6$, $N_r = 3$, and $K = 3$ simultaneously transmitted 16-QAM data streams. The schemes considered are: the proposed codebook designs for the objectives of minimization of the sum of MSEs (Grassmann-6 bits- Sum MSE), minimization of the average BER (Grassmann-6 bits- Min BER); the optimal zero-forcing design for any Schur-convex design objective with perfect CSI (ZF DFE - Perfect CSI); and the limited feedback schemes in [52], which are based on feeding back the detection ordering (Ordering Feedback - ZF DFE) and (Ordering Feedback2 - ZF DFE). The lower curve for each method represents the BER performance obtained under the assumption of correct previous decisions.

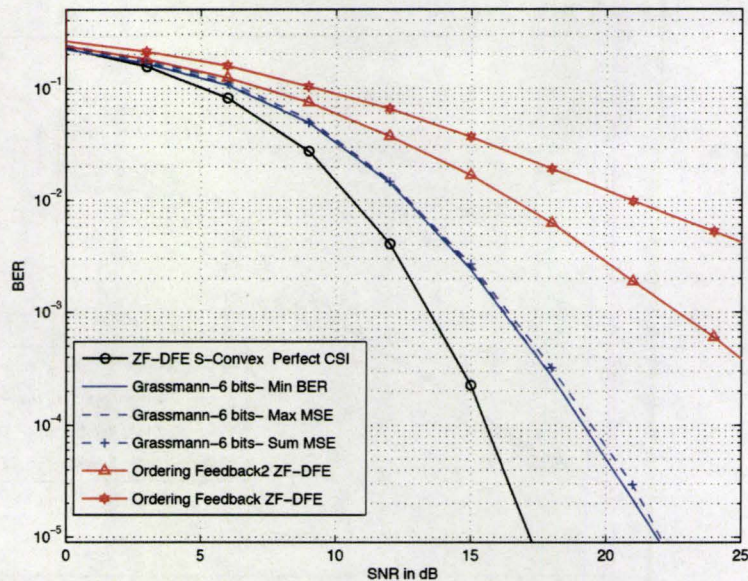


Figure 3.3: BER performance of various MIMO transmission schemes with zero-forcing DFE for a system with $N_t = 5$, $N_r = 4$, and $K = 4$ simultaneously transmitted 16-QAM data streams. The schemes considered are: the proposed codebook designs for the objectives of minimization of the sum of MSEs (Grassmann-6 bits- Sum MSE), minimization of the average BER (Grassmann-6 bits- Min BER); the optimal zero-forcing design for any Schur-convex design objective with perfect CSI (ZF DFE - Perfect CSI); and the limited feedback schemes in [52], which are based on feeding back the detection ordering (Ordering Feedback - ZF DFE) and (Ordering Feedback2 - ZF DFE).

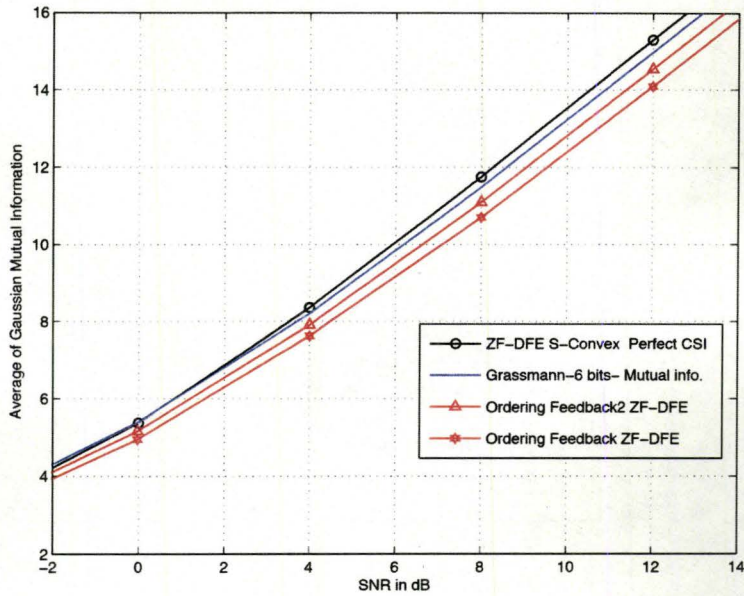


Figure 3.4: Average of Gaussian mutual information in (3.17) for various MIMO transmission schemes with zero-forcing DFE for a system with $N_t = 5$, $N_r = 4$, and $K = 4$. The schemes considered are: the proposed codebook designs for Gaussian mutual information objective (Grassmann-6 bits- Mutual info); the optimal zero-forcing design for any Schur-convex design objective with perfect CSI (ZF DFE - Perfect CSI); and the limited feedback schemes in [52], which are based on feeding back the detection ordering (Ordering Feedback - ZF DFE) and (Ordering Feedback2 - ZF DFE).

of those constructed from unitary matrices, and they do not necessarily minimize the distortion measures. Note that for all error performance figures in this paper, the simulation results of all ZF-DFE methods include the effect of error propagation. For reference, in Fig 3.2 we also provide the performance under the assumption of correct previous decisions; i.e., no error propagation. We observe that at high SNRs, the practical performance of the optimal zero-forcing DFE transceiver for the case of perfect CSI and the proposed designs based on Grassmann codebooks are close to their corresponding performance in absence of error propagation. This also holds for the permutation feedback scheme (Ordering Feedback2 ZF-DFE).

Analogous performance advantages to those in Fig 3.2 are observed in Fig 3.3, which shows the performance for a MIMO system with $N_t = 5$ transmit antennas and $N_r = 4$ receive antennas that transmits $K = 4$ data streams. The size of each permutation-based codebook is 120 matrices, while the size of each Grassmann codebook is 64 matrices.

In Fig 3.4 we compare several different methods in terms of the Gaussian mutual information that they achieve. We consider a system with $N_t = 5$, $N_r = 4$, and $K = 4$, and we plot the average, over 1000 channel realizations, of the Gaussian mutual information achieved by the ZF-DFE transceiver with the quantized precoder; i.e., the average of the values of (3.17) achieved by the quantized precoder. For the proposed scheme we consider a Grassmann codebook design and precoder selection based on the maximization of the Gaussian mutual information (Grassmann-6 bits- Mutual info.), and a codebook that consists of 64 unitary matrices. We make comparisons with the limited feedback schemes in [52] (Ordering Feedback ZF-DFE and Ordering Feedback2 ZF-DFE), whose permutation-based codebooks contain 120 matrices. We observe that the proposed Grassmann codebook with precoder selection based on the maximization of the Gaussian mutual information provides the closest performance

to the optimal ZF-DFE design for the case of perfect CSI, which was presented in Section 3.3.

3.6.2 Comparisons with Limited Feedback Linear Zero-forcing Schemes

In Fig 3.5, we consider a MIMO system with $N_t = 5$ transmit antennas and $N_r = 4$ receive antennas that transmits $K = 4$ independent data streams. We compare the performance of the proposed ZF-DFE schemes that use Grassmann codebooks with that of the corresponding linear zero-forcing schemes that use Grassmann codebooks with the same feedback rate [48]. We consider linear limited feedback schemes with different precoder selection criteria, namely minimization of the total MSE (LinZF-Grassmann-6 bits Sum MSE), and maximization of the minimum eigen value of the overall channel **HP** (LinZF-Grassmann-6 bits Max MSE), which corresponds to minimization of the maximum MSE [48]. We also provide performance comparisons with the zero-forcing DFE transceiver design for perfect CSI that simultaneously optimizes any Schur-Convex design criteria, and with the corresponding optimal zero-forcing linear transceiver designs for perfect CSI that minimize the total MSE or the average BER. Unlike the DFE case, these two design criteria result in different precoder designs [58]. In Fig. 3.5, we observe that the proposed zero-forcing DFE systems with limited feedback perform better than the corresponding linear schemes; as is to be expected, c.f. Lemma 3.3. Similar performance advantages are observed in Fig 3.6 for a MIMO system with $N_t = 4$ transmit antennas and $N_r = 3$ receive antennas that transmits $K = 3$ independent data streams.

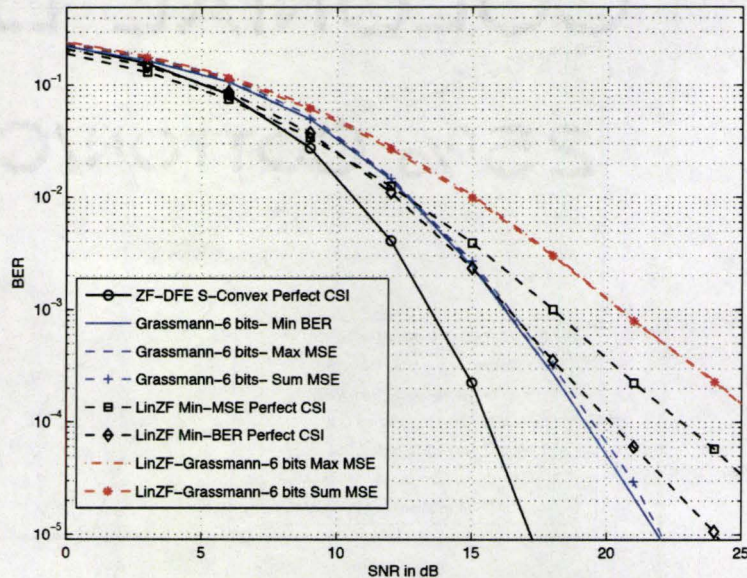


Figure 3.5: BER performance of various MIMO transmission schemes with zero-forcing linear and DFE systems with $N_t = 5, N_r = 4$, and $K = 4$ simultaneously transmitted 16-QAM data streams. The schemes considered are: the proposed code-book designs for the objectives of minimization of the sum of MSEs (Grassmann-6 bits- Sum MSE), minimization of the average BER (Grassmann-6 bits- Min BER); the optimal zero-forcing design for any Schur-convex design objective with perfect CSI (ZF DFE - Perfect CSI); the optimal linear zero-forcing design for minimum MSE (LinZF Min-MSE Perfect CSI) and minimum average BER (LinZF Min-BER Perfect CSI) [58]; and the linear zero-forcing limited feedback schemes in [48] for minimum total MSE (LinZF-Grassmann-6 bits Sum MSE) and minimum maximum MSE (LinZF-Grassmann-6 bits Max MSE).

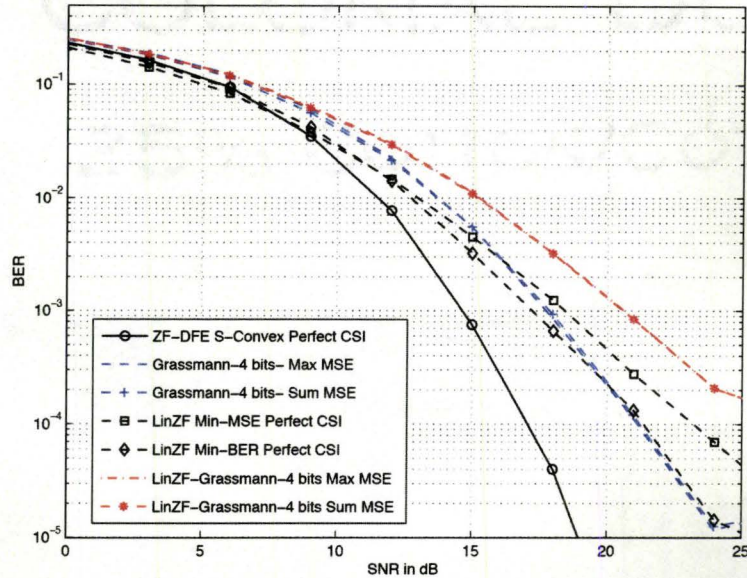


Figure 3.6: BER performance of various MIMO transmission schemes with zero-forcing linear and DFE systems with $N_t = 4, N_r = 3$, and $K = 3$ simultaneously transmitted 16-QAM data streams. The schemes considered are: the proposed codebook designs for the objectives of minimization of the sum of MSEs (Grassmann-6 bits- Sum MSE), minimization of the average BER (Grassmann-6 bits- Min BER); the optimal zero-forcing design for any Schur-convex design objective with perfect CSI (ZF DFE - Perfect CSI); the optimal linear zero-forcing design for minimum MSE (LinZF Min-MSE Perfect CSI) and minimum average BER (LinZF Min-BER Perfect CSI) [58]; and the linear zero-forcing limited feedback schemes in [48] for minimum total MSE (LinZF-Grassmann-6 bits Sum MSE) and minimum maximum MSE (LinZF-Grassmann-6 bits Max MSE).

3.7 Conclusion

In this chapter, we considered the design of multiple-input multiple-output communication systems with zero-forcing decision feedback equalization (DFE) when only limited rate feedback from the receiver to the transmitter is available. We considered schemes in which the receiver uses its CSI to select the best available precoder from a codebook of precoders and then feeds back the index of this precoder to the transmitter using a small number of bits. To facilitate the development of the limited feedback scheme, a unified design framework was developed for the joint design of the precoder and the zero-forcing DFE receiver when perfect channel state information is available at both the transmitter and the receiver. We then characterized the statistical distribution of the optimal precoder in a standard Rayleigh fading environment, and showed that codebooks constructed from Grassmann packings minimize an upper bound on an average distortion measure. Our simulation studies showed that the proposed limited feedback scheme can provide significantly better performance with a lower feedback rate than the existing schemes in which the detection order is fed back to the transmitter.

Part II

Multi-user Systems

Chapter 4

Robust Linear Broadcasting with QoS Constraints: SINR Formulations

In the first part of the thesis, we considered single-user MIMO systems, and we proposed novel design frameworks for non-linear MIMO transceivers that employ interference (pre-)subtraction. These design frameworks were developed for communication scenarios that assume the availability of perfect channel state information (CSI) at both the transmitter and the receiver, and scenarios with limited feedback that assume perfect CSI at the receiver only and a low-rate feedback channel between the receiver and the transmitter. However, as we pointed out in Chapter 1, the performance of multi-user systems is more dependent on the availability (and the quality) of the users' channel state information, and hence the focus of the second part of this thesis will be on the design of robust multi-user transceivers that explicitly take into account channel uncertainty in their design formulations.

In this chapter, we consider the design of linear precoders (beamformers) for

broadcast channels with Quality of Service (QoS) constraints for each user, in scenarios with uncertain channel state information at the transmitter. We consider a deterministically-bounded model for the channel uncertainty of each user, and the goal is to design a robust precoder that minimizes the total transmission power required to satisfy the users' QoS constraints for all channels within a specified uncertainty region around the transmitter's estimate of each user's channel. Since this problem is not known to be computationally tractable, we will derive three conservative design approaches that yield convex and computationally-efficient restrictions of the original design problem. The three approaches yield semidefinite program (SDP) formulations that offer different trade-offs between the degree of conservatism and the size of the SDP. We will also show how these conservative approaches can be used to derive efficiently-solvable quasi-convex restrictions of some related design problems, including the robust counterpart to the problem of maximizing the minimum signal-to-interference-plus-noise-ratio (SINR) subject to a given power constraint. Our simulation results indicate that in the presence of uncertain CSI the proposed approaches can satisfy the users' QoS requirements for a significantly larger set of uncertainties than existing methods, and require less transmission power to do so.

4.1 Introduction

The design of wireless broadcasting schemes that satisfy the quality of service (QoS) requirements of the intended receivers (users) is of growing interest in interactive communication applications and in the downlink of cellular systems with differentiated services. Employing multiple antennas at the transmitter (base station) of a wireless downlink offers the potential for a substantial improvement in the quality of service

(QoS) that the base station can offer to the assigned users. This potential can be realized by precoding the data symbols intended for each user in a manner that mitigates the multiuser interference at the (non-cooperating) receivers, and hence improves the fidelity of the received signals. The transmitter's ability to mitigate interference at the receivers is dependent on the availability of (accurate) channel state information (CSI) for all the users' channels. For scenarios in which one can assume perfect CSI is available at the transmitter, the problem of designing a linear precoder¹ that minimizes the transmitted power required to satisfy a set of QoS constraints specified by the users has been considered in [59–64], and in [28, 65–68] for the case of non-linear precoding.

In practice, the CSI that is available at the transmitter is subject to uncertainties that arise from a variety of sources, such as estimation error, channel quantization and short channel coherence time, and downlink precoder design methods that assume perfect CSI are particularly sensitive to these uncertainties; e.g., [8, 9]. This suggests that one ought to incorporate robustness to channel uncertainty into the formulation of the precoder design problem. One approach to doing so is to consider a bounded model for the errors in the transmitter's estimate of the (deterministic) autocorrelation matrices of the channel [61, 69]. This uncertainty model may be suitable for systems with uplink-downlink reciprocity in which the transmitter can estimate the users' channels. We will adopt an alternative approach in which we consider a bounded model for the error in the transmitter's estimate of the channels. This uncertainty model is particularly useful for systems in which users feed back quantized channel measurements to the transmitter, as knowledge of the quantization codebooks can be used to bound the quantization error. For this bounded channel uncertainty model, we consider the design of a linear precoder that minimizes the

¹Since we will focus on scenarios in which each user has a single antenna, linear precoding is analogous to downlink beamforming.

transmitted power required to ensure that each user's QoS requirement is satisfied for all channels within the specified uncertainty region. This problem is not known to be computationally tractable [70], and in order to obtain design methods that are known to be tractable we will obtain three conservative design approaches that yield convex and computationally-efficient restrictions of the original design problem.² The three approaches yield semidefinite program (SDP) formulations that offer different trade-offs between the degree of conservatism and the size of resulting SDP.

We will also show how these conservative design approaches can be used to obtain efficiently-solvable quasi-convex formulations of certain restrictions of related design problems. In particular, we consider the problem of determining the largest uncertainty region for which the QoS requirements can be satisfied for all channels within the region using finite transmission power. This problem is of considerable interest in scenarios in which the channel uncertainty is dominated by the quantization error incurred in a quantized feedback scheme. In that case, one might wish to choose the rate of the channel quantization scheme to be large enough (and the quantization cells small enough) for it to be possible to design a robust precoder with finite power. We provide quasi-convex formulations of conservative approaches to this problem that can be efficiently solved using a one-dimensional bisection search. We also consider the robust counterpart of the problem of maximizing the weakest user's signal-to-interference-plus-noise-ratio subject to a given power constraint on the transmitter (e.g., [63, 64]), and we provide quasi-convex formulations of conservative approaches to that design problem, too. Our numerical experiments will illustrate the impact that our proposed designs can have on a number of performance metrics. In particular, these experiments indicate that proposed approaches can satisfy the users' QoS

²Since these problems are restrictions of the original problem, the transmission power of the designed precoder is larger than (or equal to) the power that would be required if a tractable method for solving the original problem was available.

requirements for a significantly larger set of uncertainties than existing methods, and require less transmission power to do so.

4.2 System Model

We consider a broadcast scenario with N_t antennas at the transmitter which are used to send independent messages to K receivers, each of which has a single antenna. Let $\mathbf{s} \in \mathbb{C}^K$ be the vector of data symbols intended for each receiver. The transmitter generates a vector of transmitted signals, $\mathbf{x} \in \mathbb{C}^{N_t}$, by linearly precoding the vector \mathbf{s}

$$\mathbf{x} = \mathbf{P}\mathbf{s} = \sum_{j=1}^K \mathbf{p}_j s_j, \quad (4.1)$$

where \mathbf{p}_j is the j^{th} column of the precoding matrix \mathbf{P} , and s_j is the j^{th} element of \mathbf{s} . Without loss of generality, we will assume that $\mathbb{E}\{\mathbf{s}\mathbf{s}^H\} = \mathbf{I}$, and hence, the total transmitted power is given by

$$\text{tr}(\mathbf{P}^H \mathbf{P}) = \sum_{k=1}^K \|\mathbf{p}_k\|^2. \quad (4.2)$$

At the k^{th} receiver, the received signal y_k is given by

$$y_k = \mathbf{h}_k \mathbf{x} + n_k, \quad (4.3)$$

where $\mathbf{h}_k \in \mathbb{C}^{1 \times N_t}$ is a row vector³ representing the channel gains from the transmitting antennas to the k^{th} receiver, and n_k represents the zero-mean additive white noise at the k^{th} receiver, whose variance is $\sigma_{n_k}^2$. We will find it convenient to use the vector notation:

$$\mathbf{y} = \mathbf{H}\mathbf{x} + \mathbf{n}, \quad (4.4)$$

³Although treating \mathbf{h}_k as a row vector is a mild abuse of notation, it is standard practice.

where \mathbf{H} is the broadcast channel matrix whose k^{th} row is \mathbf{h}_k , and the noise vector \mathbf{n} has covariance matrix $\mathbf{E}\{\mathbf{nn}^H\} = \text{Diag}(\sigma_{n_1}^2, \dots, \sigma_{n_K}^2)$.

We consider broadcast scenarios in which each receiver has a quality of service requirement that is specified in terms of a lower bound on its signal-to-interference-plus-noise-ratio

$$\text{SINR}_k = \frac{|\mathbf{h}_k \mathbf{p}_k|^2}{\sum_{j=1, j \neq k}^K |\mathbf{h}_k \mathbf{p}_j|^2 + \sigma_{n_k}^2} \geq \gamma_k. \quad (4.5)$$

This SINR constraint represents a rather general constraint on the minimum quality of service received by the k^{th} user. Indeed, the SINR constraint can be translated into an equivalent constraint on the symbol error rate or the achievable data rate; e.g., [71].

4.2.1 Precoding with QoS Constraints: Perfect CSI Case

Given perfect CSI at the transmitter, the design of a precoder that minimizes the total transmitted power required to satisfy the users' QoS constraints can be stated as:

$$\min_{\mathbf{P}} \sum_{k=1}^K \|\mathbf{p}_k\|^2 \quad (4.6a)$$

$$\text{subject to } \frac{|\mathbf{h}_k \mathbf{p}_k|^2}{\sum_{j=1, j \neq k}^K |\mathbf{h}_k \mathbf{p}_j|^2 + \sigma_{n_k}^2} \geq \gamma_k. \quad (4.6b)$$

This is a convex optimization problem in the precoding matrix \mathbf{P} , and can be efficiently solved [59–64]. Indeed, if we make the following definitions,

$$\underline{\mathbf{h}}_k = \begin{bmatrix} \text{Re}\{\mathbf{h}_k\} & \text{Im}\{\mathbf{h}_k\} \end{bmatrix}, \quad (4.7)$$

$$\underline{\mathbf{P}} = \begin{bmatrix} \text{Re}\{\mathbf{P}\} & \text{Im}\{\mathbf{P}\} \\ -\text{Im}\{\mathbf{P}\} & \text{Re}\{\mathbf{P}\} \end{bmatrix}, \quad (4.8)$$

$$\underline{\mathbf{p}}_k = \begin{bmatrix} \text{Re}\{\mathbf{p}_k\} \\ -\text{Im}\{\mathbf{p}_k\} \end{bmatrix}, \quad (4.9)$$

we can formulate (4.6) as the following second order cone program (SOCP) with real variables⁴ [64]:

$$\min_{\mathbf{P}, t} t \quad (4.10a)$$

$$\text{subject to } \|\text{vec}([\mathbf{p}_1, \dots, \mathbf{p}_K])\| \leq t, \quad (4.10b)$$

$$\|[\mathbf{h}_k \mathbf{P}, \sigma_{n_k}]\| \leq \beta_k \mathbf{h}_k \mathbf{p}_k, \quad 1 \leq k \leq K, \quad (4.10c)$$

where $\beta_k = \sqrt{1 + 1/\gamma_k}$.

The primary goal of this chapter is to obtain robust counterparts to (4.10) that mitigate the impact of imperfect CSI. Before we derive those counterparts, we would like to point out that when \mathbf{H} has full row rank (which requires that $K \leq N_t$), the perfect CSI problem (with finite SINR requirements) is always feasible. (The robust counterparts will not share this property.) Indeed, one feasible solution is to chose \mathbf{P} to be the product of the right inverse of \mathbf{H} and a diagonal power loading matrix with sufficiently large loadings. In practice, however, one may wish to constrain the transmission power in various ways, such as constraining the average power transmitted by each individual antenna (e.g., [72]), $E\{|x_n|^2\} \leq P_n$, $1 \leq n \leq N_t$. Another useful power constraint arises from the imposition of a spatially-shaped bound (e.g., [73], [74]) on the transmitted power, $E\{\mathbf{x}^H \mathbf{Q}(\theta) \mathbf{x}\} \leq P_{\text{shape}}(\theta)$ for all $\theta \in \Theta$, where $\mathbf{Q}(\theta) = \mathbf{v}(\theta) \mathbf{v}^H(\theta)$, with $\mathbf{v}(\theta)$ being the “steering vector” (e.g., [75]) of the transmitter’s antenna array in the direction θ , $P_{\text{shape}}(\theta)$ is the maximum allowable power in the direction of θ , and Θ is the set of angles of interest. The later case is of particular interest in cellular systems in which interference to neighboring cells needs to be controlled; e.g., [3, 76]. Although we will focus on robust versions of the formulation in (4.10) in the presence of channel uncertainty, in Appendix D we will

⁴In this chapter and the following one, we have preferred to use formulations with real variables in order to facilitate computational cost comparisons of different proposed approaches; See Tables 4.1 and 5.1.

show how these two types of power constraints can be easily incorporated into our robust formulations.

4.2.2 Bounded Channel Uncertainty Model

We will model the channel uncertainty using a deterministically-bounded additive uncertainty set. More specifically, we will model the k^{th} user's channel as:

$$\mathbf{h}_k = \hat{\mathbf{h}}_k + \mathbf{e}_k, \quad (4.11)$$

where $\hat{\mathbf{h}}_k$ is the transmitter's estimate of the k^{th} user's channel, and \mathbf{e}_k is the corresponding estimation error. In order to avoid making any assumptions on the statistics of \mathbf{e}_k , we will merely assume that it lies in the ball $\|\mathbf{e}_k\| \leq \delta_k$, for some given δ_k . This model is a convenient one for systems in which the channel state information is quantized at the receivers and fed back to the transmitter; e.g., [8]. In particular, if the quantizer is (almost) uniform, then the quantization cells in the interior of the quantization region can be "covered" by balls of size δ_k . A similar bounded uncertainty model has been used in the context of generic beamforming systems [77–79], where it is the error in the estimate of the steering vector that is being bounded, and in CDMA systems [80].

By using the vector $\underline{\mathbf{e}}_k = [\text{Re}\{\mathbf{e}_k\}, \text{Im}\{\mathbf{e}_k\}]$, the uncertainty set of each channel can be described by the following (spherical) region:

$$\mathcal{U}_k(\delta_k) = \{\underline{\mathbf{h}}_k \mid \underline{\mathbf{h}}_k = \hat{\underline{\mathbf{h}}}_k + \underline{\mathbf{e}}_k, \|\underline{\mathbf{e}}_k\| \leq \delta_k\}. \quad (4.12)$$

4.3 Precoding with QoS Constraints: Uncertain CSI Case

Given the model for the channel uncertainty in (4.12), our goal is to design a robust precoding matrix that minimizes the transmitted power required to ensure that the users' QoS requirements are satisfied for all channels $\underline{\mathbf{h}}_k$ within the uncertainty region $\mathcal{U}_k(\delta_k)$. Using the SOCP formulation in (4.10), this design problem can be formulated as the following semi-infinite SOCP⁵:

$$\min_{\underline{\mathbf{P}}, t} t \quad (4.13a)$$

$$\text{s. t.} \quad \|\text{vec}([\underline{\mathbf{p}}_1, \dots, \underline{\mathbf{p}}_K])\| \leq t, \quad (4.13b)$$

$$\|[\underline{\mathbf{h}}_k \underline{\mathbf{P}}, \sigma_{n_k}]\| \leq \beta_k \underline{\mathbf{h}}_k \underline{\mathbf{p}}_k, \quad \forall \underline{\mathbf{h}}_k \in \mathcal{U}_k(\delta_k), \quad 1 \leq k \leq K. \quad (4.13c)$$

For later convenience, any precoder of finite power that satisfies (4.13c) will be said to provide a robust QoS guarantee.

Since $\underline{\mathbf{h}}_k$ is present on both the left and right hand sides of each SOC constraint in (4.13c), the left and right hand sides of (4.13c) vary together and share the same ellipsoidal uncertainty region. That joint variation appears to make this problem difficult to solve, but the formal treatment of the computational tractability of this problem remains an open problem [70, 81]. Some insight can be obtained by using a standard transformation (via the Schur Complement Theorem [22]) to write the SOC constraint $\|[\underline{\mathbf{h}}_k \underline{\mathbf{P}}, \sigma_{n_k}]\| \leq \beta_k \underline{\mathbf{h}}_k \underline{\mathbf{p}}_k$ as an equivalent linear matrix inequality (LMI) [82]

$$\mathbf{F}_k(\underline{\mathbf{P}}, \underline{\mathbf{h}}_k) = \begin{bmatrix} \beta_k \underline{\mathbf{h}}_k \underline{\mathbf{p}}_k & [\underline{\mathbf{h}}_k \underline{\mathbf{P}}, \sigma_{n_k}] \\ [\underline{\mathbf{h}}_k \underline{\mathbf{P}}, \sigma_{n_k}]^T & (\beta_k \underline{\mathbf{h}}_k \underline{\mathbf{p}}_k) \mathbf{I}_{(2K+1)} \end{bmatrix} \geq \mathbf{0}. \quad (4.14)$$

⁵Observe that (4.13c) contains an infinite number of second-order cone constraints, one for each $\underline{\mathbf{h}}_k \in \mathcal{U}_k(\delta_k)$.

By substituting $\underline{\mathbf{h}}_k = \hat{\underline{\mathbf{h}}}_k + \underline{\mathbf{e}}_k$ in (4.14), the inequality $\mathbf{F}_k(\underline{\mathbf{P}}, \underline{\mathbf{h}}_k) \geq \mathbf{0}$ takes the form:

$$\bar{\mathbf{F}}_k(\underline{\mathbf{P}}, \hat{\underline{\mathbf{h}}}_k, \mathbf{M}_k) = \mathbf{F}_k(\underline{\mathbf{P}}, \hat{\underline{\mathbf{h}}}_k) + \mathbf{M}_k \mathbf{R}_k(\underline{\mathbf{P}}, \beta_k) + \mathbf{R}_k^T(\underline{\mathbf{P}}, \beta_k) \mathbf{M}_k^T \geq \mathbf{0}, \quad (4.15)$$

where the matrices \mathbf{M}_k and $\mathbf{R}_k(\underline{\mathbf{P}}, \beta_k)$ are:

$$\mathbf{M}_k = \mathbf{I}_{(2K+2)} \otimes \underline{\mathbf{e}}_k, \quad (4.16)$$

$$\mathbf{R}_k(\underline{\mathbf{P}}, \beta_k) = \begin{bmatrix} \frac{1}{2}\beta_k \underline{\mathbf{p}}_k & [\underline{\mathbf{P}}, \mathbf{0}] \\ \mathbf{0} & (\frac{1}{2}\beta_k) \mathbf{I}_{(2K+1)} \otimes \underline{\mathbf{p}}_k \end{bmatrix}. \quad (4.17)$$

From (4.16), we observe that the uncertainty matrix \mathbf{M}_k belongs to a subspace \mathcal{M} of block diagonal matrices with equal blocks. Specifically,

$$\mathcal{M} = \{\mathbf{M} \mid \mathbf{M} = \mathbf{I}_{(2K+2)} \otimes \underline{\mathbf{e}}, \underline{\mathbf{e}} \in \mathbb{R}^{1 \times 2N_t}\}. \quad (4.18)$$

Hence, the spectral norm of \mathbf{M}_k is $\|\mathbf{M}_k\| = \|\underline{\mathbf{e}}_k\| \leq \delta_k$. Using (4.14)–(4.18), the robust QoS design problem in (4.13) can also be formulated as the following semi-infinite robust semidefinite program (SDP):

$$\min_{\underline{\mathbf{P}}, t} t \quad (4.19a)$$

$$\text{s. t.} \quad \|\text{vec}([\underline{\mathbf{p}}_1, \dots, \underline{\mathbf{p}}_K])\| \leq t, \quad (4.19b)$$

$$\bar{\mathbf{F}}_k(\underline{\mathbf{P}}, \hat{\underline{\mathbf{h}}}_k, \mathbf{M}_k) \geq \mathbf{0}, \quad \forall \mathbf{M}_k \in \mathcal{M}, \|\mathbf{M}_k\| \leq \delta_k, \quad 1 \leq k \leq K. \quad (4.19c)$$

A general instance of (4.19) is NP-hard for a general subspace \mathcal{M} , [83]; see also [81, 84]. This result and the undetermined tractability of the robust SOCP in (4.13) suggest that in order to obtain a robust design technique that is guaranteed to be computationally tractable, we will need to modify the formulation of (4.13) or (4.19). In the following section, we will present three conservative design approaches that yield convex and efficiently-solvable restrictions of (4.13) and (4.19). These approaches are conservative in the sense that they guarantee that the SINR constraints

are satisfied for a larger set of channel uncertainties than that described in (4.12), and hence the resulting transmission power is larger than (or equal to) that of an optimal solution to (4.13), if such a solution could be found. The three approaches yield SDP formulations that offer different trade-offs between the degree of conservatism and the size of the resulting SDP (and hence its computational cost).

4.4 Conservative Approaches to Robust Precoder Design with QoS Constraints

4.4.1 Robust SOCP with Independent Uncertainty

In this section, we will work directly with the robust SOCP formulation in (4.13). The presence of $\underline{\mathbf{h}}_k$ on both the left and right hand sides of each SOC constraint in (4.13c) means that these terms vary together and share the same ellipsoidal uncertainty region. We will obtain a conservative robust design by assuming independent uncertainties for $\underline{\mathbf{h}}_k$ on the left and right hand sides of (4.13c). Relaxing the common uncertainty structure in this way will result in a tractable restriction of (4.13) that can be formulated as an SDP. To obtain that SDP, we will use the following lemma [81]:

Lemma 4.1. *Consider the robust SOCP:*

$$\begin{aligned} \min_{\mathbf{x}} \quad & \mathbf{c}^T \mathbf{x} \\ \text{s. t.} \quad & \|\mathbf{A}\mathbf{x} + \mathbf{b}\| \leq \mathbf{f}^T \mathbf{x} + g \quad \forall \mathbf{A} \in \mathcal{Y}, \mathbf{f} \in \mathcal{W}, \end{aligned}$$

where the ellipsoidal uncertainty regions $\mathcal{Y} = \{\mathbf{A} \mid \mathbf{A} = \mathbf{A}^0 + \sum_{j=1}^y \theta_j \mathbf{A}^j, \|\boldsymbol{\theta}\| \leq 1\}$ and $\mathcal{W} = \{\mathbf{f} \mid \mathbf{f} = \mathbf{f}^0 + \sum_{j=1}^w \phi_j \mathbf{f}^j, \|\boldsymbol{\phi}\| \leq 1\}$ are independent. This robust SOCP is

equivalent to the following SDP:

$$\begin{aligned}
 & \min_{\mathbf{x}, \mu, \lambda} \quad \mathbf{c}^T \mathbf{x} \\
 & \text{s. t.} \quad \begin{bmatrix} \lambda - \mu & \mathbf{0} & (\mathbf{A}^0 \mathbf{x} + \mathbf{b})^T \\ \mathbf{0} & \mu \mathbf{I} & [\mathbf{A}^1 \mathbf{x} \dots \mathbf{A}^y \mathbf{x}]^T \\ \mathbf{A}^0 \mathbf{x} + \mathbf{b} & [\mathbf{A}^1 \mathbf{x} \dots \mathbf{A}^y \mathbf{x}] & \lambda \mathbf{I} \end{bmatrix} \geq \mathbf{0}, \\
 & \quad \begin{bmatrix} \mathbf{f}^0{}^T \mathbf{x} + g - \lambda & [\mathbf{f}^1{}^T \mathbf{x} \dots \mathbf{f}^w{}^T \mathbf{x}] \\ [\mathbf{f}^1{}^T \mathbf{x} \dots \mathbf{f}^w{}^T \mathbf{x}]^T & (\mathbf{f}^0{}^T \mathbf{x} + g - \lambda) \mathbf{I} \end{bmatrix} \geq \mathbf{0}.
 \end{aligned}$$

□

By writing $\underline{\mathbf{h}}_k = \hat{\underline{\mathbf{h}}}_k + \underline{\mathbf{e}}_k = \hat{\underline{\mathbf{h}}}_k + \delta_k \mathbf{u}$, $\|\mathbf{u}\| \leq 1$, and invoking Lemma 4.1, we obtain the following SDP formulation of a conservative version of (4.13):

$$\min_{\underline{\mathbf{P}}, \mu, \lambda, t} \quad t \tag{4.22a}$$

$$\text{s. t.} \quad \|\text{vec}([\underline{\mathbf{p}}_1, \dots, \underline{\mathbf{p}}_K])\| \leq t, \tag{4.22b}$$

$$\mathbf{A}_k(\underline{\mathbf{P}}, \lambda_k, \mu_k, \delta_k) = \begin{bmatrix} \lambda_k - \mu_k & \mathbf{0} & [\hat{\underline{\mathbf{h}}}_k \underline{\mathbf{P}}, \sigma_{n_k}] \\ \mathbf{0} & \mu_k \mathbf{I}_{2N_t} & \delta_k [\underline{\mathbf{P}}, \mathbf{0}] \\ [\hat{\underline{\mathbf{h}}}_k \underline{\mathbf{P}}, \sigma_{n_k}]^T & \delta_k [\underline{\mathbf{P}}, \mathbf{0}]^T & \lambda_k \mathbf{I}_{(2K+1)} \end{bmatrix} \geq \mathbf{0}, \quad 1 \leq k \leq K, \tag{4.22c}$$

$$\mathbf{B}_k(\underline{\mathbf{P}}, \lambda_k, \delta_k, \beta_k) = \begin{bmatrix} \beta_k \hat{\underline{\mathbf{h}}}_k \underline{\mathbf{P}}_k - \lambda_k & \delta_k \beta_k \underline{\mathbf{p}}_k^T \\ \delta_k \beta_k \underline{\mathbf{p}}_k & (\beta_k \hat{\underline{\mathbf{h}}}_k \underline{\mathbf{P}}_k - \lambda_k) \mathbf{I}_{2N_t} \end{bmatrix} \geq \mathbf{0}, \quad 1 \leq k \leq K. \tag{4.22d}$$

This problem can be efficiently solved using general purpose implementations of interior point methods; e.g., SeDuMi [85].

4.4.2 Robust SDP with Unstructured Uncertainty

In this section and the following one, we will obtain two conservative robust designs from the SDP formulation in (4.19) of the original design problem. The difficulty of solving (4.19) arises from the particular structure that the matrix \mathbf{M}_k must possess. In this section we will show that if we restrict the robust design so that the SINR targets are to be satisfied for all $\|\mathbf{M}_k\| \leq \delta_k$ rather than just those $\mathbf{M}_k \in \mathcal{M}$ that satisfy $\|\mathbf{M}_k\| \leq \delta_k$, then one can obtain an efficiently-solvable problem. That is, we will show that by replacing (4.19c) by

$$\bar{\mathbf{F}}_k(\underline{\mathbf{P}}, \underline{\mathbf{h}}_k, \mathbf{M}_k) \geq \mathbf{0}, \quad \forall \|\mathbf{M}_k\| \leq \delta_k, \quad 1 \leq k \leq K, \quad (4.23)$$

one can obtain a restriction of (4.19) that can be efficiently solved.

Although (4.23) is simpler than (4.19c), it still represents an infinite set of LMIs, one for each \mathbf{M}_k that satisfies $\|\mathbf{M}_k\| \leq \delta_k$. However, by using the following lemma, which is a special case of a more general result in [84], this semi-infinite LMI constraint can be precisely transformed into a single LMI.

Lemma 4.2. *Let $\mathbf{F}(\mathbf{x})$ be a symmetric matrix, and let $\mathbf{F}(\mathbf{x})$ and $\mathbf{R}(\mathbf{x})$ be affine functions of \mathbf{x} . Then*

$$\bar{\mathbf{F}}(\mathbf{x}, \mathbf{M}) = \mathbf{F}(\mathbf{x}) + \mathbf{M}\mathbf{R}(\mathbf{x}) + \mathbf{R}^T(\mathbf{x})\mathbf{M}^T \geq \mathbf{0}, \quad \forall \|\mathbf{M}\| \leq \delta \quad (4.24)$$

if and only if there exists a scalar τ such that

$$\begin{bmatrix} \mathbf{F}(\mathbf{x}) - \tau\mathbf{I} & \mathbf{R}^T(\mathbf{x}) \\ \mathbf{R}(\mathbf{x}) & \tau\delta^{-2}\mathbf{I} \end{bmatrix} \geq \mathbf{0}.$$

□

By applying the result of Lemma 4.2 to the LMIs in (4.23), we obtain the following efficiently-solvable SDP formulation for a conservative approach to the robust

precoder design problem:

$$\min_{\mathbf{P}, t, \tau_1, \dots, \tau_K} t \quad (4.25a)$$

$$\text{s. t. } \|\text{vec}([\mathbf{p}_1, \dots, \mathbf{p}_K])\| \leq t, \quad (4.25b)$$

$$\begin{bmatrix} \mathbf{F}_k(\mathbf{P}, \hat{\mathbf{h}}_k) - \tau_k \mathbf{I}_{(2K+2)} & \mathbf{R}^T(\mathbf{P}, \beta_k) \\ \mathbf{R}(\mathbf{P}, \beta_k) & \tau_k \delta_k^{-2} \mathbf{I}_q \end{bmatrix} \geq \mathbf{0}, \quad 1 \leq k \leq K, \quad (4.25c)$$

where $\mathbf{F}_k(\mathbf{P}, \hat{\mathbf{h}}_k)$ and $\mathbf{R}(\mathbf{P}, \beta_k)$ were defined in (4.14) and (4.17), respectively, and $q = 4N_t(K + 1)$.

4.4.3 Robust SDP with Structured Uncertainty

The efficiently-solvable conservative formulation in (4.25) was obtained by relaxing the structural constraint $\mathbf{M}_k \in \mathcal{M}$ in (4.19). In this section we will obtain a less conservative formulation of (4.19) that results in an SDP that retains this structural constraint.

We begin with a definition. Given an arbitrary subspace of matrices $\tilde{\mathcal{M}}$, let $\mathcal{B}_{\tilde{\mathcal{M}}}$ denote the following set of matrices associated with $\tilde{\mathcal{M}}$:

$$\mathcal{B}_{\tilde{\mathcal{M}}} = \{(\mathbf{S}, \mathbf{T}, \mathbf{G}) \mid \mathbf{S}\mathbf{M} = \mathbf{M}\mathbf{T}, \mathbf{G}\mathbf{M} = -\mathbf{M}^T\mathbf{G}^T, \quad \forall \mathbf{M} \in \tilde{\mathcal{M}}\}. \quad (4.26)$$

For the subspace \mathcal{M} in (4.18), applying (4.26) yields:

$$\mathbf{T} = \mathbf{S} \otimes \mathbf{I}_{2N_t}, \quad \mathbf{G} = \mathbf{0}, \quad (4.27)$$

where $\mathbf{S} \in \mathbb{R}^{(2K+2) \times (2K+2)}$. Although the construction of $\mathcal{B}_{\mathcal{M}}$ may appear to be arbitrary, it enables us to develop an SDP formulation of a conservative design that retains the structure $\mathbf{M}_k \in \mathcal{M}$. To do so, we will use the following result, which is a special case of a more general result in [84].

Lemma 4.3. *Consider the following robust SDP problem:*

$$\begin{aligned} & \min_{\mathbf{x}} \quad \mathbf{c}^T \mathbf{x} \\ & \text{s. t.} \quad \bar{\mathbf{F}}(\mathbf{x}, \mathbf{M}) = \mathbf{F}(\mathbf{x}) + \mathbf{M}\mathbf{R}(\mathbf{x}) + \mathbf{R}^T(\mathbf{x})\mathbf{M}^T \geq \mathbf{0}, \quad \forall \mathbf{M} \in \tilde{\mathcal{M}}, \|\mathbf{M}\| \leq \delta, \end{aligned}$$

where $\mathbf{F}(\mathbf{x})$ and $\mathbf{R}(\mathbf{x})$ are affine functions of \mathbf{x} , and the subspace $\tilde{\mathcal{M}}$ is arbitrary. Let $\mathcal{B}_{\tilde{\mathcal{M}}}$ denote the set of matrices in (4.26) associated with $\tilde{\mathcal{M}}$. An upper bound on the optimal value of this robust SDP and a corresponding solution \mathbf{x} can be obtained by solving the following SDP:

$$\begin{aligned} & \min_{\mathbf{x}, \mathbf{S}, \mathbf{T}, \mathbf{G}} \quad \mathbf{c}^T \mathbf{x} \\ & \text{s. t.} \quad (\mathbf{S}, \mathbf{T}, \mathbf{G}) \in \mathcal{B}_{\mathcal{M}}, \\ & \quad \mathbf{S} \geq \mathbf{0}, \\ & \quad \begin{bmatrix} \mathbf{F}(\mathbf{x}) - \mathbf{S} & \mathbf{R}^T(\mathbf{x}) + \mathbf{G} \\ \mathbf{R}(\mathbf{x}) - \mathbf{G} & \delta^{-2}\mathbf{T} \end{bmatrix} \geq \mathbf{0}. \end{aligned}$$

□

By applying Lemma 4.3 to (4.19), using the characterization of $\mathcal{B}_{\mathcal{M}}$ in (4.27), it can be shown that the solution of the following SDP generates a conservative solution to the original design problem:

$$\begin{aligned} & \min_{\substack{\mathbf{P}, t \\ \mathbf{S}_k = \mathbf{S}_k^T, 1 \leq k \leq K}} \quad t \end{aligned} \tag{4.30a}$$

$$\text{s. t.} \quad \|\text{vec}([\mathbf{p}_1, \dots, \mathbf{p}_K])\| \leq t, \tag{4.30b}$$

$$\begin{bmatrix} \mathbf{F}_k(\mathbf{P}, \hat{\mathbf{h}}_k) - \mathbf{S}_k & \mathbf{R}^T(\mathbf{P}, \beta_k) \\ \mathbf{R}(\mathbf{P}, \beta_k) & \delta_k^{-2}\mathbf{S}_k \otimes \mathbf{I}_{2N_t} \end{bmatrix} \geq \mathbf{0}, \quad 1 \leq k \leq K, \tag{4.30c}$$

where $\mathbf{F}_k(\mathbf{P}, \hat{\mathbf{h}}_k)$ and $\mathbf{R}(\mathbf{P}, \beta_k)$ are as defined in the previous section, and we have exploited the fact that (4.30c) implies that $\mathbf{S}_k \otimes \mathbf{I} \geq \mathbf{0}$ and hence that $\mathbf{S}_k \geq \mathbf{0}$, which

eliminates the constraints that would have been generated by the constraint $\mathbf{S} \geq \mathbf{0}$ in Lemma 4.3. We would like to point out that the SDP in (4.25) is the special case of the SDP in (4.30) that is obtained when $\mathbf{S}_k = \tau_k \mathbf{I}$. Therefore, the solution of (4.30) yields a tighter upper bound on the minimum power required to solve the original problem than the solution of (4.25).

4.4.4 Some Comparisons

As we have just pointed out, the structured robust SDP in (4.30) yields a tighter upper bound on the minimum transmission power than the unstructured SDP in (4.25). Furthermore, our numerical experiments suggest that the unstructured SDP in (4.25) provides a tighter upper bound than that obtained from the robust SOCP with independent uncertainties in (4.22). Given this performance hierarchy, it is of interest to examine the relative size and structure of each of the proposed formulations, and that of the design problem for the case of perfect CSI; c.f. (4.10). We have collected this information in Table 4.1, where the “core” design variables are the $2N_t K$ unique elements of $\underline{\mathbf{P}}$ and the scalar t . In the robust SOCP formulation, each (unique) element of $\underline{\mathbf{P}}$ enters all of the LMIs in (4.22c) and one of the LMIs in (4.22d), and in the robust SDP formulations, each element of $\underline{\mathbf{P}}$ enters all the LMIs. The additional variables in the robust SOCP formulation are the $2K$ scalars, λ_k and μ_k . Each λ_k is involved in 2 LMIs (one from the set in (4.22c) and one from the set in (4.22d)) and each μ_k is involved in only one. The additional variables in the unstructured robust SDP formulation are the K scalars τ_k , and each one is involved in only one LMI. In the structured robust SDP formulation, the additional variables take the form of the K symmetric matrices \mathbf{S}_k , each of which is of size $(2K + 2) \times (2K + 2)$ and is involved in only one LMI. In addition to the structure of the additional variables, Table 4.1 also emphasizes the fact that the constraints in the two robust SDP approaches have the

same structure, while that of the robust SOCP approach is somewhat simpler. These observations show that the improved bounds provided by the robust SDP approaches do incur an increase of the size of the SDP. However, our numerical experiments in Section 4.6 suggest that in some applications the improved performance will justify this increase in size.

Table 4.1: A comparison of the size and structure of various design methods

Method	Number of Variables		Number of Constraints	
	Core	Additional	SOC num; size	LMI num; size
Perfect CSI (4.10)	$2N_t K + 1$		1; $2N_t K + 1$ K ; $K + 2$ K lin. equalities	
Robust SOCP (4.22)	$2N_t K + 1$	$2K$	1; $2N_t K + 1$	K ; $2N_t + 2K + 2$ K ; $2N_t + 1$
Robust SDP, Unst. (4.25)	$2N_t K + 1$	K	1; $2N_t K + 1$	K ; $2(K + 1)(2N_t + 1)$
Robust SDP, Struct. (4.30)	$2N_t K + 1$	$K(K + 1)(2K + 3)$	1; $2N_t K + 1$	K ; $2(K + 1)(2N_t + 1)$

4.4.5 Maximum Allowable Uncertainty Size

Up until this point, we have focused on problems in which the goal has been to minimize the transmission power required to guarantee that the SINR of each user exceeds the required value for every channel uncertainty in the bounded set in (4.12). As mentioned in Section 4.2, for the class of systems with full row rank channel matrices, \mathbf{H} , the QoS requirements can always be satisfied in the absence of channel uncertainty, but this is not the case when the transmitter's model for the channel is inaccurate. This fact raises the question of whether one can determine, for a given set of channel estimates, the largest uncertainty set for which the robust QoS guarantee can be made. That is, find the largest value of δ , namely δ_{\max} , such that (4.13) (or (4.19)) has a finite solution. This problem is of interest in the design of quantization codebooks for feeding back estimates of the channel to the transmitter. In particular, one may wish to choose the rate of the codebooks to be large enough (and the quantization cells small enough) so that it is possible to design a robust precoder with finite power. As we will point out below, we can obtain efficiently solvable formulations for lower bounds on δ_{\max} by using the conservative approaches to the robust QoS design problem.

Using the first conservative approach in Section 4.4.1, it can be shown that the optimal value of the following problem is a lower bound on δ_{\max} :

$$\max_{\underline{\mathbf{P}}, \mu, \lambda, \rho} \rho \quad (4.31a)$$

$$\text{s. t. } \mathbf{A}_k(\underline{\mathbf{P}}, \lambda_k, \mu_k, \rho) \geq \mathbf{0}, \quad 1 \leq k \leq K, \quad (4.31b)$$

$$\mathbf{B}_k(\underline{\mathbf{P}}, \lambda_k, \rho, \beta_k) \geq \mathbf{0}, \quad 1 \leq k \leq K. \quad (4.31c)$$

where $\mathbf{A}_k(\underline{\mathbf{P}}, \lambda_k, \mu_k, \rho)$ and $\mathbf{B}_k(\underline{\mathbf{P}}, \lambda_k, \rho, \beta_k)$ are as defined in (4.22c) and (4.22d), respectively. Although similar to (4.22), the above problem is not jointly convex in $\underline{\mathbf{P}}$ and ρ , since the constraints (4.31b) and (4.31c) are not jointly affine. However, this

problem is quasi-convex (c.f. [82]), and an optimal solution can be efficiently found using a one-dimensional bisection search on ρ in which the problem solved at each step is the convex feasibility problem corresponding to (4.31) with a fixed value for ρ .

Using the structured robust SDP approach in Section 4.4.3, it can be shown that $\delta_{\max} \geq (\alpha^*)^{-1/2}$, where α^* is the optimal value of the following quasi-convex optimization problem

$$\begin{aligned} \min_{\substack{\underline{\mathbf{P}}, \alpha \\ \mathbf{S}_k = \mathbf{S}_k^T, 1 \leq k \leq K}} \quad & \alpha & (4.32a) \\ \text{s. t.} \quad & \begin{bmatrix} \mathbf{F}_k(\underline{\mathbf{P}}, \hat{\mathbf{h}}_k) - \mathbf{S}_k & \mathbf{R}^T(\underline{\mathbf{P}}, \beta_k) \\ \mathbf{R}(\underline{\mathbf{P}}, \beta_k) & \alpha \mathbf{S}_k \otimes \mathbf{I}_{2N_t} \end{bmatrix} \geq \mathbf{0}, \quad 1 \leq k \leq K. & (4.32b) \end{aligned}$$

(The unstructured robust SDP approach leads to the special case in which $\mathbf{S}_k = \tau_k \mathbf{I}$.) This problem can be solved using bisection search on α . Furthermore, by observing that the constraints in (4.32b) can be written as

$$\alpha \begin{bmatrix} \mathbf{0} & \mathbf{0} \\ \mathbf{0} & \mathbf{S}_k \otimes \mathbf{I}_{2N_t} \end{bmatrix} - \begin{bmatrix} -\mathbf{F}_k(\underline{\mathbf{P}}, \hat{\mathbf{h}}_k) + \mathbf{S}_k & -\mathbf{R}^T(\underline{\mathbf{P}}, \beta_k) \\ -\mathbf{R}(\underline{\mathbf{P}}, \beta_k) & \mathbf{0} \end{bmatrix} \geq \mathbf{0}, \quad 1 \leq k \leq K, \quad (4.33)$$

one can show that (4.32) is equivalent to minimizing the largest generalized eigenvalue of a pair of (block diagonal) symmetric matrices that depend affinely on the decision variables [84, 86]. Identifying (4.32) as lying within this class of problems is of interest because efficient algorithms that exploit the structure of the constituent matrices in (4.33) are available for such problems; c.f. [86, 87].

4.5 Fair SINR Maximization

In the previous section, we considered problems that required each user to be provided with an SINR that is at least as large as a given SINR requirement, even in the

presence of uncertainty. In this section, we consider the related problem of maximizing the SINR of the “weakest” user subject to a transmitted power constraint, in scenarios with uncertain CSI. Problems of this form are sometimes called max-min fair SINR problems; e.g., [63,64]. While most formulations of max-min fair SINR problems have focussed on the case of perfect CSI, under the bounded uncertainty model in (4.12) the robust max-min fair SINR problem can be stated as⁶

$$\max_{\underline{\mathbf{P}}, \gamma_0} \gamma_0 \quad (4.34a)$$

$$\text{s. t. } \text{SINR}_k \geq \gamma_0, \quad \forall \underline{\mathbf{h}}_k \in \mathcal{U}_k(\delta_k), \quad 1 \leq k \leq K, \quad (4.34b)$$

$$\frac{1}{2} \text{tr}(\underline{\mathbf{P}}\underline{\mathbf{P}}^T) \leq P_{\text{total}}. \quad (4.34c)$$

By defining $\beta_0 = \sqrt{1 + 1/\gamma_0}$ and using the SOC characterization of the QoS constraints in (4.10c), this problem can be cast as the following (semi-infinite) quasi-convex optimization problem (see [64] for a related formulation for the case of perfect CSI)

$$\min_{\underline{\mathbf{P}}, \beta_0} \beta_0 \quad (4.35a)$$

$$\text{s. t. } \|\underline{\mathbf{h}}_k \underline{\mathbf{P}}, \sigma_{n_k}\| \leq \beta_0 \underline{\mathbf{h}}_k \underline{\mathbf{P}}_k, \quad \forall \underline{\mathbf{h}}_k \in \mathcal{U}_k(\delta_k), \quad 1 \leq k \leq K, \quad (4.35b)$$

$$\|\text{vec}([\underline{\mathbf{p}}_1, \dots, \underline{\mathbf{p}}_K])\| \leq P_{\text{total}}. \quad (4.35c)$$

⁶Although we will not discuss them here, the “per-antenna” and “shaping” power constraints discussed in Appendix D can be easily incorporated into the proposed framework.

Efficient formulations for precoders that minimize upper bounds on β_0 (and hence maximize lower bounds on γ_0) can be obtained by applying the conservative approaches of Section 4.4 to (4.35). In particular, by applying the robust SOCP approach in Section 4.4.1, one obtains the following quasi-convex problem:

$$\min_{\underline{\mathbf{P}}, \mu, \lambda, \beta_0} \beta_0 \quad (4.36a)$$

$$\text{s. t. } \mathbf{A}_k(\underline{\mathbf{P}}, \lambda_k, \mu_k, \delta_k) \geq \mathbf{0}, \quad 1 \leq k \leq K, \quad (4.36b)$$

$$\mathbf{B}_k(\underline{\mathbf{P}}, \lambda_k, \delta_k, \beta_0) \geq \mathbf{0}, \quad 1 \leq k \leq K, \quad (4.36c)$$

$$\|\text{vec}([\underline{\mathbf{p}}_1, \dots, \underline{\mathbf{p}}_K])\| \leq P_{\text{total}}, \quad (4.36d)$$

where $\mathbf{A}_k(\underline{\mathbf{P}}, \lambda_k, \mu_k, \delta_k)$ and $\mathbf{B}_k(\underline{\mathbf{P}}, \lambda_k, \delta_k, \beta_0)$ were defined in (4.22c) and (4.22c), respectively. This problem can be efficiently solved by using a bisection search on β_0 in which problem solved at each step is the convex feasibility problem generated by (4.36) with a fixed value of β_0 . Similarly, the structured robust SDP approach of Section 4.4.3 yields the following quasi-convex problem that can also be efficiently solved using a bisection search on β_0 :

$$\min_{\substack{\underline{\mathbf{P}}, \beta_0 \\ \mathbf{S}_k = \mathbf{S}_k^T, 1 \leq k \leq K}} \beta_0 \quad (4.37a)$$

$$\text{s. t. } \begin{bmatrix} \mathbf{F}_k(\underline{\mathbf{P}}, \hat{\mathbf{h}}_k) - \mathbf{S}_k & \mathbf{R}^T(\underline{\mathbf{P}}, \beta_0) \\ \mathbf{R}(\underline{\mathbf{P}}, \beta_0) & \delta_k^{-2} \mathbf{S}_k \otimes \mathbf{I}_{2N_t} \end{bmatrix} \geq \mathbf{0}, \quad 1 \leq k \leq K, \quad (4.37b)$$

$$\|\text{vec}([\underline{\mathbf{p}}_1, \dots, \underline{\mathbf{p}}_K])\| \leq P_{\text{total}}. \quad (4.37c)$$

4.6 Numerical Results

In this section we will compare the performance of the three proposed approaches to robust QoS precoding, namely the robust SOCP design (RSOCP) with independent uncertainty in Section 4.4.1, the unstructured robust SDP (RSDP-Unstruct.) in

Section 4.4.2, and the robust SDP that preserves structure (RSDP-Struct.) in Section 4.4.3. We will also provide performance comparisons with some existing approaches, namely the robust autocorrelation matrix approach in [61,62] (Robust Correl. Appr.), and the robust downlink power loading approach in [69]. The approach in [69] requires the beamforming vectors to be specified, and we will consider two choices: the columns of the pseudo-inverse of $\hat{\mathbf{H}}$ (Robust Power Load. 1); and the beamforming vectors obtained by assuming that $\hat{\mathbf{H}}$ is the actual channel and using the existing methods for QoS precoding with perfect CSI [59–64] (Robust Power Load. 2). The approaches in [61,62] and [69] are based on uncertainty models that are different from the one in (4.12), and from each other. The approach in [61,62] considers a model in which the spectral norm of the error in the (deterministic) autocorrelation matrix $\mathbf{C}_k = \mathbf{h}_k^H \mathbf{h}_k$ is bounded, and in the approach in [69] the Frobenius norm of the error in \mathbf{C}_k is bounded. However, by bounding these norms of \mathbf{C}_k in terms of the norm of \mathbf{e}_k , a comparable uncertainty set can be generated.⁷ We will compare these schemes in an environment with $N_t = 3$ transmit antennas and $K = 3$ users. In our experiments, we will evaluate performance statistics for the standard case of independent Rayleigh fading channels in which the coefficients of the fading channels are modeled as being independent proper complex Gaussian random variables with zero-mean and unit variance, and the receivers' noise sources are modeled as zero-mean, additive, white, and Gaussian with unit variance.

In our first experiment, we randomly generated 2000 realizations of the set of channel estimates $\{\hat{\mathbf{h}}_k\}_{k=1}^K$ and examined the performance of each method in the

⁷A bound on the spectral norm of the error in the matrix \mathbf{C}_k can be obtained as follows: $\|(\hat{\mathbf{h}}_k + \mathbf{e}_k)^H (\hat{\mathbf{h}}_k + \mathbf{e}_k) - \hat{\mathbf{h}}_k^H \hat{\mathbf{h}}_k\| = \|\hat{\mathbf{h}}_k^H \mathbf{e}_k + \mathbf{e}_k^H \hat{\mathbf{h}}_k + \mathbf{e}_k^H \mathbf{e}_k\| \leq \|\hat{\mathbf{h}}_k^H \mathbf{e}_k\| + \|\mathbf{e}_k^H \hat{\mathbf{h}}_k\| + \|\mathbf{e}_k^H \mathbf{e}_k\| = 2\|\hat{\mathbf{h}}_k\| \|\mathbf{e}_k\| + \|\mathbf{e}_k\|^2$. The same bound also holds for the Frobenius norm, since the matrices on the immediate right hand side of the inequality are all rank one. Furthermore, the uncertainty $\mathbf{e}_k = \delta_k \hat{\mathbf{h}}_k / \|\hat{\mathbf{h}}_k\|$ achieves this upper bound with equality for both norms. (See also [88].) That said, the uncertainty models in [61,62,69] accommodate matrices that are not positive semidefinite, whereas the model proposed in Section 4.2.2 always results in a positive semidefinite autocorrelation.

presence of equal uncertainty, $\delta_k = \delta, \forall k$. The QoS requirement of each user is that the SINR is at least 10 dB. For each set of channel estimates and for each value of δ we determined whether each design method is able to generate a precoder (of finite power) that guarantees that the SINR constraints are satisfied in the presence of the modeled uncertainty. In Fig. 4.1 we provide the percentage of the 2000 channel realizations for which each method generated a precoder with finite power, as a function of the size of the uncertainty. From this figure, it is clear that the RSDP approach that preserves the structure of the uncertainty is able to provide robust QoS guarantees for a significantly larger percentage of the channels and for significantly larger uncertainty sets than the other methods. The unstructured SDP approach provides a reasonable degree of robustness to channel uncertainty compared to that provided by the RSOCP approach, the robust autocorrelation approach in [61,62], and the robust power loading approach in [69].

In our second experiment, we selected those sets of channel estimates from the 2000 sets used in the first experiment for which all design methods were able to provide robust QoS guarantees for all uncertainties with $\delta \leq 0.015$. We calculated the average, over the 609 such channel environments, of the transmitted power required to achieve these robust QoS guarantees and we have plotted the results for different values of δ in Fig. 4.2(a). The average transmitted power approaches infinity for a certain value of δ when for one (or more) of the channel estimates the method under consideration cannot provide the robust QoS guarantee with finite power. The excellent performance of the structured RSDP method and the good performance of the unstructured RSDP method that were apparent in Fig. 4.1 are also apparent in Fig. 4.2(a). In Fig. 4.2(b), we provide a detail of Fig. 4.2(a) in order to demonstrate the relative difference in the performance of the RSOCP approach, the robust autocorrelation approach in [61,62], and the robust power loading approach in [69].

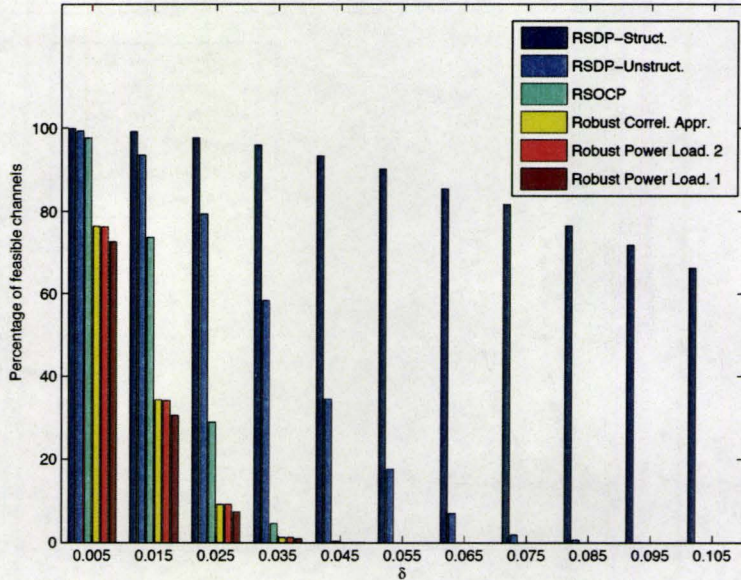
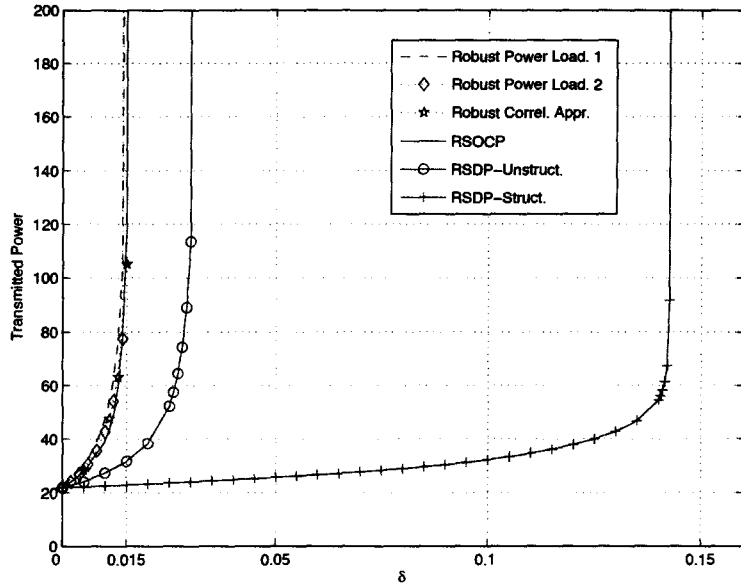


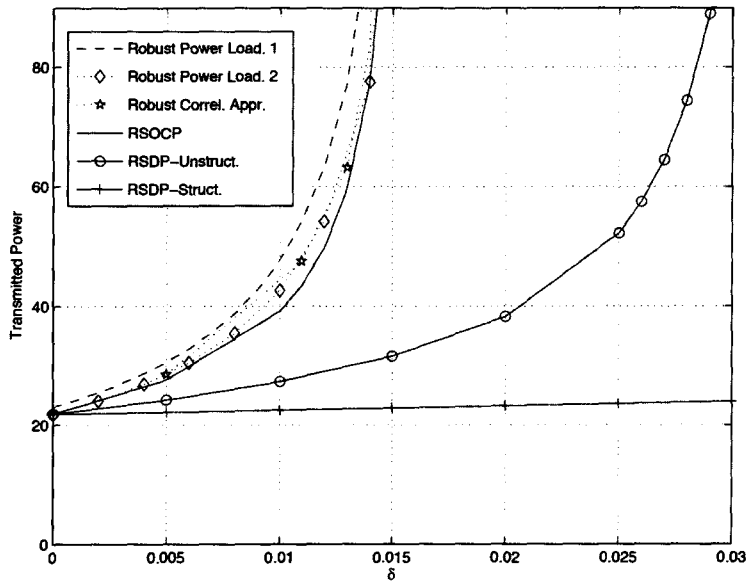
Figure 4.1: Percentage of channel realizations for which the robust QoS guarantee can be made against the uncertainty size δ , for a system with $N_t = 3$ and $K = 3$.

In the third experiment, we used the 2000 randomly generated realizations of the estimates of the channel environments from the first experiment, and for each scenario we used the methods in Section 4.4.5 to find lower bounds on the value of the uncertainty, δ_{\max} , above which each design method is unable guarantee the SINR requirements in the presence of the modeled uncertainty. In these experiments the size of uncertainty was the same for each user (i.e., $\delta_k = \delta, \forall k$), and the minimum SINR requirement of each user was 10 dB. In Fig. 4.3 we plot the cumulative distribution function (CDF) of the lower bound on δ_{\max} for each method. From this figure, it is clear that the relative performance of each method under this performance metric is similar to that established from the first two experiments.

In the fourth experiment, we examine the performance of the 2000 randomly generated realizations of the set of channel estimates $\{\hat{\mathbf{h}}_k\}_{k=1}^K$ in the presence of equal uncertainty, $\delta_k = \delta = 0.05, \forall k$. The SINR requirements of the three users are equal



(a)



(b)

Figure 4.2: Average of the transmitted power $\text{tr}(\mathbf{P}^H \mathbf{P})$, on a linear scale, versus uncertainty size δ for a system with $N_t = 3$ and $K = 3$. Part (b) is a detail of part (a).

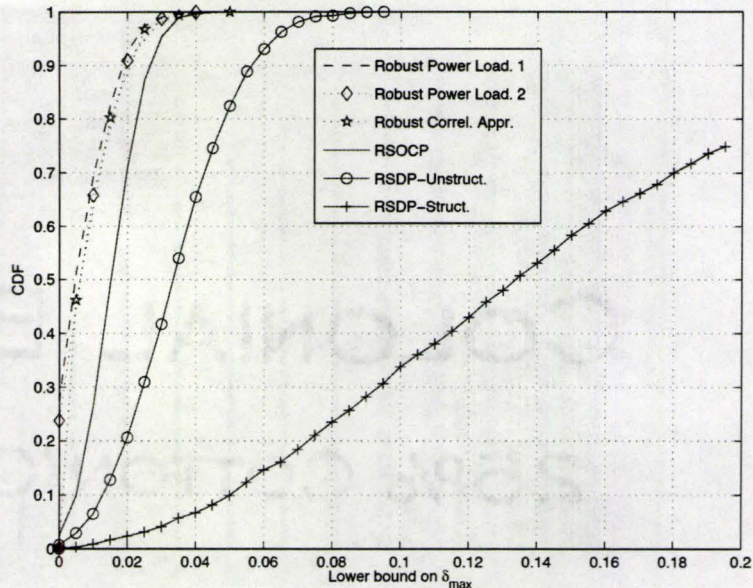


Figure 4.3: The (empirical) cumulative distribution function (CDF) of lower bounds on δ_{\max} for a system with $N_t = 3$ and $K = 3$.

and varied from 0 to 25 dB. For each set of channel estimates and for each value of the required SINR we determined whether each design method is able to generate a precoder (of finite power) that guarantees the required SINRs. In Fig. 4.4 we provide a histogram of the fraction of the 2000 channel realizations for which each method generated a precoder with finite power. From this figure, it is clear that both robust SDP approaches are able to provide robust QoS guarantees for a wider range of required SINRs than the other methods, with the structured SDP approach having a significant advantage.

In the fifth experiment, we selected all the sets of channel estimates from the 2000 sets used in the previous experiment for which all design methods were able to provide robust QoS guarantees for all SINRs less than or equal to 6dB. We calculated the average, over the 264 such channel environments, of the transmitted power required to achieve these robust QoS guarantees. We have plotted the equal SINR requirement

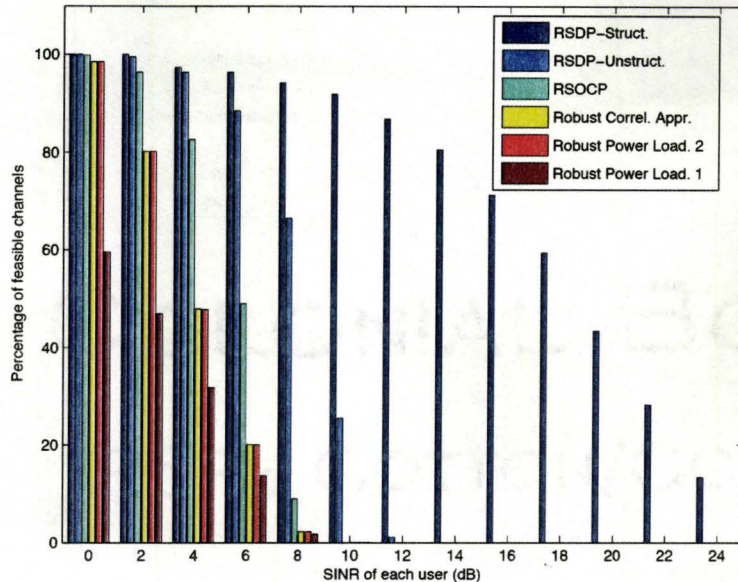


Figure 4.4: Percentage of channel realizations for which the robust QoS guarantee can be made against the required SINRs, for a system with $N_t = 3$ and $K = 3$.

of each user versus the average transmitted power in Fig. 4.5. In order to assess the additional power required to achieve robustness, we have included the corresponding curve for the case of perfect CSI at the transmitter; c.f. [59–64] and (4.10). This figure illustrates the saturation effect that channel uncertainty imposes on the growth of the SINR of each user with the transmitted power. This effect was observed in [8] for non-robust linear precoding on the MISO downlink with quantized CSI. Fig. 4.5 also illustrates the role that robust precoding can play in extending the SINR interval over which linear growth with the transmitted power can be achieved. This is particularly evident for the robust SDP approaches.

In the sixth experiment, we examine the performance of the 2000 randomly generated realizations of the set of channel estimates $\{\hat{\mathbf{h}}_k\}_{k=1}^K$ in the presence of equal uncertainty, $\delta_k = \delta = 0.05, \forall k$. The SINR requirements of the three users are equal and varied from 0 to 25 dB. For each set of channel estimates, we determine the

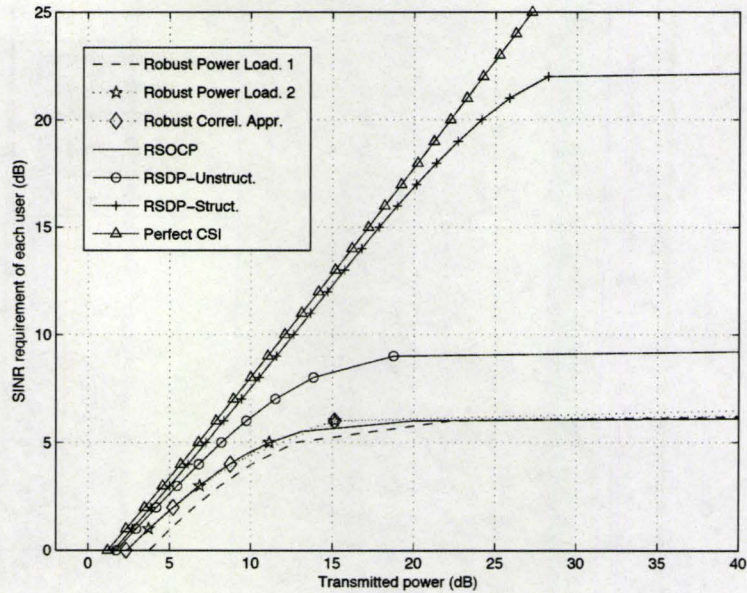


Figure 4.5: Maximum achievable (equal) SINRs against the average transmitted power, for a system with $N_t = 3$ and $K = 3$.

maximum value of the SINR, SINR_{\max} , above which each design method is unable to guarantee the SINR requirements. In Fig. 4.6 we plot the CDF of SINR_{\max} for each method. From this figure, it is clear that the three proposed approaches are able to provide SINR guarantees for significantly larger values of SINR than the robust power loading approaches in [69] and the robust autocorrelation approach in [61,62].

In the last experiment, we assess the degree of conservatism of each method by studying the statistics of the actual received SINRs for channel realizations within a given uncertainty bound. Scenarios in which the actual SINRs are likely to be significantly higher than the requested SINRs indicate that the transmitter adopts a more conservative approach that requires higher transmitted power. Ideally, when perfect CSI is available at the transmitter, the actual received SINRs are equal to the requested ones, i.e., all QoS constraints are achieved with equality [59–64]. In this experiment, we selected the sets of channel estimates from the 2000 sets used in

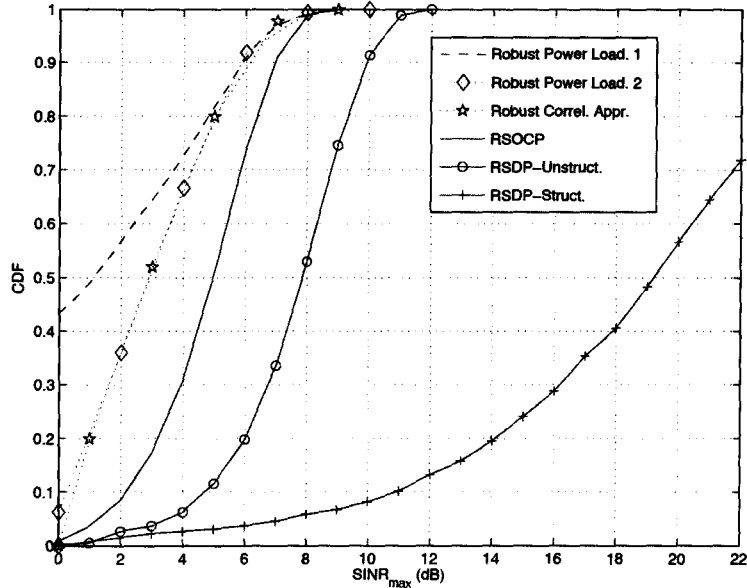


Figure 4.6: The (empirical) cumulative distribution function (CDF) of SINR_{\max} for a system with $N_t = 3$ and $K = 3$.

the first experiment for which all design methods were able to provide robust QoS guarantees of 10 dB for all users for the uncertainty bound $\delta = 0.015$. For each of the 609 such channel environments, we randomly generated 100 channel uncertainties that were uniformly distributed in direction and whose norms were equal to 0.01. In Fig. 4.7 we plot the CDF of the actual received SINRs for each design method. To help interpret this figure, in Tab. 4.2 we have provided the average transmission powers of each design method. It is apparent from Fig. 4.7 and Tab. 4.2 that the proposed approaches are able to save transmission power by reducing the likelihood that a user's SINR requirement is substantially over-satisfied.

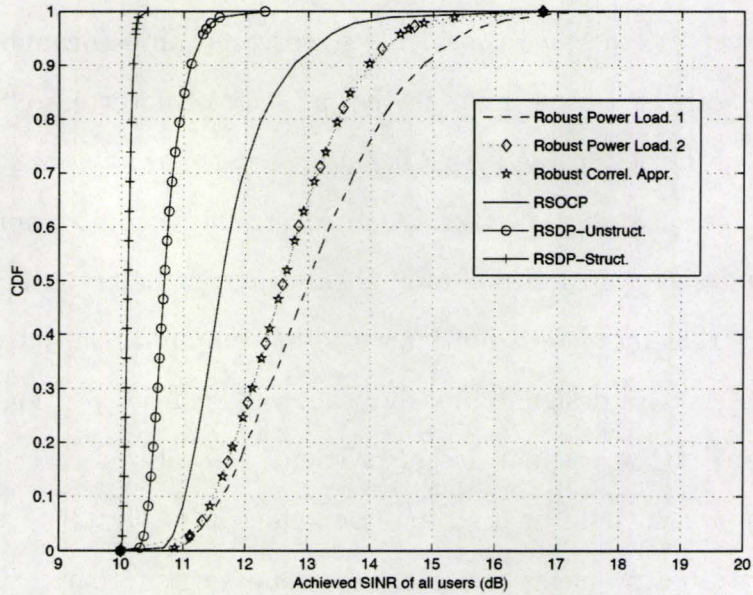


Figure 4.7: The (empirical) cumulative distribution function (CDF) of the actual received SINRs for a system with $N_t = 3$ and $K = 3$ and a target SINR of 10 dB.

Table 4.2: Transmission powers for Fig. 4.7

Approach	Transmission Power, $\text{tr}(\mathbf{P}^H \mathbf{P})$
Robust Power Load. 1	44.70
Robust Power Load. 2	42.64
Robust Autocorr.	42.60
RSOCP	39.19
RSDP-Unstruct	27.31
RSDP-Struct	22.49

4.7 Conclusion

In this chapter, we have considered linear precoding (beamforming) for broadcast channels with QoS constraints in the presence of uncertain CSI at the transmitter. We studied the design of a robust linear precoder that minimizes the total transmitted power while satisfying the users' QoS constraints for all channel realizations within a bounded uncertainty region around the transmitter's estimate of each user's channel. Since that problem is not known to be computationally tractable, we presented three conservative design approaches that yield convex and computationally-efficient restrictions of the original design problem. We also showed how the conservative design approach could be used to obtain efficiently-solvable quasi-convex restrictions of some related problems, including the robust counterpart of the problem of maximizing the minimum SINR subject to a given power constraint. As illustrated by the simulations, the proposed approaches can satisfy the users' QoS requirements for a significantly larger set of uncertainties than existing methods, and require less transmission power to do so. In the following chapter, we present a different approach to the design of robust broadcast channels with QoS requirements in which each user's QoS requirement is formulated as a constraint on the mean square error in its signal. This approach can be applied to both linear and non-linear transceivers, and robust design formulations can be obtained for a more general class of bounded uncertainties than those in treated by the approaches presented in this chapter.

Chapter 5

Robust Non-Linear and Linear Broadcasting with QoS Constraints: MSE Formulations

In the previous chapter, we developed robust linear precoding designs for broadcast channels with users' QoS requirements in the presence of bounded uncertainty at the transmitter. The QoS requirements were formulated as constraints on the SINR of each user's received signal. In this chapter, we adopt a different approach to the design of robust transceivers for broadcast channels with bounded uncertainty. We formulate each user's QoS requirement as a constraint on the mean square error (MSE) in its received signal, and we show that these MSE constraints imply constraints on the received signal-to-interference-plus-noise-ratio (SINR). Using the MSE constraints, we present a unified approach to the design of linear and non-linear transceivers with QoS requirements that must be satisfied in the presence of bounded channel uncertainty. The proposed designs overcome the limitations of the approaches of Chapter 4 that provide conservative designs or are only applicable to the case of linear precoding.

Furthermore, we provide computationally-efficient design formulations for a rather general model of bounded channel uncertainty that subsumes many natural choices for the uncertainty region. We also consider the problem of the robust counterpart to precoding schemes that maximize the fidelity of the weakest user's signal subject to a power constraint. For this problem, we provide quasi-convex formulations, for both linear and non-linear transceivers, that can be efficiently solved using a one-dimensional bisection search. Our numerical results demonstrate that in the presence of bounded uncertainty in the transmitter's knowledge of users' channels, the proposed designs provide guarantees for a larger range of QoS requirements than other approaches that consider bounded channel uncertainty models, and require less transmission power in providing these guarantees.

5.1 Introduction

For the downlink of cellular systems in which each receiver has a single antenna and the QoS requirements were formulated as constraints on the signal-to-interference-plus-noise (SINR) of each user, the design of a linear precoder that minimizes the transmitter power required to guarantee that each user's QoS requirement is satisfied for all admissible channels was considered in Chapter 4. While the methods proposed in Chapter 4 provide tractable design formulations and significant improvements in performance over previous existing designs, those approaches have two limitations. First, they are not directly applicable to non-linear precoding schemes, such as Tomlinson-Harashima precoding (THP). Second, when QoS is quantified in an SINR sense, the robust linear QoS problem resulted in designs whose tractability is an open problem; see also [70]. In order to obtain tractable designs, a conservative design approach was taken, and that approach requires the SINR constraints

to be satisfied for a superset of channels that subsumes the original bounded set of admissible channels.

In this chapter, we address both these limitations by providing tractable formulations (in the form of semidefinite programs) of both linear and non-linear downlink precoding schemes that minimize the transmitted power required to ensure that each user's QoS requirement is satisfied for all admissible channels, without expanding the admissible set. We formulate each user's QoS requirement as a constraint on the mean square error (MSE) in each user's received signal, and we show these MSE constraints imply constraints on the received SINR of each user. Since the QoS is measured in terms of MSE, our approach is immediately applicable to non-linear Tomlinson-Harashima precoding, and the resulting designs include those for linear precoding as a special case. Furthermore, the proposed designs (for the linear case) are obtained with lower computational cost than those based on SINR formulations of the QoS requirements in Chapter 4.

We will present a unified treatment of a rather general bounded model for the channel uncertainty that can represent uncertainty regions resulting from a variety of sources of imperfection, including channel quantization errors. The model naturally includes channel uncertainty regions that are described using intersection of multiple uncertainty sets, e.g., the interval constraints on the entries of each user's channel that would arise from scalar quantization. While we will provide exact robust design formulations for these types of uncertainties, we will also provide conservative formulations that reduce the computational complexity of the design for these cases.

Analogous to Sections 4.4.5 and 4.5, the proposed design approaches of this chapter can be extended to obtain efficiently-solvable quasi-convex formulations of some related design problems. In particular, we consider the robust counterpart of the problem of maximizing the fidelity of the weakest user's signal (minimizing the largest

MSE among the users). For precoding schemes that assume perfect CSI at the transmitter, this problem was studied for the case of linear precoding schemes in [63, 64]. For the bounded channel uncertainty model, tractable conservative approaches to the robust counterpart of this problem for linear precoders were provided in Section 4.5 (for the case of SINR constraints), but the problem has remained open for the case of non-linear precoding. We provide quasi-convex formulations of this robust minimax problem (for MSE constraints), for both non-linear and linear precoding schemes. These formulations can be efficiently solved using a one-dimensional bisection search, or by formulating the problem as a generalized eigenvalue problem; e.g., [86].

We also consider the problem of determining the largest uncertainty region for which the QoS requirements can be satisfied for all admissible channels using finite transmission power. This problem is of considerable interest in the design of quantization codebooks for quantized channel feedback schemes. In that case, one might wish to choose the rate of the channel quantization scheme to be large enough (and the quantization cells small enough) for it to be possible to design a robust precoder with finite power. We provide quasi-convex formulations of this problem, too.

Our numerical results demonstrate the effectiveness of the proposed approach. In particular, the proposed designs provide guaranteed satisfaction of a larger set of QoS requirements than other approaches that consider bounded channel uncertainty models, even when the QoS requirements are specified in terms of SINRs, and that they expend less transmission power in satisfying these requirements.

5.2 System Model

We consider the downlink of a multiuser cellular communication system with N_t antennas at the transmitter and K users, each with one receive antenna. We consider

systems in which Tomlinson-Harashima precoding (THP) is used at the transmitter for multi-user interference pre-subtraction; e.g., [10, 16]. As shown in Fig. 5.1, TH precoding can be modelled using a feedback matrix $\mathbf{B} \in \mathbb{C}^{K \times K}$ and a feedforward precoding matrix $\mathbf{P} \in \mathbb{C}^{N_t \times K}$. Since linear precoding is the special case of the THP model in which $\mathbf{B} = \mathbf{0}$, we will focus our development on the THP case and will extract the special case results for linear precoding as they are needed.

The vector $\mathbf{s} \in \mathbb{C}^K$ in Fig. 5.1 contains the data symbol destined for each user, and we assume that s_k is chosen from a square QAM constellation \mathcal{S} with cardinality M and that $\mathbb{E}\{\mathbf{s}\mathbf{s}^H\} = \mathbf{I}$. The Voronoi region of the constellation \mathcal{V} is a square whose side length is D .¹ In absence of the modulo operation, the output symbols of the feedback loop in Fig. 5.1, v_k , would be generated successively according to $v_k = s_k - \sum_{j=1}^{k-1} \mathbf{B}_{k,j} v_j$, where only the previously precoded symbols v_1, \dots, v_{k-1} are subtracted. Hence, \mathbf{B} is a strictly lower triangular matrix. The role of the transmitter's modulo operation is to ensure that v_k remains within the boundaries of \mathcal{V} , and its effect is equivalent to the addition of the complex quantity $i_k = i_k^{re} D + j i_k^{imag} D$ to v_k , where $i_k^{re}, i_k^{imag} \in \mathbb{Z}$, and $j = \sqrt{-1}$. Using this observation, we obtain the standard linearized model of the transmitter that does not involve a modulo operation, as shown in Fig. 5.2; e.g., [10]. For that model,

$$\mathbf{v} = (\mathbf{I} + \mathbf{B})^{-1} \mathbf{u}, \quad (5.1)$$

where $\mathbf{u} = \mathbf{i} + \mathbf{s}$ is the modified data symbol. As a result of the modulo operation, the elements of \mathbf{v} are almost uncorrelated and uniformly distributed over the Voronoi region \mathcal{V} [10, Th. 3.1]. Therefore, the symbols of \mathbf{v} will have slightly higher average energy than the input symbols \mathbf{s} . (This slight increase in the average energy is termed precoding loss [10].) For example, for square M -ary QAM we have $\sigma_v^2 = \mathbb{E}\{|\mathbf{v}_k|^2\} =$

¹The length of the side of the constellation D is equal to $\sqrt{M}d$, where d is the distance between two successive constellation points along either of the basis directions.

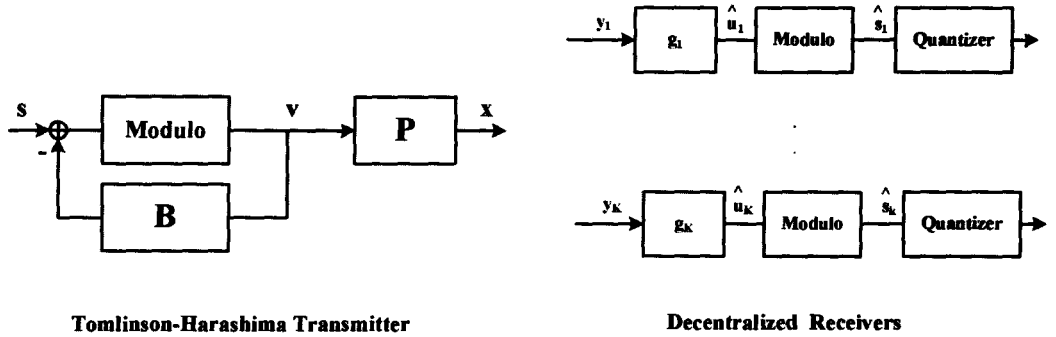


Figure 5.1: Broadcast channel with Tomlinson-Harashima precoding at the transmitter.

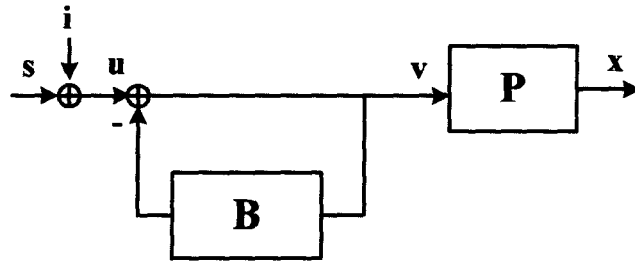


Figure 5.2: Equivalent linear model for the transmitter.

$\frac{M}{M-1}E\{|s_k|^2\}$ for all k except the first one [10]. For moderate to large values of M this power increase can be neglected and $E\{\mathbf{v}\mathbf{v}^H\} = \mathbf{I}$ is often used; e.g., [10,13,16]. Hence, the average transmitted power constraint can be written as $E_{\mathbf{v}}\{\mathbf{x}^H\mathbf{x}\} = \text{tr}(\mathbf{P}^H\mathbf{P})$.

The signals received at each user, y_k , can be written as

$$y_k = \mathbf{h}_k\mathbf{x} + n_k = \mathbf{h}_k\mathbf{P}(\mathbf{I} + \mathbf{B})^{-1}\mathbf{u} + n_k, \quad (5.2)$$

where $\mathbf{h}_k \in \mathbb{C}^{1 \times N_t}$ is a row vector representing the channel gains from the transmitting antennas to the k^{th} receiver, and n_k represents the zero-mean additive white noise at the k^{th} receiver, whose variance is $\sigma_{n_k}^2$. At each receiver, the equalizing gain g_k is used to obtain an estimate $\hat{u}_k = g_k\mathbf{h}_k\mathbf{P}(\mathbf{I} + \mathbf{B})^{-1}\mathbf{u} + g_k n_k$ of the modified data symbol \mathbf{u}_k . Following this linear receive processing step, the modulo operation is used to obtain

\hat{s} . In terms of the modified data symbols, we can define the error signal

$$\hat{u}_k - u_k = (g_k \mathbf{h}_k \mathbf{P} - \mathbf{m}_k - \mathbf{b}_k) \mathbf{v} + g_k n_k, \quad (5.3)$$

where \mathbf{m}_k and \mathbf{b}_k are the k^{th} rows of the matrices \mathbf{I} and \mathbf{B} , respectively. The error signal in (5.3) is equivalent to $\hat{s}_k - s_k$ when the integer i_k is eliminated by the modulo operation at the receiver, which occurs with high probability even at reasonably low SINRs. Using this error signal, the Mean Square Error (MSE) of the k^{th} user is given by

$$\begin{aligned} \text{MSE}_k &= \text{E}\{|\hat{u}_k - u_k|^2\} = \|g_k \mathbf{h}_k \mathbf{P} - \mathbf{m}_k - \mathbf{b}_k\|^2 + |g_k|^2 \sigma_{n_k}^2 \\ &= \left\| \begin{bmatrix} g_k \mathbf{h}_k \mathbf{P} - \mathbf{m}_k - \mathbf{b}_k & g_k \sigma_k \end{bmatrix} \right\|^2. \end{aligned} \quad (5.4)$$

5.3 Transceiver Design with MSE Constraints: Perfect CSI case

In this chapter, we will consider downlink scenarios in which each user has a quality of service constraint that is expressed in the form of an upper bound on its mean square error, MSE_k . The formulation of QoS design problem in terms of the MSEs is motivated by the following result.

Lemma 5.1. *For any given set of user's channels $\{\mathbf{h}_k\}_{k=1}^K$, if there exists a transceiver design $\mathbf{P}, \mathbf{B}, g_k$ that guarantees that $\text{MSE}_k \leq \zeta_k$, then that design also guarantees that $\text{SINR}_k \geq (1/\zeta_k) - 1$.*

Proof. See Appendix E. □

As we will point out below, in the case in which accurate CSI is available at the transmitter, a stronger result holds, namely that $\text{SINR}_k = (1/\zeta_k) - 1$. The statement

in Lemma 5.1 implies that if we guarantee that the MSE is below a certain threshold for all channels in a given set, then this implies a guarantee on the SINR for all channels in the same set. This implication enables us to develop robust QoS designs based on MSE constraints. As we will show in the remaining sections of the chapter, doing so leads to designs with better performance, lower complexity and broader applicability than existing designs in [62, 69] and in Chapter 4, that are based on SINR constraints, even though the QoS constraints are specified in terms of SINR.

In order to facilitate our development of robust precoding schemes with QoS constraints, we will briefly consider the design problem for the case in which the transmitter has accurate knowledge of the users' channels. Iterative design approaches for the perfect CSI case have been considered in [28, 66, 68], and the design problem was considered under zero-forcing criteria in [65, 67]. Our approach to the perfect CSI case includes deriving a convex conic formulation of the Tomlinson-Harashima transceiver with QoS constraints. This formulation will enable us to develop robust counterparts for the case of bounded channel uncertainty, and will allow the incorporation of different power constraints on the transmitter. In the case of perfect CSI, the design of the downlink transceiver components \mathbf{P} , \mathbf{B} and g_k so as to minimize the total transmitted power subject to satisfying the users' MSE requirements can be formulated as

$$\min_{\mathbf{P}, \mathbf{B}, g_k} \|\text{vec}(\mathbf{P})\|^2 \quad (5.5a)$$

$$\text{subject to} \quad \left\| \left[g_k \mathbf{h}_k \mathbf{P} - \mathbf{m}_k - \mathbf{b}_k, \quad g_k \sigma_k \right] \right\|^2 \leq \zeta_k. \quad (5.5b)$$

In the following lemma, we will show that g_k can be chosen to be real without loss of generality.

Lemma 5.2. *Consider the design problem in (5.5). If $\{|g_k| e^{j\theta_k}\}$, \mathbf{P} , and \mathbf{B} are the optimal equalization gains, precoding matrix and feedback matrix, respectively, then*

$\{|g_k|\}$, $\mathbf{P} \text{Diag}(e^{j\theta_1}, \dots, e^{j\theta_K})$, $\text{Diag}(e^{-j\theta_1}, \dots, e^{-j\theta_K})$ $\mathbf{B} \text{Diag}(e^{j\theta_1}, \dots, e^{j\theta_K})$ are also optimal.

Proof. Consider the transceiver whose parameters are $\{|g_k|\}$, $\mathbf{P} \text{Diag}(e^{j\theta_1}, \dots, e^{j\theta_K})$, $\text{Diag}(e^{-j\theta_1}, \dots, e^{-j\theta_K})$ $\mathbf{B} \text{Diag}(e^{j\theta_1}, \dots, e^{j\theta_K})$. Then, the left hand side of the MSE constraint of the k^{th} user in (5.5b) can be written as

$$\left\| \begin{bmatrix} e^{j(\theta_1 - \theta_k)} & (|g_k| \mathbf{h}_k \mathbf{p}_1 e^{j\theta_k} - b_{k,1}) \\ \vdots & \vdots \\ e^{j(\theta_{k-1} - \theta_k)} & (|g_k| \mathbf{h}_k \mathbf{p}_{k-1} e^{j\theta_k} - b_{k,k-1}) \\ & (|g_k| \mathbf{h}_k \mathbf{p}_k e^{j\theta_k} - 1) \\ e^{j(\theta_{k+1} - \theta_k)} & (|g_k| \mathbf{h}_k \mathbf{p}_{k+1} e^{j\theta_k}) \\ \vdots & \vdots \\ e^{j(\theta_K - \theta_k)} & (|g_k| \mathbf{h}_k \mathbf{p}_K e^{j\theta_k}) \\ & |g_k| \sigma_k \end{bmatrix} \right\|^T = \left\| \begin{bmatrix} (|g_k| e^{j\theta_k} \mathbf{h}_k \mathbf{p}_1 - b_{k,1}) \\ \vdots \\ (|g_k| e^{j\theta_k} \mathbf{h}_k \mathbf{p}_{k-1} - b_{k,k-1}) \\ (|g_k| e^{j\theta_k} \mathbf{h}_k \mathbf{p}_k - 1) \\ (|g_k| e^{j\theta_k} \mathbf{h}_k \mathbf{p}_{k+1}) \\ \vdots \\ (|g_k| e^{j\theta_k} \mathbf{h}_k \mathbf{p}_K) \\ |g_k| e^{j\theta_k} \sigma_k \end{bmatrix} \right\|^T, \quad (5.6)$$

where \mathbf{p}_j is the j^{th} column of \mathbf{P} . By extracting the unitary factor $\text{Diag}(e^{j(\theta_1 - \theta_k)}, \dots, e^{j(\theta_K - \theta_k)}, e^{-j\theta_k})$ right hand side of (5.6) and exploiting the unitary invariance of the 2-norm, we obtain the equality in (5.6). The right hand side of (5.6) is the MSE of k^{th} user for the transceiver whose parameters are $\{|g_k| e^{j\theta_k}\}$, \mathbf{P} , and \mathbf{B} . Furthermore, both transceivers have the same total transmitted power. \square

Using the result of Lemma 5.2, the definitions in (4.7-4.9), and the following definitions

$$\underline{\mathbf{b}}_k = \begin{bmatrix} \text{Re}\{\mathbf{b}_k\}/g_k & \text{Im}\{\mathbf{b}_k\}/g_k \end{bmatrix}, \quad (5.7)$$

$$\underline{\mathbf{m}}_k = \begin{bmatrix} \text{Re}\{\mathbf{m}_k\} & \text{Im}\{\mathbf{m}_k\} \end{bmatrix}, \quad (5.8)$$

$$f_k = 1/g_k, \quad (5.9)$$

where, by definition, $\text{Im}\{\mathbf{m}_k\} = \mathbf{0}$, the design problem in (5.5) can be formulated as a convex Second Order Cone Program (SOCP)

$$\min_{\mathbf{P}, \mathbf{B}, f_k, t} t \quad (5.10a)$$

$$\text{subject to } \|\text{vec}(\mathbf{P})\| \leq t, \quad (5.10b)$$

$$\|[\mathbf{h}_k \mathbf{P} - f_k \mathbf{m}_k - \mathbf{b}_k, \sigma_{n_k}]\| \leq \sqrt{\zeta_k f_k} \quad 1 \leq k \leq K. \quad (5.10c)$$

This problem can be efficiently solved using general purpose implementations of interior point methods [89,90]; e.g., SeDuMi [85]. It can be shown using a contradiction argument that the solution to (5.10) results in $\text{MSE}_k = \zeta_k$ for all k . This equality enables a stronger conclusion than that Lemma 5.1, namely that in the case of perfect CSI, $\text{SINR}_k = 1/\text{MSE}_k - 1$, e.g., [28]. Another advantage of the convex conic formulation in (5.10) is the possibility to include shaping constraints (e.g., [73,91]) on the power transmitted from the antennas; See Appendix D. These constraints are expressed as either second order cone or positive semidefiniteness constraints on the precoding matrix \mathbf{P} . The SOCP formulation can also incorporate multi-cell designs with per-cell power constraints on sets of antennas that belong to the same cell. These per-cell power constraints can also be formulated as second order cone constraints on \mathbf{P} ; See [92,93]. More importantly, however, the convex formulation in (5.10) enables us to derive robust counterparts of the original design problem in (5.5) for the uncertainty models presented in the following section.

5.4 General Class of Bounded Channel Uncertainty Models

We will consider an additive uncertainty model of the form:

$$\mathcal{U}_k(\delta_k, \Phi_k, \mathbf{Q}_k) = \{\underline{\mathbf{h}}_k \mid \underline{\mathbf{h}}_k = \hat{\underline{\mathbf{h}}}_k + \underline{\mathbf{e}}_k = \hat{\underline{\mathbf{h}}}_k + \sum_{j=1}^J w_k^{(j)} \phi_k^{(j)}, \mathbf{w}_k^T \mathbf{Q}_k \mathbf{w}_k \leq \delta_k^2\}, \quad (5.11)$$

where $\hat{\underline{\mathbf{h}}}_k$ is the transmitter's estimate of the k^{th} user's channel, and $\underline{\mathbf{e}}_k$ is the corresponding error. The above model enables us to treat several different uncertainty regions in a unified way. For example, it can model the following uncertainty sets:

- **Ellipsoidal and Spherical Uncertainty Sets:** By choosing $\mathbf{Q}_k = \mathbf{I}$, the uncertainty set in (5.11) describes an ellipsoidal uncertainty region around the channel estimate $\hat{\underline{\mathbf{h}}}_k$. The spherical uncertainty set in (4.12) with center $\hat{\underline{\mathbf{h}}}_k$ and radius δ_k is the special case that arises when Φ_k , the matrix whose rows are $\phi_k^{(j)}$, is selected to be \mathbf{I}_{2N_t} .
- **Interval Uncertainty Sets:** Interval constraints on each element of $\underline{\mathbf{h}}_k$ can also be modeled as uncertainty sets of the form in (5.11). By taking Φ_k to be \mathbf{I}_{2N_t} and \mathbf{Q}_k to be the matrix whose only non-zero element is $Q_{ii} = 1$, then the uncertainty set in (5.11) models an interval constraint on the i^{th} entry of the error $\underline{\mathbf{h}}_k$. Interval constraints on multiple entries of $\underline{\mathbf{h}}_k$ can be represented as the intersection of uncertainty sets on the form (5.11); see Section 5.5.1.

The additive uncertainty model in (5.11) is useful for systems in which the channel state information is quantized at the receivers and fed back to the transmitter; e.g., [8, 9, 79, 94, 95]. If a vector quantizer is employed at the receivers, then the quantization cells in the interior of the quantization region can be often approximated by

ellipsoids [96]. This ellipsoidal approximation can be substantially better than spherical approximation when the channel coefficients are correlated, e.g., [97, 98]. On the other hand, if a simple scalar quantizer is employed, the quantization regions can be modeled using a set of interval constraints.

5.5 Transceiver Design with MSE Constraints: Uncertain CSI Case

In this section, we will design a robust transceiver that minimizes the total transmitted power necessary to guarantee that the users' MSE requirements are satisfied for all admissible channels $\underline{\mathbf{h}}_k$ in the uncertainty region $\mathcal{U}_k(\delta_k)$ in (5.11). Using the formulation in (5.10), this robust problem can be stated as

$$\min_{\underline{\mathbf{P}}, \underline{\mathbf{B}}, f_k, t} t \tag{5.12a}$$

$$\text{s. t. } \|\text{vec}(\underline{\mathbf{P}})\| \leq t, \tag{5.12b}$$

$$\|[\underline{\mathbf{h}}_k \underline{\mathbf{P}} - f_k \underline{\mathbf{m}}_k - \underline{\mathbf{b}}_k, \sigma_{n_k}]\| \leq \sqrt{\zeta_k} f_k \quad \forall \underline{\mathbf{h}}_k \in \mathcal{U}_k(\delta_k), \quad 1 \leq k \leq K. \tag{5.12c}$$

This is a semi-infinite conic programming problem. In particular, the constraint (5.12c) represents K infinite sets of second order cone (SOC) constraints, one for each $\underline{\mathbf{h}}_k \in \mathcal{U}_k(\delta_k)$. However, we can precisely characterize each of these infinite sets of SOC constraints using a single Linear Matrix Inequality (LMI), as stated in the following formulation. (A derivation of this formulation is provided in Appendix F.)

Design Formulation 1. *The robust transceiver design problem in (5.12) is equivalent*

to the following semidefinite program (SDP)

$$\min_{\substack{t \\ \mu, t \\ \mathbf{P}, \mathbf{B}, f_k}} t \quad (5.13a)$$

$$s. t. \quad \|\text{vec}(\mathbf{P})\| \leq t, \quad (5.13b)$$

$$\mathbf{A}_k(\zeta_k, \delta_k) = \begin{bmatrix} \sqrt{\zeta_k} f_k - \mu_k & \mathbf{0} & [\hat{\mathbf{h}}_k \mathbf{P} - \mathbf{m}_k f_k - \mathbf{b}_k, \sigma_{n_k}] \\ \mathbf{0} & \mu_k \mathbf{Q}_k & \delta_k [\Phi_k \mathbf{P}, \mathbf{0}] \\ [\hat{\mathbf{h}}_k \mathbf{P} - f_k \mathbf{m}_k - \mathbf{b}_k, \sigma_{n_k}]^T & \delta_k [\Phi_k \mathbf{P}, \mathbf{0}]^T & \sqrt{\zeta_k} f_k \mathbf{I} \end{bmatrix} \geq \mathbf{0},$$

$$1 \leq k \leq K. \quad (5.13c)$$

□

This result shows that the original design problem in (5.12) with an infinite set of constraints is equivalent to the convex SDP in (5.13) that can be efficiently solved using interior point methods, e.g., [85]. Such equivalence is an advantage of the structure of the uncertain parameter of the SOC representation, in (5.12c). In these SOC constraints, the channels \mathbf{h}_k , and consequently the uncertain parameters, exist only on one side of the SOC. Hence, exact characterization of these SOC with uncertain parameters can be obtained. In contrast, when the QoS requirements are of the form of bounds on the SINR, then even in the case of linear precoding, both sides of the SOC constraints that enforce the QoS requirement depend on \mathbf{h}_k , and the resulting design problem is not known to be tractable [70, pp. 7]. In Chapter 4 this unknown tractability was addressed by taking a conservative approach to the robust design problem. As demonstrated by (5.13), for the case of MSE constraints the robust QoS design problem can be efficiently solved without introducing conservatism.

5.5.1 Case of Intersecting Uncertainty Sets for each \mathbf{h}_k

The formulation of the design problem in (5.12) extends naturally to the case in which the uncertainty region for each \mathbf{h}_k is described as the intersection of more than one uncertainty set \mathcal{U}_k^ℓ of the form (5.11); that is, the uncertainty set is of the form

$$\tilde{\mathcal{U}}_k = \bigcap_{\ell=1}^L \mathcal{U}_k^\ell(\delta_k, \Phi_k, \mathbf{Q}_k^\ell). \quad (5.14)$$

Note that there is no restriction in assuming that each \mathcal{U}_k^ℓ has the same uncertainty parameters δ_k and Φ_k , since \mathbf{Q}_k^ℓ in (5.11) can be chosen to accommodate different sizes and geometrical regions. Examples of constraint sets of the form in (5.14) include the interval constraints on each entry of $\underline{\mathbf{h}}_k$ that arise when scalar quantization is employed.

Although the design formulation involving uncertainty sets of the form (5.14) is natural extension of that in (5.12), it can be shown, based on [99], that the resulting problem is NP-hard. In particular, the transformations that lead to the efficiently-solvable formulations of (5.12) [cf. (5.13)] do not extend to this case. However, by adopting a conservative approach one can obtain an efficiently-solvable approximation to the problem with the uncertainty set in (5.14). This conservative approach involves enveloping (5.14) in a superset that can be described more efficiently, and then requiring the MSE constraints to be satisfied for all channels in this superset. Using the derivation in Appendix F, one obtains the following conservative design formulation that has the same number of LMIs as that in (5.13).

Design Formulation 2. *The solution of robust transceiver design problem in (5.12) for the intersection of uncertainty sets in (5.14) is upper-bounded by the solution of*

the following SDP

$$\min_{\substack{t \\ \boldsymbol{\mu}, t \\ \mathbf{P}, \mathbf{B}, f_k}} t \quad (5.15a)$$

$$s. t. \quad \|\text{vec}(\mathbf{P})\| \leq t, \quad (5.15b)$$

$$\mathbf{B}_k(\zeta_k, \delta_k) =$$

$$\begin{bmatrix} \sqrt{\zeta_k} f_k - \sum_{\ell=1}^L \mu_k^\ell & \mathbf{0} & [\hat{\mathbf{h}}_k \mathbf{P} - f_k \mathbf{m}_k - \mathbf{b}_k, \sigma_{n_k}] \\ \mathbf{0} & \sum_{\ell=1}^L \mu_k^\ell \mathbf{Q}_k^\ell & \delta_k [\Phi_k \mathbf{P}, \mathbf{0}] \\ [\hat{\mathbf{h}}_k \mathbf{P} - f_k \mathbf{m}_k - \mathbf{b}_k, \sigma_{n_k}]^T & \delta_k [\Phi_k \mathbf{P}, \mathbf{0}]^T & \sqrt{\zeta_k} f_k \mathbf{I} \end{bmatrix} \geq \mathbf{0},$$

$$1 \leq k \leq K. \quad (5.15c)$$

□

5.5.2 Largest Feasible Uncertainty Size

In this section we consider the related design problem of finding the largest value of the uncertainty size δ , namely δ_{\max} , for which there exists a robust transceiver of finite power that satisfies the MSE constraints for all admissible channels in the uncertainty region of size δ_{\max} . As demonstrated in Section 4.4.5, this problem is connected to the problem of designing codebooks for the quantization of the users' channels. The codebook design needs to yield quantization regions that can be "covered" by uncertainty sets of size δ_{\max} in order for the robust transceiver design problem to be feasible. Using the problem formulation in (5.13), finding the value of δ_{\max} is equivalent to solving

$$\max_{\mathbf{P}, \mathbf{B}, f_k, \boldsymbol{\mu}, \rho} \rho \quad (5.16a)$$

$$s. t. \quad \mathbf{A}_k(\zeta_k, \rho) \geq \mathbf{0}, \quad 1 \leq k \leq K, \quad (5.16b)$$

where $\mathbf{A}_k(\zeta_k, \rho)$ is defined in (5.13c). Since ρ is an optimization variable rather than a design parameter, the bilinear terms in $\mathbf{A}_k(\zeta_k, \rho)$ mean that the design problem in (5.16) is not jointly convex in the design variables ρ and $\underline{\mathbf{P}}$. However, the problem is quasi-convex (c.f. [82]), and an optimal solution can be efficiently found using a one-dimensional bisection search on ρ in which the problem solved at each step is the convex feasibility problem corresponding to (5.16) with a fixed value for ρ . For the case of the intersection of uncertainty regions in (5.14), the conservative constraint $\mathbf{B}_k(\zeta_k, \rho)$ in (5.15c) may be used in place of (5.16b). In that case, the optimal value of the design problem becomes a lower bound on δ_{\max} . It is worth observing that largest uncertainty size for the special case of linear precoding is less than that of its THP counterpart. This follows by observing that finding δ_{\max} in the linear precoding case solves a restriction of the problem (5.16) in which $\underline{\mathbf{B}}$ is set to $\mathbf{0}$.

5.5.3 Robust Broadcasting with QoS requirements: MSE versus SINR constraints

In Section 5.5 we presented design formulations for non-linear and linear broadcasting transceivers with QoS requirements under bounded channel uncertainty. These QoS requirements are formulated as MSE constraints. This design approach provides some attractive features compared to conservative design approaches in Chapter 4 in which the QoS requirements were formulated as constraints on the SINR. With that formulation of QoS constraints, the work in Chapter 4 was restricted to linear precoders and to uncertainty models consisting of a single spherical uncertainty region for each channel. Furthermore, in order to ensure tractability, a conservative design approach was taken in the design. Beside being applicable to non-linear Tomlinson-Harashima

precoding schemes, the design approach of Section 5.5 provides exact design formulations for a class of uncertainty models that encompasses many common uncertainty regions. Furthermore, it enables generalization to the case in which the uncertainty is described by multiple, and possibly different, intersecting regions. Finally, the design approach proposed in Section 5.5 requires substantially less computational effort than the approach in Chapter 4. In Table 5.1, we provide comparisons of the sizes of the SDPs associated with Design Formulation 1, for both linear and non-linear transceivers, and for that of the best conservative approach, namely the “Structured SDP” approach in Section 4.4.3. For the sake of comparison, we would like to point out that the dimension of the uncertainty ellipsoid, J , is less than or equal the dimension of \mathbf{e}_k which is $2N_t$. For spherical uncertainty regions $J = 2N_t$. It can be seen from this table that the proposed approaches requires $O(K^3)$ fewer variables than the “Structured SDP” approach for linear precoding in Section 4.4.3, and that the size of the linear matrix inequalities (LMI) is also reduced from $O(KN_t)$ to $O(K + N_t)$.

Table 5.1: A comparison of the sizes of Design Formulation 1 and that of the Structured SDP approach in Section 4.4.3

Method	Number of Variables	Number of Constraints	
		SOC num; size	LMI num; size
Structured SDP	$K(K + 1)(2K + 3) + 2N_t K + 1$	1; $2N_t K + 1$	$K; 2(K + 1)(2N_t + 1)$
Design Form. 1 - Linear	$(2N_t + 2)K + 1$	1; $2N_t K + 1$	$K; 2(K + 1) + J$
Design Form. 1 - THP	$(2N_t + K + 1)K + 1$	1; $2N_t K + 1$	$K; 2(K + 1) + J$

5.6 Robust Counterpart of Fair Minimax Transceiver Design

In the previous section, the focus was on the robust counterpart of the transceiver design problem that minimizes the total transmitted power subject to the satisfaction of the users' MSE constraints. In this section, we consider the related problem of minimizing the maximum MSE among all users subject to a transmitted power constraint, in scenarios with uncertain CSI. This design problem provides a notion of fairness amongst the users based on the value of their MSEs. The problem was addressed in Section 4.5 for a notion of fairness that is based on the SINR of the users' signals. We can formulate the robust counterpart of the design problem of minimizing the maximum MSE among all users under the channel uncertainty model in (5.11) as the following semi-infinite quasi-convex optimization problem

$$\min_{\mathbf{P}, \mathbf{B}, f_k, \sqrt{\zeta_0}} \sqrt{\zeta_0} \quad (5.17a)$$

$$\text{s. t.} \quad \left\| [\mathbf{h}_k \mathbf{P} - f_k \mathbf{m}_k - \mathbf{b}_k, \sigma_{n_k}] \right\| \leq \sqrt{\zeta_0} f_k, \quad \forall \mathbf{h}_k \in \mathcal{U}_k(\delta_k), \quad 1 \leq k \leq K, \quad (5.17b)$$

$$\frac{1}{2} \text{tr}(\mathbf{P}\mathbf{P}^T) \leq P_{\text{total}}. \quad (5.17c)$$

Using the characterization in (5.13c) of the infinite set of SOC constraints in (5.17b), this design problem can be formulated as the following quasi-convex optimization problem

$$\min_{\mathbf{P}, \mathbf{B}, f_k, \sqrt{\zeta_0}} \sqrt{\zeta_0} \quad (5.18a)$$

$$\text{s. t.} \quad \mathbf{A}_k(\zeta_0, \delta_k) \geq \mathbf{0}, \quad 1 \leq k \leq K, \quad (5.18b)$$

$$\|\text{vec}(\mathbf{P})\| \leq \sqrt{2 P_{\text{total}}}. \quad (5.18c)$$

This problem can be efficiently solved by using a bisection search on $\sqrt{\zeta_0}$ in which problem solved at each step is the convex feasibility problem generated by (5.18) with a fixed value of $\sqrt{\zeta_0}$. Alternatively, we can observe that each constraint in (5.18b) can be written as

$$\sqrt{\zeta_0} \begin{bmatrix} f_k & \mathbf{0} & \mathbf{0} \\ \mathbf{0} & \mathbf{0} & \mathbf{0} \\ \mathbf{0} & \mathbf{0} & f_k \mathbf{I} \end{bmatrix} - \begin{bmatrix} \mu_k & \mathbf{0} & -[\hat{\mathbf{h}}_k \mathbf{P} - f_k \mathbf{m}_k - \mathbf{b}_k, \sigma_{n_k}] \\ \mathbf{0} & \mu_k \mathbf{Q}_k & -\delta_k[\Phi_k \mathbf{P}, \mathbf{0}] \\ -[\hat{\mathbf{h}}_k \mathbf{P} - f_k \mathbf{m}_k - \mathbf{b}_k, \sigma_{n_k}]^T & -\delta_k[\Phi_k \mathbf{P}, \mathbf{0}]^T & \mathbf{0} \end{bmatrix} \geq \mathbf{0}. \quad (5.19)$$

Hence, (5.17) is equivalent to minimizing the largest generalized eigenvalue of a pair of (block diagonal) symmetric matrices that depend affinely on the decision variables [84, 86] — a problem that takes the form

$$\min_{\mathbf{x}, \alpha} \alpha \quad (5.20a)$$

$$\text{s. t. } \alpha \mathbf{A}^1(\mathbf{x}) - \mathbf{A}^2(\mathbf{x}) \geq \mathbf{0}, \quad (5.20b)$$

$$\mathbf{A}^1(\mathbf{x}) \geq \mathbf{0}. \quad (5.20c)$$

$$\mathbf{B}(\mathbf{x}) \geq \mathbf{0}. \quad (5.20d)$$

This observation allows us to employ more efficient algorithms, e.g., [86, 87], that exploit the structure of the constituent matrices in (5.19).

5.7 Numerical Studies

In this section, we demonstrate the performance of the proposed robust QoS designs for non-linear Tomlinson-Harashima precoding (RTHP-order 1, 2) and linear precoding (RLin) that were presented in Section 5.5, provides comparisons with other existing approaches that assume bounded channel uncertainty models. For Tomlinson-Harashima precoding, ordering of the users' channels is necessary prior to precoding. Finding the optimal ordering requires an exhaustive search over all possible permutations of the transmitter's estimate of the users' channels $\hat{\mathbf{h}}_k$, and instead of that we have implemented two suboptimal ordering methods. The first method applies the BLAST ordering in [36] to the transmitter's estimate of the users' channels. The second method is a generalization of the ordering method in [38] that selects a channel ordering that minimizes the reciprocals of the received SINRs when the precoder matrix \mathbf{P} is an identity matrix. In our generalization, the ordering selection criterion is minimizing the sum of each user's SINR requirements divided by its received SINR (when $\mathbf{P} = \mathbf{I}$), a quantity that is proportional to the power necessary for each user to achieve its SINR requirement.

In our numerical studies we consider a spherical uncertainty region of radius δ_k for each user. This model will facilitate the comparisons with other existing approaches for the linear precoding model, namely the robust autocorrelation matrix approach in [61, 62] (Robust Correl. Appr.), the robust power loading approach (RLin-PL1) using SINR constraints in [69], and the robust power loading approach (RLin-PL2) using MSE constraints in [79]. We will also provide comparisons with the conservative approach to robust linear precoding with SINR constraints in Chapter 4. The work in Chapter 4 presented three conservative approaches and we are comparing with the best conservative approach, namely the "Structured SDP" approach in Section 4.4.3.

As we make the comparisons, we would like to point out that these approaches to robust linear QoS precoding do not extend to Tomlinson-Harashima precoding, but the approaches proposed herein are inherently applicable to both linear and Tomlinson-Harashima precoders.

In order to totally specify the schemes used in our comparisons, we point out that the approaches in [69] and [79] require the beamforming vectors (normalized columns of \mathbf{P}) to be specified. We will use the zero-forcing beamforming vectors (the columns of the pseudo-inverse of $\hat{\mathbf{H}}$). In addition, the approaches in [61,62] and [69] are based on uncertainty models that are different from the one in (5.11), and from each other. The approach in [61,62] considers a model in which the spectral norm of the error in the (deterministic) autocorrelation matrix $\mathbf{C}_k = \mathbf{h}_k^H \mathbf{h}_k$ is bounded, and in the approach in [69] the Frobenius norm of the error in \mathbf{C}_k is bounded. However, by bounding these norms of \mathbf{C}_k in terms of the norm of \mathbf{e}_k , we can obtain the smallest uncertainty set for \mathbf{C}_k that contains all the channels in the set specified by $\|\mathbf{e}_k\| \leq \delta_k$. Furthermore, the uncertainty $\mathbf{e}_k = \delta_k \hat{\mathbf{h}}_k / \|\hat{\mathbf{h}}_k\|$ lies on the boundaries of the uncertainty sets for \mathbf{C}_k in [61,62] and [69].² We will compare these schemes in an environment with $N_t = 3$ transmit antennas and $K = 3$ users. In our experiments, we will evaluate performance statistics for the standard case of independent Rayleigh fading channels in which the coefficients of the fading channels are modeled as being independent circular complex Gaussian random variables with zero-mean and unit variance, and the receivers' noise sources are modeled by zero-mean, additive, white,

²As mentioned in Chapter 4, a bound on the spectral norm of the error in the matrix \mathbf{C}_k can be obtained as follows: $\|(\hat{\mathbf{h}}_k + \mathbf{e}_k)^H (\hat{\mathbf{h}}_k + \mathbf{e}_k) - \hat{\mathbf{h}}_k^H \hat{\mathbf{h}}_k\| = \|\hat{\mathbf{h}}_k^H \mathbf{e}_k + \mathbf{e}_k^H \hat{\mathbf{h}}_k + \mathbf{e}_k^H \mathbf{e}_k\| \leq \|\hat{\mathbf{h}}_k^H \mathbf{e}_k\| + \|\mathbf{e}_k^H \hat{\mathbf{h}}_k\| + \|\mathbf{e}_k^H \mathbf{e}_k\| = 2\|\hat{\mathbf{h}}_k\| \|\mathbf{e}_k\| + \|\mathbf{e}_k\|^2$. The same bound also holds for the Frobenius norm, since the matrices on the immediate right hand side of the inequality are all rank one. Furthermore, the uncertainty $\mathbf{e}_k = \delta_k \hat{\mathbf{h}}_k / \|\hat{\mathbf{h}}_k\|$ achieves this upper bound with equality for both norms. Therefore, the chosen bound on \mathbf{C}_k is the smallest (achievable) bound such that all the channels in the set specified by $\|\mathbf{e}_k\| \leq \delta_k$ lie in the uncertainty sets of the methods in [61,62,69], and the admissible uncertainty $\mathbf{e}_k = \delta_k \hat{\mathbf{h}}_k / \|\hat{\mathbf{h}}_k\|$ lie on the boundaries of these sets. (See also [88].)

and circular Gaussians with unit variance.

5.7.1 Performance Comparisons against SINR Requirements

In this comparison, we randomly generated 2000 realizations of the set of channel estimates $\{\hat{\mathbf{h}}_k\}_{k=1}^K$ and examined the performance of each method in the presence of uncertainties of equal sizes, $\delta_k = \delta = 0.05, \forall k$. The SINR requirements of the three users are also equal. For each set of channel estimates and for each value of the required SINR we determined whether each design method is able to generate a precoder (of finite power) that guarantees the required SINRs. In Fig. 5.3 we plot the fraction of the 2000 channel realizations for which each method generated a precoder with finite power against the (equal) SINR requirements of the users. From this figure, it is clear that the proposed robust designs for linear (RLin) and non-linear (RTHP-order 1, 2) precoding satisfy the SINR requirements for larger percentages of channels. The robust conservative approach for linear precoding (RLin-Conservative) in Section 4.4.3 and the power loading method in [79] achieve the QoS requirements for a percentage of channels that is quite close to that of the proposed linear approach (RLin). However, the proposed approach (RLin) has a significantly lower computational cost than the conservative approach (RLin-Conservative); see Table 5.1. Furthermore, this approach is also applicable to non-linear Tomlinson-Harashima precoding (RTHP-order 1, 2) with a slight increase in the computational cost.

For the robust linear power loading approach (RLin-PL2) in [79], the QoS design problem in terms of MSE constraints was justified as a heuristic measure for the SINR requirements. However, using Lemma 5.1 we showed that the MSE constraint of each user implies a minimum achieved SINR. Furthermore, there does not appear to be a direct extension of the power loading approach in [79] (nor that in [69]) to

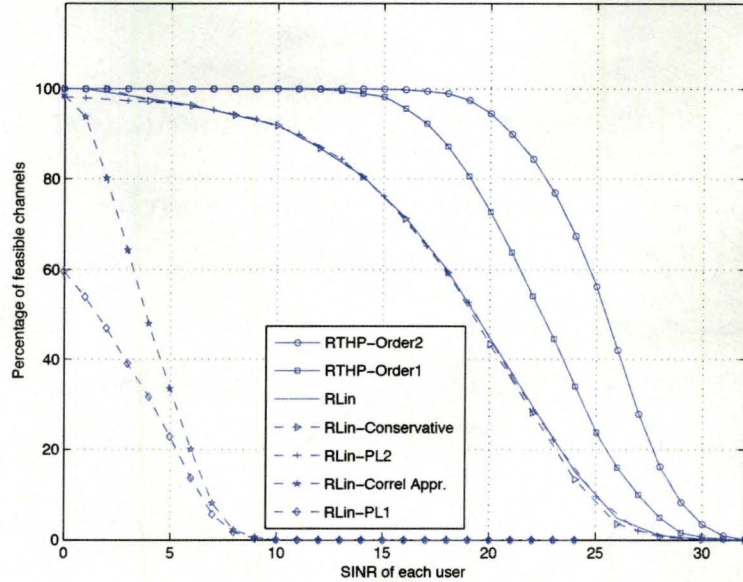


Figure 5.3: Percentage of the 2000 channel realizations for which the robust QoS guarantee can be made against the required SINRs, for a system with $N_t = 3$ and $K = 3$.

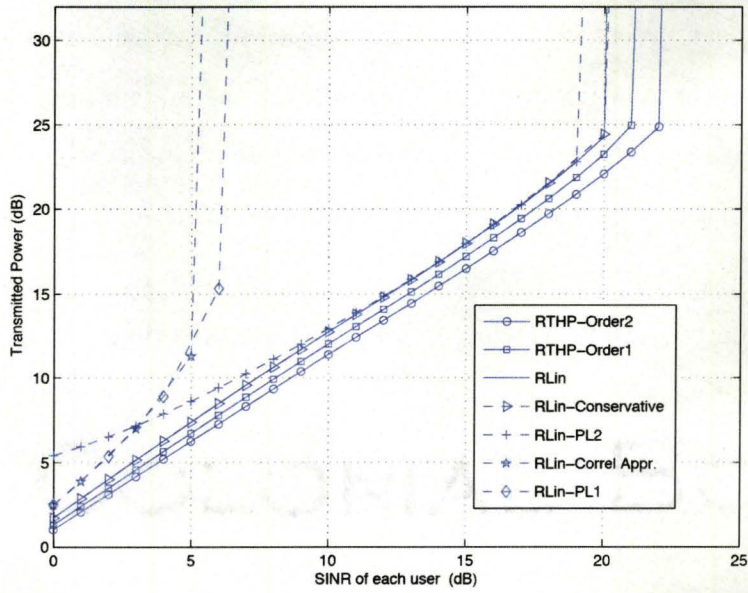
TH precoding.

For the comparison in Fig. 5.4(a), we selected all the sets of channel estimates from the 2000 sets used in the previous experiment for which all design methods were able to provide robust QoS guarantees for all SINRs less than or equal to 6dB, and we calculated the average, over the 274 such channel environments, of the transmitted power required to achieve these robust QoS guarantees. We have plotted the average transmitted power versus the equal SINR requirement of each user in Fig. 5.4(a). This figure demonstrates the saturation effect that channel uncertainty imposes on the growth of the SINR of each user with the transmitted power for both of linear and non-linear precoding. The SINR saturates at the value of SINR for which the method under consideration cannot provide the robust QoS guarantee with finite power for

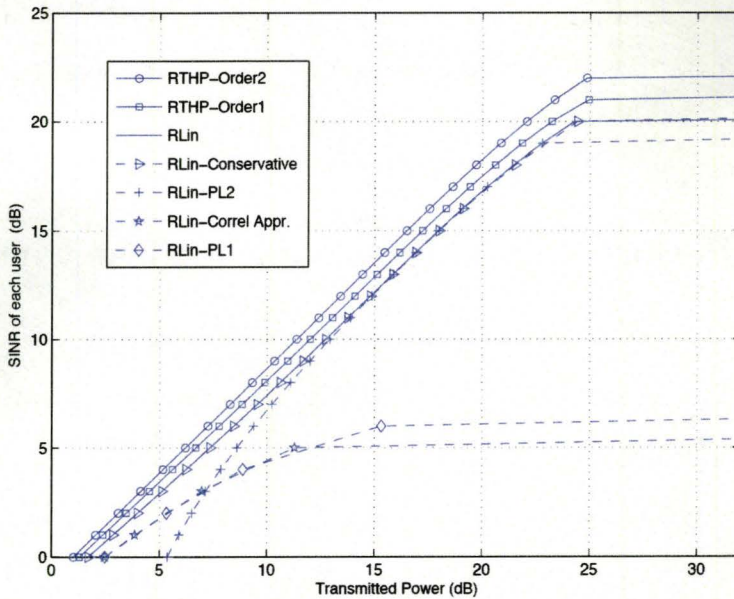
one (or more) of the channel estimates. A related effect was observed in [8] for non-robust linear precoding on the MISO downlink with quantized CSI. Fig. 5.4(a) also illustrates the role that robust precoding can play in extending the SINR interval over which linear growth with the transmitted power can be achieved. This is particularly evident for the robust non-linear approaches (RTHP-order 1, 2) and the robust linear approach (RLin). We also observe that the second ordering method for Tomlinson-Harashima precoding provides better performance than the first one, since it selects the channel ordering in a way that attempts to minimize the sum of powers necessary to achieve each SINR requirement. Since the previous experiments consider scenarios with equal SINR requirements for all users, the performance comparison curves can also be interpreted as comparisons of different approaches for the robust fair broadcasting problem simply by transposing the axes. For example, in Fig. 5.4(b) we have computed the solution to the robust fair design in Section 5.6 for the communications scenario of the second experiment, and it can be seen it is the transposed version of Fig. 5.4(a).

5.7.2 Performance Comparisons against Uncertainty Size

In this comparison, we used the 2000 randomly generated realizations of the set of channel estimates $\{\hat{\mathbf{h}}_k\}_{k=1}^K$ to examine the performance of each method in the presence of equal uncertainty, $\delta_k = \delta, \forall k$. The QoS requirement of each user is such that the SINR is at least 10 dB. In Fig. 5.5 we provide the percentage of the 2000 channel realizations for which each method generated a precoder with finite power as a function of the size of the uncertainty. From this figure, it is clear that for a large range of uncertainty sizes, the proposed non-linear approaches (RTHP-Order 1, 2) satisfy the SINR requirements for many more channel realizations than other approaches. This is due to the fact that the proposed linear approach is a



(a) Average transmitted power versus (equal) SINR requirements.



(b) Fair (equal) SINRs against the average transmitted power

Figure 5.4: Relation between transmitted power and SINR requirements for the robust QoS design problem and the robust fair problem for a system with $N_t = 3$ and $K = 3$.

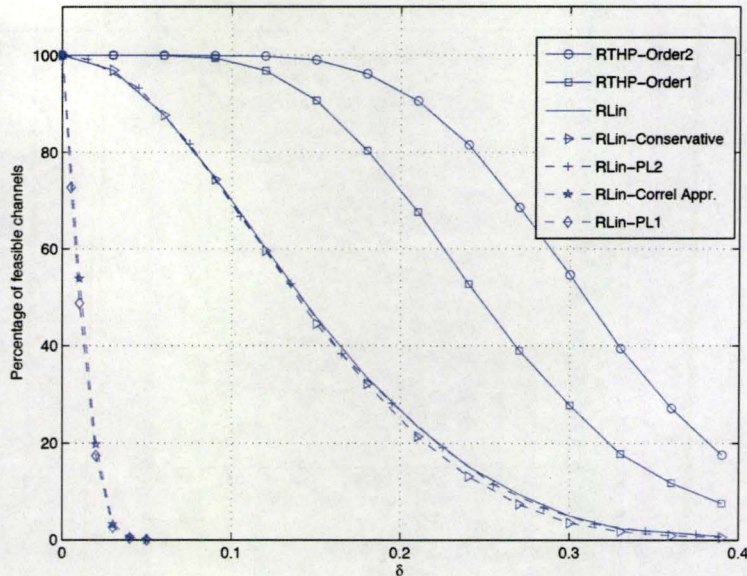


Figure 5.5: Percentage of the 2000 channel realizations for which the robust QoS guarantee can be made against the uncertainty size δ , for a system with $N_t = 3$, and $K = 3$.

special case of the proposed THP design, and the other existing linear approaches are either conservative or restricted to the optimization of powers for given transmit directions. While the performance of the conservative linear precoding approach (RLin-conservative) in Section 4.4.3 and the robust linear power loading approaches (RLin-PL2) in [79] is quite close to that of the proposed linear design (RLin) in terms of number of channel realizations for which the method satisfies the robust (SINR-based) QoS requirements, they use more power in order to achieve the QoS requirements, as shown in Fig 5.6.

In Fig 5.6, we selected those sets of channel estimates from the 2000 sets used in the previous experiment for which all design methods were able to provide robust QoS guarantees for all uncertainties with $\delta \leq 0.015$. We calculated the average, over the 614 such channel environments, of the transmitted power required to achieve these

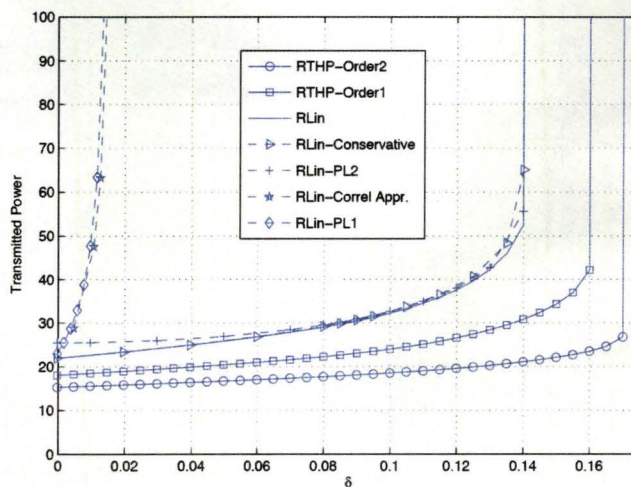


Figure 5.6: Average of the transmitted power $\text{tr}(\mathbf{P}^H \mathbf{P})$, on a linear scale, versus uncertainty size δ for a system with $N_t = 3$ and $K = 3$.

robust QoS guarantees and we have plotted the results for different values of δ in Fig. 5.6. The average transmitted power approaches infinity for a certain value of δ when for one (or more) of the channel estimates the method under consideration cannot provide the robust QoS guarantee with finite power. It is clear from Fig. 5.6 that the proposed robust Tomlinson-Harashima designs are capable of (robustly) satisfying the SINR requirements for larger values of uncertainty sizes than the other approaches. It is also apparent that they expend less power in doing so.

5.8 Conclusion

In this chapter, we have presented a unified approach to the design of robust linear and non-linear transceivers with user-specified QoS requirements subject to deterministically-bounded channel uncertainty model. The proposed approach formulated the QoS requirements in terms of MSE constraints and showed that these

constraints imply corresponding constraints on the achieved SINR of each user. Our approach provided (convex) semidefinite program formulations of the design problem that can be efficiently solved. Furthermore, these design formulations were obtained for a rather general model of bounded channel uncertainty that include many uncertainty regions. We also showed how these designs can be used to provide quasi-convex formulations for the robust counterpart of the problem of fair transceiver design that maximizes the signal quality of the user with the weakest signal. Numerical results demonstrated that under bounded uncertainty conditions, the proposed designs provided guaranteed satisfaction of a larger set of QoS requirements than the existing approaches that considered bounded uncertainty models, and that they require less transmission power in order to satisfy these requirements.

While Chapters 4 and 5 studied the design of robust designs of broadcast channels with QoS requirements for each user, in the following two chapters we will consider the complementary problem of optimizing the fidelity of the users' signals subject to a power constraint at the transmitter. In particular, we will study robust MSE designs for linear and non-linear multi-user transceivers subject to a transmission power constraint. These robust designs will be developed for both broadcast channels and multiple access channels under two different models for users' channel uncertainty: a stochastic model, and a deterministically-bounded model that is similar to the one considered in this chapter and Chapter 4.

Chapter 6

Robust Linear Transceivers for Multi-user Systems

In Chapters 4 and 5, we considered robust designs for linear and non-linear broadcast channels with quality of service constraints and uncertain channel state information (CSI) at the transmitter. In this chapter, we consider the complementary problem of optimizing the fidelity of the users' signals, measured in terms of the mean-square-error (MSE), subject to a power constraint at the transmitter. In particular, we study robust minimum MSE designs for linear multi-user transceivers, with an emphasis on downlink, that explicitly take into account the nature of channel uncertainty that arise in communication systems. For systems with uplink-downlink reciprocity, we consider a stochastic model for the channel uncertainty, and we propose an efficient algorithm for the joint design of the linear precoding matrix at the base station and the equalizing gains at the receivers so as to minimize the average mean-square-error (MSE) over the channel uncertainty. The design is based on a generalization, derived herein, of the MSE duality between the broadcast and multiple access channels (MAC) to scenarios with uncertain CSI, and on a convex formulation for the design

of robust transceivers for the dual MAC. For systems in which quantized channel feedback is employed, we consider a deterministically-bounded model for the channel uncertainty, and we study the design of robust downlink transceivers that minimize the worst-case MSE over all admissible channels. While we show that the design problem is non-convex, we also propose an iterative local optimization algorithm that is based on efficiently-solvable convex conic formulations. Our framework is quite flexible, and can incorporate a variety of power constraints. It can also be generalized to scenarios in which channel uncertainty is described as intersection of more than one bounded uncertainty region. In particular, we study a “system-wide” uncertainty model, and although the resulting design problem is still non-convex, it does result in a significantly simpler iterative local design algorithm than the “per-user” uncertainty model. Our approaches to the minimax design for the downlink can be extended to the uplink, and we provide explicit formulations for the resulting uplink designs. Simulation results indicate that the proposed approaches to robust linear transceiver design can significantly reduce the sensitivity of the downlink to uncertain CSI, and can provide improved performance over that of existing robust designs.

6.1 Introduction

As discussed in Chapter 1 and Chapters 4 and 5, the provision of multiple antennas at the base station facilitates the transmission of independent messages to different users on the downlink of a multiuser system; e.g., [62]. For these broadcast channels, the availability of accurate channel state information (CSI) at the transmitter is required in order to spatially multiplex the messages for different users by precoding them in a way that mitigates the effects of multiuser interference. Assuming that perfect CSI is available, several precoding techniques have been proposed, including the class of

schemes that apply linear precoding at the transmitter jointly with linear equalization at each receiver. Those schemes offer a desirable trade-off between performance and transmitter complexity, and examples include zero-forcing techniques for channel inversion [100, 101], regularized channel inversion [102], minimum mean square error (MMSE) techniques [103, 104], and beamforming with a prespecified signal to interference plus noise ratio (SINR) at the receivers [62, 63].

Many precoding schemes assume that the transmitter has perfect channel knowledge of all the users' channels, but in practice the CSI at the transmitter suffers from inaccuracies caused by errors in channel estimation and/or limited, delayed or erroneous feedback, and as we mentioned in Section 4.1 the performance of downlink linear precoding systems is rather sensitive to these channel uncertainties. For example, it was shown [8] that imperfect channel knowledge at the transmitter can result in the downlink becoming interference limited; i.e., the growth of SINR of each user with the transmitted power saturates.

Due to the inevitability of imperfect channel information, robust communication schemes that take into account the channel uncertainty are of interest in practice; e.g., [40, 105]. The goal of the work herein is to propose robust linear transceivers for the downlink that explicitly take into account the uncertainties in the channel model, with an emphasis on systems with a single antenna at each receiver. In systems with reciprocity between the uplink and the downlink (e.g., time division duplex systems), the base station can estimate the channel and the channel uncertainty is mainly due to channel estimation errors. In that case, a stochastic model for the uncertainty in the channel model is appropriate, and possible design approaches include those based on average performance measures, and those based on notions of outage. For these systems, we consider the joint design of the linear precoder matrix and the users' equalizing gains so as to minimize the average, over the channel uncertainty,

of the sum of the MSEs of each user. Since this design objective is not a jointly convex function of the precoding matrix and the equalizing gains, previous robust approaches considered a simpler design problem that restricts the equalizing gains to be equal (e.g., [106] [107]), or used a simpler detection model [108,109]. The proposed approach for solving the general design problem (without restricting the equalizing gains), involves the generalization of the MSE duality between the broadcast channel and multiuser access channel (MAC) [110,111] to scenarios with uncertain CSI. Using this duality, we obtain a closed-form expression that relates the desired robust broadcast transceivers to the corresponding transceivers that optimize the same performance metric for the dual MAC. The solution to the robust transceiver design problem for the dual MAC results in a closed-form expression for the optimal equalizer, and a convex conic formulation for the dual MAC optimal transmitters. Hence, by exploiting the MSE duality between BC and MAC in scenarios with uncertain CSI, we are able to transform the non-convex design problem for the BC into a convex and efficiently-solvable equivalent design problem.

For systems in which the channel is estimated and quantized at the receiver and then fed back to the transmitter (e.g., [8,9,94,95]), one has a bound on the (quantization) error and hence an appropriate approach to robust design would be to optimize the worst-case performance over errors of that size. For these systems, we study the design of robust downlink transceivers that minimize the worst-case MSE over a bounded uncertainty model of each user's channel. While we show that that design problem is non-convex, we propose an iterative local optimization algorithm that is based on efficiently-solvable convex conic formulations. The problem formulation and proposed algorithms can incorporate different bounded uncertainty models, and they can be applied to systems with per-antenna, per cell, and spatial-shaping power constraints, as well as the standard constraint on the total transmitted power.

In particular, we study a “system-wide” uncertainty model as an alternative to the “per-user” model that is suitable for large cells and for multi-cell designs. While the resulting design problem is still non-convex, it results in a significantly simpler iterative local design algorithm than the “per-user” uncertainty model. Our approaches to the minimax design for the downlink can be extended to the uplink, and we provide explicit formulations for the resulting uplink designs. Our simulation results demonstrate that the proposed approaches to robust linear transceiver design can significantly reduce the sensitivity of the downlink to uncertain CSI, and can provide improved performance over that of existing robust designs.

6.2 Broadcast Channel with Linear Transceivers

Similar to Section 4.2, we consider broadcast channels with N_t antennas at the transmitter and K receivers, each with a single antenna. Let $\mathbf{s} \in \mathbb{C}^K$ be the vector of data symbols intended for the receivers. The transmitter linearly precodes the vector \mathbf{s} to form $\mathbf{x} \in \mathbb{C}^{N_t}$,

$$\mathbf{x} = \mathbf{P}\mathbf{s} = \sum_{j=1}^K \mathbf{p}_j s_j, \quad (6.1)$$

where \mathbf{p}_j is the j^{th} column of the precoding matrix \mathbf{P} ; i.e., the beamforming weights for the j^{th} user. Without loss of generality, we will assume that $\text{E}\{\mathbf{s}\mathbf{s}^H\} = \mathbf{I}$, and hence, the total transmitted power constraint $\text{E}\{\mathbf{x}^H\mathbf{x}\} \leq P_{\text{total}}$ reduces to $\text{tr}\{\mathbf{P}^H\mathbf{P}\} \leq P_{\text{total}}$.

The signal y_k received by the k^{th} user is given by

$$y_k = \mathbf{h}_k\mathbf{x} + n_k, \quad (6.2)$$

where $\mathbf{h}_k \in \mathbb{C}^{1 \times N_t}$ is a row vector representing the channel gains from the transmitting antennas to the k^{th} receiver, and n_k is the additive zero-mean white noise at the k^{th} receiver whose variance is σ_n^2 . Collecting the received signals in the vector \mathbf{y} , we will

find it convenient to use the vector notation $\mathbf{y} = \mathbf{H}\mathbf{x} + \mathbf{n}$, where \mathbf{H} is the broadcast channel matrix whose k^{th} row is \mathbf{h}_k , and the covariance matrix of the noise vector \mathbf{n} is $E\{\mathbf{n}\mathbf{n}^H\} = \sigma_n^2\mathbf{I}$. Due to the decentralized nature of the receivers, joint processing of the received vector \mathbf{y} is not possible. Instead, each receiver will process its received signal y_k independently using a single equalizing gain g_k to obtain an estimate of its intended symbol

$$\hat{s}_k = g_k y_k. \quad (6.3)$$

Using (6.3), the mean square error MSE_k associated with the k^{th} symbol can be written as:

$$\begin{aligned} \text{MSE}_k &= E\{|\hat{s}_k - s_k|^2\} = \sum_{j=1}^K |g_k|^2 \mathbf{p}_j^H (\mathbf{h}_k^H \mathbf{h}_k) \mathbf{p}_j + \sigma_n^2 |g_k|^2 - g_k \mathbf{h}_k \mathbf{p}_k - g_k^H \mathbf{p}_k^H \mathbf{h}_k^H + 1 \\ &= \|g_k \mathbf{h}_k \mathbf{P} - \mathbf{m}_k\|^2 + \sigma_n^2 |g_k|^2, \end{aligned} \quad (6.4)$$

where \mathbf{m}_k is the i^{th} row of \mathbf{I} . Similarly, the total MSE can be written as:

$$\text{MSE} = E\{\|\hat{\mathbf{s}} - \mathbf{s}\|^2\} = \sum_{k=1}^K \text{MSE}_k = \text{tr}\{(\mathbf{GHP} - \mathbf{I})^H (\mathbf{GHP} - \mathbf{I})\} + \sigma_n^2 \|\mathbf{g}\|^2, \quad (6.5)$$

where $\mathbf{g} = (g_1, \dots, g_K)$ and $\mathbf{G} = \text{Diag}(\mathbf{g})$.

The purpose of this chapter is to determine efficient algorithms for the joint design of \mathbf{P} and \mathbf{g} with the goal of minimizing the MSE, in the presence of channel uncertainty. We will adopt the common implementation (e.g., [102, 106, 107, 109–111]) in which \mathbf{P} and \mathbf{g} are jointly designed at the basestation (using the available CSI), and the basestation informs each receiver of the equalizing gain, g_k , that it is to use. Actually, from (6.4) and (7.5) it can be seen that the phase component of each g_k can be absorbed into \mathbf{p}_k without affecting either MSE_k or MSE , and hence only the magnitude of g_k needs to be sent to the receiver k ; e.g., [110, 111]. We will point out below that this observation also applies to robust transceiver designs for scenarios with uncertain CSI that we will consider herein.

6.3 Channel Uncertainty Models

We consider additive uncertainty models for the CSI available at the transmitter:

$$\mathbf{h}_k = \hat{\mathbf{h}}_k + \mathbf{e}_k, \quad (6.6)$$

where $\hat{\mathbf{h}}_k$ is the transmitter's estimate of \mathbf{h}_k , and \mathbf{e}_k is the corresponding error. This can be equivalently written as $\mathbf{H} = \hat{\mathbf{H}} + \mathbf{E}$, where \mathbf{e}_k is the k^{th} row of \mathbf{E} . We will develop design formulations for robust transceivers under two broad models for the channel uncertainty.

6.3.1 Stochastic uncertainty model

The first model is suitable for communication schemes with reciprocity between the uplink and the downlink, which allows the transmitter to estimate the users' channels on the uplink. We will adopt a model in which the estimation errors are modelled by zero-mean random variables with covariances $\mathbb{E}\{\mathbf{e}_k^H \mathbf{e}_k\} = \sigma_{e_k}^2 \mathbf{I}$, where $\sigma_{e_k}^2$ depends on the uplink SNR of user k . This model is appropriate for scenarios in which the elements of \mathbf{h}_k have zero mean and are uncorrelated with each other and those of other users, and linear minimum mean-square error estimation is used to estimate the channels on the uplink.¹ For this stochastic uncertainty model, robust transceivers based on the average MSE will be presented in Section 6.4.

6.3.2 Bounded uncertainty model

In the second model, the error \mathbf{e}_k is assumed to be deterministically bounded. We will use the general bounded uncertainty model in Section 5.4. In this model, the

¹All our derivations extend directly to the case in which $\mathbb{E}\{\mathbf{e}_k^H \mathbf{e}_k\}$ is an arbitrary symmetric positive definite matrix, but for simplicity we will focus on the stated model.

uncertainty set of each user channel is given by:

$$\mathcal{U}_k(\delta_k, \Phi_k, \mathbf{Q}_k) = \{\mathbf{h}_k \mid \mathbf{h}_k = \hat{\mathbf{h}}_k + \mathbf{e}_k = \hat{\mathbf{h}}_k + \sum_{j=1}^J w_k^{(j)} \phi_k^{(j)}, \mathbf{w}_k^T \mathbf{Q}_k \mathbf{w}_k \leq \delta_k^2\}. \quad (6.7)$$

While Chapters 4 and 5 adopted an equivalent real formulation to (6.7), cf. (5.11), in order to facilitate computational cost comparisons of different transceiver designs with QoS, it is now more convenient to adopt the above compact complex formulation of the uncertainty model. As we mentioned in Section 5.4, the above model allows the treatment of several different uncertainty regions in a unified way. For different choices of Φ and \mathbf{Q} , it can model elliptical or spherical uncertainty sets, such as those resulting from using vector quantization at each user. For some other choices of Φ and \mathbf{Q} , it can model an interval constraint on one entry of \mathbf{h}_k ; See Section 5.4. Furthermore, we can extend this model to the case in which the uncertainty region for each \mathbf{h}_k is described as the intersection of more than one uncertainty set \mathcal{U}_k^ℓ of the form (6.7). In that case, the uncertainty set is of the form

$$\tilde{\mathcal{U}}_k = \bigcap_{\ell=1}^L \mathcal{U}_k^\ell(\delta_k, \Phi_k, \mathbf{Q}_k^\ell). \quad (6.8)$$

This is particularly useful to model interval or box constraints on each entry of \mathbf{h}_k such as those resulting from using scalar quantizer at each user; See Section 5.4. For this “per-user” bounded uncertainty model, minimax robust downlink transceivers based on the worst-case MSE will be presented in Section 6.5, for the uncertainty region in (6.7), as well as other regions.

As an alternative to this “per-user” uncertainty model, the transmitter can consider a bounded model for the error matrix $\|\mathbf{E}\| \leq \Delta$, where an estimate of $\|\mathbf{E}\|$ is

$$\|\mathbf{E}\| \leq \sqrt{\sum_{k=1}^K \|\mathbf{e}_k\|^2}. \quad (6.9)$$

For this “system-wide” uncertainty model, the channel uncertainty set can be described by

$$\mathcal{U}(\Delta) = \{\mathbf{H} \mid \mathbf{H} = \hat{\mathbf{H}} + \mathbf{E}, \|\mathbf{E}\| \leq \Delta\}, \quad (6.10)$$

and a minimax robust downlink transceiver will be presented in Section 6.6.

6.4 Statistically Robust design Via BC-MAC duality

For the stochastic uncertainty model, our objective is to jointly design the precoding matrix \mathbf{P} and the receivers’ equalizing gains g_k so as to minimize the average, over the channel estimation error, of the total MSE:

$$\overline{\text{MSE}} = \sum_{k=1}^K \overline{\text{MSE}}_k, \quad (6.11)$$

where each $\overline{\text{MSE}}_k$ is given by:

$$\overline{\text{MSE}}_k = \sum_{j=1}^K |g_k|^2 \mathbf{p}_j^H (\hat{\mathbf{h}}_k^H \hat{\mathbf{h}}_k + \sigma_{e_k}^2 \mathbf{I}) \mathbf{p}_j + \sigma_n^2 |g_k|^2 - g_k \hat{\mathbf{h}}_k^H \mathbf{p}_k - g_k \hat{\mathbf{h}}_k^H \mathbf{p}_k^H + 1. \quad (6.12)$$

It can be seen from (6.12), that each $\overline{\text{MSE}}_k$ is not a jointly convex function of \mathbf{P} and g_k .² To overcome this problem, previous approaches to the design of robust BC transceivers have considered simplifying the design by restricting all g_k to be equal [106, 107], or by using a simpler detection model [108]. In our approach, we will obtain a computationally efficient solution for the \mathbf{P} and g_k that jointly minimize (6.11) by exploiting the duality between the broadcast channel (BC) and the multiple access channel (MAC). We will start by briefly reviewing (e.g., [60, 110–115]) the dual MAC for the BC presented in Section 6.2.

²It can also be seen from (6.12) that the phase component of g_k can be absorbed in \mathbf{p}_k without changing $\overline{\text{MSE}}_k$, and hence that the basestation need only send $|g_k|$ to receiver k . This can be considered as the stochastic-model counterpart of Lemma 5.2.

6.4.1 Dual Multiple Access Channel with Linear Transceivers

By switching the roles of the transmitter and the receiver in the broadcast channel, we obtain the dual MAC that consists of K transmitters, each with a single antenna, and a receiver with N_t antennas. The channel matrix for the dual MAC is \mathbf{H}^H . Similar to the MSE expressions obtained for the BC in (6.12), we will be interested in obtaining corresponding expressions of individual MSEs in the dual MAC with linear precoding and linear multiuser reception. Because the transmitters in the dual MAC are decentralized and each have only one transmit antenna, linear precoding reduces to power loading:

$$x_k^{\text{MAC}} = p_k^{\text{MAC}} s_k^{\text{MAC}}, \quad (6.13)$$

where s_k^{MAC} and x_k^{MAC} are the data symbol and the transmitted signal of the k^{th} transmitter. Without loss of generality, we will assume that $E\{\mathbf{s}^{\text{MAC}} \mathbf{s}^{\text{MAC}H}\} = \mathbf{I}$. Hence, a total power constraint on all the transmitters can be written as $\sum_{k=1}^K |p_k^{\text{MAC}}|^2 \leq P_{\text{total}}$.

The vector of received signals \mathbf{y}^{MAC} is given by

$$\mathbf{y}^{\text{MAC}} = \mathbf{H}^H \mathbf{x}^{\text{MAC}} + \mathbf{n}^{\text{MAC}}, \quad (6.14)$$

where \mathbf{n}^{MAC} is the zero-mean receiver noise vector whose covariance matrix is $E\{\mathbf{n}^{\text{MAC}} \mathbf{n}^{\text{MAC}H}\} = \sigma_n^2 \mathbf{I}$. Using a linear multiuser receiver, $\mathbf{g}_k^{\text{MAC}} \in \mathbb{C}^{1 \times N_t}$, the base station obtains an estimate of the symbol transmitted by the k^{th} user, $\hat{s}_k^{\text{MAC}} = \mathbf{g}_k^{\text{MAC}} \mathbf{y}^{\text{MAC}}$.

Using the stochastic channel uncertainty model, the average over the channel estimation errors of the MSE associated with the estimation of \hat{s}_k^{MAC} can be written

as

$$\begin{aligned} \overline{\text{MSE}}_k^{\text{MAC}} &= \sum_{j=1}^K |p_j^{\text{MAC}}|^2 \mathbf{g}_k^{\text{MAC}} (\hat{\mathbf{h}}_j^H \hat{\mathbf{h}}_j + \sigma_{e_j}^2 \mathbf{I}) \mathbf{g}_k^{\text{MAC}H} \\ &+ \sigma_n^2 \mathbf{g}_k^{\text{MAC}} \mathbf{g}_k^{\text{MAC}H} - p_k^{\text{MAC}H} \hat{\mathbf{h}}_k \mathbf{g}_k^{\text{MAC}H} - p_k^{\text{MAC}} \mathbf{g}_k^{\text{MAC}} \hat{\mathbf{h}}_k^H + 1. \end{aligned} \quad (6.15)$$

6.4.2 BC-MAC Duality with Stochastic Uncertainty and Linear Transceivers

In this section, we will present the MSE duality result for the BC and MAC channels under the stochastic channel uncertainty model described in Section 6.3. This duality result generalizes the MSE duality between the BC and MAC channels for the perfect channel knowledge case [60, 110–114] to scenarios with uncertain CSI.³ The duality relation will be useful in obtaining a robust BC transceiver that minimizes the average MSE in terms of the corresponding transceiver of the dual MAC that minimizes the same objective.

Theorem 6.1. *Under the same total transmitted power constraint, the sets of individual average MSEs for the BC, $\{\overline{\text{MSE}}_k\}$, and for the dual MAC, $\{\overline{\text{MSE}}_k^{\text{MAC}}\}$, are equal when one uses the following transceiver designs:*

$$\mathbf{p}_k = \omega_k \mathbf{g}_k^{\text{MAC}H}, \quad g_k = \omega_k^{-1} p_k^{\text{MAC}H}, \quad (6.16)$$

where the vector of positive constants $\boldsymbol{\omega} = (\omega_1, \dots, \omega_K)$ is given by:

$$\boldsymbol{\omega}^2 = \mathbf{M}^{-1} \left[|p_1^{\text{MAC}}|^2, \dots, |p_K^{\text{MAC}}|^2 \right]^T, \quad (6.17)$$

³Note that SINR duality does not extend to the statistical model of uncertain CSI [116].

and the matrix \mathbf{M} is given by:

$$[\mathbf{M}]_{k,j} = \begin{cases} \sum_{i \neq k}^K \frac{|p_i^{\text{MAC}}|^2}{\sigma_n^2} \mathbf{g}_k^{\text{MAC}} (\hat{\mathbf{h}}_i^H \hat{\mathbf{h}}_i + \sigma_{e_i}^2 \mathbf{I}) \mathbf{g}_k^{\text{MAC}H} + \mathbf{g}_k^{\text{MAC}} \mathbf{g}_k^{\text{MAC}H} & k = j \\ -\frac{|p_k^{\text{MAC}}|^2}{\sigma_n^2} \mathbf{g}_j^{\text{MAC}} (\hat{\mathbf{h}}_k^H \hat{\mathbf{h}}_k + \sigma_{e_k}^2 \mathbf{I}) \mathbf{g}_j^{\text{MAC}H} & k \neq j. \end{cases} \quad (6.18)$$

A sketch of the proof of this result is provided in Appendix G. It is a generalization of the proof in [111] to scenarios with channel uncertainty.⁴ Using Theorem 6.1, the broadcast precoder \mathbf{P} and receiver gains g_k that jointly minimize a general function of the users' average MSEs under a total power constraint can be obtained by first obtaining the MAC transceiver that jointly minimizes the same objective and then applying the transformation in (6.17) to obtain the optimal BC transceiver. In the following section we will consider the sum of the average MSEs as an example, and we will obtain an efficiently solvable formulation for the jointly optimal transceivers for the dual MAC that minimize that objective.

6.4.3 Statistically Robust Transceiver Design for the Dual MAC

Our objective here is to find the dual MAC transmitters p_k^{MAC} and receivers $\mathbf{g}_k^{\text{MAC}}$ that jointly minimize the average MSE, $\overline{\text{MSE}}^{\text{MAC}} = \sum_{k=1}^K \overline{\text{MSE}}_k^{\text{MAC}}$. First, we will obtain an analytic expression for the optimal receiver $\mathbf{g}_k^{\text{MAC}}$ for a given set of transmitters p_i^{MAC} . Using these expressions we will then obtain a convex formulation for the optimal p_k^{MAC} under a total power constraint.

⁴In fact, the MSE duality result for the stochastic uncertainty model extends directly to the case of multiple antennas at the receivers and multiple data streams per user, analogous to the case of perfect channel knowledge in [111].

To design the $\mathbf{g}_k^{\text{MAC}}$, we observe from (6.15) that each $\overline{\text{MSE}}_k^{\text{MAC}}$ is a convex function of $\mathbf{g}_k^{\text{MAC}}$ and is independent of the other $\mathbf{g}_j^{\text{MAC}}$, $j \neq k$, and hence that it can be minimized independently. Setting the derivative of $\overline{\text{MSE}}_k^{\text{MAC}}$ with respect to $\mathbf{g}_k^{\text{MAC}}$ to zero, we obtain the following expression for the optimal $\mathbf{g}_k^{\text{MAC}}$:

$$\mathbf{g}_k^{\text{MAC}} = p_k^{\text{MAC}} \hat{\mathbf{h}}_k^H (\sum_{i=1}^K |p_i^{\text{MAC}}|^2 (\hat{\mathbf{h}}_i^H \hat{\mathbf{h}}_i + \sigma_{e_i}^2 \mathbf{I}) + \sigma_n^2 \mathbf{I})^{-1}. \quad (6.19)$$

Using this optimal value, the average total MSE reduces to

$$\overline{\text{MSE}}^{\text{MAC}} = K - N_t + \sigma_n^2 \text{tr}(\Phi^{-1}), \quad (6.20)$$

where $\Phi = \sum_{i=1}^K |p_i^{\text{MAC}}|^2 (\hat{\mathbf{h}}_i^H \hat{\mathbf{h}}_i + \sigma_{e_i}^2 \mathbf{I}) + \sigma_n^2 \mathbf{I}$.

The next step is to design the p_k^{MAC} that minimize (6.20) subject to a total transmitted power constraint $\sum_{k=1}^K |p_k^{\text{MAC}}|^2 \leq P_{\text{total}}$. By defining $q_k = |p_k^{\text{MAC}}|^2$, that problem can be formulated as:

$$\min_{q_i} \text{tr}(\sum_{i=1}^K q_i (\hat{\mathbf{h}}_i^H \hat{\mathbf{h}}_i + \sigma_{e_i}^2 \mathbf{I}) + \sigma_n^2 \mathbf{I})^{-1} \quad (6.21a)$$

$$\text{s. t. } q_i \geq 0, \quad i = 1, \dots, K, \quad \sum_{i=1}^K q_i \leq P_{\text{total}}. \quad (6.21b)$$

Using techniques similar to those in [117], this problem can be transformed into the following (convex) Semidefinite Program (SDP):

$$\min_{q_i, \mathbf{S}} \text{tr}(\mathbf{S}) \quad (6.22a)$$

$$\text{s. t. } \begin{bmatrix} \mathbf{S} & \mathbf{I} \\ \mathbf{I} & (\sum_{i=1}^K q_i (\hat{\mathbf{h}}_i^H \hat{\mathbf{h}}_i + \sigma_{e_i}^2 \mathbf{I}) + \sigma_n^2 \mathbf{I}) \end{bmatrix} \geq \mathbf{0}, \quad (6.22b)$$

$$q_i \geq 0, \quad i = 1, \dots, K, \quad \sum_{i=1}^K q_i \leq P_{\text{total}}. \quad (6.22c)$$

This SDP can be efficiently solved using self-dual interior point methods; e.g., [85].⁵

⁵Without loss of generality, we can choose each p_k^{MAC} to be the positive square root of q_k , then since ω_k in (6.16) is real, each optimal g_k will be real.

6.5 Downlink Minimax Robust Design with Individual Channel Uncertainties

In this section we present a robust transceiver design that does not rely on a statistical model of channel uncertainty, but merely assumes that the each user's channel lies within a given uncertainty set $\mathcal{U}_k(\delta_k, \Phi_k, \mathbf{Q}_k)$; c.f. (6.7). As mentioned in Section 6.3, this uncertainty model is a convenient one for systems in which a channel estimate is quantized at the receiver and fed back to the transmitter. For this type of channel uncertainty, our goal is to jointly design the precoder \mathbf{P} and equalization gains g_k so as to minimize the worst-case MSE over all admissible channels $\mathbf{h}_k \in \mathcal{U}_k(\delta_k)$, subject to a total power constraint. That is,

$$\min_{\mathbf{P}, \mathbf{g}} \max_{\mathbf{h}_k \in \mathcal{U}_k(\delta_k)} \sum_{k=1}^K \|g_k \mathbf{h}_k \mathbf{P} - \mathbf{m}_k\|^2 + \sigma_n^2 \|\mathbf{g}\|^2 \quad (6.23a)$$

$$\text{s. t. } \|\text{vec}(\mathbf{P})\|^2 \leq P_{\text{total}}. \quad (6.23b)$$

By introducing the auxiliary variables t_k , $0 \leq k \leq K$, this minimax problem can be written as the following minimization problem:

$$\min_{\mathbf{P}, \mathbf{g}, \mathbf{t}} \sum_{k=0}^K t_k^2 \quad (6.24a)$$

$$\text{s. t. } \|g_k \mathbf{h}_k \mathbf{P} - \mathbf{m}_k\| \leq t_k \quad \forall 1 \leq k \leq K, \mathbf{h}_k \in \mathcal{U}_k(\delta_k, \Phi_k, \mathbf{Q}_k), \quad (6.24b)$$

$$\sigma_n \|\mathbf{g}\| \leq t_0, \quad (6.24c)$$

along with (6.23b).⁶ The constraint in (6.24b) represents K infinite sets of second order cone (SOC) constraints (e.g., [82, 118]), with one constraint for each $\mathbf{h}_k \in \mathcal{U}_k(\delta_k)$. However, these infinite sets of constraints can be precisely characterized by

⁶As was the case in the previous section, the formulation in (6.24) shows that phase component of g_k can be absorbed into \mathbf{p}_k . Indeed, if $\{|g_k| e^{j\theta_k}\}$ and \mathbf{P} are an optimal solution of (6.24), then $\{|g_k|\}$ and $\mathbf{P} \text{Diag}(e^{j\theta_1}, \dots, e^{j\theta_K})$ are also optimal.

the following set of K inequalities [81]:

$$\begin{bmatrix} t_k - \mu_k & \mathbf{0} & (g_k \hat{\mathbf{h}}_k \mathbf{P} - \mathbf{m}_k) \\ \mathbf{0} & \mu_k \mathbf{Q} & \delta_k(g_k \Phi \mathbf{P}) \\ (g_k \hat{\mathbf{h}}_k \mathbf{P} - \mathbf{m}_k)^H & \delta_k(g_k \Phi \mathbf{P})^H & t_k \mathbf{I} \end{bmatrix} \geq \mathbf{0}, \quad 1 \leq k \leq K, \quad (6.25)$$

where Φ is the matrix whose rows are ϕ_j . Using the characterization in (6.25), the robust transceiver design can be formulated as:

$$\min_{\mathbf{P}, \mathbf{g}, \lambda, \mu, \alpha} \alpha \quad (6.26a)$$

$$\text{s.t.} \quad \left\| \begin{bmatrix} \lambda \\ \sigma_n \mathbf{g} \end{bmatrix} \right\|^2 \leq \alpha, \quad (6.26b)$$

$$\begin{bmatrix} t_k - \mu_k & \mathbf{0} & (g_k \hat{\mathbf{h}}_k \mathbf{P} - \mathbf{m}_k) \\ \mathbf{0} & \mu_k \mathbf{Q} & \delta_k(g_k \Phi \mathbf{P}) \\ (g_k \hat{\mathbf{h}}_k \mathbf{P} - \mathbf{m}_k)^H & \delta_k(g_k \Phi \mathbf{P})^H & t_k \mathbf{I} \end{bmatrix} \geq \mathbf{0} \quad 1 \leq k \leq K, \quad (6.26c)$$

$$\|\text{vec}(\mathbf{P})\|^2 \leq P_{\text{total}}, \quad (6.26d)$$

where we have used the fact that the optimal value for t_0 is $\sigma_n \|\mathbf{g}\|$. The constraint in (6.26c) represents a set of K bilinear matrix inequalities and hence the optimization problem in (6.26) is non-convex. (In the general case, optimization problems with bilinear matrix inequalities are NP hard [119].) However, given initial values for \mathbf{P} and \mathbf{g} , one can find a locally optimal solution by iteratively optimizing over \mathbf{P} for fixed \mathbf{g} , and over \mathbf{g} for fixed \mathbf{P} . Each of those problems is implicit in (6.26) and is a convex conic program that can be efficiently solved; e.g., [85]. One natural choice of the starting point for this iterative design would be the transceiver designed for the case in which the estimates $\hat{\mathbf{h}}_k$ are assumed to be the actual channels; e.g., [102, 110].

The formulation in (6.23) employs a simple constraint on the transmitted power. However, other types of power constraints can be incorporated into the design without

compromising the convex conic nature of the steps in the proposed iterative algorithm. In particular, one can incorporate per-antenna power constraints, per-cell power constraints, and spatial masking constraints as second order cone (SOC) constraints or linear matrix inequality constraints on \mathbf{P} ; See Appendix D.

6.5.1 Multiple Intersecting Uncertainties for Each User

The problem formulation in (6.23) can be generalized to the case in which the uncertainty region $\tilde{\mathcal{U}}_k$ for each \mathbf{h}_k is described as the intersection of more than one uncertainty set of the form (6.7); cf. (6.8). In that case, the problem is at least as hard as the case of a single uncertainty set (the special case of (6.8) when $L = 1$). In particular, in the general case when \mathcal{U}_k is replaced by $\tilde{\mathcal{U}}_k$ it is not possible to characterize the infinite set of constraints of the form in (6.24b) by a polynomial (in N_t) number of constraints [99]. Therefore, the number of constraints in the subproblems in an iterative local optimization algorithm analogous to that described above for the problem in (6.26) grows faster than any polynomial in N_t . As a result, each of these subproblems is NP-hard, even though they remain convex. However, by adopting a conservative approach one can obtain an efficiently-solvable approximation to the problem with the uncertainty set in (6.8). This conservative approach involves enveloping (6.8) in a superset that can be described more efficiently, and then minimizing the maximum MSE in this superset. Using the superset characterization in [99] of sets of the form (6.8), it can be shown that the solution of robust transceiver design problem in (6.23) for the intersection of uncertainty sets in (6.8) is

upper-bounded by the solution of the following optimization problem

$$\min_{\substack{\mathbf{P}, \mathbf{g}, \\ \mathbf{t}, \mu_k, \alpha}} \alpha \quad (6.27a)$$

$$\text{s.t.} \quad \left\| \begin{bmatrix} \sigma_n \mathbf{g} \\ \mathbf{t} \end{bmatrix} \right\|^2 \leq \alpha, \quad (6.27b)$$

$$\begin{bmatrix} t_k - \sum_{\ell} \mu_k^{\ell} & \mathbf{0} & (g_k \hat{\mathbf{h}}_k \mathbf{P} - \mathbf{m}_k) \\ \mathbf{0} & \sum_{\ell} \mu_k^{\ell} \mathbf{Q}_k^{\ell} & \delta_k(g_k \Phi_k \mathbf{P}) \\ (g_k \hat{\mathbf{h}}_k \mathbf{P} - \mathbf{m}_k)^H & \delta_k(g_k \Phi_k \mathbf{P})^H & t_k \mathbf{I} \end{bmatrix} \geq \mathbf{0}, \quad (6.27c)$$

$$\|\text{vec}(\mathbf{P})\|^2 \leq P_{\text{total}}. \quad (6.27d)$$

Similar to (6.26), a local optimal solution can be found by employing an alternative optimization algorithm that optimizes over \mathbf{P} and \mathbf{B} for fixed \mathbf{g} , and over \mathbf{g} and \mathbf{B} for fixed \mathbf{P} . In this conservative approach, those (convex) problems can be efficiently solved.

6.6 Downlink Minimax Robust Design with Overall Channel Uncertainty

The robust minimax design in (6.26) for the “per-user” channel uncertainty model contains K bilinear matrix inequalities, one for each user. In this section, we consider the alternative “system-wide” channel uncertainty model in (6.10), namely $\|\mathbf{E}\| \leq \Delta$, and we will show that the resulting robust minimax design involves only one nonlinear matrix inequality. Therefore, the computational cost of the conic programs used in the iterative algorithm is reduced. This approach may be suitable for downlink systems involving cells with large number of users or for multi-cell designs.

As in the previous section, our goal is to jointly design the precoder \mathbf{P} and the

equalization gains g_k so as to minimize the worst-case MSE over all admissible channels, subject to a total power constraint. The design problem can be formally stated as:

$$\min_{\mathbf{P}, \mathbf{G}=\text{Diag}(\mathbf{g})} \max_{\|\mathbf{E}\| \leq \Delta} \text{tr}\{(\mathbf{I} - \mathbf{GHP})^H(\mathbf{I} - \mathbf{GHP})\} + \sigma_n^2 \|\mathbf{g}\|^2 \quad (6.28a)$$

$$\text{s. t. } \|\text{vec}(\mathbf{P})\|^2 \leq P_{\text{total}}, \quad (6.28b)$$

and using the auxiliary variables w_0 and w_1 , that minimax problem can be precisely transformed into the following minimization problem:

$$\min_{\mathbf{P}, \mathbf{G}=\text{Diag}(\mathbf{g}), w_0, w_1} w_0 + w_1 \quad (6.29a)$$

$$\text{s.t. } \text{tr}(\mathbf{I} - \mathbf{G}(\hat{\mathbf{H}} + \mathbf{E})\mathbf{P})^H(\mathbf{I} - \mathbf{G}(\hat{\mathbf{H}} + \mathbf{E})\mathbf{P}) \leq w_1 \quad \forall \|\mathbf{E}\| \leq \Delta, \quad (6.29b)$$

$$\sigma_n^2 \|\mathbf{g}\|^2 \leq w_0, \quad (6.29c)$$

$$\|\text{vec}(\mathbf{P})\|^2 \leq P_{\text{total}}. \quad (6.29d)$$

Like (6.24), this problem has an infinite set of constraints, namely (6.29b). (Furthermore, we can also choose \mathbf{g} to be a real vector, without loss of generality.) The first step in the transformation of (6.29b) into a single constraint is the application of the following lemma.

Lemma 6.1 ([120]). *Let $\mathbf{M} \in \mathbb{C}^{K \times K}$ be a Hermitian matrix. Then there exists a scalar s and a matrix $\mathbf{Z} \geq \mathbf{0}$ such that the constraint $\text{tr}(\mathbf{M}) \leq t$ is equivalent to the following representation:*

$$t - Ks - \text{tr}(\mathbf{Z}) \geq 0, \quad (6.30)$$

$$\mathbf{M} \leq \mathbf{Z} + s\mathbf{I}. \quad (6.31)$$

While Lemma 6.1 considers a single matrix \mathbf{M} , it can be directly extended to a set of matrices by applying the lemma to an element of that set of matrices with the

largest trace. Applying that extension to (6.29b) yields a single constraint of the form in (6.30) and the set of constraints $(\mathbf{I} - \mathbf{G}(\hat{\mathbf{H}} + \mathbf{E})\mathbf{P})^H(\mathbf{I} - \mathbf{G}(\hat{\mathbf{H}} + \mathbf{E})\mathbf{P}) \leq \mathbf{Z} + s\mathbf{I}$, $\forall \|\mathbf{E}\| \leq \Delta$. Using the Schur Complement Theorem [22], that set of quadratic matrix inequalities can be transformed into the following set of bilinear matrix inequalities:

$$\begin{bmatrix} \mathbf{Z} + s\mathbf{I} & (\mathbf{I} - \mathbf{G}(\hat{\mathbf{H}} + \mathbf{E})\mathbf{P})^H \\ (\mathbf{I} - \mathbf{G}(\hat{\mathbf{H}} + \mathbf{E})\mathbf{P}) & \mathbf{I} \end{bmatrix} \geq \mathbf{0} \quad \forall \|\mathbf{E}\| \leq \Delta. \quad (6.32)$$

By moving terms containing \mathbf{E} to the right-hand side of the inequality, we can re-write (6.32) as:

$$\begin{bmatrix} \mathbf{Z} + s\mathbf{I} & (\mathbf{I} - \mathbf{G}\hat{\mathbf{H}}\mathbf{P})^H \\ (\mathbf{I} - \mathbf{G}\hat{\mathbf{H}}\mathbf{P}) & \mathbf{I} \end{bmatrix} \geq \begin{bmatrix} \mathbf{0} \\ \mathbf{G} \end{bmatrix} \mathbf{E} \begin{bmatrix} \mathbf{P} & \mathbf{0} \end{bmatrix} + \begin{bmatrix} \mathbf{P}^H \\ \mathbf{0} \end{bmatrix} \mathbf{E}^H \begin{bmatrix} \mathbf{0} & \mathbf{G}^H \end{bmatrix} \quad \forall \|\mathbf{E}\| \leq \Delta. \quad (6.33)$$

To cast (6.33) as a single matrix inequality we use the following lemma:

Lemma 6.2 ([121]). *Let \mathbf{A} be a Hermitian matrix. Then $\mathbf{A} \geq \mathbf{C}^H \mathbf{X}^H \mathbf{B} + \mathbf{B}^H \mathbf{X} \mathbf{C}$ for all $\|\mathbf{X}\| \leq \Delta$ if and only if there exists a $\lambda \geq 0$ such that*

$$\begin{bmatrix} \mathbf{A} - \lambda \mathbf{C}^H \mathbf{C} & -\Delta \mathbf{B}^H \\ -\Delta \mathbf{B} & \lambda \mathbf{I} \end{bmatrix} \geq \mathbf{0}.$$

Applying Lemma 6.2 with $\mathbf{B} = [\mathbf{P} \ \mathbf{0}]$, and $\mathbf{C} = [\mathbf{0} \ \mathbf{G}^H]$, the robust minimax

design in (6.28) can be formulated as

$$\min_{\substack{\mathbf{P}, \mathbf{G} = \text{Diag}(\mathbf{g}), \mathbf{Z}, \\ s, \lambda, w_0, w_1}} w_0 + w_1 \quad (6.34a)$$

$$\text{s. t. } \begin{bmatrix} \mathbf{Z} + s\mathbf{I} & (\mathbf{I} - \mathbf{G}\hat{\mathbf{H}}\mathbf{P})^H & -\Delta\mathbf{P}^H \\ (\mathbf{I} - \mathbf{G}\hat{\mathbf{H}}\mathbf{P}) & \mathbf{I} - \lambda\mathbf{G}\mathbf{G}^H & \mathbf{0} \\ -\Delta\mathbf{P} & \mathbf{0} & \lambda\mathbf{I} \end{bmatrix} \geq \mathbf{0} \quad (6.34b)$$

$$w_1 - Ks - \text{tr}(\mathbf{Z}) \geq 0, \quad (6.34c)$$

$$s \geq 0, \quad (6.34d)$$

$$\sigma_n^2 \|\mathbf{g}\|^2 \leq w_0, \quad (6.34e)$$

$$\|\text{vec}(\mathbf{P})\|^2 \leq P_{\text{total}}. \quad (6.34f)$$

Although this problem has a finite number of inequalities, like (6.26), the presence of the non-linear matrix inequality in (6.34b) renders (6.34) a non-convex optimization problem. However, one can use an iterative algorithm to obtain a locally optimal solution. For the iterations with fixed \mathbf{g} , the problem in (6.34) represents a convex conic optimization problem that can be solved more efficiently than the corresponding problem in the case of “per-user” channel uncertainty model, c.f., (6.26). For the iterations with fixed \mathbf{P} , one can interchange the choices of \mathbf{B} and \mathbf{C} in the application of Lemma 6.2 to obtain an equivalent inequality to (6.34b) that is linear in \mathbf{g} . The resulting problem is also an efficiently-solvable convex conic optimization problem.

As was the case with the results in Section 6.4.2, the results in this section extend directly to the case of multiple antennas at the receivers and multiple data streams per user. For such scenarios, \mathbf{G} is a block diagonal matrix (with rectangular blocks).

6.7 Uplink Minimax Robust Designs

The proposed design framework for minimax robust transceivers for the downlink is quite general and can be applied to uplink systems as well. In this section we will provide explicit formulations of the minimax robust designs for the dual MAC. As mentioned in Section 6.4, the channel matrix for the dual MAC is \mathbf{H}^H , and we will define $\mathbf{p}^{\text{MAC}} = (p_1^{\text{MAC}}, \dots, p_K^{\text{MAC}})$ and \mathbf{G}^{MAC} to be the matrix whose rows are $\mathbf{g}_k^{\text{MAC}}$.

To derive the robust “per-user” minimax design, we first observe that MSE expression for the k^{th} user in the uplink is function is function of all channels, not just its own. While these multiple sources of uncertainty can complicate the design, one can write the total MSE as

$$\text{MSE}^{\text{MAC}} = \sum_{k=1}^K \|\mathbf{G}^{\text{MAC}} \mathbf{h}_k^H p_k^{\text{MAC}} - \mathbf{m}_k^T\|^2 + \sigma_n^2 \text{tr}((\mathbf{G}^{\text{MAC}})^H \mathbf{G}^{\text{MAC}}), \quad (6.35)$$

where each term of the summation is subject to uncertainty from one source only. Using (6.35) and the analysis in Section 6.5, the uplink robust minimax design with the “per-user” uncertainty model can be formulated as

$$\min_{\substack{\mathbf{G}^{\text{MAC}}, \mathbf{p}^{\text{MAC}} \\ \lambda, \mu, \beta}} \beta \quad (6.36a)$$

$$\text{s.t.} \quad \left\| \left[\sigma_n \text{vec}(\hat{\mathbf{G}}^{\text{MAC}}) \right] \right\|^2 \leq \beta \quad (6.36b)$$

$$\begin{bmatrix} \lambda_k - \mu_k & \mathbf{0} & (\mathbf{G}^{\text{MAC}} \hat{\mathbf{h}}_k^H p_k^{\text{MAC}} - \mathbf{m}_k^T)^H \\ \mathbf{0} & \mu_k \mathbf{I} & \delta_k (\mathbf{G}^{\text{MAC}} p_k^{\text{MAC}})^H \\ (\mathbf{G}^{\text{MAC}} \hat{\mathbf{h}}_k^H p_k^{\text{MAC}} - \mathbf{m}_k^T) & \delta_k (\mathbf{G}^{\text{MAC}} p_k^{\text{MAC}}) & \lambda_k \mathbf{I} \end{bmatrix} \geq \mathbf{0},$$

$$1 \leq k \leq K, \quad (6.36c)$$

$$\|\mathbf{p}^{\text{MAC}}\|^2 \leq P_{\text{total}}. \quad (6.36d)$$

Similarly, the uplink robust minimax design with the “system-wide” model of uncertainty can be formulated as

$$\min_{\substack{\mathbf{G}^{\text{MAC}}, \mathbf{Z}, s, \lambda, w_0, w_1, \\ \mathbf{P}^{\text{MAC}} = \text{Diag}(\mathbf{p}^{\text{MAC}})}} w_0 + w_1 \quad (6.37a)$$

$$\text{s.t.} \quad \begin{bmatrix} \mathbf{Z} + s\mathbf{I} & (\mathbf{I} - \mathbf{G}^{\text{MAC}} \hat{\mathbf{H}}^H \mathbf{P}^{\text{MAC}})^H & -\Delta(\mathbf{P}^{\text{MAC}})^H \\ (\mathbf{I} - \mathbf{G}^{\text{MAC}} \hat{\mathbf{H}}^H \mathbf{P}^{\text{MAC}}) & \mathbf{I} - \lambda \mathbf{G}^{\text{MAC}} (\mathbf{G}^{\text{MAC}})^H & \mathbf{0} \\ -\Delta \mathbf{P}^{\text{MAC}} & \mathbf{0} & \lambda \mathbf{I} \end{bmatrix} \geq \mathbf{0} \quad (6.37b)$$

$$s \geq 0, \quad (6.37c)$$

$$\sigma_n^2 \|\text{vec}(\mathbf{G}^{\text{MAC}})\|^2 \leq w_0, \quad (6.37d)$$

$$\|\mathbf{p}^{\text{MAC}}\|^2 \leq P_{\text{total}}. \quad (6.37e)$$

As with the case with the downlink, these optimization problems are non-convex, but one can employ a local iterative algorithm in which a convex conic program is solved at each iteration.

6.8 Simulation Studies

In order to compare the performance of the proposed robust designs with existing approaches, we have simulated these methods for the cases of uncoded QPSK and 16-QAM transmission over independent block fading Rayleigh channels (without shadowing). We considered downlink scenarios with $N_t = 4$ and 5 antennas, and $K = 4$ users, at different distances from the base station. The first two users are assumed to be far from the base station and their channels coefficients are modeled as being independent circularly symmetric complex Gaussian random variables with zero mean and unit variance. The other two users are assumed to be closer to the base station

and their channel coefficients are generated using the above model but with variances equal to 10.⁷ We will plot the average bit error rate (BER) over all users against the signal-to-noise-ratio, which is defined as $\text{SNR} = P_{\text{total}}/(K\sigma_n^2)$. We will also plot the average BER over each pair of near and far users. The BERs are averaged over 500 channel realizations, \mathbf{H} . For each realization, we construct 100 channel estimates, $\hat{\mathbf{H}}$, using (6.6). For each estimate, we compute the robust precoder and the equalizing gains, inform each receiver of the equalizing gain g_k that it is to use, and transmit a packet of 200 uncoded symbols.

6.8.1 Statistically robust transceiver design

The channel estimation error $\mathbf{e}_k = \mathbf{h}_k - \hat{\mathbf{h}}_k$ was modelled by generating \mathbf{e}_k from a zero-mean Gaussian distribution with $E\{\mathbf{e}_k^H \mathbf{e}_k\} = \sigma_{e_k}^2 \mathbf{I}$, where we will use the same $\sigma_{e_k}^2$ for all users. This model is appropriate for a scenario in which the uplink power is controlled so that the received SNRs on the uplink are equal and independent from the downlink SNR. For convenience, we define $\epsilon^2 = E\{\mathbf{e}_k \mathbf{e}_k^H\} = N_t \sigma_{e_k}^2$.

In Fig. 6.1 we compare the performance of the statistically robust transceiver proposed in Section 6.4 with that of the regularized channel inversion approach in [102, 122], and that of the channel inversion approach in [100, 101], for a system with 4 transmit antennas, 4 users, QPSK signalling, and $\epsilon^2 = 0.01$. It can be seen that the performance of a linear transceiver in the broadcast channel is rather sensitive to the mismatch between the actual CSI and the transmitter's estimate of CSI; see also [8]. It can be also seen that while the effect of noise is dominant at low SNR, the channel uncertainty dominates at high SNR, where the proposed robust transceiver design performs significantly better than the other two approaches. Fig. 6.1 also shows that

⁷In practice, a scheduler may select the users to which data is transmitted, but in order to focus on the impact of the proposed designs, no scheduling will be considered in the simulations.

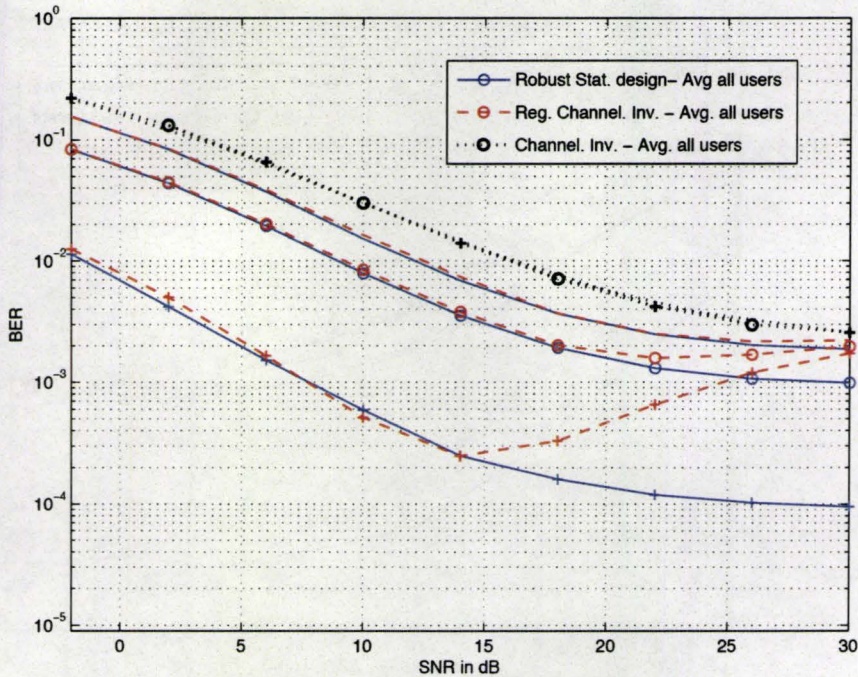


Figure 6.1: Comparison between the performance of the proposed statistically robust transceiver, the channel inversion approach in [100, 101], and regularized channel inversion [102, 122] for values of channel uncertainty $\epsilon^2 = 0.01$ for a system with $N_t = 4$ and $K = 4$ using QPSK signalling. The curves with (+) markers and no markers represent the average BER of the two near and the two far users, respectively.

in the presence of channel uncertainty, both the regularized channel inversion and channel inversion designs have the same performance limit at high SNR. This is due to the fact that the regularized method involves the addition of a regularization term whose value is inversely proportional to $P_{\text{total}}/(K\sigma_n^2)$; see [102].

In Fig. 6.2 we compare the performance of the statistically robust transceiver with that of channel inversion approach in [100, 101], and regularized channel inversion approach in [102, 122], for a system with 5 transmit antennas, 4 users, QPSK signalling,

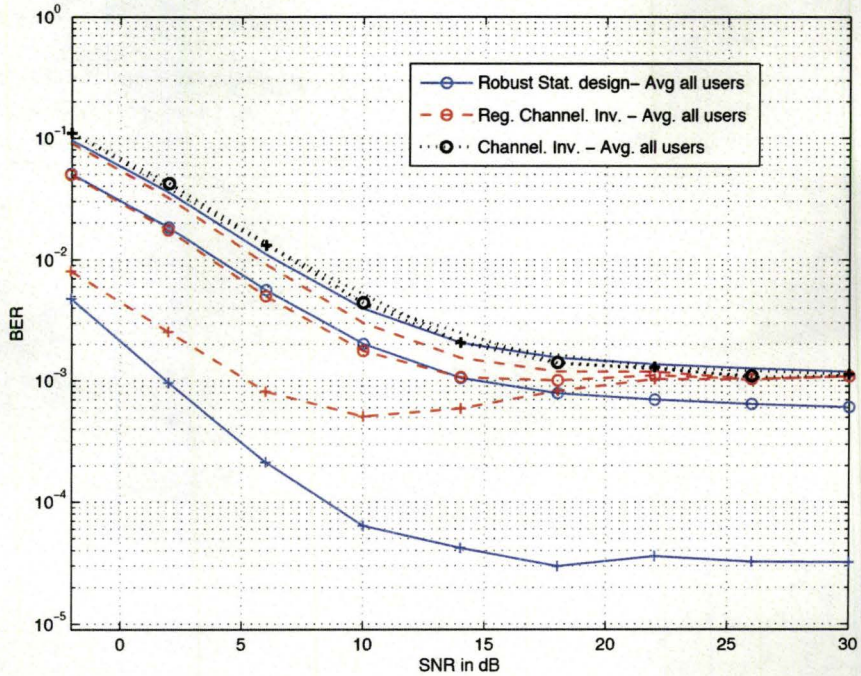


Figure 6.2: Comparison between the performance of the transceivers considered in Figure 6.1 for a system with $N_t = 5$ and $\epsilon^2 = 0.1$. The legend is the same as that in Figure 6.1.

and uncertainty value $\epsilon^2 = 0.1$. The impact of the robust design is apparent in the average performance of the two near users for the whole SNR range, and in the average performance of all users at high SNRs.

For Fig. 6.3 we consider a system with 16-QAM signalling, 5 transmit antennas and 4 users, and we compare the performance of the proposed statistically robust transceiver with that of the robust regularized channel inversion approach in [107], which restricts all the receiver gains g_k to be equal. It can be seen from Fig. 6.3 that significant improvement in the performance of the near users can be achieved by the proposed robust design, as it offers more degrees of freedom in the choice of the gains g_k .

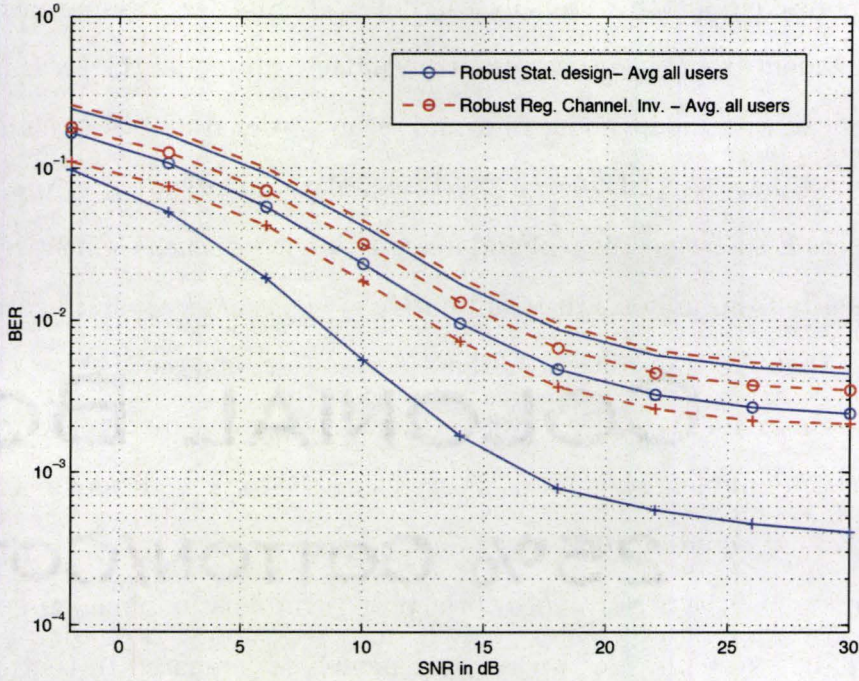


Figure 6.3: Comparison between the performance of the proposed statistically robust transceiver and the robust regularized channel inversion approach in [107] for values of channel uncertainty $\epsilon^2 = 0.03$ for a system with $N_t = 5$ and $K = 4$ using 16-QAM signalling. The curves with (+) markers and no markers represent the average BER of the two near and the two far users, respectively.

6.8.2 Robust minimax transceiver designs

In systems that use feedback to provide the transmitter with quantized version of the CSI, the information available to the transmitter will include the designed quantization codebooks and the statistics of the error resulting from the use of these codebooks; e.g., $E\{(\mathbf{h}_k - \hat{\mathbf{h}}_k)(\mathbf{h}_k - \hat{\mathbf{h}}_k)^H\} = \epsilon^2$. Since we assume each user's channel is independent from the others, the transmitter can model the error matrix \mathbf{E} as being zero mean with independent rows and second order statistics given by $E\{\mathbf{E}\mathbf{E}^H\} = \epsilon^2\mathbf{I}$. Thus, we have $\|E\{\mathbf{E}\mathbf{E}^H\}\| = \epsilon^2$. To simulate quantization errors, we will generate matrices \mathbf{E} such that the real and imaginary parts of each element E_{ij} are drawn independently from uniform distribution $U(-\sqrt{\frac{3}{2N_t}}\epsilon, \sqrt{\frac{3}{2N_t}}\epsilon)$, and hence $E\{\mathbf{E}\mathbf{E}^H\} = \epsilon^2\mathbf{I}$. Given that the transmitter will have access to ϵ , and since $\Delta^2 = \|\mathbf{E}^H\mathbf{E}\|$, an appropriate choice for Δ , for the “system-wide” uncertainty model, is ϵ . For the “per-user” uncertainty model, when all users are using the same codebooks, all δ_k are equal and one can use equation (6.9) to set $\delta_k = \epsilon/\sqrt{K}$.

In Fig. 6.4 the performance of the proposed robust minimax approaches with “per-user” and “system-wide” uncertainty models is compared to that of the regularized channel inversion approach in [102,122] in the presence of uniformly distributed quantization errors with $\epsilon^2 = 0.03$ for a system with $N_t = 5$, $K = 4$ and 16-QAM signalling. It can be seen that performance of the minimax approach with the “system-wide” uncertainty model is reasonably close to the minimax approach with “per-user” uncertainty, especially in terms of the average performance of all users. Both approaches provide improved performance over the non-robust approach in terms of the average BER and significantly improved performance in terms of the BER of the near users. In Fig. 6.5, a comparison is made with the non-robust of channel inversion approach in [100,101], for a similar system with $\epsilon^2 = 0.05$, and similar performance advantages are observed.

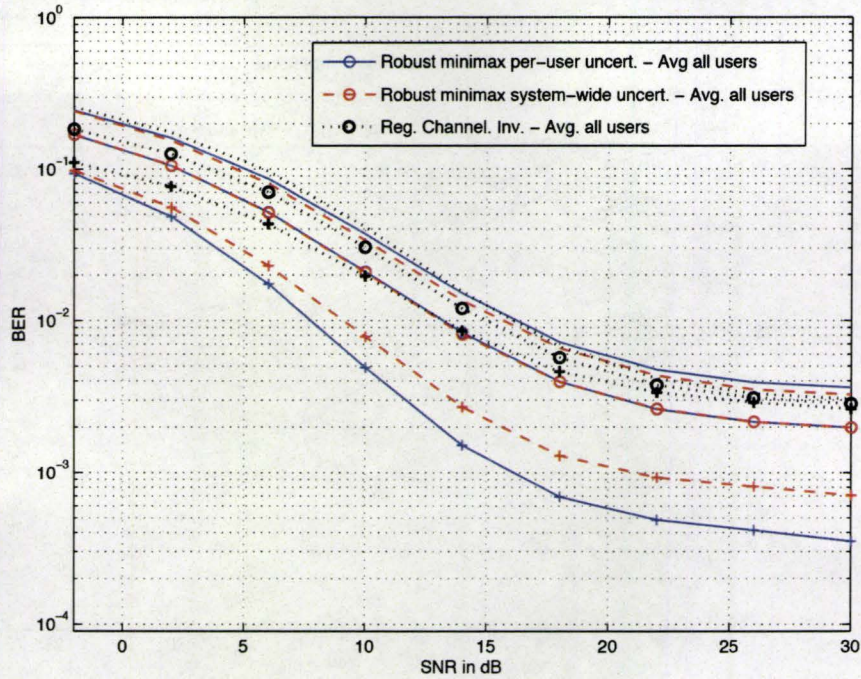


Figure 6.4: Comparison between the performance of the proposed robust minimax approaches with “per-user” and “system-wide” uncertainty models, and the regularized channel inversion approach in [102, 122] in the presence of uniformly distributed quantization errors with $\epsilon^2 = 0.03$ for a system with $N_t = 5$ and $K = 4$ using 16-QAM signalling. The curves with (+) markers and no markers represent the average BER of the two near and the two far users, respectively.

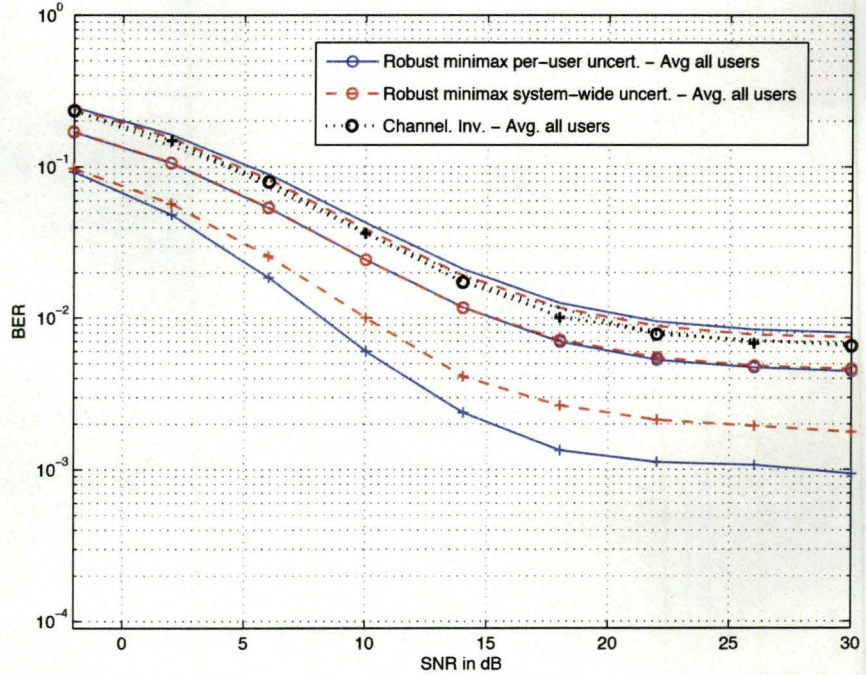


Figure 6.5: Comparison between the performance of the proposed robust minimax approaches with “per-user” and “system-wide” uncertainty models, and the channel inversion approach in [100, 101] in the presence of uniformly distributed quantization errors with $\epsilon^2 = 0.05$ for a system with $N_t = 5$ and $K = 4$ using 16-QAM signalling. The curves with (+) markers and no markers represent the average BER of the two near and the two far users, respectively.

6.9 Conclusion

In this chapter, we considered statistical and minimax robust joint designs for linear transceivers for multiuser communication systems. For the statistical approach, we have presented a robust design for the broadcast channel transceivers that jointly minimize the average, over the channel estimation errors, of the sum of the MSEs of each user. By generalizing the MSE duality between the broadcast channel (BC) and multiple access channel (MAC) to schemes with channel estimation errors, we have shown that the robust design for the broadcast channel can be obtained from an efficiently-solvable conic programming formulation for the robust transceivers for the dual MAC. For the minimax approach, we have provided a formulation for the robust downlink transceivers that maximize the worst-case performance for “per-user” and “system-wide” channel uncertainty models. We also proposed computationally-tractable iterative algorithms for obtaining locally optimal solutions to these two design problems. The problem formulation and proposed algorithms can be applied to systems with per-antenna, per-cell, and spatial-shaping power constraints, as well as a constraint on the total transmitted power. We showed that proposed minimax downlink transceiver designs can be applied to the design of uplink transceivers as well. Our simulation results demonstrated that the proposed approaches to the robust linear transceiver design can significantly reduce the sensitivity of the downlink to uncertain CSI, and can provide improved performance over that of existing robust designs. In the next chapter, we will demonstrate how these robust designs can be generalized to non-linear transceivers.

Chapter 7

Robust Non-Linear Transceivers for Multi-user Systems

In Chapter 6, we studied the design of linear multi-user transceivers that are robust to uncertainty in the users' channel state information (CSI). In this chapter, we generalize those robust design approaches to non-linear transceivers under stochastic and deterministically-bounded models of channel uncertainty. For the stochastic model, we study the joint design of a Tomlinson-Harashima precoder (THP) at the base station and the equalizing gains at the receivers so as to minimize the average, over channel uncertainty, of the total mean-square-error (MSE). By generalizing the MSE duality between the broadcast channel (BC) with THP and the multiple access channel (MAC) with decision feedback equalization (DFE) to scenarios with uncertain CSI, we obtain a relation between the desired robust broadcast transceivers and the corresponding transceivers that optimize the same performance metric for the dual multiple access channel. For the deterministically-bounded model of the channel uncertainty, we study the robust design of THP transceivers for the BC that minimize the maximum MSE over all set admissible channels. Similar to the case of

linear transceiver, we show that the design problem is non-convex and we propose an iterative local optimization algorithm that is based on efficiently-solvable convex subproblems. The robust minimax framework is also generalized to multiple access channels with DFE and bounded channel uncertainty. Simulation results show the proposed robust approaches can result in significant reduction of the sensitivity of THP transceivers to channel uncertainty.

7.1 Introduction

A fundamental assumption of Tomlinson-Harashima Precoding (THP) is the availability of perfect Channel State Information (CSI) at the transmitter. Perfect CSI enables the transmitter to precisely pre-subtract the terms that would interfere at the receivers. Based on the assumption of perfect CSI at the transmitter, several different approaches for designing THP for broadcast channels have been proposed, including zero-forcing designs [16, 123–125], and minimum mean square error (MMSE) designs [126, 127].

In practical downlink scenarios, the CSI available at the transmitter is generally inaccurate; see Sections 4.1 and 6.1. Furthermore, the performance of THP is particularly sensitive to inaccuracies in CSI, e.g., [128]. Motivated by the sensitivity of both broadcast channels and THP to channel uncertainty, we design, herein, robust THP transceivers under two different models of the uncertainty in the CSI: a stochastic model, and a deterministically bounded model.

As mentioned in Section 6.3.1, the stochastic model of channel uncertainty is particularly suitable for systems in which the uncertainty is dominated by the effects of channel estimation errors, such as time division duplex systems with short

“ping-pong” time. For these systems, we consider the joint design of a Tomlinson-Harashima precoder and the users’ equalizing gains to minimize the average, over the channel uncertainty, of the total MSE. Previous attempts to solve this problem have considered a simpler design problem by restricting all the users’ equalizing gains to be equal [106, 129], or by using a simpler detection model [109]. In our approach we will preserve all the degrees of freedom, and will exploit the duality, derived herein, between the broadcast with THP and the multiple access channel (MAC) with decision feedback equalization (DFE), under a statistical model of CSI. More generally, the duality result that we will derive will enable us to obtain robust designs for broadcast channels with THP that optimize objective functions of the the average MSEs, by solving the same design problem for a dual MAC with a DFE. By doing so, we extend to the case of imperfect CSI earlier work on the duality, in the MSE sense, of the BC with THP and MAC with a DFE assuming perfect CSI [127, 130].

The bounded model of channel uncertainty, cf. Section 6.3.2, can be suitable for systems in which each user quantizes its channel information and feeds it back to the transmitter using a limited feedback channel. Using the general bounded uncertainty model in Section 6.3.2, we consider the design of robust THP transceivers for the downlink that minimize the maximum MSE over all admissible channels. We show that the design problem is non-convex and we propose an iterative local optimization algorithm that is based on efficiently-solvable convex subproblems. We also generalize the robust minimax designs to multiple access channels with DFE and bounded channel uncertainty. Simulation results show the proposed robust approaches can result in significant reduction of the sensitivity of THP-based transceivers to channel uncertainty, and can provide improved performance over that of existing robust designs.

7.2 System Model

We consider broadcast channels (BC) with N_t antennas at the base station and K users, each with one antennas. The focus of this chapter will be on BC transceivers that employ Tomlinson-Harashima precoding (THP) at the transmitter. As mentioned in Section 5.2, multi-user interference pre-subtraction and spatial pre-equalization are implemented using feedback and feed forward processing, respectively, as shown in in Fig. 7.1. The elements of the vector output, \mathbf{v} , of the feedback loop in Fig. 7.1 are generated sequentially by computing $v_k = s_k - \sum_{j=1}^{k-1} B_{kj} v_j$, where s_k is the symbol intended for the k^{th} user, which is chosen from a constellation whose Voronoi region is \mathcal{V} , and $\mathbf{B} \in \mathbb{C}^{K \times K}$ is a strictly lower triangular feedback matrix. To prevent v_k from growing outside \mathcal{V} , the modulo operation is then applied to each v_k . The vector \mathbf{v} is subsequently linearly precoded using the feed forward matrix $\mathbf{P} \in \mathbb{C}^{N_t \times K}$ to generate the transmitted vector \mathbf{x} ,

$$\mathbf{x} = \mathbf{P}\mathbf{v}. \quad (7.1)$$

As mentioned in Chapters 2 and 5, when the elements of \mathbf{s} are chosen from a square QAM constellation with cardinality M , the Voronoi region \mathcal{V} is a square of length D , and the modulo operation with respect to \mathcal{V} corresponds to performing separate modulo- D operations on the real and imaginary parts of v_k . This is equivalent to the addition of the complex quantity $i_k = i_k^{re} D + j i_k^{imag} D$ to v_k , where $i_k^{re}, i_k^{imag} \in \mathbb{Z}$, and $j = \sqrt{-1}$, and using this observation leads the standard linearized model of the transmitter as shown in Fig. 7.2; e.g., [10]. For this equivalent model, the vector \mathbf{v} is a linear function of the modified data vector $\mathbf{u} = \mathbf{s} + \mathbf{i}$,

$$\mathbf{v} = (\mathbf{I} + \mathbf{B})^{-1} \mathbf{u}. \quad (7.2)$$

As a result of the modulo operation at the transmitter, the elements of \mathbf{v} are almost uncorrelated and uniformly distributed over \mathcal{V} , [10, Th. 3.1], and hence they will have

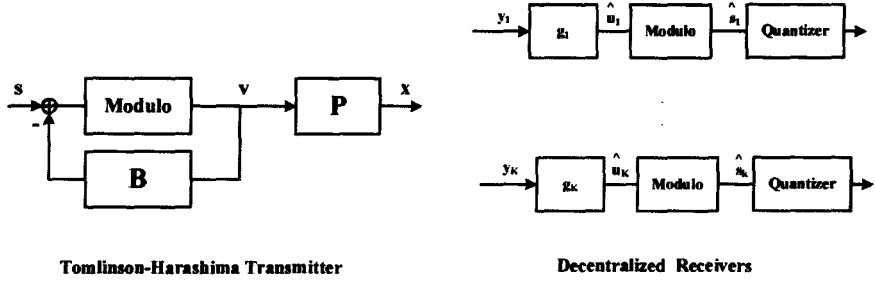


Figure 7.1: BC with Tomlinson-Harashima precoding.

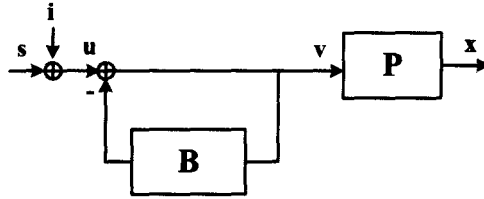


Figure 7.2: Equivalent linear model for the transmitter.

slightly higher average energy than the input symbols of \mathbf{s} ; something that is often called precoding loss [10]. For example, for square M -ary QAM we have $E\{|v_k|^2\} = \frac{M}{M-1}E\{|s_k|^2\}$ for $k = 2, \dots, K$, and $E\{|v_1|^2\} = E\{|s_1|^2\}$, [10]. For moderate to large values of M this power increase can be neglected and the approximation $E\{\mathbf{v}\mathbf{v}^H\} = \mathbf{I}$ is often used; e.g., [13, 16]. Under the assumption of negligible precoding loss, the average transmitted power constraint becomes $E_{\mathbf{v}}\{\mathbf{x}^H\mathbf{x}\} = \text{tr}(\mathbf{P}^H\mathbf{P}) \leq P_{\text{total}}$.

The signal received by the k^{th} user, y_k , can be written as

$$y_k = \mathbf{h}_k \mathbf{x} + n_k, \quad (7.3)$$

where $\mathbf{h}_k \in \mathbb{C}^{1 \times N_t}$ is a row vector representing the channel gains from the transmitting antennas to the k^{th} receiver, and n_k is the additive zero-mean white noise at the k^{th} receiver whose variance is σ_n^2 . The K equations on the form (7.3) can be written as

$$\mathbf{y} = \mathbf{H}\mathbf{x} + \mathbf{n},$$

where \mathbf{h}_k is k^{th} row of the broadcast channel matrix, \mathbf{H} , and the noise vector \mathbf{n} has zero-mean and covariance matrix is $E\{\mathbf{nn}^H\} = \sigma_n^2 \mathbf{I}$. Since the receivers operate independently, each receiver processes its received signal y_k using a single equalizing gain g_k to obtain the estimate, $\hat{u}_k = g_k y_k$, followed by a modulo operation to obtain \hat{s}_k . Assuming negligible precoding loss and that the vector \mathbf{i} is eliminated by the receivers' modulo operation, the error signal $\hat{u}_k - u_k$ is equivalent to $\hat{s}_k - s$, and can be used to define the mean square error,

$$\begin{aligned} \text{MSE}_k &= E_{\mathbf{v}}\{|\hat{u}_k - u_k|^2\} = \sum_{j=1}^K |g_k|^2 \mathbf{p}_j^H (\mathbf{h}_k^H \mathbf{h}_k) \mathbf{p}_j + \sigma_n^2 |g_k|^2 - g_k \mathbf{h}_k \mathbf{p}_k - \mathbf{p}_k^H \mathbf{h}_k^H g_k^H \\ &\quad - \sum_{j=1}^{k-1} \mathbf{p}_j^H \mathbf{h}_k^H g_k^H B_{kj} - \sum_{j=1}^{k-1} B_{kj}^H g_k \mathbf{h}_k \mathbf{p}_j + \sum_{j=1}^{k-1} |B_{kj}|^2 + 1 \\ &= \|g_k \mathbf{h}_k \mathbf{P} - \mathbf{m}_k - \mathbf{b}_k\|^2 + \sigma_n^2 |g_k|^2, \end{aligned} \quad (7.4)$$

where \mathbf{m}_k and \mathbf{b}_k are the i^{th} row of \mathbf{I} and \mathbf{B} , respectively. Similarly, the total MSE can be written as:

$$\text{MSE} = \sum_{k=1}^K \text{MSE}_k = \text{tr}\{(\mathbf{GHP} - \mathbf{I} - \mathbf{B})^H (\mathbf{GHP} - \mathbf{I} - \mathbf{B})\} + \sigma_n^2 \|\mathbf{g}\|^2, \quad (7.5)$$

where $\mathbf{g} = (g_1, \dots, g_K)$ and $\mathbf{G} = \text{Diag}(\mathbf{g})$.

7.3 Statistically Robust design Via BC-MAC duality

For the statistical uncertainty model in Section 6.3.1, our objective is to jointly design the feedback and precoding matrices, \mathbf{B} and \mathbf{P} , and the receivers' equalizing gains, g_k , so as to minimize the average, over the channel estimation error, of the total MSE:

$$\overline{\text{MSE}} = \sum_{k=1}^K \overline{\text{MSE}}_k, \quad (7.6)$$

where each $\overline{\text{MSE}}_k$ is given by (cf. (7.4))

$$\begin{aligned} \overline{\text{MSE}}_k = & \sum_{j=1}^K |g_k|^2 \mathbf{p}_j^H (\hat{\mathbf{h}}_k^H \hat{\mathbf{h}}_k + \sigma_{e_k}^2 \mathbf{I}) \mathbf{p}_j + \sigma_n^2 |g_k|^2 - g_k \hat{\mathbf{h}}_k \mathbf{p}_k - \mathbf{p}_k^H \hat{\mathbf{h}}_k^H g_k \\ & - \sum_{j=1}^{k-1} \mathbf{p}_j^H \hat{\mathbf{h}}_k^H g_k^H B_{kj} - \sum_{j=1}^{k-1} B_{kj}^H g_k \hat{\mathbf{h}}_k \mathbf{p}_j + \sum_{j=1}^{k-1} |B_{kj}|^2 + 1. \end{aligned} \quad (7.7)$$

Previous attempts to this design problem have involved the restriction that all g_k be equal [106, 129], or have employed a simpler detection model [109]. In our approach we will preserve all the degrees of freedom, and will exploit the duality, derived herein, between the broadcast channel with TH precoding and the multiple access channels with DFE, under a statistical model of the error of the CSI. Using this duality, we will jointly design the transceiver parameters \mathbf{B} , \mathbf{P} , and g_k so as to minimize (7.6). Our duality result also enable us to obtain robust designs of broadcast channels with TH precoding that optimize objectives that are functions of the the average MSEs, not just the sum, by solving the same design problem for a dual MAC with a DFE.

7.3.1 Dual Multiple Access Channel with Non-Linear Transceivers

By reversing the direction of the communication in the broadcast channel (BC) with Tomlinson-Harashima precoding in Fig. 7.1, we obtain a dual multiple access channel (MAC) in which K transmitters, each with a single antenna, communicate to a base station with N_t antennas that employ successive interference cancelation detector based on decision feedback equalization (DFE); see Fig 7.3. To obtain duality, the users are detected using the reverse order of the BC precoding order; i.e., detection starts with the K^{th} user. Because the transmitters in the dual MAC are decentralized and each has only one transmit antenna, linear precoding reduces to power loading:

$$x_k^{\text{MAC}} = p_k^{\text{MAC}} s_k^{\text{MAC}}, \quad (7.8)$$

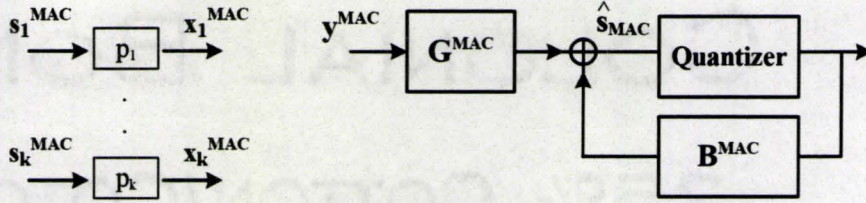


Figure 7.3: The Dual MAC with decision feedback equalization.

where s_k^{MAC} and x_k^{MAC} are the data symbol and the transmitted signal of the k^{th} transmitter. Without loss of generality, we will assume that $E\{\mathbf{s}^{\text{MAC}}\mathbf{s}^{\text{MAC}H}\} = \mathbf{I}$. Hence, a total power constraint on all the transmitters can be written as $\sum_{k=1}^K |p_k^{\text{MAC}}|^2 \leq P_{\text{total}}$.

The channels between the transmitters and the receiver of the dual MAC can be represented by \mathbf{H}^H (e.g., [115]) and hence the vector of received signals \mathbf{y}^{MAC} is given by

$$\mathbf{y}^{\text{MAC}} = \mathbf{H}^H \mathbf{x}^{\text{MAC}} + \mathbf{n}^{\text{MAC}}, \quad (7.9)$$

where \mathbf{n}^{MAC} is the zero-mean receiver noise vector with $E\{\mathbf{n}^{\text{MAC}}\mathbf{n}^{\text{MAC}H}\} = \sigma_n^2 \mathbf{I}$. As shown in Fig. 7.3, the operation of the DFE can be represented by a feedforward matrix $\mathbf{G}^{\text{MAC}} \in \mathbb{C}^{K \times N_r}$ and a strictly upper triangular feedback matrix $\mathbf{B}^{\text{MAC}} \in \mathbb{C}^{K \times K}$. Assuming correct previous decisions, the input to the quantizer, $\hat{\mathbf{s}}^{\text{MAC}}$, can be written as

$$\hat{\mathbf{s}}^{\text{MAC}} = (\mathbf{G}^{\text{MAC}} \mathbf{H}^H \mathbf{P}^{\text{MAC}} - \mathbf{B}^{\text{MAC}}) \mathbf{s}^{\text{MAC}} + \mathbf{G}^{\text{MAC}} \mathbf{n}^{\text{MAC}}, \quad (7.10)$$

where $\mathbf{P}^{\text{MAC}} = \text{Diag}(p_1^{\text{MAC}}, \dots, p_K^{\text{MAC}})$. Using the stochastic channel uncertainty

model in Section 6.3.1, the average over channel estimation errors of the MSE associated with the estimate \hat{s}_k^{MAC} is

$$\begin{aligned} \overline{\text{MSE}}_k^{\text{MAC}} &= \sum_{j=1}^K |p_j^{\text{MAC}}|^2 \mathbf{g}_k^{\text{MAC}} (\hat{\mathbf{h}}_j^H \hat{\mathbf{h}}_j + \sigma_{e_j}^2 \mathbf{I}) \mathbf{g}_k^{\text{MAC}H} + \sigma_n^2 \mathbf{g}_k^{\text{MAC}} \mathbf{g}_k^{\text{MAC}H} - p_k^{\text{MAC}H} \hat{\mathbf{h}}_k \mathbf{g}_k^{\text{MAC}H} \\ &\quad - \mathbf{g}_k^{\text{MAC}} \hat{\mathbf{h}}_k^H p_k^{\text{MAC}} - \sum_{j=k+1}^K (p_j^{\text{MAC}H} \hat{\mathbf{h}}_j \mathbf{g}_k^{\text{MAC}H} B_{kj}^{\text{MAC}} + B_{kj}^{\text{MAC}H} \mathbf{g}_k^{\text{MAC}} \hat{\mathbf{h}}_j^H p_j^{\text{MAC}}) \\ &\quad + \sum_{j=k+1}^K |B_{kj}^{\text{MAC}}|^2 + 1, \end{aligned} \quad (7.11)$$

where $\mathbf{g}_k^{\text{MAC}}$ is the k^{th} row of \mathbf{G}^{MAC} .

7.3.2 BC-MAC Duality with Stochastic Uncertainty and Non-Linear Transceivers

In this section, we will present the MSE duality result between the broadcast channel with TH precoding and the multiple access channel with DFE under the stochastic channel uncertainty model described in Section 6.3.1. This duality result generalizes the MSE duality between the BC with TH precoding and the MAC with DFE for the perfect channel knowledge case [127, 130] to scenarios with uncertain CSI. It is also a generalization of the duality results for linear transceivers in [92, 93].

Theorem 7.1. *Assume that there is no precoding loss in the THP in the BC and no error propagation in DFE in the dual MAC. Then, under the same constraint on the total transmitted power, the sets of individual average MSEs for the BC, $\{\overline{\text{MSE}}_k\}$, and for the dual MAC, $\{\overline{\text{MSE}}_k^{\text{MAC}}\}$, are the same for the following transceiver design*

$$\mathbf{p}_k = \omega_k \mathbf{g}_k^{\text{MAC}H}, \quad g_k = \omega_k^{-1} p_k^{\text{MAC}H}, \quad B_{kj} = \frac{\omega_j}{\omega_k} B_{jk}^{\text{MAC}}, \quad (7.12)$$

where the vector of positive constants $\boldsymbol{\omega} = (\omega_1, \dots, \omega_K)$ is given by:

$$\boldsymbol{\omega}^2 = \mathbf{M}^{-1} \left[|p_1^{\text{MAC}}|^2, \dots, |p_K^{\text{MAC}}|^2 \right]^T, \quad (7.13)$$

and the elements of the matrix \mathbf{M} are given by:

$$M_{ki} = \begin{cases} -\frac{|p_k^{\text{MAC}}|^2}{\sigma_n^2} \mathbf{g}_i^{\text{MAC}} (\hat{\mathbf{h}}_k^H \hat{\mathbf{h}}_k + \sigma_{e_k}^2 \mathbf{I}) \mathbf{g}_i^{\text{MAC}H} & k < i \\ -\frac{|p_k^{\text{MAC}}|^2}{\sigma_n^2} \mathbf{g}_i^{\text{MAC}} (\hat{\mathbf{h}}_k^H \hat{\mathbf{h}}_k + \sigma_{e_k}^2 \mathbf{I}) \mathbf{g}_i^{\text{MAC}H} - \frac{|B_{ik}^{\text{MAC}}|^2}{\sigma_n^2} + \frac{1}{\sigma_n^2} \mathbf{g}_i^{\text{MAC}} \hat{\mathbf{h}}_k^H p_k^{\text{MAC}} B_{ik}^{\text{MAC}H} \\ + \frac{1}{\sigma_n^2} B_{ik}^{\text{MAC}} p_k^{\text{MAC}H} \hat{\mathbf{h}}_k \mathbf{g}_i^{\text{MAC}H} & k > i \\ \mathbf{g}_k^{\text{MAC}} \mathbf{g}_k^{\text{MAC}H} - \sum_{j \neq k} M_{jk} & k = i. \end{cases} \quad (7.14)$$

The proof is similar to that presented in Appendix G. Using Theorem 7.1, an optimal design of the BC transceiver that jointly minimizes the sum of the average MSEs, $\overline{\text{MSE}}$, under a total power constraint can be obtained by first obtaining the optimal MAC transceiver that jointly minimizes $\overline{\text{MSE}}^{\text{MAC}}$, and then applying the transformation (7.13) to obtain the optimal BC transceiver. Although, this duality extends to arbitrary functions of the set of average MSEs $\{\overline{\text{MSE}}_k\}$, and is not restricted to the sum, for reasons of simplicity we will focus on the case of the sum in the next section.

7.3.3 Statistically Robust Transceiver Design for the Dual MAC

In this section, we will obtain a statistically robust design of the dual MAC transceiver that jointly minimizes $\overline{\text{MSE}}^{\text{MAC}} = \sum_{k=1}^K \overline{\text{MSE}}_k^{\text{MAC}}$. We will first obtain an analytic expression for the optimal receiver, \mathbf{B}^{MAC} and $\mathbf{g}_k^{\text{MAC}}$, for a given set of transmitters p_k^{MAC} , and then we will then obtain an optimization formulation for the optimal p_k^{MAC} under a total power constraint.

From equation (7.11), we observe that each $\overline{\text{MSE}}_k^{\text{MAC}}$ is a smooth convex function

of the k^{th} row of \mathbf{B}^{MAC} and is independent of the other rows. Hence, $\overline{\text{MSE}}_k^{\text{MAC}}$ can be minimized independently. Indeed, by setting the stationary point $\overline{\text{MSE}}_k^{\text{MAC}}$ with respect to k^{th} row of \mathbf{B}^{MAC} to zero, we obtain the optimal values of the elements of \mathbf{B}^{MAC}

$$B_{kj}^{\text{MAC}} = \mathbf{g}_k^{\text{MAC}} \hat{\mathbf{h}}_k^H p_j^{\text{MAC}}. \quad (7.15)$$

Substituting the resulting expression for the optimal \mathbf{B}^{MAC} in (7.11), we find that each resulting $\overline{\text{MSE}}_k^{\text{MAC}}$ is a convex function of $\mathbf{g}_k^{\text{MAC}}$ and is independent of $\mathbf{g}_j^{\text{MAC}}$ for $j \neq k$. Hence, each $\overline{\text{MSE}}_k^{\text{MAC}}$ is optimized by setting

$$\mathbf{g}_k^{\text{MAC}} = p_k^{\text{MAC}} \hat{\mathbf{h}}_k^H \mathbf{S}_k, \quad (7.16)$$

where

$$\mathbf{S}_k = \left(\sum_{i=1}^k |p_i^{\text{MAC}}|^2 (\hat{\mathbf{h}}_i^H \hat{\mathbf{h}}_i + \sigma_{e_i}^2 \mathbf{I}) + \sigma_n^2 \mathbf{I} \right)^{-1} \quad (7.17)$$

Using the optimal receiver parameters in (7.15) and (7.16), the sum of the average MSEs can be expressed as

$$\overline{\text{MSE}}^{\text{MAC}} = K - \sum_{k=1}^K |p_k^{\text{MAC}}|^2 \hat{\mathbf{h}}_k^H \mathbf{S}_k \hat{\mathbf{h}}_k. \quad (7.18)$$

Similar to scenarios in which channel state information is available [130], the expression in (7.18) is differentiable function of $|p_i^{\text{MAC}}|^2$, and hence a (locally) optimal solution to the minimization of (7.18) under a total power constraint can be found by applying a standard iterative algorithm.

7.4 Robust Design with Bounded Channel Uncertainties

In this section we present a robust transceiver design for the second uncertainty region, which does not rely on a statistical model of channel uncertainty, and merely assumes

that the each user's channel lies within a given uncertainty set $\mathcal{U}_k(\delta_k, \Phi_k, \mathbf{Q}_k)$ in (6.7). For this type of channel uncertainty, our goal is to jointly design the transmitter (i.e., \mathbf{B} and \mathbf{P}), and the equalizing gains of the receivers, g_k , so as to minimize the worst-case MSE over all admissible channels $\mathbf{h}_k \in \mathcal{U}_k(\delta_k, \Phi_k, \mathbf{Q}_k)$, subject to a total power constraint, and \mathbf{B} being a strictly lower triangular matrix. That is,

$$\min_{\mathbf{B}, \mathbf{P}, \mathbf{g}} \max_{\mathbf{h}_k \in \mathcal{U}_k(\delta_k)} \sum_{k=1}^K \|g_k \mathbf{h}_k \mathbf{P} - \mathbf{m}_k - \mathbf{b}_k\|^2 + \sigma_n^2 \|\mathbf{g}\|^2 \quad (7.19a)$$

$$\text{s. t. } B_{ij} = 0 \quad 1 \leq i \leq j \leq K, \quad (7.19b)$$

$$\|\text{vec}(\mathbf{P})\|^2 \leq P_{\text{total}}. \quad (7.19c)$$

This minimax problem can be simplified by rewriting it as the following minimization problem

$$\min_{\mathbf{B}, \mathbf{P}, \mathbf{g}, \mathbf{t}} \sum_{k=0}^K t_k^2 \quad (7.20a)$$

$$\text{s.t. } \|g_k \mathbf{h}_k \mathbf{P} - \mathbf{m}_k - \mathbf{b}_k\| \leq t_k \quad \forall 1 \leq k \leq K, \mathbf{h}_k \in \mathcal{U}_k(\delta_k, \Phi_k, \mathbf{Q}_k), \quad (7.20b)$$

$$\sigma_n \|\mathbf{g}\| \leq t_0, \quad (7.20c)$$

$$B_{ij} = 0 \quad 1 \leq i \leq j \leq K, \quad (7.20d)$$

$$\|\text{vec}(\mathbf{P})\|^2 \leq P_{\text{total}}. \quad (7.20e)$$

Using the finite characterization of infinite second order cone (SOC), cf. (6.25), the robust transceiver design can be formulated as:

$$\min_{\mathbf{B}, \mathbf{P}, \mathbf{g}, \mathbf{t}, \mu, \alpha} \alpha \quad (7.21a)$$

$$\text{s.t.} \quad \left\| \begin{bmatrix} \sigma_n \mathbf{g} \\ \mathbf{t} \end{bmatrix} \right\|^2 \leq \alpha, \quad (7.21b)$$

$$\begin{bmatrix} t_k - \mu_k & \mathbf{0} & \mathbf{a}_k \\ \mathbf{0} & \mu_k \mathbf{Q} & \delta_k(g_k \Phi \mathbf{P}) \\ \mathbf{a}_k^H & \delta_k(g_k \Phi \mathbf{P})^H & t_k \mathbf{I} \end{bmatrix} \geq \mathbf{0} \quad \leq k \leq K, \quad (7.21c)$$

$$B_{ij} = 0 \quad 1 \leq i \leq j \leq K, \quad (7.21d)$$

$$\|\text{vec}(\mathbf{P})\|^2 \leq P_{\text{total}}, \quad (7.21e)$$

where \mathbf{a}_k is a placeholder for $(g_k \hat{\mathbf{h}}_k \mathbf{P} - \mathbf{m}_k - \mathbf{b}_k)$, and we have used the fact that the optimal value for t_0 is $\sigma_n \|\mathbf{g}\|$. Similar to the linear transceiver case in Chapter 6, the constraint in (7.21c) represents a set of K bilinear matrix inequalities and hence the optimization problem in (7.21) is non-convex. (In the general case, optimization problems with bilinear matrix inequalities are NP hard [119].) However, given initial values for \mathbf{P} , \mathbf{B} and \mathbf{g} , one can find a locally optimal solution by iteratively optimizing over \mathbf{P} and \mathbf{B} for fixed \mathbf{g} , and over \mathbf{g} and \mathbf{B} for fixed \mathbf{P} . Each of those problems is implicit in (7.21) and is a convex conic program that can be efficiently solved. The choice of the initial point for this iterative design can be the transceiver designed for the case in which the estimates $\hat{\mathbf{h}}_k$ are assumed to be the actual channels; e.g., [127].

Similarly, for the case of uncertainty regions $\tilde{\mathcal{U}}_k$ in (6.8) that are described as the intersection of more than one uncertainty set of the form (6.7), it can be shown that a conservative robust design can be formulated as:

$$\min_{\substack{\mathbf{B}, \mathbf{P}, \mathbf{g}, \\ t, \mu_k^\ell, \alpha}} \alpha \quad (7.22a)$$

$$\text{s.t.} \quad \|\left[\begin{smallmatrix} \sigma_n \mathbf{g} \\ t \end{smallmatrix} \right]\|^2 \leq \alpha, \quad (7.22b)$$

$$\left[\begin{array}{ccc} t_k - \sum_{\ell} \mu_k^\ell & \mathbf{0} & \mathbf{a}_k \\ \mathbf{0} & \sum_{\ell} \mu_k^\ell \mathbf{Q}_k^\ell & \delta_k(g_k \Phi_k \mathbf{P}) \\ \mathbf{a}_k^H & \delta_k(g_k \Phi_k \mathbf{P})^H & t_k \mathbf{I} \end{array} \right] \geq \mathbf{0}, \quad 1 \leq k \leq K, \quad (7.22c)$$

$$B_{ij} = 0 \quad 1 \leq i \leq j \leq K, \quad (7.22d)$$

$$\|\text{vec}(\mathbf{P})\|^2 \leq P_{\text{total}}. \quad (7.22e)$$

Similar to (7.21), a local optimal solution can be found by employing an alternative optimization algorithm that optimizes over \mathbf{P} and \mathbf{B} for fixed \mathbf{g} , and over \mathbf{g} and \mathbf{B} for fixed \mathbf{P} .

7.5 Uplink Minimax Robust Designs

In this section we will provide explicit formulations of the minimax robust designs for the dual MAC.

To derive the robust minimax design, we first observe that the MSE expression for the k^{th} user in the uplink is function is a function of all channels, not just its own. While these multiple sources of uncertainty can complicate the design, one can write the total MSE as

$$\text{MSE}^{\text{MAC}} = \sum_{k=1}^K \|\mathbf{G}^{\text{MAC}} \mathbf{h}_k^H p_k^{\text{MAC}} - \mathbf{m}_k^H - (\mathbf{b}_k^{\text{MAC}})^H\|^2 + \sigma_n^2 \text{tr}\{(\mathbf{G}^{\text{MAC}})^H \mathbf{G}^{\text{MAC}}\}, \quad (7.23)$$

where each term of the summation is subject to uncertainty from one source only. Using (7.23) and the analysis in Section 7.4, the uplink robust minimax design can

be formulated as

$$\min_{\substack{\mathbf{B}^{\text{MAC}}, \mathbf{G}^{\text{MAC}}, \\ \mathbf{p}^{\text{MAC}}, t, \mu, \beta}} \beta \quad (7.24a)$$

$$\text{subject to} \quad (7.24b)$$

$$\| [\sigma_n \text{vec}(\mathbf{G}_t^{\text{MAC}})] \|^2 \leq \beta, \quad (7.24c)$$

$$\begin{bmatrix} t_k - \mu_k & \mathbf{0} & (\mathbf{a}_k^{\text{MAC}})^H \\ \mathbf{0} & \mu_k \mathbf{Q}_k & \delta_k(p_k^{\text{MAC}} \Phi_k \mathbf{G}^{\text{MAC}}) \\ \mathbf{a}_k^{\text{MAC}} & \delta_k(p_k^{\text{MAC}} \Phi_k \mathbf{G}^{\text{MAC}})^H & t_k \mathbf{I} \end{bmatrix} \geq \mathbf{0}, \quad \leq k \leq K, \quad (7.24d)$$

$$B_{ij} = 0 \quad 1 \leq j \leq i \leq K, \quad (7.24e)$$

$$\|\mathbf{p}^{\text{MAC}}\|^2 \leq P_{\text{total}}, \quad (7.24f)$$

where $\mathbf{a}_k^{\text{MAC}}$ is a placeholder for $\mathbf{G}^{\text{MAC}} \mathbf{h}_k^H p_k^{\text{MAC}} - \mathbf{m}_k^T - (\mathbf{b}_k^{\text{MAC}})^H$. Similarly, conservative formulations can be obtained for the robust uplink designs with multiple intersecting uncertainty sets for each channel. As was the case with the downlink, both problems are non-convex, but one can employ a local iterative algorithm in which a convex conic program is solved at each iteration. In the formulation in (7.24), the power constraint is a constraint on the total power transmitted by the users; cf. (7.24f). This constraint can be replaced by individual power constraints of the form $|p_k^{\text{MAC}}|^2 \leq P_{\text{total-k}}$ without disturbing the convex structure of the problem.

7.6 Simulation Studies

In order to compare the performance of the proposed robust design with the existing approaches, we have simulated these methods for the cases of QPSK transmission over independent Rayleigh fading channels. We will plot the average bit error rate (BER) over all users against the signal-to-noise-ratio, which is defined as

SNR = $P_{\text{total}}/(K\sigma_n^2)$. In our simulations, the coefficients of the channel matrix \mathbf{H} are modeled as being independent circularly symmetric complex Gaussian random variables with zero mean. All THP transceivers assume a given ordering of the users. Since finding an optimal ordering will involve an exhaustive search over $K!$ possible arrangements, a suboptimal ordering is usually employed. We will choose the suboptimal ordering proposed for MMSE Tomlinson-Harashima transceiver design in [126], using the transmitter's channel estimate $\hat{\mathbf{H}}$. This ordering will be used for all methods, including the proposed robust transceiver.

7.6.1 Statistically Robust Designs

To model the error \mathbf{e}_k between the actual channel \mathbf{h}_k and the estimated channel at the transmitter $\hat{\mathbf{h}}_k$, \mathbf{e}_k is generated from a zero-mean Gaussian distribution with $E\{\mathbf{e}_k^H \mathbf{e}_k\} = \sigma_{e_k}^2 \mathbf{I}$. In our simulation, we will use the same $\sigma_{e_k}^2$ for all users. This model is appropriate for a scenario in which the uplink power is controlled so that the received SNRs on the uplink are equal and independent from the downlink SNR. For convenience, we define $\epsilon^2 = E\{\mathbf{e}_k \mathbf{e}_k^H\} = N_t \sigma_{e_k}^2$.

In Fig. 7.4 we compare the performance of the statistically robust Tomlinson-Harashima transceiver proposed in Section 7.3 with that of the zero-forcing Tomlinson-Harashima transceiver design (ZF-THP) in [124, 125], and the MMSE Tomlinson-Harashima transceiver design (MMSE-THP) in [126] for a system with 4 transmit antennas, 4 users, and QPSK signalling. In Fig. 7.4, the performance of each method is plotted for values of $\epsilon^2 = 0.05, 0.1$. It can be seen that the performance of Tomlinson-Harashima precoding in the broadcast channel is rather sensitive to the mismatch between the actual CSI and the transmitter's estimate of CSI. It can be also seen that while the effect of noise is dominant at low SNR, the channel uncertainty dominates at high SNR, where the proposed robust transceiver design performs

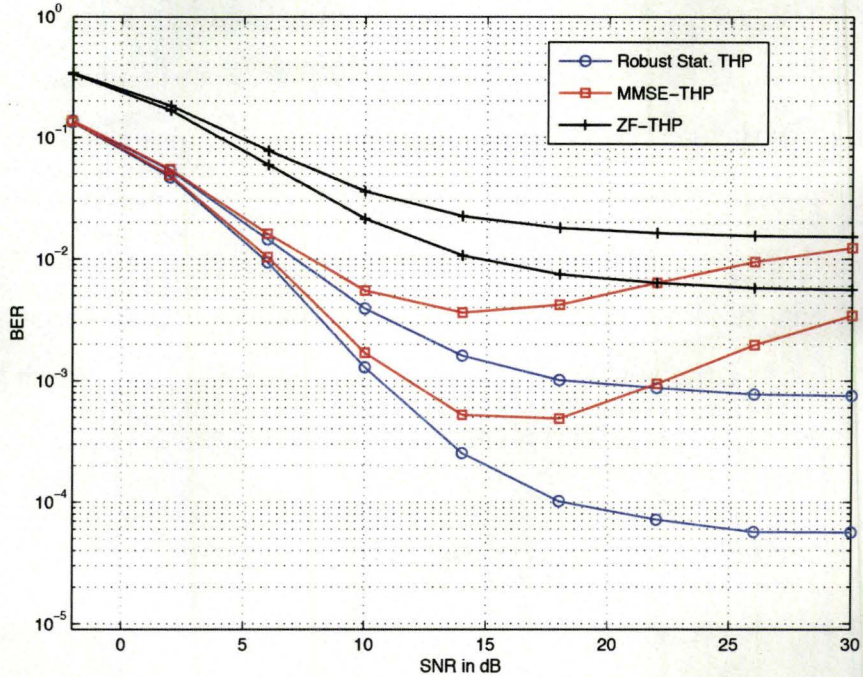


Figure 7.4: Comparison between the performance of the proposed statistically robust Tomlinson-Harashima transceiver, zero-forcing Tomlinson-Harashima transceiver design (ZF-THP) in [124, 125], and the MMSE Tomlinson-Harashima transceiver design (MMSE-THP) in [126] for values of channel uncertainty $\epsilon^2 = 0.05, 0.1$ for a system with $N_t = 4$ and $K = 4$ using QPSK signalling. The upper performance curve of each method corresponds to channel uncertainty $\epsilon^2 = 0.1$

significantly better than the other two approaches. Fig. 7.4 also shows that in the presence of channel uncertainty, both the ZF-THP and MMSE-THP designs have the same performance limit at high SNR. This is due to the fact that the MMSE method involves the addition of a regularization term whose value is inversely proportional to $P_{\text{total}}/(K\sigma_n^2)$; see [126].

For Fig. 7.5 we consider a system with $N_t = 4$ antennas and $K = 4$ users. In addition to the previous two designs, ZF-THP [124, 125] and MMSE-THP [126], that

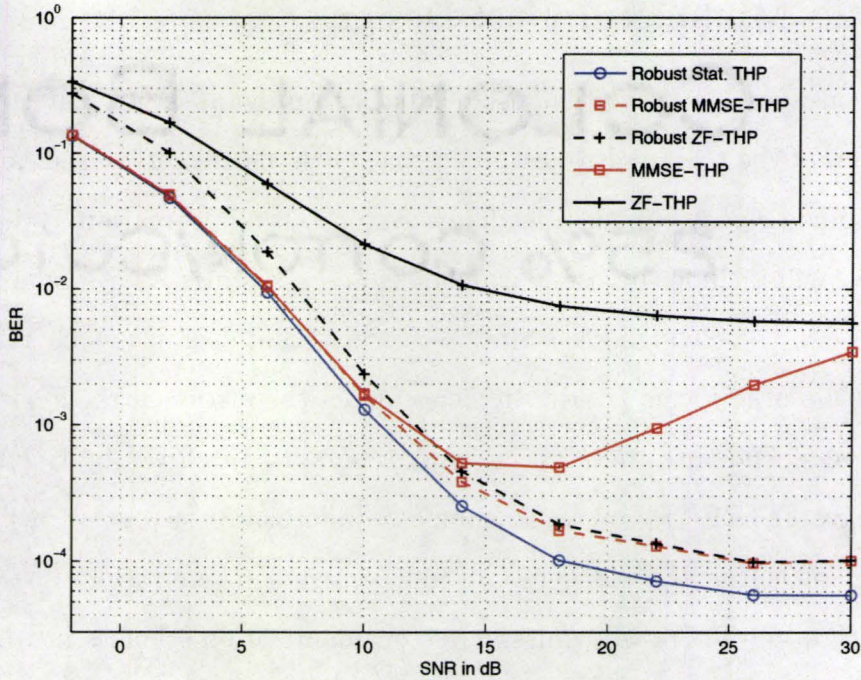


Figure 7.5: Comparison between the performance of the proposed statistically robust THP transceiver, zero-forcing THP transceiver design (ZF-THP) in [124, 125], and the MMSE THP transceiver design (MMSE-THP) in [126], robust zero-forcing THP (Robust ZF-THP) approach introduced in [106], and the robust MMSE Tomlinson-Harashima (Robust MMSE-THP) approach introduced in [129], for values of channel uncertainty $\epsilon^2 = 0.05$ for a system with $N_t = 4$ and $K = 4$ using QPSK signalling.

assume precise CSI, we will also compare the performance of the statistically robust transceiver proposed in Section 7.3 with that of the robust zero-forcing Tomlinson-Harashima (Robust ZF-THP) approach introduced in [106], and the robust MMSE Tomlinson-Harashima (Robust MMSE-THP) approach introduced in [129]. These two approaches restrict the all gains g_k to be equal. It can be seen from Fig. 7.5 that improvement in the performance can be achieved by the proposed robust design as it offers more degrees of freedom in the choice of the gains g_k .

7.6.2 Minimax Robust Designs

We considered systems that use feedback to provide the transmitter with quantized version of the CSI, and we assumed that all K users employ the same vector quantization codebooks. In these feedback systems, the information available to the transmitter will include the users' codebooks and the statistics of the error resulting from the use of these codebooks. Since we assume that each user's channel is independent from the others, the transmitter can model the error matrix \mathbf{E} as being zero mean with independent rows \mathbf{e}_k and second order statistics given by $\mathbf{E}\{\mathbf{E}\mathbf{E}^H\} = \epsilon^2\mathbf{I}$. Thus, we have $\|\mathbf{E}\{\mathbf{E}\mathbf{E}^H\}\| = \epsilon^2$. To simulate quantization errors, we will generate matrices \mathbf{E} such that the elements are independent and uniformly distributed such that $\mathbf{E}\{\mathbf{E}\mathbf{E}^H\} = \epsilon^2\mathbf{I}$. We will consider vector quantization schemes in which the transmitter employs a robust THP transceiver designed using spherical uncertainty regions $\|\mathbf{e}_k\| \leq \delta_k$. To estimate δ_k , we observe that an appropriate estimate of $\|\mathbf{E}\|$ can be ϵ , and since $\|\mathbf{E}\| \leq \sqrt{\sum_k \mathbf{e}_k^2}$, one can choose $\delta_k = \epsilon/\sqrt{K}$.

In the third experiment, we compare the performance of the robust minimax Tomlinson-Harashima transceiver proposed in Section 7.4 with that of the zero-forcing Tomlinson-Harashima transceiver design (ZF-THP) in [124, 125], and the MMSE Tomlinson-Harashima transceiver design (MMSE-THP) in [126]. In Fig. 7.6, the performance of each method is plotted for values of $\epsilon^2 = 0.03, 0.05$. It can be seen that the performance of the downlink with interference pre-subtraction is rather sensitive to the mismatch between the actual CSI and the transmitter's estimate of CSI. It can be also seen that while the effect of noise is dominant at low SNR, the channel uncertainty dominates at high SNR, where the proposed robust transceiver design performs significantly better than the other two approaches. Fig. 7.6 also shows that in the presence of channel uncertainty, both the ZF-THP and MMSE-THP designs have the same performance limit at high SNR. This is due to the fact that the MMSE method

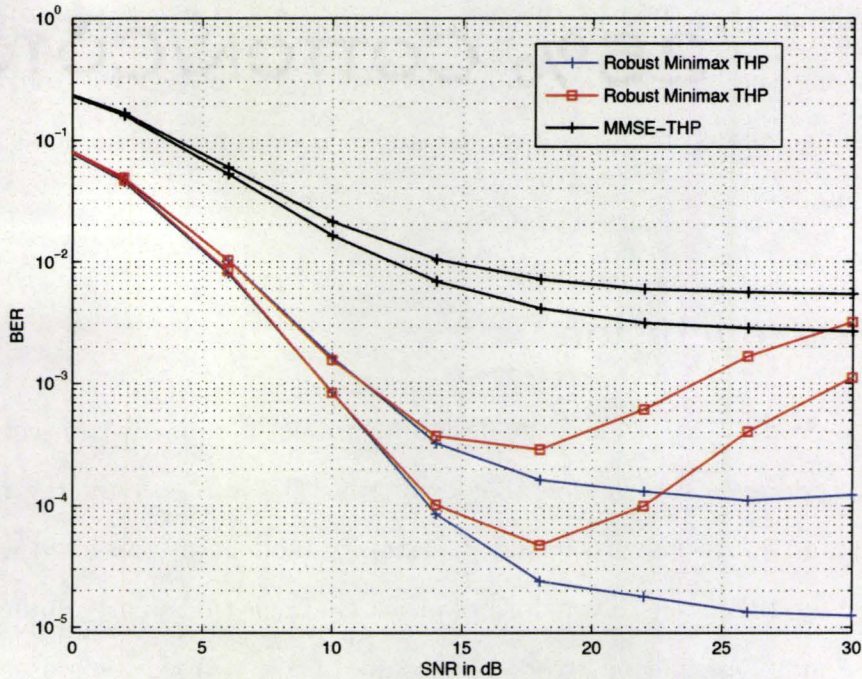


Figure 7.6: Comparison between the performance of the proposed robust minimax Tomlinson-Harashima transceiver, zero-forcing Tomlinson-Harashima transceiver design (ZF-THP) in [124, 125], and the MMSE Tomlinson-Harashima transceiver design (MMSE-THP) in [126] for values of channel uncertainty $\epsilon^2 = 0.03, 0.05$ for a system with $N_t = 4$ and $K = 4$ using QPSK signalling. The upper performance curve of each method corresponds to channel uncertainty $\epsilon^2 = 0.05$

involves the addition of a regularization term whose value is inversely proportional to $P_{\text{total}}/(K\sigma_n^2)$; see [126].

In the fourth experiment, we simulate a scenario with two different sets of users' locations from the base station. The first two users are assumed to be close to the base station and their channel coefficients are generated using the above model but with variances equal to 10. The other two users are assumed to be farther from the base stations and their channel coefficients are generated using unit variance. We

plot the average BER of all users in addition to the average BER of the two near users and the far users for value of $\epsilon^2 = 0.1$. It can be seen from Fig. 7.7 that the advantage offered by using a robust design is even more significant in the case of the near users.

7.7 Conclusion

In this chapter, we studied the design for robust non-linear transceivers with sequential interference subtraction that explicitly take into account the nature of channel uncertainty. For the stochastic uncertainty model, we presented an optimal robust design for THP transceivers for broadcast channels that jointly minimizes the average, over channel estimation errors, of the sum of the MSEs of each user. By generalizing the MSE duality between the broadcast channel with Tomlinson-Harashima precoding and the multiple access channel with decision feedback equalization to schemes with channel estimation errors, we have obtained the desired robust broadcast transceivers in terms of the robust transceivers that optimize the same performance metric for the dual multiple access channel. This approach allowed the derivation of an optimal statistically robust design that preserves all the available degrees of freedom. For the bounded uncertainty model, we presented a minimax robust design of THP transceivers that maximizes the worst-case performance. The proposed uncertainty model is general and encompasses many bounded uncertainty regions. We also generalize the robust designs to the case in which the channel uncertainty is described by multiple intersecting bounded regions, and to multiple access channels with DFE transceivers and bounded channel uncertainty. Simulation studies demonstrated that the proposed approaches can significantly reduce the sensitivity of the downlink to uncertainty in the CSI, and can provide improved performance over that of existing

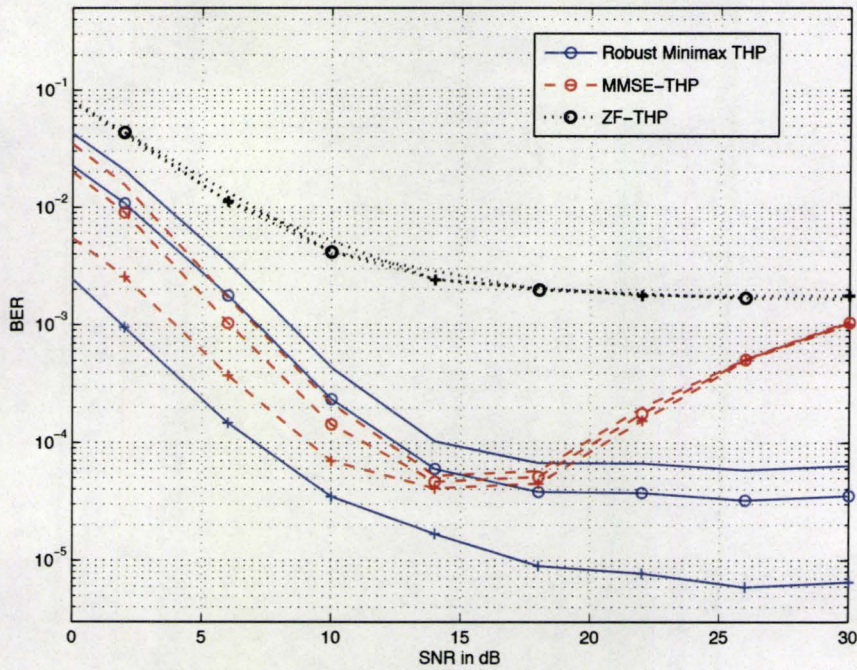


Figure 7.7: Comparison between the performance of the proposed robust minimax Tomlinson-Harashima transceiver, zero-forcing Tomlinson-Harashima transceiver design (ZF-THP) in [124, 125], and the MMSE Tomlinson-Harashima transceiver design (MMSE-THP) in [126] for values of channel uncertainty $\epsilon^2 = 0.1$ for a system with $N_t = 4$ and $K = 4$ using QPSK signalling. The curves with (+) markers and no markers represent the average BER of the two near and the two far users, respectively.

robust designs.

Chapter 8

Summary and Future Directions

This chapter summarizes the contributions of this thesis, and proposes some future research directions.

8.1 Summary

The thesis studied the joint design of the transmitter and the receiver for single-user and multi-user MIMO systems. These transceiver designs are developed under different assumptions of the available channel knowledge.

In the single-user part of the thesis, a novel design framework was developed for non-linear MIMO transceivers with interference (pre-) subtraction that assume perfect channel state information (CSI) at both the transmitter and the receiver. The framework unifies the design of two dual non-linear MIMO systems: transceivers with Tomlinson-Harashima precoding (THP), and transceivers with decision feedback equalization (DFE). It provides optimal transceiver designs for many design objectives that have been open problems. Using concepts from majorization and convex optimization theories, the framework generates closed-form optimal designs for two

broad classes of communication objectives, namely those that are Schur-convex and Schur-concave functions of the logarithms of the MSEs of each data stream. For the class of Schur-convex objectives, the optimal transceiver results in equal individual MSEs, and simultaneously minimizes the total MSE, minimizes the average bit error rate, and maximizes the Gaussian mutual information, among many other objectives. This property cannot be achieved by any linear transceiver. Furthermore, that optimal design yields objective values that are superior to the corresponding optimal objective value for a linear transceiver. For the class Schur-concave objectives, the optimal non-linear transceiver reduces to the optimal linear transceiver. The derivation of this framework resulted in a more developed understanding of non-linear MIMO transceivers that is comparable to that of the linear transceivers.

The single-user part of the thesis also presented a generalization of the framework to communications schemes operating in a limited feedback regime and employing zero-forcing decision feedback equalization. In that regime, only the receiver has CSI, and it uses that CSI to select the best available precoder from a codebook of precoders and then feeds back the index of this precoder to the transmitter over a limited rate feedback channel. For these communication schemes, the statistical distribution of the optimal precoder matrix was derived, and it was showed that codebooks constructed from Grassmann packings minimize an upper bound on average distortion measures for many design objectives.

The multi-user part of the thesis studied the design of robust multi-user transceivers that explicitly include the channel uncertainty in the design formulations.

The first component of the multi-user part developed robust broadcasting transceivers that are designed to satisfy each user's quality of service (QoS) requirements subject to bounded channel uncertainty at the transmitter. The QoS

requirements were formulated as either constraints on the signal-to-interference-plus-noise-ratio (SINR) of each user or as constraints on the mean square error (MSE) each user's received signal. Using the theories of robust and convex optimization, efficiently solvable convex design approaches were developed for both QoS formulations. These design approaches were then employed to generate tractable quasi-convex design formulations for other problems such as the robust fair broadcasting problem. It was also shown that the MSE formulation of the QoS requirements can yield designs with lower computational costs, and they can be obtained for a wider class of bounded models of channel uncertainty.

The second component of the multi-user part developed robust multiuser transceivers based on mean-square error (MSE) performance criteria subject to a transmission power constraint. The transceivers were designed for both broadcast channels (BC) and multiple access channels (MAC), and they include both linear and non-linear designs. The designs were obtained for two main channel uncertainty models. The first model is the stochastic uncertainty model that suits multi-user systems with uplink-downlink reciprocity. The robust transceivers for this uncertainty model were designed so as to minimize the average, over channel uncertainty, of functions of the MSEs, and they were obtained based on a derived generalization of the mean square error (MSE) duality between the broadcast channels and multiple access channels to scenarios with uncertain channels. This duality also showed that the optimal robust BC transceiver can be generated, using a linear transformation, from the corresponding MAC transceiver for the same objective, thus allowing robust BC design problems to be obtained by solving the more tractable MAC designs. The second channel uncertainty model is a deterministically-bounded one that suits systems with quantized channel feedback from the users. The robust transceivers for this uncertainty model were designed so as minimize the worst-case

value of the total MSE, over all admissible channels. The results for this uncertainty model included a proof of NP-hardness of the design problem, and computationally-tractable iterative approaches that are based on convex formulation of each iteration. The presented approach incorporated a wide range bounded uncertainty models as well as a variety of power constraints.

8.2 Future Directions

The results presented in the thesis can be the basis for the pursuit of other related future research directions. The following points are examples of these directions.

- It will be interesting to study the existence of a unifying design framework, similar to the one developed in Chapter 2, for MIMO transceiver with maximum likelihood (ML) receivers. Since MIMO transceivers with lattice-based detection or with (vector) lattice precoding can be thought as generalizations of MIMO transceivers with DFE or THP, respectively, it would also be worth studying the development of a design framework for these two dual MIMO transceivers.
- The limited feedback scheme presented in Chapter 3 could be combined with adaptive bit and/or power loading in order to bridge the gap between its performance and that the corresponding system with perfect CSI at the transmitter.
- The proposed robust multi-user transceivers can be combined with multi-user scheduling and selection algorithm that that would explicitly take into account the nature of the channel uncertainty.
- Unifying design frameworks were developed for linear single-user MIMO transceivers in [6] and for non-linear transceiver in Chapter 3, and those framework unified the design for a wide range of design objectives. On the other

hand, no such generalizing framework exists for multi-user transceivers, either linear or non-linear. The lack of such frameworks is a significant hindrance to the design of optimal transceivers for an arbitrary design objective in the multi-user case. Possible future directions can explore the existence of such framework in the multi-user case for both the broadcast channel and multiple access channels.

These research directions, among other ones, are being considered by the author of this thesis.

Appendix A

Proofs of Schur-convex objectives

Minimization of total MSE The objective here is to minimize $g(\mathbf{e}^l) = \sum_{i=1}^K e^{l_i}$, which has the form of $g(\mathbf{e}^l) = \sum_{i=1}^K f(l_i)$ for the strictly convex function $f(\mathbf{x}_i) = e^{\mathbf{x}_i}$. Hence, $g(\mathbf{e}^l)$ is a strictly Schur-convex function of \mathbf{l} , [29, p. 64].

Minimization of product of MSEs This objective can be written as: minimize $g(\mathbf{e}^l) = \sum_{i=1}^K l_i$. Since this is the sum of each l_i , it is both a Schur-convex and a Schur-concave function of \mathbf{l} , [29].

Minimization of p-norm of MSEs In this case, the objective is to minimize $g(\mathbf{e}^l) = (\sum_{i=1}^K (e^{l_i})^p)^{1/p}$, $p \geq 1$, which has the form $g(\mathbf{e}^l) = h(f(l_1), \dots, f(l_K))$, where $h(\mathbf{x}_1, \dots, \mathbf{x}_K) = (\sum_{i=1}^K |\mathbf{x}_i|^p)^{1/p}$ is Schur-convex and is an increasing function of each argument, and $f(x) = e^x$ is a convex function. It follows from the composition properties of Schur-convex functions [29] that $g(\mathbf{e}^l)$ is a Schur-convex function. Although minimization of the total MSE is a special case of the p -norm minimization for $p = 1$, the proof used for the total MSE case provides the stronger result of strict Schur-convexity.

Maximization of product of SINRs This objective can be written as: minimize $g(e^{\mathbf{l}}) = -\sum_{i=1}^K \log(e^{-\mathbf{l}_i} - 1)$. Since $-g(e^{\mathbf{l}})$ is the sum of the concave function $f(x) = \log(e^{-x} - 1)$ applied to each \mathbf{l}_i , $-g(e^{\mathbf{l}})$ is a Schur-concave function of \mathbf{l} [29, p. 64], and it follows that $g(e^{\mathbf{l}})$ is Schur-convex.

Maximization of harmonic mean of SINRs In this case the objective is to minimize $g(e^{\mathbf{l}}) = \sum_{i=1}^K \frac{1}{\text{SINR}_i} = \sum_{i=1}^K \frac{1}{e^{-\mathbf{l}_i} - 1}$, $\mathbf{l}_i < 0$. Since each MSE satisfies $0 \leq e^{\mathbf{l}_i} < 1$, we will restrict our proof to the case of $\mathbf{l}_i < 0$. We observe that $g(e^{\mathbf{l}})$ is a sum of the strictly convex function $f(x) = 1/(e^{-x} - 1)$, for $x < 0$, applied to each \mathbf{l}_i . Hence, $g(e^{\mathbf{l}})$ is a strictly Schur-convex function.

Minimization of average BER Assuming that each data stream employs the same constellation, the average BER is $g(e^{\mathbf{l}}) = \frac{1}{K} \sum_{i=1}^K \text{BER}(\text{SINR}_i)$, where $\text{BER}(\cdot)$ is the bit error rate of the chosen constellation as a function of the SINR, and $\text{SINR}_i = e^{-\mathbf{l}_i} - 1$. As pointed out in Section 2.5.3, for many constellations the bit error rate function $\text{BER}(\text{SINR})$ can be closely approximated by

$$\text{BER}(\text{SINR}) = c_2 Q(\sqrt{c_1 \text{SINR}}), \quad (\text{A.1})$$

where c_1 and c_2 are constants that depend on the constellation. If each $\text{BER}(e^{-\mathbf{l}_i} - 1)$ is a (strictly) convex function of \mathbf{l}_i , it follows that their sum $g(e^{\mathbf{l}})$ is (strictly) Schur-convex. To show the convexity of $\text{BER}(e^{-\mathbf{l}_i} - 1)$, we obtain the second derivative of (A.1) with respect to \mathbf{l}_i :

$$\frac{d^2 \text{BER}}{d\mathbf{l}_i^2} = \frac{c_2 c_1^{1/2} e^{-\frac{c_1}{2}(y^{-1}-1)}}{4\sqrt{2\pi} y^{3/2} (1-y)^{3/2}} (2y^2 - (c_1 + 1)y + c_1), \quad (\text{A.2})$$

where $y = e^{\mathbf{l}_i}$. Since the first term is non-negative for all values of the MSE, the sign of the second derivative is determined by the quadratic term $(2y^2 - (c_1 + 1)y + c_1)$. To check the sign of this term, we have to consider two cases:

- For values of the constellation constant c_1 such that the discriminant of the quadratic equation is negative, the second derivative is non-negative for all the range of the MSE. Hence, the expression for BER in (A.1) is convex function of l_i . This case includes BPSK and M -ary QAM with $M \leq 16$.
- For values of the constellation constant c_1 such that discriminant of the quadratic equation is non-negative, the second derivative is non-negative for the range of MSE $y \leq y_r$, where $y_r = (c_1 + 1 - \sqrt{c_1^2 - 6c_1 + 1})/4$ is a root of the quadratic equation. In this case, which applies to M -ary constellations with $M \geq 16$, the BER expression in (A.1) will be convex for all SINRs above the small threshold $1/y_r - 1$.

Appendix B

Proofs of Schur-concave objectives

Minimization of harmonic mean of MSEs This corresponds to the minimization of $g(\mathbf{e}^{\mathbf{l}}) = \frac{1}{\sum_{i=1}^K e^{-\mathbf{l}_i}}$, where the denominator is the sum of a convex function $f(x) = e^{-x}$ applied to each \mathbf{l}_i . Hence, the denominator is a Schur-convex function [29, p. 64]. Since $g(\mathbf{e}^{\mathbf{l}})$ is a decreasing function of a Schur-convex function, it follows that $g(\mathbf{e}^{\mathbf{l}})$ is Schur-concave [29, p. 61].

Maximization of p -norm of SINRs In this case, the objective is to minimize: $g(\mathbf{e}^{\mathbf{l}}) = -(\sum_{i=1}^K (e^{-\mathbf{l}_i} - 1)^p)^{1/p}$, $p \geq 1$. We observe that $-g(\mathbf{e}^{\mathbf{l}})$ has the form $g(\mathbf{e}^{\mathbf{l}}) = h(f(\mathbf{l}_1), \dots, f(\mathbf{l}_K))$, where $h(\mathbf{x}_1, \dots, \mathbf{x}_K) = (\sum_{i=1}^K |\mathbf{x}_i|^p)^{1/p}$ is Schur-convex and is an increasing function of each argument [29], and that $f(x) = e^{-x} - 1$ is a convex function. It follows from composition rules of Schur-convex functions [29, p. 63] that $-g(\mathbf{e}^{\mathbf{l}})$ is a Schur-convex function. Hence, $g(\mathbf{e}^{\mathbf{l}})$ is Schur-concave.

Minimization of a subclass of weighted product of MSEs Minimization of the weighted product of the individual MSEs (or, equivalently, the weighted geometric mean of the MSEs) corresponds to minimization of the objective $g(\mathbf{e}^{\mathbf{l}}) = \log \prod_{i=1}^K (e^{\mathbf{l}_i})^{a_i} = \sum_{i=1}^K a_i \mathbf{l}_i$. Assuming that \mathbf{l}_i are in decreasing order, then $g(\mathbf{e}^{\mathbf{l}})$ is a

Schur-concave function when the weights a_i are in ascending order [6, 29]. A special case of this objective is the unweighted product, for which all $a_k = 1$. That function is both Schur-concave and Schur-convex; see Appendix A.

Appendix C

Proof of Theorem 3.1

C.1 Optimal Precoder for Schur-convex Functions

If $g(e^{\mathbf{l}})$ is a Schur convex function of \mathbf{l} , then from Lemma 3.1 we have that

$$g(e^{\bar{\mathbf{l}}}) \leq g(e^{\mathbf{l}}), \quad (\text{C.1})$$

and the optimal value is obtained when all l_i are equal to

$$l_i = \frac{1}{K} \ln \det(\mathbf{N}). \quad (\text{C.2})$$

Hence, all MSEs are equal to $\mathbf{E}_{ii} = \mathbf{L}_{ii}^2 = \sqrt[K]{\det(\mathbf{N})}$. Since the objective is an increasing function of the individual MSEs, the design goal reduces to minimizing $\det \mathbf{N}$ subject to the power constraint on the precoder and to the constraint that diagonal elements of the Cholesky factor of \mathbf{N} are all equal. We will start by characterizing the family of precoders that minimize $\det(\mathbf{N})$ subject to the power constraint, then we will show that there is a member of this family that yields a Cholesky factor of \mathbf{N} with equal diagonal elements. Minimizing $\det(\mathbf{N})$ is equivalent to maximizing $\det(\mathbf{P}^H \mathbf{H}^H \mathbf{H} \mathbf{P})$, and the family of optimal precoders to maximize this objective subject to a power constraint is given by the following lemma.

Lemma C.1. *The family of optimal precoders that maximizes $\det(\mathbf{P}^H \mathbf{H}^H \mathbf{H} \mathbf{P})$ subject to a power constraint $\text{tr}(\mathbf{P}^H \mathbf{P}) \leq P_{\text{total}}$ is given by:*

$$\mathbf{P} = \sqrt{\frac{P_{\text{total}}}{K}} \mathbf{U}_{\mathbf{H},1} \mathbf{V}, \quad (\text{C.3})$$

where $\mathbf{U}_{\mathbf{H},1} \in \mathbb{C}^{N_t \times K}$ contains the eigen vectors of $\mathbf{H}^H \mathbf{H}$ corresponding to the K largest eigen values, and $\mathbf{V} \in \mathbb{C}^{K \times K}$ is a unitary matrix degree of freedom.

Proof. Let $\mathbf{H}^H \mathbf{H} = \mathbf{U}_{\mathbf{H}} \boldsymbol{\Lambda}_{\mathbf{H}} \mathbf{U}_{\mathbf{H}}^H$ be the eigenvector decomposition of the $\mathbf{H}^H \mathbf{H}$ such that eigenvalues are in descending order. Let the singular value decomposition of the precoding matrix be given by:

$$\mathbf{P} = \mathbf{U}_{\mathbf{P}} \begin{bmatrix} \boldsymbol{\Phi} \\ \mathbf{0} \end{bmatrix} \mathbf{V} = \mathbf{U}_{\mathbf{P},1} \boldsymbol{\Phi} \mathbf{V}. \quad (\text{C.4})$$

Now, the objective of the maximization can written as:

$$\begin{aligned} \det(\mathbf{P}^H \mathbf{H}^H \mathbf{H} \mathbf{P}) &= \det(\mathbf{V}^H \boldsymbol{\Phi} \mathbf{U}_{\mathbf{P},1}^H \mathbf{U}_{\mathbf{H}} \boldsymbol{\Lambda}_{\mathbf{H}} \mathbf{U}_{\mathbf{H}}^H \mathbf{U}_{\mathbf{P},1} \boldsymbol{\Phi} \mathbf{V}) \\ &= \det(\mathbf{W}_1^H \boldsymbol{\Lambda}_{\mathbf{H}} \mathbf{W}_1) \det(\boldsymbol{\Phi}^2) \end{aligned} \quad (\text{C.5})$$

where $\mathbf{W}_1 = \mathbf{U}_{\mathbf{H}}^H \mathbf{U}_{\mathbf{P},1}$ is a matrix with orthonormal columns ($\mathbf{W}_1^H \mathbf{W}_1 = \mathbf{I}$). Using Hadamard inequality, the first term in Eq. (C.5) is maximized when \mathbf{W}_1 consists of first K columns of \mathbf{I} . Accordingly, $\mathbf{U}_{\mathbf{P},1}$ is the first K columns of $\mathbf{U}_{\mathbf{H}}$.

Next, we choose $\boldsymbol{\Phi} = \text{Diag}(\boldsymbol{\Phi}_{11}, \dots, \boldsymbol{\Phi}_{KK})$ to maximize $\det(\boldsymbol{\Phi}^2)$ subject to $\sum_{i=1}^K \boldsymbol{\Phi}_{ii}^2 = P_{\text{total}}$. We observe that $\ln \det(\boldsymbol{\Phi}^2) = \sum_{i=1}^K \ln(\boldsymbol{\Phi}_{ii}^2)$ is a Schur-concave function of $\boldsymbol{\Phi}_{ii}^2$ and is maximized when all $\boldsymbol{\Phi}_{ii}^2$ are equal to $\frac{P_{\text{total}}}{K}$ [29]. \square

To complete the design of \mathbf{P} , we need to select \mathbf{V} such that the Cholesky decomposition of $\mathbf{N} = \mathbf{L}\mathbf{L}^H$ yields an \mathbf{L} factor with equal diagonal elements. Using (C.3) we have that

$$\begin{aligned} \mathbf{N} &= \frac{K\sigma_n^2}{P_{\text{total}}} \left(\mathbf{V}^H \boldsymbol{\Lambda}_{\mathbf{H},1}^{-1/2} \right) \left(\boldsymbol{\Lambda}_{\mathbf{H},1}^{-1/2} \mathbf{V} \right) \\ &= \mathbf{L}\mathbf{L}^H = \mathbf{R}^H \mathbf{R} = (\mathbf{Q}\mathbf{R})^H (\mathbf{Q}\mathbf{R}), \end{aligned} \quad (\text{C.6})$$

where $\Lambda_{\mathbf{H},1}$ is the diagonal matrix containing the largest K eigen values of $\mathbf{H}^H\mathbf{H}$, and \mathbf{Q} is a matrix with orthonormal columns. Therefore, finding \mathbf{V} is equivalent to finding a \mathbf{V} such that QR decomposition of $(\Lambda_{\mathbf{H},1}^{-1/2}\mathbf{V})$ has an R-factor with equal diagonal. This problem was solved in [14,53], and \mathbf{V} can be obtained by applying the algorithms therein to the matrix $\Lambda_{\mathbf{H},1}^{-1/2}$.

C.2 Optimal Precoder for Schur-concave Functions

If $g(e^{\mathbf{l}})$ is a Schur-concave function of \mathbf{l} , then from Lemma 3.1 we have that $g(e^{\mathbf{l}})$ is minimized when $\mathbf{L}_{ii}^2 = \lambda_i(\mathbf{N})$, and that this equality holds when \mathbf{L} is normal matrix. Since \mathbf{L} is a lower triangular matrix, in order for it to be normal it must be a diagonal matrix [22]. The optimal \mathbf{C} in that case is \mathbf{I} , and hence $\mathbf{B} = \mathbf{0}$. That is, in the case of Schur-concave functions of \mathbf{l} , the optimal ZF-DFE design results in zero-forcing linear equalization.

Appendix D

Incorporating different power constraints

In this appendix we show how different power constraints can be incorporated in our formulations. Consider a set of per-antenna power constraints, $E\{|x_n|^2\} \leq P_n$, one for each $1 \leq n \leq N_t$, where P_n is the bound on the power transmitted from the n^{th} antenna. Each of these constraints can be written as

$$\sum_{k=1}^K [\underline{\mathbf{p}}_k]_n^2 + [\underline{\mathbf{p}}_k]_{n+N_t}^2 \leq P_n, \quad (\text{D.1})$$

where $[\cdot]_n$ denotes the n^{th} element of a vector. This is a convex quadratic constraint on the elements of $\underline{\mathbf{p}}_k$, and can be formulated as a second order cone constraint and directly accommodated in (4.10) and all the subsequent robust counterparts.

The shaping constraint $E\{\mathbf{x}^H \mathbf{Q}(\theta) \mathbf{x}\} \leq P_{\text{shape}}(\theta)$ can be written as

$$\sum_{k=1}^K \underline{\mathbf{p}}_k^T \underline{\mathbf{Q}}(\theta) \underline{\mathbf{p}}_k \leq P_{\text{shape}}(\theta), \quad \forall \theta \in \Theta, \quad (\text{D.2})$$

where $\underline{\mathbf{Q}}(\theta)$ is defined analogously to (4.8). A convenient way in which this constraint

can be incorporated into (4.10) is to write

$$\|\text{vec}(\underline{\mathbf{Q}}(\theta)^{1/2}[\underline{\mathbf{p}}_1, \dots, \underline{\mathbf{p}}_K])\| \leq \sqrt{P_{\text{shape}}(\theta)}, \quad \forall \theta \in \Theta. \quad (\text{D.3})$$

Whenever the set Θ is discrete and finite, this set of SOCs constraints can be easily incorporated in (4.10) without compromising our approach. Integral constraints of the form

$$\int_{\theta_1}^{\theta_2} \mathbf{E}\{\mathbf{x}^H \underline{\mathbf{Q}}(\theta) \mathbf{x}\} d\theta \leq \int_{\theta_1}^{\theta_2} P_{\text{shape}}(\theta) d\theta \quad (\text{D.4})$$

can be accommodated in a similar way.

The power constraints considered above all have the SOCP formulations, but they all fall into the more general class of shaping constraints

$$\underline{\mathbf{P}}^T \underline{\mathbf{Q}} \underline{\mathbf{P}} \leq \mathbf{C}_{\text{shape}}, \quad (\text{D.5})$$

for given $\underline{\mathbf{Q}} > \mathbf{0}$ and $\mathbf{C}_{\text{shape}}$, that have been previously studied for the single user case [71]. Using the Schur Complement Theorem [22], this constraint is equivalent to the LMI

$$\mathbf{C}(\underline{\mathbf{P}}) = \begin{bmatrix} \mathbf{C}_{\text{shape}} & \underline{\mathbf{P}}^T \\ \underline{\mathbf{P}} & \underline{\mathbf{Q}}^{-1} \end{bmatrix} \geq \mathbf{0}, \quad (\text{D.6})$$

and hence constraints of the form in (D.5) can be easily incorporated into our approach.

Appendix E

Proof of Lemma 5.1

Consider the quantity $(\hat{u}_k - u_k)$ in equation (5.3). Assuming correct removal of i_k , we have

$$\hat{s}_k - s_k = (g_k \mathbf{h}_k \mathbf{P} - \mathbf{m}_k - \mathbf{b}_k) \mathbf{v} + g_k n_k, \quad (\text{E.1})$$

or equivalently,

$$\hat{s}_k = a_k s_k + \sum_{i \in \mathcal{I}_k} a_i s_i + a_0 n_k, \quad (\text{E.2})$$

where \mathcal{I}_k is the set of interfering symbols with s_k . Using (E.2), we can write¹

$$\mathbb{E}\{|\hat{s}_k|^2\} = |a_k|^2 + \sum_{i \in \mathcal{I}_k} |a_i|^2 + |a_0|^2 \sigma_k^2, \quad (\text{E.3})$$

$$\mathbb{E}\{|\hat{s}_k - s_k|^2\} = |a_k - 1|^2 + \sum_{i \in \mathcal{I}_k} |a_i|^2 + |a_0|^2 \sigma_k^2, \quad (\text{E.4})$$

$$= \mathbb{E}\{|\hat{s}_k|^2\} + 1 - 2 \operatorname{Re}\{\mathbf{a}_k\}, \quad (\text{E.5})$$

$$1 + 1/\operatorname{SINR}_k = \mathbb{E}\{|\hat{s}_k|^2\}/|a_k|^2. \quad (\text{E.6})$$

¹We assume that the interfering symbols from the other users, $\{s_i\}_{i \in \mathcal{I}_k}$, are independent from each other, from s_k , and from the additive noise.

Consider the MSE constraint $E\{|\hat{s}_k - s_k|^2 = E\{|\hat{s}_k|^2\} + 1 - 2 \operatorname{Re}\{a_k\}\} \leq \zeta_k \leq 1$. This can be written as

$$E\{|\hat{s}_k|^2\}(1 - \zeta_k) \leq 2 \operatorname{Re}\{a_k\}(1 - \zeta_k) - (1 - \zeta_k)^2 \quad (\text{E.7})$$

$$= \operatorname{Re}^2\{a_k\} - (\operatorname{Re}\{a_k\}) - (1 - \zeta_k))^2 \leq |a_k|^2. \quad (\text{E.8})$$

The latter inequality is equivalent to $1 + 1/\operatorname{SINR}_k \leq 1/(1 - \zeta_k)$, or equivalently $\operatorname{SINR}_k \geq (1/\zeta_k) - 1$.

Appendix F

Derivation of Design Formulations 1 and 2

The derivations are based on the following lemma which is a concatenation of two results in [99]:

Lemma F.1. *Consider the SOC constraint $\|\mathbf{Ax} + \mathbf{b}\| \leq y$ for every $[\mathbf{A}, \mathbf{b}]$ in the uncertainty region given by*

$$\begin{aligned} \mathcal{U} &= \left\{ [\mathbf{A}, \mathbf{b}] \mid [\mathbf{A}, \mathbf{b}] = [\mathbf{A}^0, \mathbf{b}^0] + \sum_{j=1}^J \theta_j [\mathbf{A}^j, \mathbf{b}^j], \boldsymbol{\theta} \in \mathcal{V} \right\} \\ \mathcal{V} &= \left\{ \boldsymbol{\theta} \mid \boldsymbol{\theta}^T \mathbf{Q}^\ell \boldsymbol{\theta} \leq 1, \ell = 1, \dots, L \right\}, \end{aligned} \quad (\text{F.1})$$

where $\mathbf{Q}^\ell \geq \mathbf{0}$. Then the set \mathcal{S}_1 of pairs (\mathbf{x}, y) satisfying $\|\mathbf{Ax} + \mathbf{b}\| \leq y$ for every $[\mathbf{A}, \mathbf{b}] \in \mathcal{U}$ is subset of the set \mathcal{S}_2 of pairs (\mathbf{x}, y) such that there exist non-negative scalars μ^1, \dots, μ^L satisfying

$$\begin{bmatrix} y - \sum_{\ell=1}^L \mu^\ell & \mathbf{0} & (\mathbf{A}^0 \mathbf{x} + \mathbf{b}^0)^T \\ \mathbf{0} & \sum_{\ell=1}^L \mu^\ell \mathbf{Q}^\ell & [\mathbf{A}^1 \mathbf{x} + \mathbf{b}^1 \dots \mathbf{A}^J \mathbf{x} + \mathbf{b}^J]^T \\ \mathbf{A}^0 \mathbf{x} + \mathbf{b}^0 & [\mathbf{A}^1 \mathbf{x} + \mathbf{b}^1 \dots \mathbf{A}^J \mathbf{x} + \mathbf{b}^J] & y \mathbf{I} \end{bmatrix} \geq \mathbf{0}. \quad (\text{F.2})$$

When $L = 1$, $\mathcal{S}_1 = \mathcal{S}_2$. □

To derive Design Formulation 1, we use the channel uncertainty model in (5.11) to write the left hand side of each MSE constraint in (5.12c) as follows

$$\begin{aligned}
 [\hat{\mathbf{h}}_k \mathbf{P} - f_k \mathbf{m}_k - \mathbf{b}_k, \sigma_{n_k}] &= [\hat{\mathbf{h}}_k \mathbf{P} - f_k \mathbf{m}_k - \mathbf{b}_k, \sigma_{n_k}] + \left[\sum_{j=1}^J w_k^{(j)} \phi_k^{(j)} \mathbf{P}, 0 \right] \\
 &= [\hat{\mathbf{h}}_k \mathbf{P} - f_k \mathbf{m}_k - \mathbf{b}_k, \sigma_{n_k}] + \sum_{j=1}^J \theta_k^{(j)} [\delta_k \phi_k^{(j)} \mathbf{P}, 0],
 \end{aligned} \tag{F.3}$$

where $\theta_k^{(j)} = w_k^{(j)} / \delta_k$, hence $\boldsymbol{\theta}_k^T \mathbf{Q} \boldsymbol{\theta}_k \leq 1$. By comparing (F.3) to (F.1), we can invoke Lemma F.1 with $L = 1$ to show the equivalence between the SOC constraints in (5.12c) and the corresponding LMIs in (5.13c). The non-negativity constraints on each μ_k is implied by positive semidefiniteness of the diagonal blocks of the matrices in (5.12c). The derivation of Design Formulation 2 is similar, but when $L \geq 2$ the application of Lemma F.1 results in a conservative design formulation, and hence an upper bound on the required transmission power.

Appendix G

Proof of Theorem 6.1

We start by considering linearly related transceivers for BC and dual MAC:

$$\mathbf{p}_k = \omega_k \mathbf{g}_k^{\text{MAC}^H}, \quad g_k = \chi_k p_k^{\text{MAC}^H}, \quad (\text{G.1})$$

and we find the necessary conditions for ω_k and χ_k such that set of MSEs in BC and dual MSE are equal. By setting $\overline{\text{MSE}}_k = \overline{\text{MSE}}_k^{\text{MAC}}$ and substituting the values \mathbf{p}_k and g_k from (G.1), we obtain a set of K equations. From the equality of coefficients the term in $p_k^{\text{MAC}} \mathbf{g}_k^{\text{MAC}} \hat{\mathbf{h}}_k^H$ (or $p_k^{\text{MAC}^H} \hat{\mathbf{h}}_k \mathbf{g}_k^{\text{MAC}^H}$) on both sides we have $\chi_k = 1/\omega_k$. Using this relation, the set of K equations reduces to the following linear system in $\boldsymbol{\omega}^2$:

$$\mathbf{M} \boldsymbol{\omega}^2 = \left[|p_1^{\text{MAC}}|^2, \dots, |p_K^{\text{MAC}}|^2 \right]^T, \quad (\text{G.2})$$

where \mathbf{M} was defined in (6.18). We observe that \mathbf{M} has strictly dominant diagonal elements and negative off-diagonal elements, hence it is non-singular and the elements of \mathbf{M}^{-1} are non-negative. Adding all equations in the linear system in (G.2) results in $\sum_{k=1}^K \omega_k^2 \mathbf{g}_k^{\text{MAC}} \mathbf{g}_k^{\text{MAC}^H} = \sum_{k=1}^K |p_k^{\text{MAC}}|^2$, i.e., total transmitted power in BC and dual MAC are the same.

Bibliography

- [1] Z. Liu, Y. Xin, and G. B. Giannakis, "Space-time-frequency coded OFDM over frequency-selective fading channels," vol. 50, no. 20, pp. 2465–2476, Oct. 2002.
- [2] G. Caire and K. R. Kumar, "Information theoretic foundations of adaptive coded modulation," *Proc. IEEE*, vol. 95, no. 12, pp. 2274–2298, Dec 2007.
- [3] A. Goldsmith, S. A. Jafar, N. Jindal, and S. Vishwanath, "Capacity limits of MIMO channels," *IEEE J. Select. Areas Commun.*, vol. 21, no. 5, pp. 684–702, June 2003.
- [4] S. A. Jafar and A. Goldsmith, "Transmitter optimization and optimality of beamforming for multiple antenna systems," *IEEE Trans. Wireless Commun.*, vol. 3, no. 4, pp. 1165–1175, July 2004.
- [5] A. Scaglione, G. B. Giannakis, and S. Barbarossa, "Redundant filterbank precoders and equalizers. Part I: Unification and optimal designs," *IEEE Trans. Signal Processing*, vol. 47, no. 7, pp. 1988–2006, July 1999.
- [6] D. P. Palomar, J. M. Cioffi, and M. A. Lagunas, "Joint Tx-Rx beamforming design for multicarrier MIMO channels: A unified framework for convex optimization," *IEEE Trans. Signal Processing*, vol. 51, no. 9, pp. 2381–2401, Sept. 2003.

- [7] F. Xu, T. N. Davidson, J. Zhang, and K. M. Wong, "Design of block transceivers with decision feedback detection," *IEEE Trans. Signal Processing*, vol. 54, no. 3, pp. 965–978, Mar. 2006.
- [8] N. Jindal, "MIMO broadcast channels with finite rate feedback," *IEEE Trans. Inform. Theory*, vol. 52, no. 11, pp. 5045–5059, Nov. 2006.
- [9] P. Ding, D. J. Love, and M. D. Zoltowski, "Multiple antenna broadcast channels with shape feedback and limited feedback," *IEEE Trans. Signal Processing*, vol. 55, pp. 3417–3428, July 2007.
- [10] R. F. H. Fischer, *Precoding and Signal Shaping for Digital Transmission*, Wiley, New York, 2002.
- [11] J. M. Cioffi and G. D. Forney, "Generalized decision-feedback equalization for packet transmission with ISI and Gaussian noise," in *Communications, Computation, Control and Signal Processing*, A. Paulraj, V. Roychowdhury, and C. Schaper, Eds., chapter 4, pp. 79–127. Kluwer, 1997.
- [12] J. Yang and S. Roy, "Joint transmitter-receiver optimization for multi-input multi-output systems with decision feedback," *IEEE Trans. Inform. Theory*, vol. 40, no. 5, pp. 1334–1347, Sept. 1994.
- [13] O. Simeone, Y. Bar-Ness, and U. Spagnolini, "Linear and nonlinear preequalization/equalization for MIMO systems with long-term channel state information at the transmitter," *IEEE Trans. Wireless Commun.*, vol. 3, no. 2, pp. 373–378, Mar. 2004.
- [14] J. Zhang, A. Kavcic, and K. M. Wong, "Equal-diagonal QR decomposition and its application to precoder design for successive-cancellation detection," *IEEE Trans. Inform. Theory*, vol. 51, no. 1, pp. 154–172, Jan. 2005.

- [15] Y. Jiang, J. Li, and W.W. Hager, "Joint transceiver design for MIMO communications using geometric mean decomposition," *IEEE Trans. Signal Processing*, vol. 53, no. 10, pp. 3791–3803, Oct. 2005.
- [16] C. Windpassinger, R. F. H. Fischer, T. Vencel, and J. B. Huber, "Precoding in multiantenna and multiuser communications," *IEEE Trans. Wireless Commun.*, vol. 3, no. 4, pp. 1305–1316, Jul. 2004.
- [17] Y. Jiang, D. P. Palomar, and M. K. Varanasi, "Precoder optimization for nonlinear MIMO transceiver based on arbitrary cost function," in *Proc. Conf. Inform. Sci. Syst.*, Baltimore, Mar. 2007.
- [18] Y. Jiang and D. P. Palomar, "MIMO transceiver design via majorization theory," *Foundations and Trends in Communications and Information Theory*, vol. 3, no. 4–5, pp. 331–551, 2006.
- [19] M. Schubert and H. Boche, "User ordering and power allocation for optimal multiantenna precoding/decoding," in *Proc. ITG Wkshp Smart Antennas*, Munich, March 2004, pp. 174–181.
- [20] A. Scaglione, P. Stoica, S. Barbarossa, G.B. Giannakis, and H. Sampath, "Optimal designs for space-time linear precoders and decoders," *IEEE Trans. Signal Processing*, vol. 50, no. 5, pp. 1051–1064, May 2002.
- [21] J. M. Cioffi, G. P. Dudevoir, M. V. Eyuboglu, and G. D. Forney, Jr., "MMSE decision-feedback equalizers and coding—Part I: Equalization results," *IEEE Trans. Commun.*, vol. 43, no. 10, pp. 2582–2594, Oct. 1995.
- [22] R. A. Horn and C. R. Johnson, *Matrix Analysis*, Cambridge University Press, Cambridge, U.K., 1985.

- [23] H. Weyl, "Inequalities between the two kinds of eigenvalues of a linear transformation," *Proc. Nat. Acad. Sci.*, vol. 35, pp. 408–411, July 1949.
- [24] T. Guess and M. K. Varanasi, "Multiuser decision-feedback receivers for the general Gaussian multiple-access channel," in *Proc. Allerton Conf. Communications, Control, Computing*, Monticello, IL, Oct. 1996.
- [25] T. Guess and M. K. Varanasi, "An information-theoretic framework for deriving canonical decision-feedback receivers in Gaussian channels," *IEEE Trans. Inform. Theory*, vol. 51, no. 1, pp. 173–187, 2005.
- [26] T. Guess, "Optimal sequences for CDMA with decision-feedback receivers," *IEEE Trans. Inform. Theory*, vol. 49, no. 4, pp. 886–900, April 2003.
- [27] L. Li, Y. Yao, and H. Li, "Transmit diversity and linear and decision-feedback equalizations for frequency-selective fading channels," *IEEE Trans. Veh. Technol.*, vol. 52, no. 5, pp. 1217–1231, Sept. 2003.
- [28] M. Schubert and S. Shi, "MMSE transmit optimization with interference pre-compensation," in *Proc. Veh. Tech. Conf.*, Stockholm, May 2005, vol. 2, pp. 845–849.
- [29] A. W. Marshal and I. Olkin, *Inequalities: Theory of Majorization and its Applications*, Academic Press, New York, 1979.
- [30] H. S. Witsenhausen, "A determinant maximization problem occurring in the theory of data communication," *SIAM J. Appl. Math.*, vol. 29, pp. 515–522, 1975.

- [31] Y. Jiang, J. Li, and W.W. Hager, "Uniform channel decomposition for MIMO communications," *IEEE Trans. Signal Processing*, vol. 53, no. 11, pp. 4283–4294, Nov. 2005.
- [32] J. Zhang, T. N. Davidson, and K. M. Wong, "Uniform decomposition of mutual information using MMSE decision feedback detection," in *Proc. Int. Symp. Info. Theory*, Sept. 2005, pp. 714–718.
- [33] K. Cho and D. Yoon, "On the general BER expression of one- and two-dimensional amplitude modulations," *IEEE Trans. Commun.*, vol. 50, no. 7, pp. 1074–1080, July 2002.
- [34] L. Yang and L. Hanzo, "A recursive algorithm for the error probability evaluation of M-QAM," *IEEE Commun. Lett.*, vol. 4, no. 10, pp. 304–306, Oct. 2000.
- [35] S. S. Chan, T. N. Davidson, and K. M. Wong, "Asymptotically minimum BER linear block precoders for MMSE equalisation," *IEE Proc. Commun.*, vol. 151, no. 4, pp. 297–304, Aug. 2004.
- [36] G. D. Golden, C. J. Foschini, R. A. Valenzuela, and P. W. Wolniansky, "Detection algorithm and initial laboratory results using V-BLAST space-time communication architecture," *Electron. Lett.*, vol. 35, no. 1, pp. 14–16, 7 Jan. 1999.
- [37] G. Ginis and J. M. Cioffi, "On the relation between V-BLAST and the GDFE," *IEEE Commun. Letters*, vol. 5, no. 9, pp. 364–366, 2001.
- [38] C. Windpassinger, T. Vencel, and R. F. H. Fischer, "Precoding and loading for BLAST-like systems," in *Proc. IEEE Int. Conf. Commun.*, Anchorage, May 2003, vol. 5, pp. 3061–3065.

- [39] D. Love, R. W. Heath Jr., W. Santipach, and M. L. Honig, "What is the value of limited feedback for MIMO channels?," *IEEE Commun. Mag.*, vol. 42, no. 10, pp. 54–59, 2004.
- [40] A. Narula, M. J. Lopez, M. D. Trott, and G. W. Wornell, "Efficient use of side information in multiple-antenna data transmission over fading channels," *IEEE J. Select. Areas Commun.*, vol. 16, no. 8, pp. 1423–1436, Oct. 1998.
- [41] E. Visotsky and U. Madhow, "Space-time transmit precoding with imperfect feedback," *IEEE Trans. Inform. Theory*, vol. 47, no. 6, pp. 2632–2639, 2001.
- [42] D. J. Love, R. W. Heath Jr., and T. Strohmer, "Grassmannian beamforming for multiple-input multiple-output wireless systems," *IEEE Trans. Inform. Theory*, vol. 49, no. 10, pp. 2735–2747, Oct. 2003.
- [43] K. K. Mukkavilli, A. Sabharwal, E. Erkip, and B. Aazhang, "On beamforming with finite rate feedback in multiple-antenna system," *IEEE Trans. Inform. Theory*, vol. 49, no. 10, pp. 2562–2579, Oct. 2003.
- [44] W. Santipach and M. L. Honig, "Asymptotic performance of MIMO wireless channels with limited feedback," in *Proc. IEEE Mil. Commun. Conf.*, Boston, Oct. 2003, vol. 1, pp. 141–146.
- [45] P. Xia and G. B. Giannakis, "Design and analysis of transmit-beamforming based on limited-rate feedback," *IEEE Trans. Signal Processing*, vol. 54, no. 5, pp. 1853–1863, 2006.
- [46] J. C. Roh and B. D. Rao, "Transmit beamforming in multiple-antenna systems with finite rate feedback: A VQ-based approach," *IEEE Trans. Inform. Theory*, vol. 52, no. 3, pp. 1101–1112, 2006.

- [47] Z. Yan, K. M. Wong, and Z.-Q. Luo, "Optimal diagonal precoder for multi-antenna communication systems," *IEEE Trans. Signal Processing*, vol. 53, pp. 2089 – 2100, 2005.
- [48] D. J. Love and R. W. Heath Jr., "Limited feedback unitary precoding for spatial multiplexing systems," *IEEE Trans. Inform. Theory*, vol. 51, no. 8, pp. 2967–2976, Aug. 2005.
- [49] D. J. Love and R. W. Heath Jr., "Limited feedback unitary precoding for orthogonal space-time block codes," *IEEE Trans. Signal Processing*, vol. 53, no. 1, pp. 64–73, Jan. 2005.
- [50] G. Jongren and M. Skoglund, "Quantized feedback information in orthogonal space-time block coding," *IEEE Trans. Inform. Theory*, vol. 50, no. 10, pp. 2473–2486, 2004.
- [51] Y. Bae and J. Lee, "Antenna selection for MIMO systems with sequential nulling and cancellation," in *Proc. Conf. Information Sciences Systems*, Princeton, March 2006, pp. 745–749.
- [52] Y. Jiang and M. K. Varanasi, "A novel spatial multiplexing architecture with finite rate feedback," in *Proc. Conf. Information Sciences Systems*, Princeton, March 2006, pp. 755–760.
- [53] Y. Jiang, W. W. Hager, and J. Li, "The geometric mean decomposition," *Linear Algebra Appl.*, vol. 396, pp. 373–384, 2005.
- [54] A. Edelman, T. A. Arias, and S. T. Smith, "The geometry of algorithms with orthogonality constraints," *SIAM J. Matrix Anal. Applicat.*, vol. 20, no. 2, pp. 303–353, 1998.

- [55] J. H. Manton, "Optimization algorithms exploiting unitary constraints," vol. 50, no. 3, pp. 635–650, Mar. 2002.
- [56] A. Barg and D. Yu. Nogin, "Bounds on packings of spheres in the Grassmann manifold," *IEEE Trans. Inform. Theory*, vol. 48, no. 9, pp. 2450–2454, Sept. 2002.
- [57] B. M. Hochwald, T. L. Marzetta, T. J. Richardson, W. Sweldens, and R. Urbanke, "Systematic design of unitary space-time constellations," *IEEE Trans. Inform. Theory*, vol. 46, no. 6, pp. 1962–1973, Sept. 2000.
- [58] Y. Ding, T. N. Davidson, Zhi-Quan Luo, and K. M. Wong, "Minimum BER block precoders for zero-forcing equalization," *IEEE Trans. Signal Processing*, vol. 51, no. 9, pp. 2410–2423, Sept. 2003.
- [59] F. Rashid-Farrokhi, L. Tassiulas, and K. J. R. Liu, "Joint optimal power control and beamforming in wireless networks using antenna arrays," *IEEE Trans. Commun.*, vol. 46, no. 10, pp. 1313–1324, Oct. 1998.
- [60] F. Rashid-Farrokhi, K. J. R. Liu, and L. Tassiulas, "Transmit beamforming and power control for cellular wireless systems," *IEEE J. Select. Areas Commun.*, vol. 16, no. 8, pp. 1437–1450, Oct. 1998.
- [61] M. Bengtsson and B. Ottersten, "Optimal downlink beamforming using semidefinite optimization," in *Proc. 37th Allerton Conf. Comm., Control, Computing*, Monticello, IL, 1999, pp. 987–996.
- [62] M. Bengtsson and B. Ottersten, "Optimal and suboptimal transmit beamforming," in *Handbook of Antenna in Wireless Communications*, L. C. Godara, Ed., chapter 18. CRC Press, Boca Raton, FL, August 2001.

- [63] M. Schubert and H. Boche, "Solution of the multiuser downlink beamforming problem with individual SINR constraints," *IEEE Trans. Veh. Technol.*, vol. 53, pp. 18–28, Jan. 2004.
- [64] A. Wiesel, Y.C. Eldar, and S. Shamai, "Linear precoding via conic optimization for fixed MIMO receivers," *IEEE Trans. Signal Processing*, vol. 54, no. 1, pp. 161–176, Jan. 2006.
- [65] F. C.-H. Fung, W. Yu, and T. J. Lim, "Non-linear multi-user precoding for multi-antenna downlink channels using independent MSE constraints," in *Proc. 22nd Biennial Symposium on Communications*, Kingston, Ontario, May 2004.
- [66] R. Doostnejad, T. Lim, and E. Sousa, "Joint precoding and beamforming design for the downlink in a multiuser MIMO system," in *Wireless Mobile Computing, Networking, Commun.*, Montreal, Aug. 2005, vol. 1, pp. 153– 159.
- [67] L. Sanguinetti and M. Morelli, "Non-linear pre-coding for multiple-antenna multi-user downlink transmissions with different QoS requirements," *IEEE Trans. Commun.*, vol. 6, no. 3, pp. 852 – 856, March 2007.
- [68] M. Schubert and H. Boche, "Iterative multiuser uplink and downlink beamforming under SINR constraints," *IEEE Trans. Signal Processing*, vol. 53, no. 7, pp. 2324– 2334, July 2005.
- [69] M. Biguesh, S. Shahbazpanahi, and A.B. Gershman, "Robust downlink power control in wireless cellular systems," *EURASIP J. Wireless Commun. Networking*, vol. 2, pp. 261–272, 2004.
- [70] D. Bertsimas and M. Sim, "Tractable approximations to robust conic optimization problems," *Math. Program.*, vol. 107, no. 1, 2006.

- [71] D.P. Palomar, M.A. Lagunas, and J.M. Cioffi, "Optimum linear joint transmit-receive processing for MIMO channels with QoS constraints," *IEEE Trans. Signal Processing*, vol. 52, no. 5, pp. 1179–1197, May 2004.
- [72] T. Lan and W. Yu, "Input optimization for multi-antenna broadcast channels with per-antenna power constraints," in *Proc. IEEE Global Telecommun. Conf.*, Dallas, Dec. 2004, pp. 420–424.
- [73] D. P. Palomar, "Unified framework for linear MIMO transceivers with shaping constraints," *IEEE Commun. Letters*, vol. 8, no. 12, pp. 697–699, 2004.
- [74] D. Hammarwall, M. Bengtsson, and B. Ottersten, "On downlink beamforming with indefinite shaping constraints," *IEEE Trans. Signal Processing*, vol. 54, no. 9, pp. 3566–3580, Sept. 2006.
- [75] H. L. Van Trees, *Optimum Array Processing*, Wiley, New York, 2002.
- [76] P. Zetterberg, M. Bengtsson, D. McNamara, P. Karlsson, and M. Beach, "Performance of multiple-receive multiple-transmit beamforming in WLAN-type systems under power or EIRP constraints with delayed channel estimates," in *Proc. IEEE Veh. Technol. Conf.*, Birmingham, AL, May 2002, pp. 1906–1910.
- [77] S. A. Vorobyov, A. B. Gershman, and Z.-Q. Luo, "Robust adaptive beamforming using worst-case performance optimization: a solution to the signal mismatch problem," *IEEE Trans. Signal Processing*, vol. 51, no. 2, pp. 313–324, Feb. 2003.
- [78] R. G. Lorenz and S. P. Boyd, "Robust minimum variance beamforming," *IEEE Trans. Signal Processing*, vol. 53, no. 5, pp. 1684–1696, May 2005.

- [79] M. Payaro, A. Pascual-Iserte, and M. Lagunas, "Robust power allocation designs for multiuser and multiantenna downlink communication systems through convex optimization," *IEEE J. Select. Areas Commun.*, vol. 25, no. 7, pp. 1390–1401, Sept. 2007.
- [80] S. Cui, M. Kisiailiou, Z.-Q. Luo, and Z. Ding, "Robust blind multiuser detection against signature waveform mismatch based on second-order cone programming," *IEEE Trans. Commun.*, vol. 4, no. 4, pp. 1285–1291, July 2005.
- [81] A. Ben-Tal and A. Nemirovski, "Robust convex optimization," *Math. Oper. Res.*, vol. 23, no. 4, pp. 769–805, 1998.
- [82] S. Boyd and L. Vandenberghe, *Convex Optimization*, Cambridge University Press, Cambridge, U.K., 2004.
- [83] L. El Ghaoui and H. Le Bret, "Robust solutions to least-squares problems with uncertain data," *SIAM J. Matrix Anal. Appl.*, vol. 18, pp. 1035–1064, 1997.
- [84] L. El-Ghaoui, F. Oustry, and H. Le Bret, "Robust solutions to uncertain semidefinite programs," *SIAM J. Optim.*, vol. 9, pp. 33–52, 1998.
- [85] J. Sturm, "Using SeDuMi 1.02, a MATLAB toolbox for optimization over symmetric cones," *Optim. Methods Softw.*, vol. 11, pp. 625–653, 1999.
- [86] S. Boyd and L. El Ghaoui, "Method of centers for minimizing generalized eigenvalues," *Linear Algebra Appl.*, vol. 188, no. 189, pp. 63–111, 1993.
- [87] Y. Nesterov and A. Nemirovskii, "An interior-point method for generalized linear-fractional programming," *Math. Program.*, vol. 69, no. 1, pp. 177–204, 1995.

- [88] T.-L. Tung and K. Yao, "Robust downlink power-control for DS-CDMA system with multimedia services," in *IEEE Wkshp Signal Processing Advances Wireless Commun.*, Rome, June 2003, pp. 532–536.
- [89] Y. Nesterov and A. Nemirovsky, *Interior polynomial methods in convex programming: Theory and applications*, SIAM, Philadelphia, PA, 1994.
- [90] Y. Nesterov and M. Todd, "Primal-dual interior-point methods for self scaled cones," *SIAM J. Optim.*, vol. 8, pp. 324–364, 1998.
- [91] M. Botros Shenouda and T. N. Davidson, "Convex conic formulations of robust downlink precoder designs with quality of service constraints," *IEEE J. Select. Topics Signal Processing*, vol. 1, no. 4, pp. 714–724, Dec. 2007.
- [92] M. Botros Shenouda and T. N. Davidson, "Linear multiuser transceivers: Robustness via worst scenario MSE approach," *Proc. IEEE WCNC*, Las Vegas, April 2008.
- [93] M. Botros Shenouda and T. N. Davidson, "On the design of linear transceivers for multi-user systems with channel uncertainty," To appear in *IEEE J. Select. Areas Commun.*, Submitted July 2007, Accepted Dec. 2007.
- [94] T. Yoo, N. Jindal, and A. Goldsmith, "Multi-antenna downlink channels with limited feedback and user selection," *IEEE J. Select. Areas Commun.*, vol. 25, no. 7, pp. 1478–1491, Sept. 2007.
- [95] K. Huang, R. W. Heath Jr., and J. G. Andrews, "Multiuser limited feedback for wireless multi-antenna communication," in *Proc. Int. Symp. Inform. Theory*, Nice, June 2007.

- [96] J. Zheng, E. R. Duni, and B. D. Rao, "Analysis of multiple-antenna systems with finite-rate feedback using high-resolution quantization theory," *IEEE Trans. Signal Processing*, vol. 55, no. 4, pp. 1461–1476, April 2007.
- [97] J. Zheng and B. D. Rao, "Analysis of multiple antenna systems with finite-rate channel information feedback over spatially correlated fading channels," *IEEE Trans. Signal Processing*, vol. 55, no. 6, pp. 4612–4626, Sept. 2007.
- [98] M. Barlaud, P. Sole, JM Moureaux, M. Antonini, and P. Gauthier, "Elliptical codebook for lattice vector quantization," in *Proc. IEEE Int. Conf. on Acoustics, Speech, Signal Processing*, Minneapolis, 1993.
- [99] A. Ben-Tal, A. Nemirovski, and C. Roos, "Robust solutions of uncertain quadratic and conic-quadratic problems," *SIAM J. Optim.*, vol. 13, no. 2, pp. 535–560, Oct. 2002.
- [100] Q. H. Spencer, A. L. Swindlehurst, and M. Haardt, "Zero-forcing methods for downlink spatial multiplexing in multiuser MIMO channels," *IEEE Trans. Signal Processing*, vol. 52, no. 2, pp. 461–471, Feb. 2004.
- [101] L. Choi and R. Murch, "A transmit processing technique for multiuser MIMO systems using a decomposition approach," *IEEE Trans. Commun.*, vol. 3, no. 1, pp. 20–24, Jan. 2004.
- [102] C. Peel, B. Hochwald, and A. Swindlehurst, "A vector-perturbation technique for near-capacity multiantenna multiuser communication — Part I: Channel inversion and regularization," *IEEE Trans. Commun.*, vol. 53, no. 1, pp. 195–202, Jan. 2005.

- [103] W. Jang, B. Vojcic, and R. Pichholtz, "Joint transmitter-receiver optimization in synchronous multiuser communications over multipath channels," *IEEE Trans. Commun.*, vol. 46, no. 2, pp. 269–278, Feb. 1998.
- [104] M. Joham, W. Utschick, and J. Nosske, "Linear transmit processing in MIMO communications systems," *IEEE Trans. Signal Processing*, vol. 53, no. 8, pp. 2700–2712, Aug. 2005.
- [105] E. Vistorsky and U. Madhow, "Space-time transmit precoding with imperfect feedback," *IEEE Trans. Inform. Theory*, vol. 47, no. 6, pp. 2632–2639, Sept. 2001.
- [106] R. Hunger, F. Dietrich, M. Joham, and W. Utschick, "Robust transmit zero-forcing filters," in *Proc. ITG Wkshp Smart Antennas*, Munich, Mar. 2004, pp. 130–137.
- [107] F. A. Dietrich, R. Hunger, M. Joham, and W. Utschick, "Robust transmit Wiener filter for time division duplex systems," in *Proc. IEEE Int. Symp. Signal Processing Inform. Tech.*, Darmstadt, Germany, 2003, pp. 415–418.
- [108] M. Botros Shenouda and T. N. Davidson, "Robust linear precoding for uncertain MISO broadcast channels," in *Proc. IEEE Int. Conf. Acoustics, Speech, Signal Processing*, Toulouse, May 2006, pp. IV–37–IV–40.
- [109] M. Botros Shenouda and T. N. Davidson, "Tomlinson-Harashima precoding for broadcast channels with uncertainty," *IEEE J. Select. Areas Commun.*, vol. 25, no. 7, pp. 1380–1389, Sept. 2007.
- [110] S. Shi and M. Schubert, "MMSE transmit optimization for multi-user multi-antenna systems," in *Proc. IEEE Int. Conf. on Acoustics, Speech, Signal Processing*, Philadelphia, Mar. 2005, vol. 3.

- [111] A. Mezghani, M. Joham, R. Hunger, and W. Utschick, "Transceiver design for multi-user MIMO systems," in *Proc. ITG Wkshp Smart Antennas*, Castle Reisensburg, Germany, 2006.
- [112] N. Jindal, S. Vishwanath, and A. Goldsmith, "On the duality of Gaussian multiple-access and broadcast channels," *IEEE Trans. Inform. Theory*, vol. 50, no. 5, pp. 768–783, 2004.
- [113] S. Vishwanath, N. Jindal, and A. Goldsmith, "Duality, achievable rates, and sum capacity of Gaussian MIMO broadcast channel," *IEEE Trans. Inform. Theory*, vol. 49, pp. 2658–2668, Aug 2003.
- [114] P. Viswanath and D. Tse, "Sum capacity of the vector Gaussian broadcast channel and uplink-downlink duality," *IEEE Trans. Inform. Theory*, vol. 49, pp. 1912–1921, Aug 2003.
- [115] W. Yu, "Uplink-downlink duality via minimax duality," *IEEE Trans. Inform. Theory*, vol. 52, no. 2, pp. 361–374, 2006.
- [116] E. Jorswieck, "Lack of duality between SISO Gaussian MAC and BC with statistical CSIT," *IEE Electron. Lett.*, vol. 42, no. 25, pp. 1466 – 1468, Dec. 2006.
- [117] Z.-Q. Luo, T. N. Davidson, G.B. Giannakis, and K. M. Wong, "Transceiver optimization for block-based multiple access through ISI channels," *IEEE Trans. Signal Processing*, vol. 52, no. 4, pp. 1037–1052, April 2004.
- [118] Z.-Q. Luo and W. Yu, "An introduction to convex optimization for communications and signal processing," *IEEE J. Select. Areas Commun.*, vol. 24, no. 8, pp. 1426–1438, Aug. 2006.

- [119] O. Toker and H. Ozbay, "On the NP-hardness of solving bilinear matrix inequalities and simultaneous stabilization with static output feedback," in *Proc. IEEE American Control Conf.*, Seattle, 1995, pp. 2525–2526.
- [120] A. Ben-Tal and A. Nemirovski, *Lectures on Modern Convex Optimization: Analysis, Algorithms, and Engineering Applications*, SIAM, Philadelphia, 2001.
- [121] Y. C. Eldar, A. Ben-Tal, and A. Nemirovski, "Robust mean-squared error estimation in the presence of model uncertainties," *IEEE Trans. Signal Processing*, vol. 53, no. 1, pp. 168–181, Jan. 2005.
- [122] M. Joham, K. Kusume, M. Gzara, W. Utschick, and J. Nossék, "Transmit Wiener filter for the downlink of TDD DS-CDMA systems," in *Proc. 7th IEEE Int. Symp. Spread Spectrum Technology and Applications*, Prague, Sep. 2002, pp. 9–13.
- [123] R. F. H. Fischer, C. Windpassinger, A. Lampe, and J. B. Huber, "MIMO precoding for decentralized receivers," in *Proc. Int. Symp. Inform. Theory*, Lausanne, Switzerland, Jul. 2002, p. 496.
- [124] M. Joham, J. Brehmer, A. Voulgarelis, and W. Utschick, "Multiuser spatio-temporal Tomlinson-Harashima precoding for frequency selective vector channels," in *Proc. ITG Wkshp Smart Antennas*, Munich, Mar. 2004, pp. 208–215.
- [125] R. Hunger, M. Joham, and W. Utschick, "Extension of linear and nonlinear transmit filters for decentralized receivers," in *Proc. European Wireless Conf.*, Nicosia, April 2005, pp. 40–46.
- [126] M. Joham, J. Brehmer, and W. Utschick, "MMSE approaches to multiuser spatio-temporal Tomlinson-Harashima precoding," in *Proc. 5th Int. ITG Conf. Source and Channel Coding*, Erlangen, Jan. 2004, pp. 387–394.

- [127] M. Schubert and S. Shi, "MMSE transmit optimization with interference pre-compensation," in *Proc. IEEE Veh. Technol. Conf.*, May-1 June 2005, vol. 2, pp. 845–849.
- [128] W. Shi and R. Wesel, "The effect of mismatch on decision-feedback equalization and Tomlinson-Harashima precoding," in *Proc. Asilomar Conf. Signals, Syst., Comput.*, 1998.
- [129] F. A. Dietrich, P. Breun, and W. Utschick, "Robust Tomlinson-Harashima precoding for the wireless broadcast channel," *IEEE Trans. Signal Processing*, vol. 55, no. 2, pp. 631–644, Feb. 2007.
- [130] A. Mezghani, R. Hunger, M. Joham, and W. Utschick, "Iterative THP transceiver optimization for multi-user MIMO systems based on weighted sum-MSE minimization," in *Proc. IEEE Wkshp. Signal Process Signal Processing Advances in Wireless Commun.*, Cannes, 2-5 July 2006.